

Modeling Terrestrial Paleobiogeochemistry - Linking Fire, Biochemistry, Humans, and Climate

THÈSE N° 5721 (2013)

PRÉSENTÉE LE 24 MAI 2013

À LA FACULTÉ DE L'ENVIRONNEMENT NATUREL, ARCHITECTURAL ET CONSTRUIT
GROUPE KAPLAN
PROGRAMME DOCTORAL EN ENVIRONNEMENT

ÉCOLE POLYTECHNIQUE FÉDÉRALE DE LAUSANNE

POUR L'OBTENTION DU GRADE DE DOCTEUR ÈS SCIENCES

PAR

Mirjam PFEIFFER

acceptée sur proposition du jury:

Prof. A. Meibom, président du jury
Prof. J. O. Kaplan, directeur de thèse
Dr G. Krinner, rapporteur
Dr B. Poulter, rapporteur
Dr N. E. Zimmermann, rapporteur



ÉCOLE POLYTECHNIQUE
FÉDÉRALE DE LAUSANNE

Suisse
2013

Acknowledgements

This work would not have been possible without the support of those around me who provided expertise, facilities, and encouragement.

I would like to thank my thesis supervisor, Dr. Jed O. Kaplan, for offering me the possibility to write this thesis, and for donating his time, expertise and patience to my work. Without his encouragement and guidance this thesis would not have been completed or written. The discussions I had with him over the course of the last four years were a valuable contribution to this thesis. He always had an open ear for my questions and concerns, and the willingness to offer his expertise for the solution of diverse technical problems. His technical and editorial advice was essential to the completion of this dissertation and has taught me valuable lessons and insights on the workings of academic research in general.

I would also like to express my gratitude to my colleagues and good friends Pamela Collins, Kristen Krumhardt, and Achille Mauri. Thank you for your encouragement and the patient support offered through the ups and downs of my research. It was a pleasure to share this exciting time and benefit from your expertise. I appreciated the good-spirited discussions that we had relating to my research, and the spontaneous exchange of ideas and solutions for small technical issues.

A big thank you goes to Dr. Basil Davis, who was always there to patiently listen to my ideas and concerns and willing to offer advice and guidance. Writing this thesis would not have been the same without him.

A special thank you goes to Dr. Shawn Koppenhoefer for all the technical support provided throughout my thesis. Without his maintenance of personal computers and server system the simulations that produced the results presented in this thesis clearly would not have been possible.

Funding for my thesis was provided by grants from the Swiss National Science Foundation (PP0022-1190049) and the Italian Ministry for Research and Education (FIRB RBID08LNFJ) for the Research Project CASTANEA. In addition am indebted to Dr. Michel Bierlaire and Dr. Marc Parlange for providing support and funding to complete my thesis. Without the support and guidance provided by EPFL's doctoral school, this thesis would not have been completed.

I would also like to acknowledge Marie Sudki for dealing with various travel refunds and organizational issues. I owe her a special thank you for being there and listening to me when I needed to talk. Although I cannot acknowledge all of them by name, I would also like to thank all the nice people in my department for a great time and many vivid discussions and conversations.

Acknowledgements

Outside EPFL, I owe my gratitude to Dr. Sönke Zaehle from MPI Jena for sharing code from ORCHIDEE-CN and personal guidance that enabled me to perform the simulations for the Gerzensee study.

With respect to the Gerzensee study, I would like to single out Dr. Brigitta Ammann and thank her explicitly for sharing her immeasurable knowledge about the Gerzensee site, and for the kind support that she provided while I was completing the Gerzensee manuscript for the Paleocube Special Issue.

A special thank you goes to Dr. Allan Spessa from MPI Mainz for the fruitful discussions we had during the development of LMfire. His input clarified a number of open questions on SPITFIRE. The time he dedicated to the LMfire-manuscript clearly helped to improve my thesis.

I would also like to thank the members of my thesis committee, Dr. Benjamin Poulter, Dr. Gerhard Krinner, Dr. Niklaus Zimmermann, and Dr. Anders Meibom, for the time that they invested to read my thesis, and for coming to Lausanne to attend my thesis defense.

My personal thanks go to Klaus and Christiana for all the moral support and constant encouragement provided throughout the last four years. They have shared the ups and downs that I experienced while working on this thesis and always offered consolation and advice when needed most.

I am immeasurably grateful for the loving support and understanding of my wonderful fiancé Martin who was constantly at my side and encouraging me throughout my thesis. I am deeply thankful for all the help and technical expertise from his side, including the time that he spent helping me layout my thesis. Thank you for accepting me exactly the way I am, and thank you for being who you are!

And finally, I would like to thank all those people who contributed to the successful completion of my thesis without being specifically mentioned here.

Lausanne, April 16, 2013

M. P.

Summary

Quantitative assessment of terrestrial ecosystem processes over large spatial and temporal scales requires models that synthesize the knowledge obtained from measurements and empirical observation data. Changes in environmental conditions trigger reactions of biogeochemical cycles, alter vegetation distribution and composition, and affect disturbance regimes. Linked to the global change debate within the last decade, the focus of science has shifted beyond the carbon cycle and models are expanded to represent processes related to non-carbon trace gas exchange between biosphere and atmosphere with a specific emphasis on the nitrogen cycle. Disturbance has been recognized as a factor that cannot be neglected when simulating vegetation cover using Dynamic Global Vegetation Models (DGVMs), and most DGVMs include at least a simple scheme representing fire as disturbance factor in terrestrial ecosystems.

In this thesis I investigate the effect of the large abrupt warming at the transition from Oldest Dryas to Bølling on terrestrial nitrous oxide (N_2O) emissions at the Gerzensee site in Switzerland using a biogeochemical model that simulates terrestrial nitrogen uptake and release, including N_2O emissions. Evidence from polar ice core records for a large, rapid increase in atmospheric N_2O concentrations that occurred concurrent with the abrupt warming at the end of the last glacial period suggests a reorganization of the terrestrial nitrogen cycle for the time of the transition. The Gerzensee site provides a detailed scenario of climate and vegetation composition change based on multiproxy data that allows to study the sensitivity of terrestrial N_2O emissions to abrupt climate change. In addition, the abundant presence of the symbiotic nitrogen fixing species *Hippophaë rhamnoides* (L.) as an early colonizing pioneer on freshly exposed immature glacial soils likely contributed to a quick nitrogen enrichment of soils. My simulation study comes to the conclusion that already without additional nitrogen fixation through *H. rhamnoides* the reconstructed climate warming and wetting results in more than a tripling of local N_2O emissions. Additional nitrogen input via biological nitrogen fixation results in a further increase in emissions. The results therefore suggest that local reactions of emissions to abrupt climate change could have been even faster than the overall atmospheric concentration changes observed in polar ice. The positive reaction of emissions to the presence of the nitrogen-fixing pioneer species indicates that nitrogen enrichment of soils due to symbiotic N-fixation during early primary succession not only facilitates the establishment of vegetation on immature soils, but can also have considerable influence on biogeochemical cycles and the release of reactive nitrogen trace gases to the atmosphere.

Climatically relevant trace gases such as CO_2 , CO, CH_4 , NO_x , and aerosols are also emitted

Summary

by vegetation fires. Process-based fire models linked to DGVMs allow assessing the impact of global wildfire on centennial to multi-millennial timescales. In this thesis I present LMfire, a new fire module that is particularly suited to investigate climate-human-fire relationships on multi-millennial timescales prior to the Industrial Revolution. It includes explicit calculation of natural ignitions, the representation of multi-day burning and coalescence of fires, the calculation of fire spread in different vegetation types, and a new representation of anthropogenic burning under preindustrial conditions that distinguishes different human-fire relationships for hunter-gatherers, pastoralists, and farmers. An evaluation of the new fire model against remote-sensing based estimates of burned area at regional and global scale reveals those parts of the world where modern anthropogenic fire management has significantly altered natural fire regimes. The new fire module shows a considerably enhanced representation of natural fire in those parts of the world where lightning ignitions are scarce and natural fire dominates the fire regime, e.g., in remote areas of the boreal forest and the subarctic.

In the third part of my thesis I present an application of the new fire module to test the hypothesis that fire use by Paleolithic hunter-gatherers during the time of the Last Glacial Maximum (LGM) in Europe may have been a significant contribution to produce the open, steppe-like vegetation reconstructed from pollen. Most DGVMs have difficulties in reproducing the high degree of landscape openness in Europe during the LGM and overestimate tree cover albeit colder and dryer climatic conditions and lower atmospheric CO₂ concentrations. I argue that inclusion of anthropogenic fire into DGVMs may be the key to simulating vegetation patterns that are in better agreement with proxy-reconstructions. Based on four model simulations separately testing the effect of naturally caused fires vs. natural and additional human fire for the LGM and preindustrial time, a quantification of changes in average annual area burned and simulated tree cover is possible. The results show that already relatively small increases in average annual area burned due to additional human ignitions may result in a remarkable reduction of tree cover, and a dominance of grassy/herbaceous plant functional types as suggested by data-based reconstructions. The usage of fire by forager people in Europe during the LGM may therefore have been an important factor leading to the high degree of landscape openness and the predominance of steppe-type flora that vegetation models cannot reproduce based solely on cold and dry climatic conditions and low atmospheric CO₂.

Keywords: Terrestrial nitrogen cycle, abrupt climate change, N₂O emissions, Gerzensee, DGVM fire modeling, LMfire, preindustrial anthropogenic fire, LGM, Europe, steppe-vegetation, hunter-gatherer burning

Zusammenfassung

Eine Quantifizierung terrestrischer Ökosystemprozesse für große räumliche und zeitliche Skalen erfordert Modelle um das aus Messungen und empirischen Beobachtungsdaten gewonnene Wissen zusammenzufassen. Veränderungen von Umweltbedingungen führen zu Reaktionen biogeochemischer Kreisläufe, verändern die Verbreitungsmuster und Zusammensetzung von Vegetation und beeinflussen Störungsregimes. Im Rahmen der Global Change Diskussionen während des letzten Jahrzehnts hat sich das Augenmerk der Wissenschaft auf Aspekte jenseits des Kohlenstoffkreislaufs gerichtet und Modelle werden nun erweitert um Prozesse wie den Austausch von nicht-kohlenstoffbasierten Spurengasen zwischen Biosphäre und Atmosphäre zu erfassen. Ein besonderer Schwerpunkt liegt hierbei auf dem Stickstoffkreislauf. Störungsprozesse sind als ein Faktor identifiziert worden der bei der Simulation von Vegetation mit DGVMs (Dynamic Global Vegetation Models) nicht vernachlässigt werden kann.

Im Rahmen dieser Dissertation untersuche ich den Effekt einer raschen drastischen Erwärmung auf terrestrische Lachgasemissionen am Gerzensee in der Schweiz für den Übergang von der Ältesten Dryas zum Bølling mittels eines Modells welches die terrestrische Aufnahme und Abgabe von Stickstoff, inklusive N_2O , simuliert. Polare Eisbohrkerne liefern Anhaltspunkte für einen raschen, ausgeprägten Anstieg der atmosphärischen N_2O Konzentration zeitgleich zu der abrupt erfolgenden Erwärmung am Ende des letzten Glazials, was eine zu dieser Zeit stattfindende Reorganisation des terrestrischen Stickstoffkreislaufes vermuten lässt. Basierend auf Multiproxy-Daten liefert der Gerzensee ein detailliertes Szenario für die Veränderung des Klimas und der Vegetationszusammensetzung, was eine Untersuchung der Empfindlichkeit terrestrischer N_2O Emissionen auf abrupte Klimaveränderung ermöglicht. Zusätzlich legt die verbreitete Anwesenheit der zur symbiotischen Stickstofffixierung fähigen Art *Hippophaë rhamnoides* (L.), die im Frühstadium der Besiedelung glazialer Böden als Pionierart auftritt, eine rasche Anreicherung der Böden mit Stickstoff nahe. Das Ergebnis der Studie zeigt bereits ohne die zusätzliche Anwesenheit des Stickstofffixierers *H. rhamnoides* mehr als eine Verdreifachung der lokalen N_2O Emissionen als Reaktion auf die Erwärmung und die feuchteren Bedingungen. Weiterer Stickstoffeintrag durch biologische Fixierung führt zu einer zusätzlichen Erhöhung der Emissionen. Dies legt die Schlussfolgerung nahe dass die Reaktion von N_2O Emissionen auf raschen Klimawandel lokal noch schneller ablaufen kann als die im polaren Eis dokumentierten Konzentrationsveränderungen anzeigen. Die positive Reaktion der Emissionen auf die Anwesenheit des symbiotischen Stickstofffixierers während der Frühsukzession ist ein Indiz dafür dass die Anreicherung des Bodens mit Stickstoff nicht

nur die Ansiedelung von Vegetation auf Rohböden erleichtert, sondern auch einen beträchtlichen Einfluss auf biogeochemische Kreisläufe und die Freisetzung von Stickstoff-Spurengasen haben kann.

Klimarelevante Spurengase wie CO_2 , CO , CH_4 , NO_x , sowie Aerosole werden auch von Vegetationsfeuern freigesetzt. In DGVMs integrierte prozessbasierte Feuermodelle ermöglichen eine Abschätzung der Auswirkung von Feuer auf globaler Skala auf Zeitskalen von Jahrhunderten bis Jahrtausenden. In dieser Dissertation stelle ich LMfire als ein neues Feuermodul für LPJ vor das auf SPITFIRE basiert und besonders gut geeignet ist um die präindustrielle Beziehung zwischen Klima, Mensch und Feuer auf Zeitskalen von Jahrtausenden zu untersuchen. Es beinhaltet die explizite Simulation natürlicher Feuerentzündung, eine Darstellung von Feuern die über eine Reihe von aufeinanderfolgenden Tagen brennen können, die Berechnung von Feuerausbreitung in verschiedenen Vegetationstypen, und eine neue Repräsentation für menschlich verursachte Feuer unter präindustriellen Bedingungen. Diese unterscheidet verschiedene Beziehungen zwischen Mensch und Feuer für Jäger und Sammler, Viehhalter und Ackerbauern. Eine Evaluierung des neuen Feuermodells gegen fernerkundungsbasierte Abschätzungen feuerbetroffener Flächen auf regionaler und globaler Skala zeigt jene Bereiche auf in denen modernes Feuermanagement durch den Menschen das natürliche Feuerregime signifikant verändert hat. Das Model zeigt eine deutlich verbesserte Darstellung von natürlicherweise auftretenden Feuern in Bereichen in denen Blitzeinschlag selten ist, gleichzeitig aber natürlich entzündete Feuer das Feuerregime beherrschen, d.h. beispielsweise in abgelegenen subarktischen und borealen Gebieten.

Im letzten Kapitel dieser Dissertation wird das neue Feuermodell angewendet um die Hypothese zu testen dass die Verwendung von Feuer durch paläolithische Jäger und Sammler während der Zeit des letzten glazialen Maximums (LGM) in Europa zur Erzeugung der offenen, steppenartigen Vegetation beitrug. Viele DGVMs haben Schwierigkeiten den aus Pollendaten rekonstruierten hohen Grad an Landschaftsoffenheit in Europa während des LGMs zu reproduzieren. Trotz kälterer und trockenerer klimatischer Bedingungen und niedrigerer atmosphärischer CO_2 -Konzentration überschätzen sie die Deckung von von Bäumen. Die Berücksichtigung von Störungsfaktoren wie menschlich verursachter Feuer in DGVMs ist möglicherweise der Schlüssel für eine Simulation von Vegetationsmustern die besser mit den proxybasierten Rekonstruktionen übereinstimmen. Basierend auf vier Simulationen die jeweils separat den Effekt von natürlich vs. natürlich und menschlich verursachten Feuern zur Zeit des LGMs und präindustrielle Bedingungen testen, lässt sich die Veränderung der jeweiligen jährlich verbrannten Fläche und simulierten Baumbedeckung quantifizieren. Die Ergebnisse zeigen dass bereits eine vergleichsweise kleine Steigerung der pro Jahr verbrannten Fläche bedingt durch von Menschen verursachtes Feuer zu einer deutlichen Reduzierung der simulierten Baumbedeckung und einer Dominanz krautiger Taxa führen kann. Der gezielte Einsatz von Feuer durch Jäger und Sammler in Europa während des LGMs war möglicherweise ein wichtiger Faktor der zu dem hohen Grad an Landschaftsoffenheit und der Vorherrschaft von Steppenflora beigetragen hat.

Schlagworte: Terrestrischer Stickstoffkreislauf, abrupte Klimaveränderung, N₂O Emissionen, Gerzensee, Feuermodellierung, DGVM, LMfire, präindustrielles anthropogenes Feuer, LGM, Europa, Steppenvegetation, Paläolithikum, Jäger-Sammler

Contents

Acknowledgements	iii
Summary (English/Deutsch)	v
List of figures	xii
List of tables	xiv
1 Introduction	1
1.1 N ₂ O emissions from terrestrial ecosystems during abrupt climatic warming	6
1.2 Modeling preindustrial natural and anthropogenic biomass burning	13
1.3 The role of hunter-gatherer burning in Europe during the Last Glacial Maximum	20
1.4 Synthesis	25
2 The effect of abrupt climatic warming on biogeochemical cycling and N₂O emissions in a terrestrial ecosystem	49
2.1 Introduction	50
2.2 Methods	52
2.2.1 Site location, period of interest, and soils	52
2.2.2 Paleoclimate scenario for O-CN	54
2.2.3 Vegetation change during the transition period	55
2.2.4 Biological nitrogen fixation	55
2.2.5 Simulation of N ₂ O emissions	57
2.3 Results	57
2.4 Discussion	60
2.4.1 Uncertainties related to the climate reconstruction	60
2.4.2 Influence of soil properties on N ₂ O emissions	61
2.4.3 Comparison of simulated N ₂ O emissions to present day measurements	63
2.4.4 Vegetation succession and nitrogen enrichment by symbiotic fixation . .	64
2.4.5 Simulated N ₂ O increase at Gerzensee and ice core records	64
2.5 Conclusions	67

Contents

3	LMfire: An improved fire module for Dynamic Global Vegetation Models	77
3.1	Introduction	78
3.2	Rationale for modifying SPITFIRE	80
3.3	Methods	80
3.3.1	Fire occurrence and ignitions	85
3.3.2	Fire behavior	94
3.3.3	Fire mortality	102
3.3.4	Datasets and model runs used for model evaluation	104
3.4	Model results and evaluation	105
3.4.1	Aboveground biomass	106
3.4.2	The organic soil layer	106
3.4.3	Fire in boreal ecosystems: The Alaska case study	107
3.4.4	Global fire under natural conditions	116
3.4.5	Comparison to contemporary observations of burned area	119
3.5	General discussion	125
3.6	Conclusions	127
3.7	Appendix	128
3.7.1	Fuel load and moisture	128
3.7.2	Rate of spread	129
3.7.3	Fire geometry and duration	132
3.7.4	Combustion of dead fuel	133
3.7.5	Fire mortality and combustion of live fuel	134
3.7.6	Fuel consumption	135
3.7.7	Trace gas emissions	137
3.8	Supplementary Figures	140
4	Role of humans and fire for vegetation in Europe during the Last Glacial Maximum	165
4.1	Introduction	165
4.2	Methods	167
4.3	Results	168
4.3.1	Changes in average annual area burned	168
4.3.2	Changes in simulated tree cover	170
4.4	Discussion	172
4.5	Conclusions	175
4.6	Supplementary Figures	177
	Curriculum Vitae	185

List of Figures

1.1	Systems analysis diagram illustrating the regulation mechanisms between plants, fires and oxygen	2
1.2	Modeled fluctuations in atmospheric oxygen concentration during Late Paleozoic	3
1.3	Schematic representation of the terrestrial nitrogen cycle	7
1.4	Dome C N ₂ O records over the past 220 ky	9
1.5	Flowchart illustrating the simulation of terrestrial N ₂ O emissions at Gerzensee during the transition from Oldest Dryas to Bølling	12
1.6	Simplified schematic of components included in LMfire.	18
1.7	Example of LMfire simulating fire occurrence on a daily time step based on fire weather conditions and occurrence of ignitions	19
1.8	Simulated and observed biomes in the northern extratropics	23
2.1	Map showing the spatial distribution of the major soil types at Gerzensee	53
2.2	Comparison of simulated annual mean temperature and temperature anomalies reconstructed from $\delta^{18}\text{O}$	56
2.3	Simulated N ₂ O emissions for the time of the abrupt Bølling warming and atmospheric N ₂ O concentrations from ice core records.	59
2.4	characteristic emissions for the three simulated PFTs and 15 tested soils (BNF0 scenario)	62
2.5	Total regional emissions for the 10-km area around Gerzensee stacked according to the contributions of the three PFTs	66
3.1	Flowchart of LPJ-LMfire	81
3.2	Maximum-to-mean-ratio (top boxplot) and minimum-to-mean-ratio (bottom boxplot) for Alaska lightning strike data	86
3.3	Simulated aboveground C-storage in living biomass	106
3.4	Simulated C-storage in the organic topsoil layer (O-horizon) newly implemented in LPJ	107
3.5	Alaska ecoregions following the scheme used by the Alaska Fire Service	109
3.6	Boxplots showing the observed and simulated area burned in Alaska between 1986 and 2010	110
3.7	Simulated and observed time series of total annual area burned	111

List of Figures

3.8	Typical daily precipitation, FDI, lightning and snowcover data for a grid pixel located in ecoregion BTA	114
3.9	Simulated fire return intervals in Alaska	115
3.10	Simulated global biomass C for different scenarios	117
3.11	Map of simulated global fire return intervals	118
3.12	Residuals between observed and simulated average annual area burned	121
3.13	Scatterplot of Monte Carlo simulation results of connectivity simulations on a 100 x 100 grid	140
3.14	Spatial distribution of the slope factor (slf)	140
3.15	Effect on global biomass caused by the changes to maximum crown area and maximum establishment rate in LPJ	141
3.16	Simulated maximum crown area for different scenarios	142
3.17	Comparison of average annual burned area fraction for different simulation scenarios	142
3.18	Seasonality of fire under natural conditions (no land use, lightning ignitions)	143
3.19	Statistical comparison between ALDS lightning observations and LIS/OTD-derived, CAPE-scaled lightning for the time period 2001-2010	144
3.20	Residuals between average annual area burned in Randerson et al. [2012] and LMfire simulation results	145
3.21	Human impact based on settlements and infrastructure (roads, powerlines, pipelines, etc.) [Ahlenius, 2005]	145
4.1	Simulated area burned for different scenarios using LMfire	169
4.2	Simulated tree cover for different scenarios using LMfire	171
4.3	Difference in annual burned area for the scenarios with and without human influence	174
4.4	Simulated area burned for different LMfire scenarios	177
4.5	Simulated forest covered areas for different LMfire scenarios	178

List of Tables

2.1	Simulated N ₂ O emissions before and after the 30-year-transition period around the Gerzensee site.	61
3.1	Explanation of LMfire variable and parameter abbreviations	83
3.2	Rate of Spread calculations before and after implementation of the O-horizon .	97
3.3	Datasets used to drive LPJ-LMfire	105
3.4	Observed and simulated mean (standard deviation) area burned and burned percent of total ecoregion area over the time period 1986-2010 by ecoregion . .	109
3.5	PFT-specific parameters in LMfire	128
3.6	Explanation of SPITFIRE variable and parameter abbreviations	137

1 Introduction

This thesis focusses on interactions between vegetation and soils, climate, biogeochemical cycles, fire, and humans in the Earth system during the last 21,000 years of Earth history. It addresses the question what potential effect abrupt climate change in the past, e.g., the transition from a glacial cold period into a warm phase, could have had on vegetation, soils, and the release of radiatively active nitrogen trace gases from terrestrial ecosystems. A detailed reconstruction of climate and vegetation composition change based on high-resolution multi-proxy data from the Swiss Gerzensee site is used to drive a terrestrial nitrogen cycle model and simulate emissions of terrestrial N_2O during an abrupt climate change event on a local to regional scale. To study the role of natural and anthropogenic fire in the past, a new fire module for Dynamic Global Vegetation Models (DGVMs) has been developed and integrated into the LPJ-DGVM as part of this thesis. The new fire module includes explicit calculation of natural and anthropogenic ignitions, the representation of fire behavior, and an assessment of fire effects with respect to vegetation mortality and trace gas emissions. An application study using the new fire module is presented that tests the sensitivity of European vegetation to human-caused fire disturbance during the time of the Last Glacial Maximum. Results from this study propose that human burning may have been an important factor for the creation of the open steppe-type vegetation reconstructed from pollen records.

Vegetation is influenced by a variety of factors in the Earth system, e.g. climate, soils and disturbance. At the same time, vegetation plays a very important role in shaping the terrestrial land surface, influences biogeochemical cycles, and affects climate through physical and chemical interactions with the atmosphere. In order to fully understand the importance of vegetation for the terrestrial land surface, it is important to consider the changes in the Earth system that were caused or reinforced by the appearance and presence of plants over the course of Earth history.

Since the first terrestrial plants evolved, the face of the Earth has been dramatically altered and reshaped. The arrival of the first simple land plants, approx. 470 million years ago, was accompanied by a dramatic reduction in atmospheric carbon causing a pronounced temperature drop and a series of ice ages [Lenton et al., 2012]. The presence of plants and the

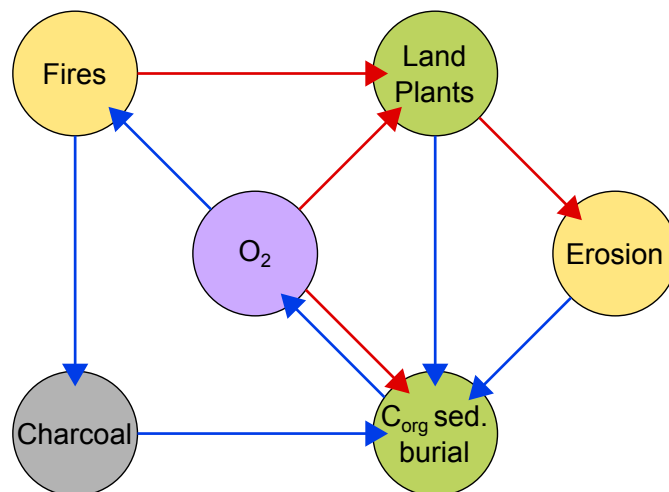


Figure 1.1: Systems analysis diagram adapted from [Berner et al., 2003] illustrating the regulation mechanisms between plants, fires and oxygen. Red arrows mark negative feedback mechanisms, while blue arrows indicate positive feedback. Elevated O₂ levels increase fire activity, which leads to a faster breakdown of organic material and changes in ecosystem form and functioning. The decrease in land biomass due to increased fire activity lowers photosynthetic O₂ production and CO₂ fixation and results in a negative feedback. In addition, high O₂ concentrations directly have adverse effects on plants via photorespiration. Charcoal production leads to enhanced preservation of organic matter and therefore more carbon burial, resulting in a positive feedback. Moreover, char acts as a fire retardant. Increased erosion due to fire destruction of land plants increases marine sedimentation and burial of organic matter and enhances O₂ production, resulting in another positive feedback mechanism.

organic acids they excreted accelerated bedrock weathering and ultimately led to the formation of first soils. As plants evolved and root systems developed, this fed back on the development of the first soils, which in return enhanced plant growth and production. Organic matter input into soils and plant exudates caused a shift from predominantly physical weathering to increasingly more chemical weathering, resulting in finer particle sizes, an accelerated release of essential nutrients from rock material, and a drawdown of atmospheric CO₂ that led to the global cooling and polar glaciations of the Devonian [Berner, 1997, Bateman et al., 1998, Moulton and Berner, 1998]. Early vascular plants with increasingly extensive root structures and their ability to fix carbon through photosynthesis accelerated the terrestrial nutrient cycle by binding, transforming and redistributing molecules from the atmosphere and elements from the lithosphere. Through the presence of plants, relatively light chemical elements such as carbon and nitrogen are withdrawn from the atmosphere and transformed into organic molecules. When plants die and their residues are decomposed part of the organically bound carbon and nitrogen is transformed and sequestered as humus [Jobbágy and Jackson, 2004]. Characterized by this ability to transform inorganic elements from atmosphere and lithosphere into organic molecules, plants as primary producers are the fundamental basis of most terrestrial ecosystems by providing other heterotrophic organisms with energy and organic matter.

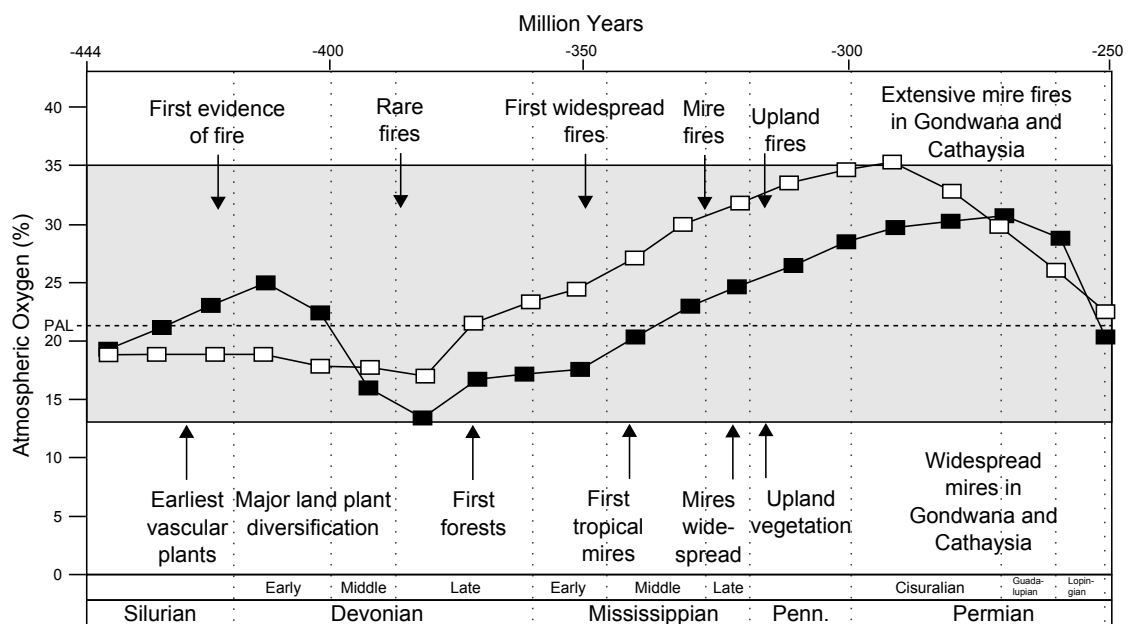


Figure 1.2: Modeled fluctuations in atmospheric oxygen concentration during Late Paleozoic from Berner et al. [2003, □] and Berner [2006, ■]. Figure adapted from Scott and Glasspool [2006]

Free oxygen produced through photosynthesis caused one of the most radical changes in Earth's atmosphere, leading to the so-called Oxygen Crisis that is supposed to have wiped out the majority of Earth's anaerobic inhabitants. Moreover, the existence of free atmospheric oxygen likely was the key trigger that caused the Huronian glaciation, possibly the longest snowball Earth episode, by reacting with atmospheric methane and thereby significantly lowering the concentration of atmospheric greenhouse gas [Holland, 2006, Frei et al., 2009, Bekker and Holland, 2012]. Moreover, the presence of oxygen in the atmosphere is one of the three key elements essential to the existence of one of the most important disturbance processes in terrestrial ecosystems: fire. In addition to oxygen, fire requires a combustion source, i.e., fuel, which is also provided by plants, and an ignition source such as lightning, sparks from rocks, meteorite impacts or volcanoes. Therefore, two out of three prerequisites for the possible occurrence of fire are linked to the existence of plants. Prior to the existence of photosynthetic organisms, low atmospheric oxygen levels would not have allowed fires to burn, and prior to the appearance of terrestrial plants lack of fuel inhibited the occurrence of fire [Pausas and Keeley, 2009]. As soon as the first terrestrial plants developed during the Silurian approx. 440 mya ago, there is evidence of fire in form of charred remains of low-growing vegetation of the earliest stomata-bearing plants [Cressler, 2001, Glasspool et al., 2004]. Early fire history on Earth is characterized by periods of higher and lower fire activity that seem to be connected to fluctuations in atmospheric oxygen levels [Scott and Glasspool, 2006]. During the Permo-Carboniferous oxygen levels as high as 35% likely stimulated more extensive wildfires, which in turn increased the breakdown of organic material and changed form and function of ecosystems [Berner et al., 2003] (see Fig. 1.1).

Chapter 1. Introduction

Through the production of oxygen and fuel, vegetation created the prerequisite to its own self-regulation as fire destroys biomass, consumes oxygen, releases CO₂, and indirectly reduces atmospheric oxygen through the destruction of photosynthetically active tissue. Fire therefore counterbalances the sequestration of carbon in plants and acts as a "global herbivore" [Bond and Keeley, 2005]. It is assumed that during early Earth history, the negative feedback mechanism between fire as a "herbivore" and vegetation helped to regulate atmospheric oxygen concentrations at levels between 15% and 25% [Watson et al., 1978, Lovelock, 1995, Kump, 1988, 1989, Lenton and Watson, 2000] (also see Figure 1.2). At the same time, ecosystems reacted to fire by promoting fire-adapted species, e.g., plant species that enhance char-forming chemical reactions as a way to create fire-retardants [Nelson, 2001] as suggested by the abundance of fusain in Late Paleozoic sediments [see, e.g., Robinson, 1989, Glasspool, 2000], or the ability for resprouting as an adaptive selection in response to fire. Fire-regimes similar to those observable at present developed early in Earth history, as indicated by evidence of understory surface fires in the Devonian [Cressler, 2001], documented fire return intervals of 3 to 35 years in Carboniferous progymnosperm communities [Beerling et al., 1998, Falcon-Lang, 2000], indicators for crown fire regimes in Carboniferous wetland lepidodendron forests [Falcon-Lang, 2000], or evidence for high-frequency, light surface fires in Jurassic gymnosperm forests [Francis, 1984]. The continuous history of fire since plants invaded land documents that vegetation coevolved with fire as one of the most important disturbance processes in ecosystems.

Aside from regulating the composition and ecology of plant ecosystems and balancing the carbon cycle, fire has both short- and long-term effects on nutrient cycles and soil fertility [Raison, 1980, Rundel, 1983]. As nitrogen in plants is predominantly allocated in fine fuel such as foliage, twigs and litter that burn most readily, and due to its low volatilization temperature of approx. 200 °C, the majority of nitrogen in burned biomass is lost in gaseous form [Vitousek and Howarth, 1991, Sampson, 1997, Caldwell et al., 2002]. Additional post-fire losses of nutrients in ash and topsoil can be caused by wind and water. However, fire also frees nitrogen that was previously bound in organic matter, leaving high concentrations of ammonium and organic nitrogen in the remaining ash and topsoil which promotes re-growth after fire [Christensen, 1973, Wan et al., 2001]. Biochar produced by wildfires has the potential to retain nitrogen in soils by enhancing NH₃ and NH₄⁺ retention, increase nitrification rates [Berglund et al., 2004, DeLuca and Sala, 2006, Ball et al., 2010] reduce N₂O emissions [Rondon et al., 2005] and NO₃⁻ leaching, enhance biological nitrogen fixation [Rondon et al., 2007], and to influence soil microbial communities [Clough and Condron, 2010]. Johnson et al. [1998] demonstrate that in semi-arid forest ecosystems fire may be more important than water with respect to nitrogen fluxes, especially with respect to nitrogen volatilization and enhanced post-fire nitrogen fixation.

The interactions and feedbacks between vegetation, nutrient cycles, fire and atmospheric trace gas composition are complex and have coevolved ever since the first terrestrial plants appeared. Much research effort during the past years has been oriented toward the understanding and quantification of these processes and feedbacks. Field studies and experiments help

to understand the underlying processes and mechanisms in more detail and provide the basis for synthesis studies. However, models are required in order to produce global-scale quantifications of fluxes related to these processes and assess changes to carbon and nutrient pools or vegetation composition. Such models synthesize the knowledge received from empirical observations and measurements and allow an evaluation of science's understanding with respect to process coupling. Dynamic Global Vegetation Models (DGVMs) combine routines to model biogeochemistry, biogeography and disturbance. They enable scientists to study the reaction of vegetation to changing environmental conditions, e.g., changing climate, with respect to shifts in potential vegetation and associated biogeochemical and hydrological cycles. Since the introduction of the term "DGVM" in 1996 (Neilson and Running), the number of different processes represented by DGVMs has continuously increased [Arneeth et al., 2009]. In the beginning, DGVMs mainly focused on aspects related to the carbon cycle and were designed to answer scientific questions related to CO₂ and partially CH₄. In contrast, non-carbon trace gases have been left aside for a long time. More recently, DGVMs are expanded to represent processes related to non-carbon trace gas exchange between terrestrial biosphere and atmosphere within unified modeling frameworks with a special focus on the nitrogen cycle [e.g., Thornton et al., 2007, Sokolov et al., 2008, Xu-Ri and Prentice, 2008, Zaehle and Friend, 2010a, Zaehle et al., 2010, Zaehle and Friend, 2010b]. With respect to disturbance, DGVMs usually include schemes to simulate wildfires, but often ignore other disturbance factors such as insect outbreaks, windthrow, or anthropogenic disturbance through forestry, agriculture and land management, although more recently attempts to include humans as disturbance factor have been made [e.g., Kaplan et al., 2011, 2012].

DGVMs and biogeochemical models allow addressing scientific questions that cannot directly be answered solely based on empirical studies and observations. For example, they are particularly valuable to investigate the effects of past or future climate change on vegetation, carbon, nutrient and water cycles, or the change of fire regimes. In my thesis, I focus on two major aspects related to vegetation modeling: a) the effect of abrupt climate change on nitrogen trace gas emissions, and b) the effects of fire on vegetation as one of the most important disturbance factors in terrestrial ecosystems. To address the first aspect, I used the nitrogen cycle module of ORCHIDEE-CN [Zaehle and Friend, 2010a] to simulate changes in N₂O emissions at the Swiss Gerzensee site over a period of abrupt climate change at the end of the last glacial. This part of my work has been published as part of a special issue in *Palaeogeography, Palaeoclimatology, Palaeoecology* on the Oldest Dryas to Bølling transition at the Gerzensee site in Switzerland, [Pfeiffer et al., 2012] and is presented in chapter 2. In chapter 3 I present a new fire module for LPJ that is based on the SPITFIRE-scheme developed by Thonicke et al. [2010]. The new fire module includes several improvements to the way in which the occurrence, behavior and the effect of fire on vegetation are simulated, e.g., by including explicit calculation of natural ignitions, the representation of multi-day burning and coalescence of fires, the calculation of rates of spread in different vegetation types, and a representation of anthropogenic biomass burning under preindustrial conditions. This work has been published as discussion paper [Pfeiffer and Kaplan, 2012] in *Geoscientific Model*

Development Discussions and has been resubmitted for final publication in *Geoscientific Model Development* after review. In chapter 4 I illustrate how the new fire routine can be used to estimate the effect of anthropogenic burning on vegetation cover in Europe during the time of the Last Glacial Maximum (LGM). Implications of this study are that the observed high degree of landscape openness during the LGM suggested by pollen records may not only have been climatically triggered, but rather could have been the result of climate effects combined with efforts from hunter-gatherer people to maintain open landscapes using fire. This manuscript is currently prepared for submission to *Nature Geoscience*.

1.1 N₂O emissions from terrestrial ecosystems during abrupt climatic warming

During more recent years it has been recognized that terrestrial ecosystems, due to their capability to sequester or release climatically relevant greenhouse gases such as CO₂, CH₄ and N₂O, play an important role in the global climate system via feedback mechanisms that amplify or attenuate climate change on regional to global scale [Heimann and Reichstein, 2008]. As large quantities of carbon are bound in vegetation and soil organic matter, attention was first mainly focused on interactions between carbon cycling and climate system [Post et al., 1990, Cox et al., 2000, Dufresne et al., 2002, Friedlingstein et al., 2006, Heimann and Reichstein, 2008]. However, more recently the role of non-carbon greenhouse gases has been recognized as an additional important factor in the climate system. Consequently, the interest on functioning and mechanisms of nutrient cycles that are involved in the production and release of non-carbon greenhouse gases has been increasing [Reilly et al., 2002].

Assessment of the role of non-carbon greenhouse gases requires a sound understanding of the underlying processes, feedbacks and sensitivities of greenhouse gas sources and sinks. For example, plant macronutrients such as nitrogen can affect atmospheric greenhouse gas concentrations directly and indirectly. While increasing atmospheric CO₂ concentrations may enhance the productivity of terrestrial ecosystem and thereby lead to an increased storage of carbon in vegetation and soils [Norby et al., 2005], this effect can be counterbalanced by feedbacks between carbon and nitrogen cycle when nitrogen availability to plants is limited and constrains CO₂-fertilization effects [Hungate et al., 2003, Luo et al., 2004, Norby et al., 2010]. Availability of mineral nitrogen for primary production is controlled by net nitrogen mineralization of plant litter and soil organic matter, which implies a strong dependency of heterotrophic respiration on plant organic matter production and its qualitative composition, as well as a temperature dependency for the microorganisms that are responsible for the breakdown of organic matter [Vitousek and Howarth, 1991, Melillo et al., 2002]. Nitrogen availability therefore indirectly controls atmospheric CO₂ concentrations by constraining how much CO₂ plants can fix, and by how fast carbon will be released from soils due to microbial breakdown of organic matter [McClaugherty et al., 1985, Taylor et al., 1989, Manzoni et al., 2008].

1.1. N₂O emissions from terrestrial ecosystems during abrupt climatic warming

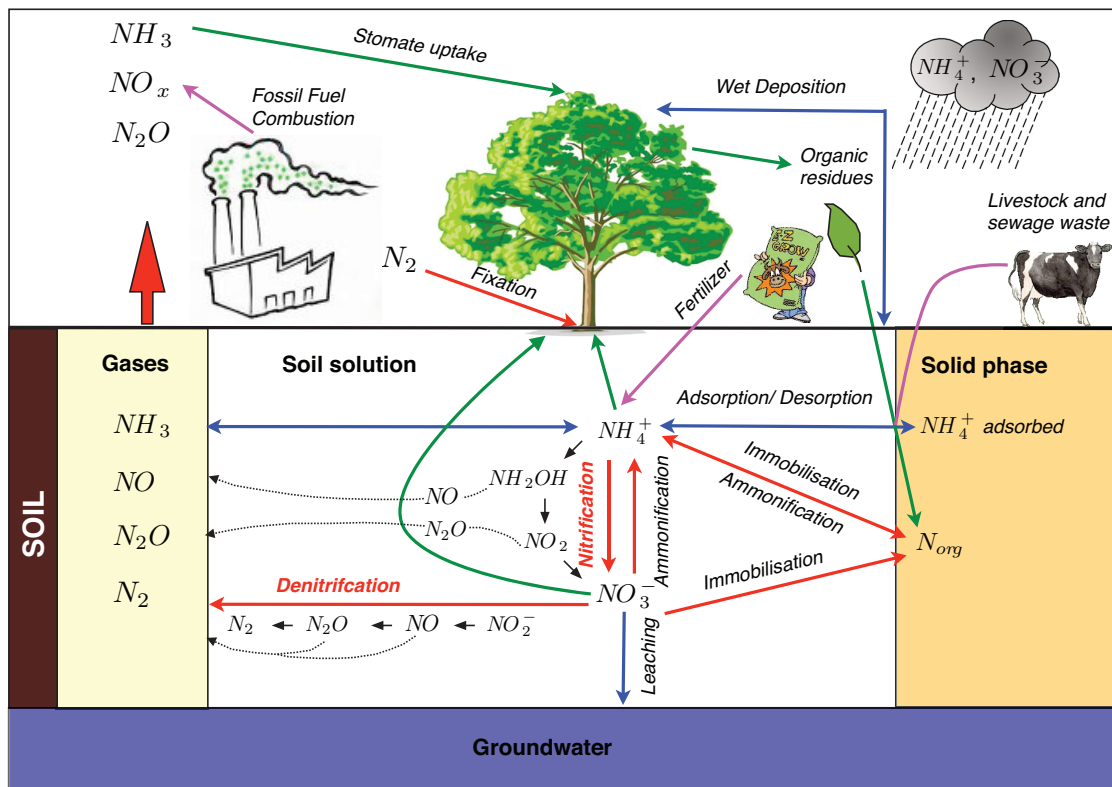


Figure 1.3: Schematic representation of the terrestrial nitrogen cycle. Processes represented by red arrows are catalyzed by soil microbial organisms and depend on temperature and soil water saturation. Blue arrows depict inorganic processes, while purple arrows represent human-related fluxes. Green arrows illustrate fluxes connected to plants.

Aside from the indirect control on atmospheric CO₂ concentrations, the nitrogen cycle itself also emits trace gases that either directly or indirectly act as greenhouse gases. Nitrous oxide (N₂O) and nitric oxides (NO_x) are gaseous intermediate products of microbial nitrification and denitrification in soils [Knowles, 1982, Vinther, 1984, Skiba et al., 1993, Kaiser et al., 1996, Maag and Vinther, 1996, Parton et al., 2001]. These nitrogen trace gases have important implications for atmospheric chemistry, air quality and climate. Although the atmospheric importance of both trace gases is generally understood, it is largely unknown how climate change effects the magnitude and timing of terrestrial emissions. Nitrogen oxides indirectly affect the global greenhouse budget by influencing the atmospheric abundance of hydroxyl radicals and the production of tropospheric ozone, the formation of SOA from biogenic precursors, as well as atmospheric breakdown of CH₄ [Kroll et al., 2005, Denman et al., 2007]. N₂O directly acts as greenhouse gas when released into the atmosphere and has a greenhouse warming potential of 289 times on a 100-year time period compared to CO₂, and an atmospheric lifetime of approx. 120 years. This makes N₂O one of the most important greenhouse gases after CO₂ and CH₄. Currently, it has a radiative forcing of approx. 0.16 W m⁻², which is 33% that of CH₄ and 9.6% that of CO₂ [Donner and Ramanathan, 1980, Forster et al., 2007, Solomon et al., 2007].

Chapter 1. Introduction

Nitrogen is an essential macronutrient for all organisms and is characterized by a complex environmental cycle involving different oxidation states and chemical species (Fig. 1.3). It exists in form of inorganic ions (NH_4^+ , NO_3^-), bound in organic molecules (N_{org}), or in gaseous form (N_2 , NH_3 , NO_x , N_2O). Biological N_2 -fixation is the largest source of natural nitrogen input to terrestrial ecosystems and currently amounts to approx. 110 Tg N yr^{-1} [Galloway et al., 2004]. In comparison, anthropogenic production of reactive nitrogen from N_2 using the Haber-Bosch process was approx. 100 Tg N yr^{-1} in the early 1990s [Kramer, 1999].

Nitrogen in reactive form can be used by plants, which take up NH_4^+ , NO_3^- , and N_{org} when living in symbiosis with N-fixing bacteria, and sometimes directly small-chain organic molecules and proteins [Schimel and Bennett, 2004, Paungfoo-Lonhienne et al., 2008]. Nitrogen bound in organic matter can be released in soils due to microbial breakdown in form of NH_4^+ , which then can be transformed to NO_3^- via nitrification (Fig. 1.3). Under anoxic conditions, microorganisms can use NO_3^- as electron acceptor and reduce it to N_2 (denitrification). Nitrification and denitrification involve several intermediate steps and products, with N_2O and NO_x being gaseous intermediates in both processes. As microorganisms are not 100% efficient in trapping these intermediate products, part of them can be emitted by soils ([see leaky pipe model, Firestone and Davidson, 1989]). Although nitrification and denitrification are the processes directly responsible for N_2O and NO_x emissions, all other processes of the nitrogen cycle also influence the emission of these trace gases as long as they directly or indirectly control the availability of NO_3^- in the soil. A quantitative assessment of nitrogen trace gas emissions from the terrestrial biosphere, e.g., through biogeochemical models, therefore requires a detailed and precise representation of all processes in the nitrogen cycle.

Denitrification is an anaerobic process that becomes relevant in parts of the soil with an oxygen partial pressure of less than 5%. As a biotic process, it is catalyzed by microorganisms and therefore temperature-dependent. N_2O emissions from nitrification and denitrification in soils are known to react sensitively to soil water content, soil temperature, and available organic nitrogen in the soil, as well as physical and chemical properties of the soil such as texture and pH [Smith et al., 1998, Stevens et al., 1998, Del Grosso et al., 2000]. From a kinetic point of view, denitrification is assumed to be most efficient in soils with prevailing warm and moist conditions, e.g., in seasonally inundated soils of the tropics [Kroeze et al., 1999, Galloway et al., 2004, Werner et al., 2007]. According to estimates of the Intergovernmental Panel on Climate Change [2001], the mean estimate of $3.0 \text{ Tg N}_2\text{O-N yr}^{-1}$ emitted from tropical forest soils accounts for approx. 18% of all atmospheric N_2 sources. Nevertheless, soils from all climate zones have the potential to emit considerable amounts of N_2O as long as the conditions for denitrification are favorable, i.e., low oxygen content due to water-filled pore-space and temperatures high enough to allow microbial activity to occur. Recently, Repo et al. [2009] published findings for discontinuous permafrost zones in subarctic East European tundra, stating that emissions from peat soils in this type of environment can be equivalent to those from tropical and agricultural soils. Due to the limited number of measurements available and the high temporal and spatial variability of N_2O fluxes, the uncertainty about the magnitude of net emissions from single ecosystems is high [e.g., Groffman et al., 2006, Seitzinger et al., 2006].

1.1. N₂O emissions from terrestrial ecosystems during abrupt climatic warming

One reason for this high uncertainty is the effect of soil nitrogen contents on N₂O emissions, which is still not very well understood. Some studies report increasing emissions from soils with elevated nitrogen content [e.g., Kitzler et al., 2006, Forster et al., 2007, Crutzen et al., 2008], while other studies do not find a significant effect, indicating that the nitrogen saturation level of ecosystems might be important [Aber et al., 1989]. To assess nitrogen saturation of ecosystems it is important to have reliable estimates for nitrogen input into ecosystems, e.g., via atmospheric deposition [Denier van der Gon and Bleeker, 2005], but there is also considerable uncertainty about atmospheric nitrogen deposition effects on soil nitrogen trace gas emissions [Pilegaard et al., 2006].

Once released to the atmosphere, the main sink for N₂O is photochemical destruction in upper troposphere and lower stratosphere, the later accounting for about 98% of the total atmospheric N₂O sink [Sowers et al., 2003], approx. 10 Tg N yr⁻¹ [Crutzen and Ehhalt, 1977] to 12.3 Tg N yr⁻¹ [Houghton, 1995]. Nevertheless, recent studies from field observations indicate that soils may function as a sink for N₂O, and that this might be of higher magnitude as generally thought [Chapuis-Lardy et al., 2007, Neftel et al., 2007]. Chapuis-Lardy et al. [2007] report that scientists observing the sink behavior of soils in field studies generally tend not to mention or explain these observations, as soils have traditionally only been considered as source of N₂O. In the future, the possibility of soils acting as sinks needs more investigation, and global scale modeling will be an important way to clarify the importance of soils as global sinks of N₂O.

A number of studies over the past decade have attempted to quantify N₂O and NO_x emissions both for the present and the past based on measurement inventories of N₂O concentrations in ice cores [Flückiger et al., 1999, Sowers et al., 2003, Spahni et al., 2005, Wolff and Spahni, 2007] and atmospheric monitoring networks (e.g., NOAA Global Air Sampling Network, by the NOAA Climate Monitoring and Diagnostic Laboratory). The ice core record shows a high variability of atmospheric N₂O concentrations that are closely correlated to polar temperature records (Fig. 1.4). This indicates that nitrogen trace gas emissions may be extremely sensitive to climate change. At the same time, given the high greenhouse warming potential of N₂O, it is conceivable that increases in its atmospheric concentration could have led to amplification of climate change during periods of rapid warming.

Early studies simulating N₂O and NO_x emissions at regional and global scale [e.g., Potter et al., 1996, Potter and Klooster, 1998, Parton et al., 2001, Sorai et al., 2007] were based on process descriptions, in some cases combined with remote sensing information and vegetation models. In general, these models take into account the following aspects:

- plant functional type specific C:N ratios
- retention of a fraction of leaf nitrogen prior to abscission
- release or sequestration of mineral nitrogen from litter decomposition
- immobilization of mineral nitrogen by microorganisms

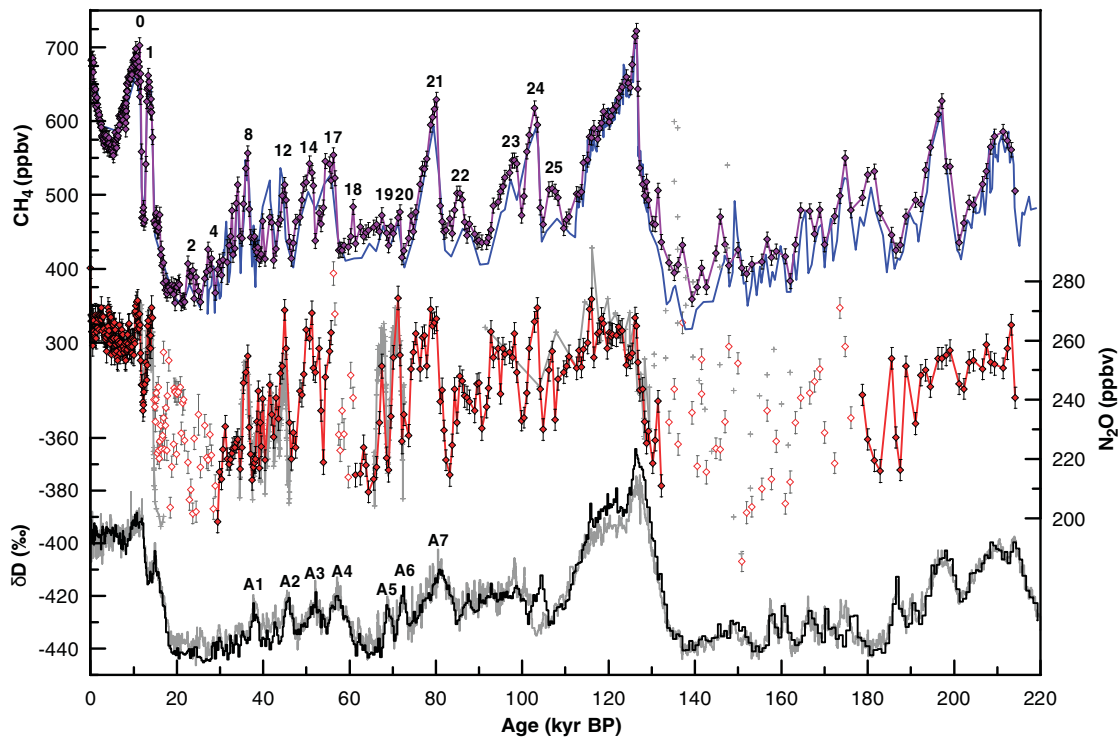


Figure 1.4: Dome C CH₄ (purple line), N₂O (red line), and δD (black line) records over the past 220 ky from Spahni et al. [2005]. Atmospheric N₂O concentrations vary considerably between glacials and interglacials, with concentrations generally being high during warm periods and lower during glacials. Concentrations change very rapidly from glacials into warm phases.

- plant uptake of mineral nitrogen
- adsorption/desorption of excess mineral nitrogen in form of NH₄⁺
- leaching of NO₃⁻ from soil to groundwater

In these biogeochemical models denitrification is either treated using a generic loss term depending on available mineral nitrogen [e.g., Friend et al., 1997, Thornton et al., 2002], or nitrification and denitrification are modeled as a function of nitrogen availability and soil moisture, as for example in Dickinson et al. [2002]. Most of these models have in common that gaseous losses are accounted for in a lumped manner without differentiating the emissions of N-gas species [Arneth et al., 2009]. More recent attempts have been made to develop fully coupled process-oriented nitrogen cycle models and integrate them into existing DGVMs, e.g., Sokolov et al. [2008], Xu-Ri and Prentice [2008], Thornton et al. [2009], Zaehle and Friend [2010a]. The process-based nitrogen cycle model included in ORCHIDEE-CN [O-CN, Zaehle and Friend, 2010a] allows to simulate gaseous losses differentiated by gas species, which is an important step towards a global quantification of terrestrial N₂O and NO_x emissions. O-CN dynamically simulates nitrogen concentrations in plants and soil, allowing carbon fluxes to respond to nitrogen status. It treats ecosystem nitrogen inputs from atmospheric deposition,

1.1. N₂O emissions from terrestrial ecosystems during abrupt climatic warming

biological nitrogen fixation, and fertilizer input, and mechanistically simulates nitrogen losses to leaching and emissions of trace gases from nitrification and denitrification [Zaehle and Friend, 2010a].

In the framework of my PhD thesis I was specifically interested in simulating N₂O emissions at the Gerzensee site in Switzerland at the time of the Oldest Dryas to Bølling transition. From the Greenland ice core record it is known that this rapid warming event was linked to a significant increase in atmospheric N₂O concentrations from approx. 210 ppbv to 260 ppbv in less than 200 years [Flückiger et al., 1999]. The Oldest Dryas is a climatic period that corresponds to Greenland stadial 2 [Björk et al., 1998], dating approx. between 18,000 and 14,650 calibrated years before present [cal. yr. BP, Magny et al., 2003]. The Bølling oscillation following the Oldest Dryas was a warm period (interstadial) dating between 14,650 and 14,000 cal. yr. BP [Magny et al., 2003]. Extensive research at Gerzensee highlights how abrupt climate change affects ecosystem behavior on a local to regional scale.

Extensive research at Gerzensee based on high-resolution multiproxy reconstructions of local climate and vegetation from pollen, plant macrofossils, $\delta^{18}\text{O}$ of lake carbonates, chironomids and charcoal [e.g., Ammann, 2000, Ammann et al., 2000, Brooks, 2000, Hofmann, 2000, Lemdahl, 2000, Tobolsky and Ammann, 2000, Wick, 2000, Schwander et al., 2000, Lotter et al., 2000, 2012, van Raden et al., 2012, Lischke et al., 2012, Nováková et al., 2012, Ammann et al., 2012, Magny, 2012, Brooks and Heiri, 2012] highlights how abrupt climate change affects ecosystem behavior on a local to regional scale. The pollen records indicate that mostly grassy or herbaceous taxa were present during the glacial cold period and mostly forest after the transition. The very similar oxygen isotope records from Greenland ice cores and European lake sediments during the Glacial Termination [von Grafenstein et al., 2000] suggest that drastic climatic changes (a warming of 5 to 6 °C within approx. one century at Gerzensee, approx. 13 °C at Greenland) occurred quasi-simultaneously on an extra-regional, probably hemispheric scale [Schwander et al., 2000]. The material available from the Gerzensee site delivers excellent information to model N₂O emissions during the time of the rapid warming using the nitrogen cycling scheme from O-CN in combination with environmental data reconstructed for the Gerzensee site (Fig. 1.5) and answer questions such as:

- How much did the total N₂O emissions change at this specific site throughout the transition?
- Which factors are most influential for simulated changes in emissions?
- Could the abundant presence of the nitrogen-fixing species *Hippophaë rhamnoides* (L.) have caused nitrogen enrichment in soils and amplified N₂O emissions?

Simulation of N₂O emission from the Gerzensee site over the time of the rapid warming from Oldest Dryas to Bølling clearly indicates that increasing annual mean temperature and precipitation lead to more than a tripling of emissions. Additional nitrogen input through

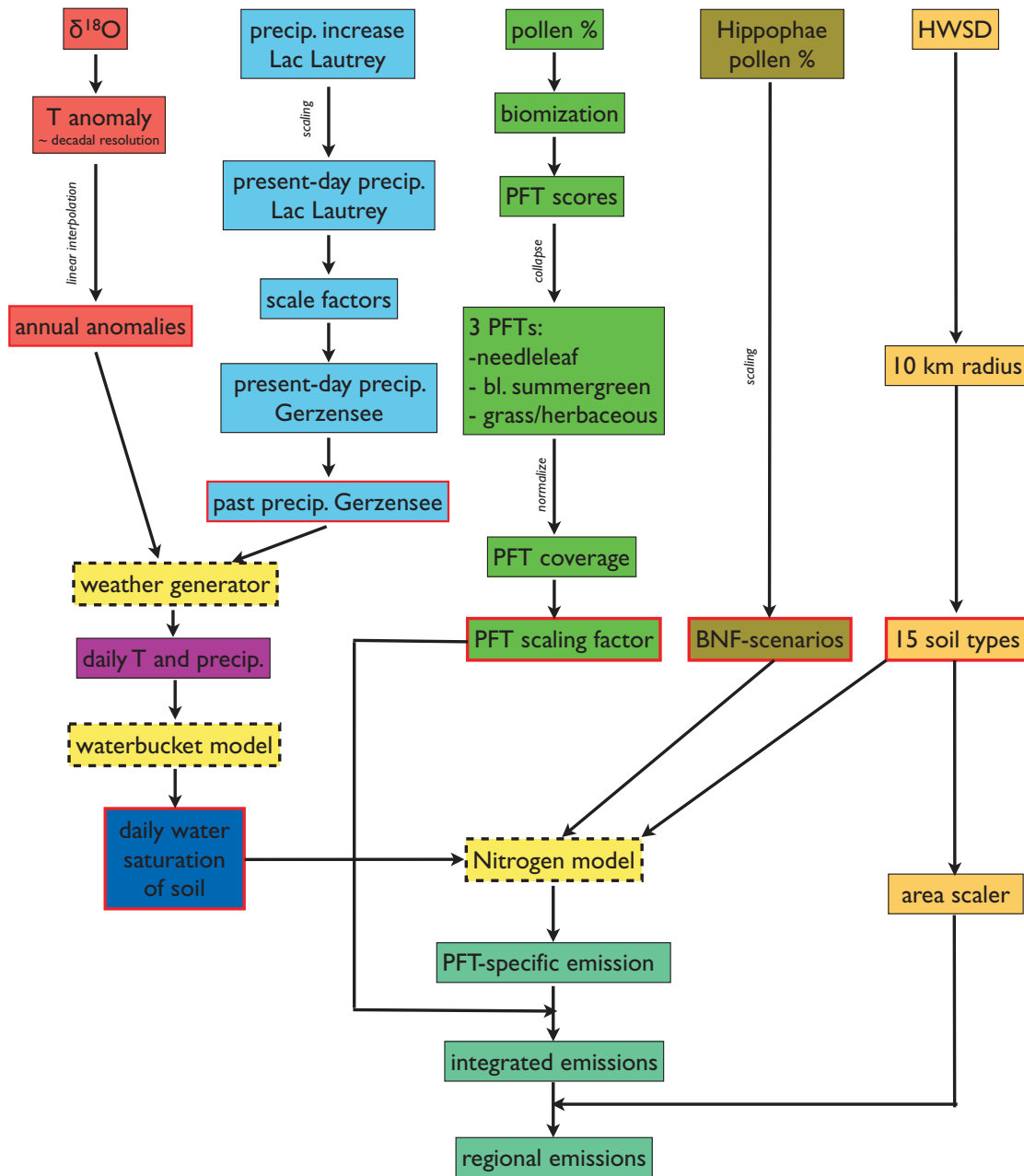


Figure 1.5: Flowchart illustrating the simulation of terrestrial N₂O emissions at Gerzensee during the transition from Oldest Dryas to Bølling using the O-CN nitrogen module and data to drive the module derived from high-resolution multiproxy data.

nitrogen fixation leads to further emission increases. The results therefore clearly suggest that local reactions of emissions to abrupt climate change could have been considerably faster than the overall atmospheric concentration changes observed in polar ice. The positive reaction of emissions to additional nitrogen input via biological fixation indicates that symbiotic N-fixers as early successional pioneers not only facilitate the establishment of vegetation by enriching

soils with nitrogen, but also have the potential to influence biogeochemical cycles.

1.2 Modeling preindustrial natural and anthropogenic biomass burning

In chapter 3 I present LMfire, a new fire module for DGVMs that allows to simulate occurrence of natural and anthropogenic wildfire. LMfire has been developed with specific focus on the simulation of anthropogenic burning during preindustrial and prehistoric time, and therefore includes a novel representation of human burning based on differing human-fire relationships according to subsistence strategy.

Wildfire modeling is challenging as factors related to vegetation type and structure, fire weather, topography and feedbacks between fire and vegetation need to be taken into account. Depending on research interest and scale of interest, wildfire spread can be modeled based on fine-scale mechanistic equations aiming for accurate, high-resolution fire behavior prediction, or broad-scale probabilistic equations. The purpose of numerical wildfire modeling is to reproduce fire behavior, e.g., rate of fire spread, fire line intensity and fuel combustion, and to estimate fire effects such as tree mortality. The results from wildfire modeling can be used to predict fire behavior from prevailing environmental conditions, e.g., to improve fire management decision-making before and during fires in order to reduce risk for public and firefighters, and to minimize damage to human assets. Conceptual fire models are based on semi-empirical equations derived from experiments in combustion chambers or wind tunnels where fuel arrays of defined particle size and fuel bulk density are burned under controlled conditions. These equations allow to estimate parameters such as rate of fire spread, fireline intensity, and flame height for given fuel complexes [Rothermel, 1972, Noble et al., 1980, Forestry Canada Fire Danger Group, 1992, Cheney et al., 1993].

Two-dimensional models using such semi-empirical relationships for high-resolution fire prediction are, e.g., the deterministic fire growth simulation models Prometheus [Tymstra et al., 2009] and FARSITE [Finney, 1998]. Prometheus simulates fire growth based on spatial input data (slope, aspect, elevation), fuel types, and weather by applying Huygens' principle of wave propagation to the rate of spread predictions from the Canadian Forest Fire Behavior Prediction System of the Canadian Forest Fire Danger Rating System [Tymstra et al., 2009]. Given heterogeneous fuel, topography and weather condition, Prometheus simulates spatially explicit fire behavior and spread. FARSITE is based on the same principle and incorporates schemes for surface fire, crown-fire, point-source fire acceleration, spotting and fuel moisture [Finney, 1998]. Similar to Prometheus, FARSITE requires spatial fuel and terrain data and information on weather and fuel moisture change with time. This type of fire models specifically has been developed to improve forecasting of wildland fire growth and support operational decisions, to help planning of prescribed burns, to supplement fire behavior training and education programs, or to study the role of fire in establishing and maintaining landscape patterns. They help to assess the effectiveness of alternative fuel management strategies, pro-

Chapter 1. Introduction

vide spatial and temporal estimates of smoke emissions, allow to study the impact of climate change scenarios on area burned, or can provide forensic support for wildfire investigations [Tymstra et al., 2009].

Instead of relying on prescribed rules based on empirical data, physics-based process models representing wildfire behavior allow the coupling of a set of very complex processes. They are often coupled with the atmosphere and apply principles from computational fluid dynamics to allow fire to feed back upon the atmosphere. FIRETEC [Linn et al., 2002] is an example for such a coupled atmosphere/wildfire behavior model. It is based on conservation of mass, momentum, and energy and includes a transport formulation to couple its physics-based wildfire model with the dynamics of the local atmosphere. A similar approach is used in NCAR's Coupled Atmosphere-Wildland Fire Environment Model [CAWFE, Coen, 2004, Clark et al., 2004], which consists of a numerical weather prediction model and a fire behavior model. The two sub-models are two-way coupled and constantly exchange information regarding heat and water vapor fluxes from fire to atmosphere, which will alter the state of the atmosphere and feed back on the fire in form of fire winds and changes in atmospheric humidity. This ultimately determines how fast and in what direction the fire will propagate. Other examples for coupled atmosphere-wildfire models are WRF-fire [Mandel et al., 2009], or the Fire Dynamics Simulator (FDS), a computational fluid dynamics model of fire-driven fluid flow developed by the National Institute of Standards and Technology of the United States Department of Commerce, in cooperation with the VTT Technical Research Centre of Finland [Mell et al., 2007].

Such complex physical models are usually applied to simulate single fires. The most physically complex models of this type with a full three-dimensional explicit treatment of combustion in wildland fuels by direct numerical simulation are so computationally demanding that they cannot be solved fast enough to be used as forecasting tools. This is partially due to the required fine atmospheric model resolution needed for the coupling between fire model and atmosphere, as the simulated fires are usually too small-scale to interact with a weather model [Coen, 2004]. Typical physical phenomena studied with such models are, e.g., the effects of transient wind conditions, the effects of non-homogeneous terrain, the effects of patchy fuel distributions, and the effects of different vertical structure on fire behavior, or interactions between inhomogeneities in vegetation, topography, and atmospheric conditions [Linn et al., 2002]. Re-simulation of real fires is used to evaluate the performance of such models and to identify potential weaknesses.

While more complex models such as FIRETEC are ideal to simulate postulated fires in critical areas for risk assessment, and to learn more about the physical processes that trigger wildfire behavior, they are too complex to be applied on larger spatial and temporal scales, e.g., to study changes in fire regimes on continental to global scale over several centuries or millennia. They are therefore not suitable to directly be included into DGVMs, although fire modules in DGVMs may share the physical process representation in a simpler form that allows the simulation of wildfires in a more generalized way on larger spatial and longer temporal scales.

1.2. Modeling preindustrial natural and anthropogenic biomass burning

For the scales relevant to DGVM applications, focus therefore needs to shift from modeling fire behavior and danger at small scales to system-specific impacts of fire at large scale [Lenihan et al., 1998].

The most simple type of fire modules incorporated into DGVMs include those used in TRIFFID [Cox, 2001], the Sheffield-DGVM [Woodward and Lomas, 2004], IBIS [Kucharik et al., 2000] or ED [Moorcroft et al., 2001]. TRIFFID represents all forms of natural disturbance, including disease, fire and herbivory, with a prescribed disturbance rate which is uniform for a given PFT and independent of climate or local land use practices [Betts et al., 2004]. This practically excludes TRIFFID from any studies focusing on changing fire regimes as a reaction to climate change. The Sheffield-DGVM simulates fire mechanistically in form of burned fraction depending on the dryness of the climate and vegetation in the gridcell. The applied relationships between moisture content of plant litter (determined by climate) and fire return intervals ignores the role of ignitions, assuming that ignitions are never limiting to fire occurrence [Woodward et al., 2001]. The Integrated Biosphere Simulator (IBIS) models fire as a simple function of litter amount and its dryness, and its effect in form of a fractional loss of biomass [Kucharik et al., 2000, Quillet et al., 2010]. ED as described in [Moorcroft et al., 2001] models fire frequency within each grid cell as a function of fuel and climate, i.e., burn rates are a function of fuel availability and local moisture conditions. Rather than modeling ignitions explicitly, they are assumed to only depend on soil moisture, and burn rates are set proportional to total aboveground biomass. Another simplification is that burning consumes aboveground vegetation completely. As none of these simple empirical schemes takes into account potential interactions and feedbacks between vegetation and fire, they are not suitable to assess the changing role of fire linked to changes in climate or human impact.

In comparison with these simple representations, fire models of intermediate complexity can represent the major processes of vegetation-fire dynamics while still being computationally inexpensive compared to operational fire models such as FIRETEC or CAWFE. Intermediate complexity models such as Glob-FIRM [Thonicke et al., 2001], Reg-FIRM [Venevsky et al., 2002], and CTEM-FIRE [Arora and Boer, 2005] have been incorporated as modules into a number of DGVMs, including LPJ [Sitch et al., 2003], CLM3 [Levis et al., 2004], ORCHIDEE [Krinner et al., 2005], SEIB-DGVM [Sato et al., 2007] and CLM4-CND [Oleson et al., 2010].

Glob-FIRM estimates fire conditions based on soil moisture and determines area burned based on the length of the fire season. Empirical observations are the basis for the established relationship between daily litter moisture status and the length of the fire season, and the length of the fire season and annual area burned [Thonicke et al., 2001]. However, Glob-FIRM ignores the need for ignitions sources by assuming that an ignition source will always be available, omits anthropogenic influences on fire regimes, and neglects the influence of wind speed on fire spread and aspects such as incomplete combustion of plant material in areas that experienced fire. Fire mortality is set to a constant PFT-specific rate and does not depend on fire intensity or duration, and annual area burned only depends on the length of the fire season and minimal fuel load. Reg-FIRM prescribes vegetation mortality using parameters

Chapter 1. Introduction

and also uses upper soil moisture as a surrogate for litter moisture which is a crucial factor in determining fire spread [Pyne et al., 1996]. Intermediate complexity fire models are therefore compromises with respect to process representation, as not all processes are represented equally well and some are completely ignored. However, depending on the research focus, not all DGVM applications need complex fire representation.

The most complex representations of fire currently adapted for DGVMs incorporate many of the concepts and equations developed for operational fire forecasting [e.g., Burgan and Rothermel, 1984, Andrews, 1986, 2007, Burgan, 1987, Andrews and Chase, 1989, Reinhardt et al., 1997, Finney, 1998, Andrews et al., 2003, 2008, Heinsch and Andrews, 2010] into a large-scale framework. The first attempts in this direction were already made in the late 1990s, e.g., the MCFIRE scheme [Lenihan et al., 1998] as part of the MC-DGVM [Bachelet et al., 2003], which allows to explicitly simulate fire spread based on work of Cohen and Deeming [1985] and calculates dead fuel consumption as a function of the moisture content of different fuel size classes [Peterson and Ryan, 1986]. MCFIRE classifies fuel in four dead fuel and three live fuel classes and calculates dead fuel moisture based on a combination of the Canadian Fine Fuel Moisture Code [van Wagner, 1987] and the National Fire Danger Rating System [Bradshaw, 1983], while live fuel moisture is connected to plant water stress [Howard, 1978]. Surface fire rate of spread is modeled based on Rothermel [1972], and crown fire using the formulation of van Wagner [1993]. Vegetation mortality and fuel consumption depend on fireline intensity, rate of spread, and the residence time of flaming and smoldering combustion [Lenihan et al., 1998]. Tree mortality is the result of crown scorching and cambial kill. The occurrence of ignitions depends on a combination of a drought threshold based on the fuel moisture of the coarsest fuel size class and the probability of fire spread.

MCFIRE already included many of the concepts that were later incorporated into SPITFIRE [SPread and InTensity of FIRE, Thonicke et al., 2010], one of the most comprehensive fire modules used in DGVMs at present. SPITFIRE essentially was developed using elements of the intermediate complexity fire model Reg-FIRM and the operational fire forecasting BEHAVE model. In recent years, SPITFIRE was integrated into a number of different DGVMs, including LPJ [Thonicke et al., 2010], LPJ-GUESS [Smith et al., 2001], LPX [Prentice et al., 2011] and the Ecosystem Demography (ED) vegetation model [Moorcroft et al., 2001, Spessa and Fisher, 2010]. SPITFIRE represents a synthesis of preceding DGVM fire models with the purpose to overcome many of the limitations of those previous fire schemes, while still being applicable on a wide spatial and temporal scale ranging from regional to global and from annual to millennial. It simulates fire danger based on climatic conditions, i.e., temperature and precipitation occurrence, and fuel moisture status using a fire danger index (FDI), and explicitly represents ignitions and physical processes determining fire spread and intensity. SPITFIRE allows lightning-caused and anthropogenic ignitions, but ignores active and passive human fire suppression. It models fire spread as a two-step process and is run for daily time steps. Fuel quantity, fuel composition, and fuel moisture status determine if an ignition will be successful, and rate of fire spread in case of a successful ignition is simulated following Rothermel's equations [Rothermel, 1972, Wilson Jr., 1982, Pyne et al., 1996]. As in MCFIRE,

1.2. Modeling preindustrial natural and anthropogenic biomass burning

dead fuel is classified into four fuel size classes. Dead fuel moisture controls fire danger, rate of spread, and completeness of combustion. Post-fire mortality depends on structural properties of the vegetation, e.g., tree height and diameter, surface fire intensity and residence time of fire. Crown scorch [Johnson, 1992, Dickinson and Johnson, 2001] and cambial death [Rigolot, 2004, Stephens and Finney, 2002] are included as the two most important causes of fire-related vegetation mortality. Emission factors based on Andreae and Merlet [2001] are used to estimate trace gas emissions from fire.

Although being very comprehensive compared to other fire modules used in DGVMs, SPITFIRE still has some shortcomings that leave space for further improvement. While at least including a scheme to parameterize anthropogenic ignitions, the formulation of anthropogenic fire ignitions in SPITFIRE based on population density and a single spatially variable parameter, $a(N_d)$ seems overly simplistic and problematic for several reasons. First, regional values for $a(N_d)$ had to be obtained by means of "an inverse method, using data on numbers of human-caused fires and population densities for various regions" [Thonicke et al., 2010]. However, the estimate of regional-scale $a(N_d)$ values based on empirical observation data on number of burned patches or fire scars is uncertain for all countries where observed fires are not separated into human versus lightning-caused fires and fire-cause attribution is not available. Second, due to being based on present-day observational data, the $a(N_d)$ parameter is strictly only valid for contemporary applications of the fire model. It is highly unlikely that the relationship between population density and anthropogenic ignitions observed at present day has been constant through time and space, especially when acknowledging the important way in which human relationship with fire has changed since the Industrial Revolution. Fire suppression technology, the mechanization of agriculture, laws and regulations governing the use of fire and prosecution of arson, urbanization, and the emergence of outdoor recreation have changed greatly over the past 150 years, concurrent with exponential increases in human population. A number of recent publications [e.g., Pyne, 1994, Pyne et al., 1996, Pyne, 2000, Bowman et al., 2009, 2011] commented on the importance of fire for humans in prehistoric and preindustrial time and the way in which industrialization and urbanization fundamentally changed this relationship in recent centuries. As cultural contexts change over time, so does the relationship that people have with fire. At present, especially in societies with a Western cultural background, fire is mostly perceived as a threat to personal property, safety, air quality and environment and therefore banished and suppressed in most places, although awareness that too much fire suppression can also be counterproductive to the long term health of ecosystems has increased in recent decades [see, e.g., ?]. One fixed parameter such as $a(N_d)$ may capture spatial variation of people-fire-relationships at present, but estimating how this parameter may have changed with time is an probably not an appropriate way of simulating changes in fire over millennia.

In addition, the assumed relationship between number of anthropogenic ignitions and population density presented in SPITFIRE is likely only applicable for present-day observations, but must not necessarily apply to preindustrial conditions. It is likely that high population densities such as in present-day Europe lead to a decline in anthropogenic fire because of

direct and indirect suppression with the emphasis on avoiding damage to life and property. However, this will not hold true for preindustrial societies that used fire for, e.g., land clearing and agricultural means. It is also not necessarily true that very low population numbers will cause very little fire, as this will totally depend on the reasons why people cause fires. If all human ignitions were accidental, then such an assumption might be valid, as less people mean less risk for potential ignitions. However, if people purposely use fire to modify landscapes, e.g., as hunter-gatherer societies such as is seen in parts of Africa at present [e.g., Eva et al., 1998], or reported in Australia and the Americas for the past [e.g., Bowman, 1998, Williams, 2002] it may take only a few dedicated individuals to cause large amounts of fire.

Another shortcoming becomes obvious when comparing annual area burned as simulated by SPITFIRE [Thonicke et al., 2010] with datasets of observed burned area, e.g., GFEDv3 [Giglio et al., 2010] or the dataset presented by Randerson et al. [2012]. Especially in high-latitude regions, e.g., in boreal and subarctic North America, SPITFIRE tends to underestimate burned area size and interannual variability in burned area compared to observations, indicating that the fundamental behavior of the model and/or the datasets used to drive the model could be improved. Specifically in places where large fires are infrequent but important in terms of ecological impact, such as in boreal and subarctic regions, interannual variability in lightning strikes cannot be neglected as it has been in SPITFIRE [Thonicke et al., 2010]. The deterministic approach of using monthly frequency of total lightning flashes, which are interpolated between months to yield a quasi-daily lightning climatology, omits the important observation that lightning usually occurs clustered in time and is correlated to precipitation events and times of atmospheric instability. Using a fixed, deterministic ignition efficiency that directly links the fire starts on a given day to lightning amount neglects stochastic variations that are characteristic for lightning-caused ignitions. Both of the latter points are crucial prerequisites for simulating fire in areas that are naturally ignition-limited, but nonetheless display infrequent large fires. Additionally, fires in SPITFIRE are restricted to an active burning period of 241 minutes per day, and are automatically extinguished after one day. As wildfires typically burn until fire weather conditions become adverse and they are extinguished, or stop burning because they run out of fuel, this restriction is unrealistic and again leads to underestimates in total area burned specifically in places where ignitions are scarce.

In order to be able to simulate anthropogenic burning for times prior to the industrial period, my co-authors and I modified the SPITFIRE-version published in Thonicke et al. [2010] by developing a novel scheme for simulating anthropogenic burning. While implementing the updated fire scheme into the LPJ-version used in my research group, I also set out to improve the deficiencies of the original SPITFIRE highlighted above in close collaboration with my thesis supervisor. The new fire module presented in Chapter 3 of this thesis (simplified illustrational chart shown in Fig. 1.6) includes a novel approach to determine lightning ignitions in a way that accounts for temporal variability in lightning occurrence and the stochasticity of lightning ignitions. Differing from SPITFIRE, ignitions are allowed to carry over from one day to the next, and new criteria for fire extinction are presented. The changes made to the original SPITFIRE scheme to incorporate these updates required additional modifications to

1.2. Modeling preindustrial natural and anthropogenic biomass burning

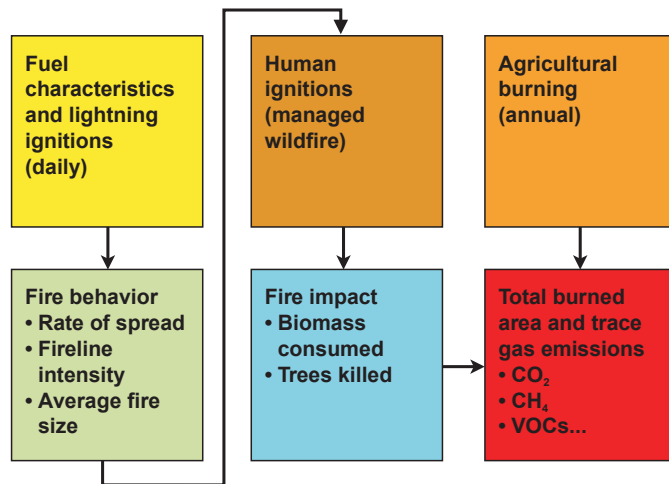


Figure 1.6: Simplified schematic of components included in LMfire.

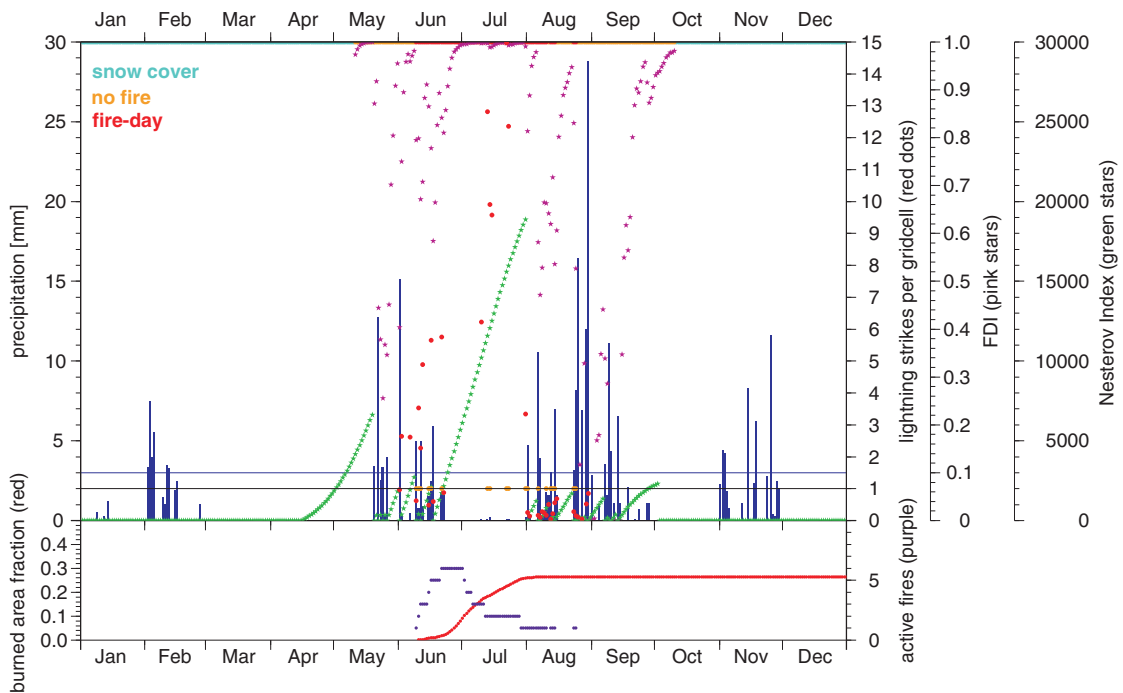


Figure 1.7: LMfire simulates fire occurrence on a daily basis based on fire weather conditions and occurrence of ignitions. The example illustrates the development of fire weather conditions (Nesterov Index, Fire Danger Index), the occurrence of snow cover, precipitation, lightning strikes, lightning ignitions (orange dots) and number of active fires over the course of a year for a grid pixel in Alaska. Fire season starts with the disappearance of the last snow in May and ends in October. The first fire is ignited in June and more fires are quickly added that keep burning through June until they start merging and burn out in August.

the LPJ-DGVM and the fire routine. In addition to the new representation of anthropogenic burning it includes explicit calculation of natural ignitions, the representation of multi-day

burning and coalescence of fires (Illustrational chart shown in Fig. 1.7), and the calculation of rates of spread in different vegetation types. Effects of landscape fragmentation on fire spread due to topographic complexity and agricultural land use are also taken into account. Compared to the original SPITFIRE scheme, the updated LMfire-scheme demonstrates a significant improvement in simulated burned area in remote areas of the boreal forest and subarctic.

Tests of the new fire model reveal that LMfire is able to simulate realistic fire regimes in Alaska, one of the key regions of the world where SPITFIRE results did not agree with observations. Improvements to a variety of aspects of the original formulation in SPITFIRE helps to more realistically represent fire occurrence, fire behavior, and fire impacts, particularly in boreal and subarctic ecosystems. A comparison of annual burned area simulated by LMfire to empirical observational data of burned area such as GFEDv3 [Giglio et al., 2010] highlights that at present almost all parts of the world are heavily influenced by human fire management, i.e., industrial fire suppression or anthropogenic biomass burning. Given that the main focus of the development of LMfire has been to create a fire module capable of simulating anthropogenic fire management prior to the industrial period, present-day active fire suppression using modern technology is not included in the new fire routine. Simulating global burning for the present day requires a different approach that takes this aspect into account. Due to the novel approach on modeling anthropogenic burning, the new LMfire-module is particularly suited to investigate climate-human-fire relationships on multi-millennial timescales prior to the Industrial Revolution. It provides a basis for further improvements, modifications and model development.

1.3 The role of hunter-gatherer burning in Europe during the Last Glacial Maximum

In Chapter 4 I present a study that investigates the potential effect of anthropogenic and natural burning on LGM vegetation on Europe using the fire module and implementation of anthropogenic burning presented in Chapter 3. The results of this simulation study highlight that already a moderate increase in burning frequency due to additional anthropogenic ignitions may have been sufficient to cause a significant decrease in simulated tree cover and produce the steppe-like conditions suggested by pollen-based vegetation reconstructions.

Human evolution took place in a naturally highly flammable environment. During the lower Pliocene, the African climate became increasingly dry [Brain, 1981, Vrba, 1988, 1995], which makes it likely that natural fires originating from lightning ignitions, volcanic activity or sparks from rock fall occurred more frequently. Originating from the savannas in Africa, the exposure to fire as a major environmental agent likely contributed to the eventual mastery of fire by hominids [Ségalen et al., 2007]. Archaeological evidence suggests that already *Homo erectus* was able to control fire as early as 1.6 million years ago and may have used it as a source for heat, light, and as protection against predators [Harris, 1978, Harris and Gowlett, 1980,

1.3. The role of hunter-gatherer burning in Europe during the Last Glacial Maximum

Bellomo, 1994). Based on fossil artefacts from *H. erectus* Wrangham et al. [1999] suggest that the use of fire for cooking may date back 1.9 million years. Direct evidence for the usage of fire based on burned bones in the Swartkrans cave dates back to 1.0-1.5 million years [Brain and A., 1988] and suggests that hominids prior the appearance of *H. sapiens* were able to control and use fire for their benefit. Archaeological evidence from Europe, e.g., Beeches Pit in East Anglia, documents the usage of fire by hominids with an age of approx. 400,000 years [Gowlett, 2006]. At Beeches Pit, evidence of fire is commonplace and occurs in form of burned flints and sharply delimited features that can be interpreted as hearths. Large tails of burned material suggest that fires were burned through prolonged periods, and maybe continuously [Gowlett, 2006]. Although preservation opportunities in Europe are poor for the time of the Middle Pleistocene due to glacial activity and erosional reworking of archaeological sites, it can be expected that sites such as Beeches Pit are not exceptional and that the mastery of fire may have been the key to a successful colonization of glacial Europe by hominids and early humans. At the transition from Middle to Upper Paleolithic, approx. 35,000-40,000 radiocarbon years ago, archaeological and fossil finds indicate that Neanderthals in Europe were confronted with modern humans. Also from this time dates the oldest documented evidence for human presence in the European Arctic [Pavlov et al., 2001, Gowlett, 2001]. Survival in this extremely cold and harsh environment would be difficult to imagine without the usage of fire and the capability for long-term planning and extended social networks [Pavlov et al., 2001, Gowlett, 2006, Roebroeks and Villa, 2011]. Roebroeks and Villa [2011] argue that the habitual and controlled use of fire in Europe dates back to the second half of the Middle Pleistocene, and conclude that both Neanderthals and modern humans used fire for a variety of different reasons including cooking, but also as a source for light and warmth and an important technological component for the production of new materials and tools. Given this early evidence for human use and control of fire, it is a reasonable assumption that at the time of the Last Glacial Maximum (LGM) in Europe approx. 21,000 years before present, fire must have been a constant companion of the humans who lived there at that time, and a valuable tool for surviving in a glacial environment.

From more modern hunter-gatherer societies it is well-known that fire is used liberally for a host of different purposes far beyond the purpose of cooking or a mere source of warmth and light [Lewis, 1985]. Hunter-gatherer societies, e.g., Native Americans or Australian Aborigines, purposely used fire as a tool for landscape management to change ecosystems for their use and survival. Differing from the image of the "noble savage" treading lightly on the land, ample evidence points to the conclusion that hunter-gatherers significantly altered the character of landscapes and abundance of wildlife species through their liberal usage of fire [Botkin, 1990, Pyne, 1994, 1997]. Highly mobile humans can significantly increase ignition density even when population numbers are small, especially when inhabiting landscapes where background fire activity is low [Wardle et al., 1997, Bowman et al., 2011]. Lewis [1973] lists at least 70 different reasons why North American hunter-gatherers burned landscapes, and other authors [e.g., Russell, 1983, Kay, 1994] have grouped reasons into different categories. In summary, reasons why hunter-gatherers may burn are for hunting, to clear ground for gathering and to

Chapter 1. Introduction

promote the growth of desired plants, to create fireproof areas and control fuel accumulation, to prevent large devastating fires in the late dry season, to manage pests, to clear areas to facilitate travel, to fell trees and clear riparian areas, and for warfare and signaling. Burning of large areas was used to provide fresh browse for prey animals, to guide prey animals into small unburned areas where they could be hunted more easily, to expose the hiding places of prey, or to drive game up against cliffs or into narrow chutes where they could be killed more easily [Lewis, 1985, Pyne, 1994, 1997, Yibarbuk et al., 2002, Bowman et al., 2004, Bowman and Prior, 2004]. Use of fire by foragers can be so extensive that forested landscapes are transformed into savannas or grassland, or persisting forest areas are opened up and freed from underbrush. In his 1982 book on fire in America, Stephen Pyne highlights that by the arrival of the first Europeans in the Americas almost all naturally drained land was burned nearly everywhere, and the sole areas of dense forest were located in areas of swamps and bogs. He explains the high degree of observed landscape openness as a result of repeated, controlled surface burns on cycles of one to three years that were occasionally interrupted by catastrophic fires and conflagrations when fires escaped and got out of control. Pyne [1997] also notes that the use of fire by native peoples to alter and manage their environment is almost universal and not only restricted to America.

The extensive evidence for use of fire as a tool for ecosystem management among hunter-gatherer societies suggests that for Paleolithic hunter-gatherers at the time of the LGM the habitual controlled use of fire could have been a valuable tool to customize their environment to their specific needs. The question that arises is: What impact could hunter-gatherer burning in Europe during the time of the LGM have had on vegetation? Vegetation reconstructions based on pollen records and plant macrofossils indicate that extensive parts of Europe were covered by steppe-like vegetation during maximum glaciation, with adjacent tundra in the ice-free northern parts of Europe [e.g., Prentice et al., 2000, Tarasov et al., 2000]. A low but persistent presence of fossil tree pollen in central and southern European records suggests that trees were not completely absent during the full glacial, although their abundance must have been drastically lower than during the Holocene [e.g., Follieri et al., 1988, Magri, 1989, Willis et al., 2000]. Whether the tree pollen found in LGM records are indicators of tree species that persisted in local refugia, or originate from long-range dispersal and reworking, is a matter of debate [e.g., Stewart and Lister, 2001, Birks and Willis, 2008, Normand et al., 2011].

Willis et al. [2000] found evidence in form of macroscopic charcoal for the presence of at least seven tree taxa in Hungary during the last full-glaciation, with types similar to those found on the southern edge of the present-day boreal forest. The additional presence of burned tree trunks and sediment layers forming a silhouette of trunk and root positions shows that trees were locally present, and that wildfires must have been an important ecological component in these ecosystems [Willis et al., 2000, Zackrisson et al., 1996]. In their 2004 review paper, Willis and van Andel present evidence based on macroscopic charcoal from 40 locations in seven central and eastern European countries that strongly points to the conclusion that at least 20 different tree taxa were continuously present during the last full-glacial interval. They compared the present-day climatic tolerances of the identified tree taxa with simulated LGM-

1.3. The role of hunter-gatherer burning in Europe during the Last Glacial Maximum

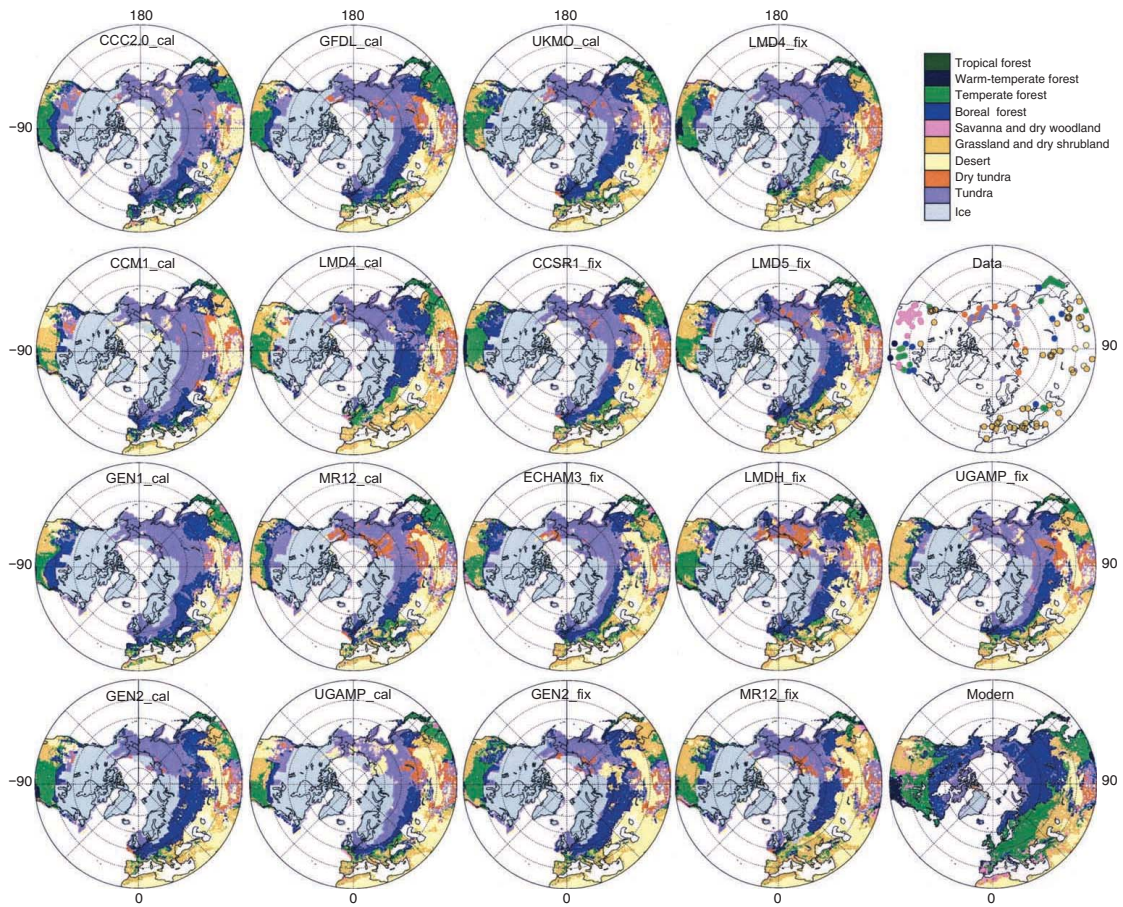


Figure 1.8: Simulated and observed biomes in the northern extratropics (north of 30°N) from Harrison and Prentice [2003] illustrating the discrepancy between modeled and reconstructed vegetation cover in Europe for the time of the LGM. Where most of the models classify vegetation cover as boreal or temperate forest for central Europe pollen-based biome reconstruction suggests grassland and dry shrubland.

climates from the Stage 3 project [Barron and Pollard, 2002, H., 2002, Barron et al., 2003, Pollard and Barron, 2003] and conclude that neither reduced temperatures and precipitation nor cold podzolic soils would suffice to exclude the identified boreal tree taxa from LGM central Europe. This is in agreement with model simulations showing evergreen taiga/montane forest as dominant vegetation type in glacial central Europe [e.g., Alfano et al., 2003, Kaplan et al., 2003].

In fact, there is a strong contradiction between Dynamic Global Vegetation Models or equilibrium biosphere models and proxy-based vegetation reconstructions, with models almost universally suggesting greater representation of trees than indicated by pollen-based biome reconstructions [see, e.g., Harrison and Prentice, 2003, Kaplan et al., 2003, Lathière et al., 2005, Strandberg et al., 2011, Woillez et al., 2011] than pollen-based vegetation cover reconstructions (Fig. 1.8). The latter come to the conclusion that steppe ecosystems were the dominant

Chapter 1. Introduction

vegetation type across northern Eurasia south of approx. 57 °N, with adjacent tundra in the north, a significantly reduced and discontinuous taiga belt, and cool mixed or temperate deciduous forests being absent from the central part of the East European Plain and the southern Ural [Tarasov et al., 2000, Prentice et al., 2000]. Where Mediterranean pollen sites indicate savanna-like ecosystems or steppe-type vegetation, pollen sites north of the Alps point to steppe-type vegetation with mixed-in tundra features where trees were largely absent [Elenka et al., 2000, and references therein].

In summary, evidence from macroscopic charcoal indicates that trees were present in glacial central Europe, and comparison to present-day climatic tolerances of boreal tree species leads to the conclusion that colder and drier climatic conditions during the full glacial would probably not suffice to exclude boreal tree taxa from central Europe during the LGM. The observed evidence for trees being present is further supported by models driven with LGM climate, which mostly simulate cold evergreen needleleaf forests for Europe. However, this contradicts the pollen-based reconstructions that are pointing to extensive steppe-type vegetation. If trees were present and climate could not exclude them from Europe, what kept them from being abundant enough to also reflect their presence more dominantly in the pollen records? Are the climate and vegetation models wrong, and climatic conditions in reality were too extreme to allow the presence of trees with the exception of some cryptic refugia with more favorable climate [Birks and Willis, 2008], or was there a factor other than climate involved that prevented Europe from being forested?

What many of the studies on full-glacial vegetation in Europe neglect is the presence of Paleolithic hunter-gatherers who were able to control and use fire to facilitate their survival under the prevailing harsh glacial conditions. Knowing how liberally more modern forager peoples used fire to manage their environment it can be assumed that Paleolithic hunter-gatherers may have used it in a similar way to shape and control their habitat. Anthropogenic fire disturbance therefore may be an explanation that could reconcile the discrepancy between the glacial vegetation cover simulated by vegetation models and the pollen-based reconstructions, which suggest that the models almost universally overestimate tree cover in Europe for the LGM. Ample evidence for the presence of trees in Europe during the LGM [e.g., Willis et al., 2000, Willis and van Andel, 2004] and the comparison of boreal trees' ecological tolerances with climatic conditions reconstructed for the LGM [Barron and Pollard, 2002, H., 2002, Barron et al., 2003, Pollard and Barron, 2003] suggests that climate and low CO₂ alone may not be sufficient to explain their low abundance. If vegetation models consistently overestimate tree cover compared to proxy-based reconstructions, there is obviously something missing in the models. If it is not the vegetation sensitivity to climate and low CO₂ that the models get wrong, or the reconstructed climate itself used to drive the models, or the proxy-based vegetation cover, then there must be an additional factor that the models are missing. With trees already being at the limit of their ability to grow due to climate, only comparably small amounts of additional disturbance may be required to significantly lower tree cover and open up the landscape. Based on the results presented in Chapter 4 I therefore suggest that the missing factor in the vegetation models may be disturbance triggered by Paleolithic hunter-gatherers

using fire to shape their environment.

1.4 Synthesis

Modeling interactions between vegetation and soils, climate, terrestrial nitrogen cycling, fire, and humans in the Earth system allows to address questions that cannot be answered based on environmental proxies alone. As environmental archives are spatially and temporally constrained, models are required as tools to integrate in space and time in order to obtain a more complete understanding of past environmental change. In addition, modeling environmental change in the past allows to evaluate the process understanding deduced from present observations with respect to the evidence preserved in paleoarchives. As no such archives are available for the future, testing models by applying them for scenarios of environmental change in the past is the only way to calibrate them for future predictions.

Combining high-resolution multiproxy data with a process-based nitrogen cycle model and applying it for a local-scale study on abrupt climate change at the end of the last glacial reveals that the reaction of terrestrial ecosystems with respect to nitrogen trace gases can be very sensitive. The results of the Gerzensee study suggest that terrestrial N₂O emissions could react very sensitively to changes in soil moisture and vegetation composition within very short time spans. By enriching soils with nitrogen and thereby providing additional substrate for nitrifying and denitrifying bacteria, early successional pioneer species such as *H. rhamnoides* have the potential to amplify climatically triggered increases of reactive nitrogen trace gases. Although *H. rhamnoides* is known to be a low pollen producer, a direct quantitative reconstruction of its spatial cover based on pollen percentages is not possible. Compared to the full range of measured emission observations from present day field campaigns, the N₂O emissions simulated for the Gerzensee site are conservative estimates. The main uncertainties in the simulated emissions are due to the exact soil conditions during the transition time being unknown, the precipitation reconstruction being tied to only two values prior and after the transition derived from pollen at Lac Lautrey, and the exact amount of nitrogen fixed by *H. rhamnoides* being unknown. As no proxy is available to reconstruct the soil conditions directly after the glacial retreat, and emissions react sensitive to soil water conditions, it is only possible to give a potential range spanned by a diverse number of different soil types. To constrain the amount of nitrogen fixed by *H. rhamnoides* more closely, pollen productivity estimates would be required for this species in order to estimate its spatial cover based on pollen percentages. For the future, uncertainties resulting from the crude precipitation reconstruction should be reduced as soon as more detailed precipitation reconstructions directly from the Gerzensee site, e.g., based on pollen or lake level reconstructions, become available. Due to the uncertainties, the Gerzensee study presented in this thesis should be understood as a scenario-based sensitivity study that is relevant for a small regional scale. However, the results are valuable in so far as they indicate the importance of the terrestrial land surface with respect to the emission of reactive nitrogen trace gases. Future simulations on a global scale should be performed in order to clarify the role of terrestrial soils as source

Chapter 1. Introduction

of N_2O during abrupt climate change. This ultimately should allow a global quantification of emissions originating from terrestrial sources vs. oceanic sources and contribute to an explanation of the observed N_2O concentration changes in polar ice.

LMfire, the new fire model developed for LPJ based on SPITFIRE, combines process-based fire modeling with an innovative scheme for modeling anthropogenic burning during preindustrial and prehistoric time based on differing subsistence strategies. As all currently existing fire models have been developed based on present day human-fire relationships, none of the existing models is suitable to simulate anthropogenic burning for the past. Relationships between observed area burned and human ignitions derived from observational data, e.g., satellite products, are only valid for the present day as they include unprecedented anthropogenic fire suppression supported by modern technological means. Such massive fire suppression is a novelty in human history and only valid for the industrial period. Historic documents and archaeological evidence points to a very different relationship between humans and fire for most of human history. Since the first hominids discovered how to control and use fire, it has been a valuable tool for humans to manage and shape their respective environment. As archeological evidence and historical observations are usually qualitative, modeling past human burning is only possible based on a number of assumptions required to transfer qualitative knowledge into quantitative information that can be represented by models. The inherently required generalizations and simplifications are a source of uncertainty and should be updated as soon as new insights and knowledge become available. In addition to the implementation of anthropogenic burning for the past, the new LMfire scheme that I present includes improvements to the calculation of daily lightning ignitions which take the stochastic nature of lightning into account. The introduction of stochasticity and inclusion of interannual variability in lightning ignitions significantly improves the performance of LMfire when it comes to modeling wildfires in areas where natural ignitions are scarce, but nevertheless sporadically cause large fires, e.g., in boreal and subarctic areas. By allowing fires to burn for multiple days and merge with other fires or previously burned areas, LMfire represents the behavior of wildfire in a more realistic way than SPITFIRE, which automatically extinguishes all ongoing fires after a maximum burn duration of 241 minutes. Although LMfire does not specifically account for active human fire suppression, it is able to represent the effect of passive fire suppression caused by landscape fragmentation due to anthropogenic land use and terrain complexity. The rate of fire spread calculations distinguish between different vegetation types, and new assumptions are made concerning the role of different fuel types for the rate of fire spread. Its newly developed features and process representation schemes make LMfire a valuable tool for all those who want to address questions related to natural and anthropogenic fire for times prior to the Industrial Revolution.

For example, LPJ-LMfire could be used to simulate the change of fire regimes over the course of the Holocene due to changes in climate and human lifestyles. The transition from hunter-gatherers to pastoralists and farmers was a profound change in lifestyle that completely changed the relationship between people, their environment, and likely the way they used fire to manage their environment. Based on a scenario of agricultural expansion over the

Holocene, LMfire could be used to model how this shift in anthropogenic lifestyle influenced global fire regimes and emissions from biomass burning. In combination with modeling land use changes and emissions of trace gases from deforestation, such simulations could be used to test the Early Anthropogenic Hypothesis of Ruddiman [2003, 2007] by assessing the combined release of greenhouse gases from anthropogenic farming and burning activities. Another interesting application could be to test which effect the collapse of the indigenous American populations following the conquest of the Americas had on fire regimes in North and South America.

As any other model, LPJ-LMfire leaves space for further improvements. Future updates should, e.g., include a scheme to represent permafrost and wetlands for a more realistic simulation of fires in peatland and tundra. To decrease LMfire's tendency to overestimate burning in tundra ecosystems, the implementation of new plant functional types specifically designed to represent tundra tussocks and shrubs should be addressed. As has already been done with respect to land use fragmentation, a similar scheme could be implemented to represent fragmentation due to water bodies. This aspect so far is missing in LMfire. Moreover, the discrepancy between calculations on a daily time step within LMfire as compared to monthly or annual time steps for the vegetation dynamics simulated by LPJ should ultimately be resolved by moving to daily time steps within LPJ. This way, carbon pools and litter production can be updated daily as well, which then provides direct daily input for LMfire.

The application of LPJ-LMfire to simulate vegetation cover and biomass burning in glacial Europe indicates that the role of Paleolithic hunter-gatherers in creating the steppe-type vegetation reconstructed from pollen records may have been important. As none of the vegetation models are able to simulate the highly open landscape indicated by pollen records solely based on glacial climate and low atmospheric CO₂ concentrations, it is likely that they are missing an additional influence factor on vegetation. The modeling experiment performed for the LGM indicates that by including additional disturbance due to human burning produces a vegetation cover that agrees far better with proxy-based vegetation reconstructions. As trees in Europe during the LGM already were at their bioclimatic limits, already moderate additional disturbance due to human burning is sufficient to significantly reduce simulated tree cover. For future studies it could be interesting to test if the results obtained for Europe are unique, or if other places in high latitudes would show a similar reaction. A global simulation for the LGM including hunter-gatherers could reveal interesting new insights concerning the question which parts of the world were most susceptible to human presence, and how much Paleolithic humans could have modified their environment opposed to conditions that would have prevailed naturally.

Bibliography

- J. D. Aber, K. J. Nadelhoffer, P. Steudler, and J. M. Melillo. Nitrogen saturation in Northern forest ecosystems. *BioScience*, 39(6):378–386, 1989.
- M. J. Alfano, E. J. Barron, D. Pollard, B. Huntley, and J. R. M. Allen. Comparison of climate model results with European vegetation and permafrost during Oxygen Isotope Stage 3. *Quaternary Research*, 59:97–107, 2003.
- B. Ammann. Biotic responses to rapid climatic changes: Introduction to a multidisciplinary study of the Younger Dryas and minor oscillations on an altitudinal transect in the Swiss Alps. *Palaeogeography, Palaeoclimatology, Palaeoecology*, 159:191–201, 2000.
- B. Ammann, H. J. B. Birks, S. J. Brooks, U. Eicher, U. von Grafenstein, W. Hofmann, G. Lemdahl, J. Schwander, K. Tobolsky, and L. Wick. Quantification of biotic responses to rapid climatic changes around the Younger Dryas. *Palaeogeography, Palaeoclimatology, Palaeoecology*, 159:313–347, 2000.
- B. Ammann, J. F. N. van Leeuwen, van der Knaap. W. O., H. Lischke, O. Heiri, and W. Tinner. Vegetation responses to rapid warming and to minor climatic fluctuations during the Late-Glacial Interstadial (GI-1) at Gerzensee (Switzerland). *Paleogeography, Palaeoclimatology, Palaeoecology*, in press:20 p., PALAEO–06206, 2012. doi: 10.1016/j.palaeo.2012.07.010.
- M. O. Andreae and P. Merlet. Emission of trace gases and aerosols from biomass burning. *Global Biogeochemical Cycles*, 15(4):955–966, 2001.
- P. L. Andrews. BEHAVE: Fire Behavior Prediction and Fuel Modeling System - Burn Subsystem, Part 1. General Technical Report INT-194, United States Department of Agriculture, Forest Service, Intermountain Research Station, Ogden, UT 84401, January 1986.
- P. L. Andrews. BehavePlus Fire Modeling System: Past, Present, and Future. Bar Harbor, ME, 23-25 October 2007. American Meteorological Society.
- P. L. Andrews and C. H. Chase. BEHAVE: fire behavior prediction and fuel modeling system - BURN subsystem, Part 2. General Technical Report INT-260, United States Department of Agriculture, Forest Service, Intermountain Research Station, Ogden, UT 84401, 1989.

Bibliography

- P. L. Andrews, C. D. Bevens, and R. C. Seli. BehavePlus Fire Modeling System, version 2.0: Users Guide. General technical report, United States Department of Agriculture, Forest Service, Rocky Mountain Research Station, Ogden, UT, 2003.
- P. L. Andrews, C. D. Bevens, and R. C. Seli. BehavePlus Fire Modeling System, version 4.0, User's Guide. General Technical Report RMRS-GTR-106WWW Revised, United States Department of Agriculture, Forest Service, Rocky Mountain Research Station, Ogden, UT, July 2008.
- A. Arneth, S. Sitch, A. Bondeau, K. Butterbach-Bahl, P. Foster, N. Gedney, N. de Noblet-Ducoudré, I. C. Prentice, M. Sanderson, K. Thonicke, R. Wania, and S. Zaehle. From biota to chemistry and climate: towards a comprehensive description of trace gas exchange between the biosphere and atmosphere. *Biogeosciences Discussions*, 6:7717–7788, 2009.
- V. K. Arora and G. J. Boer. Fire as an interactive component of dynamic vegetation models. *Journal of Geophysical Research*, 110:G02008, 2005. doi: 10.1029/2005JG000042.
- D. Bachelet, R. P. Neilson, T. Hickler, R. J. Drapek, J. M. Lenihan, M. T. Sykes, B. Smith, S. Sitch, and K. Thonicke. Simulating past and future dynamics of natural ecosystems in the United States. *Global Biogeochemical Cycles*, 17(2):1045, 2003. doi: 10.1029/2001GB001508.
- P. N. Ball, M. D. MacKenzie, T. H. DeLuca, and W. E. Holben. Wildfire and charcoal enhance nitrification and ammonium-oxidizing bacterial abundance in dry montane forest soils. *Journal of Environmental Quality*, 39:1243–1253, 2010.
- E. J. Barron and D. Pollard. High-resolution climate simulations of Oxygen Isotope Stage 3 in Europe. *Quaternary Research*, 58:296–309, 2002.
- E. J. Barron, T. H. van Andel, and D. Pollard. *Neanderthals and Modern Humans in the European Landscape during the Last Glaciation*, chapter Glacial environments II. Reconstructing the climate of Europe in the Last Glaciation, pages 57–78. McDonald Institute for Archaeological Research, Cambridge, 2003.
- R. M. Bateman, P. R. Crane, W. A. DiMichele, P. R. Kenrick, N. P. Rowe, T. Speck, and W. E. Stein. Early Evolution of Land Plants: Phylogeny, Physiology, and Ecology of the Primary Terrestrial Radiation. *Annual Review of Ecology, Evolution, and Systematics*, 29:263–292, 1998.
- D. J. Beerling, F. I. Woodward, M. R. Lomas, Wills. M. A., W. P. Quick, and P. J. Valdes. The influence of Carboniferous palaeoatmospheres on plant function: an experimental and modelling assessment. *Philosophical Transactions of the Royal Society B*, 353:131–140, 1998.
- A. Bekker and H. D. Holland. Oxygen overshoot and recovery during the early Paleoproterozoic. *Earth and Planetary Science Letters*, 317-318:295–304, 2012. doi: 10.1016/j.epsl.2011.12.012.
- R. V. Bellomo. Methods of determining early hominid behavioral activities associated with the controlled used of fire at FxJj 20 Main, Koobi Fora, Kenya. *Journal of Human Evolution*, 27: 173–195, 1994.

- L. M. Berglund, T. H. DeLuca, and O. Zackrisson. Activated carbon amends soil alters nitrification rates in Scots pine forests. *Soil Biology and Biochemistry*, 36:2067–2073, 2004.
- R. A. Berner. The Rise of Plants and Their Effect on Weathering and Atmospheric CO₂. *Science*, 25, 5312:544–546, 1997. doi: 10.1126/science.276.5312.544.
- R. A. Berner, D. J. Beerling, R. Dudley, J. M. Robinson, and R. A. Wildman, Jr. Phanerozoic Atmospheric Oxygen. *Annual Review of Earth and Planetary Sciences*, 31:105–134, 2003. doi: 10.1146/annurev.earth.31.100901.141329.
- Robert A. Berner. GEOCARBSULF: A combined model for Phanerozoic atmospheric O₂ and CO₂. *Geochimica et Cosmochimica Acta*, 70(23):5653 – 5664, 2006. ISSN 0016-7037. doi: 10.1016/j.gca.2005.11.032. URL <http://www.sciencedirect.com/science/article/pii/S0016703706002031>. <ce:title>A Special Issue Dedicated to Robert A. Berner</ce:title>.
- R. A. Betts, P. M. Cox, M. Collins, P. P. Harris, C. Huntingford, and C. D. Jones. The role of ecosystem-atmosphere interactions in simulated Amazonian precipitation decrease and forest dieback under global climate warming. *Theoretical and Applied Climatology*, 78: 157–175, 2004. doi: 10.1007/s00704-004-0050-y.
- H. J. B. Birks and K. J. Willis. Alpines, trees, and refugia in Europe. *Plant Ecology and Diversity*, 1(2):147–160, 2008.
- S. Björk, M. J. C. Walker, L. C. Cwynar, S. Johnsen, K. L. Knudsen, J. L. Lowe, and B. Wohlfahrt. An event stratigraphy for the last termination in the North Atlantic region based on the Greenland ice core record: a proposal by the INTIMATE group. *Journal of Quaternary Science*, 13:283–292, 1998.
- W. J. Bond and J. E. Keeley. Fire as a global 'herbivore': the ecology and evolution of flammable ecosystems. *Trends in Ecology and Evolution*, 20(7):387–394, 2005.
- D. B. Botkin. *Discordant Harmonies: A New Ecology for the Twenty-First Century*. Oxford University Press, New York, 1990.
- D. M. J. S. Bowman. Tansley Review No. 101 - The impact of Aboriginal landscape burning on the Australian biota. *New Phytologist*, 140:385–410, 1998.
- D. M. J. S. Bowman and L. D. Prior. Impact of Aboriginal landscape burning on woody vegetation in *Eucalyptus tetrodonta* savanna in Arnhem Land, northern Australia. *Journal of Biogeography*, 31:807–817, 2004.
- D. M. J. S. Bowman, A. Walsh, and L. D. Prior. Landscape analysis of Aboriginal fire management in Central Arnhem Land, north Australia. *Journal of Biogeography*, 31:207–223, 2004.
- D. M. J. S. Bowman, J. K. Balch, P. Artaxo, W. J. Bond, J. M. Carlson, M. A. Cochrane, C. M. D'Antonio, R. S. DeFries, J. C. Doyle, S. P. Harrison, F. H. Johnston, J. E. Keeley, M. A. Krawchuck, C. A. Kull, J. B. Marston, M. A. Moritz, I. C. Prentice, C. I. Roos, A. C. Scott,

Bibliography

- T. W. Swetnam, G. R. van der Werf, and S. J. Pyne. Fire in the Earth System. *Science*, 324: 481–485, 2009.
- D. M. J. S. Bowman, J. Balch, P. Artaxo, W. J. Bond, M. A. Cochrane, C. M. D'Antonio, R. DeFries, F. H. Johnston, J. E. Keeley, M. A. Krawchuck, C. A. Kull, M. Mack, M. A. Moritz, S. J. Pyne, C. I. Roos, A. C. Scott, N. S. Sodhi, and T. W. Swetnam. The human dimension of fire regimes on Earth. *Journal of Biogeography*, 38(12):2223–2236, 2011. doi: 10.1111/j.1365-2699.2011.02595.x.
- A. D. Bradshaw. The reconstruction of ecosystems. *Journal of Applied Ecology*, 20:1–17, 1983.
- C. K. Brain. The evolution of man in Africa: Was it a consequence of Cainozoic cooling? *Annals of the Geological Society of South Africa*, 84:1–19, 1981.
- C. K. Brain and Sillen A. Evidence from the Svarkrans cave for the earliest use of fire. *Nature*, 336:464–466, 1988.
- S. J. Brooks. Late-glacial fossil midge stratigraphies (Insecta: Diptera: Chironomidae) from the Swiss Alps. *Palaeogeography, Palaeoclimatology, Palaeoecology*, 159:261–279, 2000.
- S. J. Brooks and O. Heiri. Response of chironomid assemblages to environmental change during the early Late-glacial at Gerzensee, Switzerland. *Palaeogeography, Palaeoclimatology, Palaeoecology*, in press:9 p., PALAEO-06302, 2012. doi: 10.1016/j.palaeo.2012.10.022.
- R. E. Burgan. Concepts and Interpreted Examples In Advanced Fuel Modeling. General Technical Report INT-283, United States Department of Agriculture, Forest Service, Intermountain Research Station, Ogden, UT 84401, November 1987.
- R. E. Burgan and R. C. Rothermel. BEHAVE: Fire Behavior Prediction and Fuel Modeling System - Fuel Subsystem. General Technical Report INT-167, National Wildfire Coordinating Group, United States Department of Agriculture, United States Department of the Interior, Intermountain Forest and Range Experiment Station, Ogden, UT 84401, May 1984.
- T. G. Caldwell, D. W. Johnson, W. W. Miller, and R. G. Qualls. Forest Floor Carbon and Nitrogen Losses Due to Prescription Fire. *Soil Science Society of America Journal*, 66(1):262–267, 2002. doi: 10.2136/sssaj2002.2620.
- L. Chapuis-Lardy, N. Wrage, A. Metay, J.-L. Chotte, and M. Bernoux. Soils, a sink for N₂O? A review. *Global Change Biology*, 13:1–17, 2007.
- N. P. Cheney, J. S. Gould, and W. R. Catchpole. The Influence of Fuel, Weather and Fire Shape Variables on Fire-Spread in Grasslands. *International Journal of Wildland Fire*, 3(1):31–44, 1993.
- N. L. Christensen. Fire and the Nitrogen Cycle in California Chapparral. *Science*, 181(4094): 66–68, 1973.

- T. L. Clark, J. Coen, and D. Latham. Description of a coupled atmosphere-fire model. *International Journal of Wildland Fire*, 13:49–64, 2004.
- T. J. Clough and L. M. Condon. Biochar and the Nitrogen Cycle: Introduction. *Journal of Environmental Quality*, 39(4):1218–1223, 2010.
- J. L. Coen. Simulation of the Big Elk Fire using coupled atmosphere-fire modeling. *International Journal of Wildland Fire*, 14(1):49–59, 2004.
- J. D. Cohen and J. E. Deeming. The National Fire Danger Rating System: basic equations. General Technical Report PSW-GTR-82,23, Pacific Southwest Forest and Range Experiment Station, Berkeley, 1985.
- P. M. Cox. Description of the TRIFFID Dynamic Global Vegetation Model. Technical Report Tech. Note 24, Hadley Center, Bracknell, UK, 2001.
- P. M. Cox, R. A. Betts, C. D. Jones, S. A. Spall, and I. J. Totterdell. Acceleration of global warming due to carbon-cycle feedbacks in a coupled climate model. *Nature*, 408:184–188, 2000.
- W. L. Cressler. Evidence of Earliest Known Wildfires. *Palaeos*, 16(2):171–174, 2001.
- P. J. Crutzen and D. H. Ehhalt. Effects of Nitrogen Fertilizers and Combustion on the Stratospheric Ozone Layer. *Ambio*, 6(2/3):112–117, 1977.
- P. J. Crutzen, A. R. Mosier, K. A. Smith, and W. Winiwarter. N₂O release from agro-biofuel production negates global warming reduction by replacing fossil fuels. *Atmos. Chem. Phys.*, 8:389–395, 2008.
- S. J. Del Grosso, W. J. Parton, A. R. Mosier, D. S. Ojima, A. E. Kulmala, and S. Phongpan. General model for N₂O and N₂ gas emissions from soils due to denitrification. *Global Biogeochemical Cycles*, 14(4):1045–1060, 2000.
- T. H. DeLuca and A. Sala. Frequent fire alters nitrogen transformations in Ponderosa pine stands of the inland northwest. *Ecology*, 87:2511–2522, 2006.
- H. Denier van der Gon and A. Bleeker. Indirect N₂O emission due to atmospheric N deposition for the Netherlands. *Atmospheric Environment*, 39(5827-5838), 2005.
- K. L. Denman, G. Brasseur, G. Chidthaisong, P. Ciais, P. M. Cox, R. E. Dickinson, D. Hauglustaine, C. Heinze, E. Holland, D. Jacob, U. Lohmann, S. Ramachandran, P. Leita da Silva Dias, S. C. Wotsy, and X. Zhang. *Climate Change 2007: The Physical Science Basis. Contribution of Working Group I to the Fourth Assessment Report of the Intergovernmental Panel on Climate Change*, chapter Couplings between changes in the climate system and biogeochemistry. Cambridge University Press: Cambridge, 2007.
- M. B. Dickinson and E. A. Johnson. *Forest Fires, Behaviour and ecological effects*, chapter Fire Effects on Trees, pages 477–525. Academic Press, San Diego, 2001.

Bibliography

- R. E. Dickinson, J. A. Berry, G. B. Bonan, G. J. Collatz, C. B. Field, I. Y. Fung, M. Goulden, W. A. Hoffmann, R. B. Jackson, R. Myneni, P. J. Sellers, and M. Shaikh. Nitrogen controls on climate model evapotranspiration. *Journal of Climate*, 15:278–295, 2002.
- L. Donner and V. Ramanathan. Methane and nitrous oxide: Their effects on the terrestrial climate. *J. Atmos. Sci.*, 37:119–124, 1980.
- J.-L. Dufresne, P. Friedlingstein, M. Berthelot, L. Bopp, P. Ciais, L. Fairhead, H. Le Treut, and P. Monfray. On the magnitude of positive feedback between future climate change and the carbon cycle. *Geophysical Research Letters*, 29(10):4pp., 1405, 2002. doi: 10.1029/2001GL013777.
- H. Elenga, O. Peyron, R. Bonnefille, D. Jolly, R. Cheddadi, J. Guiot, V. Andrieu, S. Bottema, G. Buchet, J.-L. de Beaulieu, A. C. Hamilton, J. Maley, R. Marchant, R. Perez-Obiol, M. Reille, G. Riollet, L. Scott, H. Straka, D. Taylor, E. van Campo, A. Vincens, F. Laarif, and H. Jonson. Pollen-based biome reconstruction for southern Europe and Africa 18,000 yr BP. *Journal of Biogeography*, 27:621–634, 2000.
- H. D. Eva, J. P. Malingreau, J. M. Gregoire, A. S. Belward, and C. T. Mutlow. Cover The advance of burnt areas in Central Africa as detected by ERS-1 ATSR-1. *International Journal of Remote Sensing*, 19(9):1635–1637, 1998.
- H. J. Falcon-Lang. Fire ecology of the Carboniferous tropical zone. *Palaeogeography, Palaeoclimatology, Palaeoecology*, 164:355–371, 2000.
- M. A. Finney. FARSITE: Fire Area Simulator - Model Development and Evaluation. *USDA Forest Service Research Paper, Missoula, MT, RMRS-RP-4 Revised:52*, 1998.
- M. K. Firestone and E. A. Davidson. *Exchange of Trace Gases between Terrestrial Ecosystems and the Atmosphere*, chapter Microbiological basis of NO and nitrous oxide production and consumption in soil, pages 7–21. John Wiley & Sons, New York, 1989.
- J. Flückiger, A. Dällenbach, T. Blunier, B. Stauffer, T. F. Stocker, D. Raynaud, and J.-M. Barnola. Variations in atmospheric N₂O concentration during abrupt climatic changes. *Science*, 285: 227–230, 1999.
- M. Follieri, D. Magri, and L. Sadori. 250,000-year pollen record from Valle di Castiglione (Roma). *Pollen et Spores*, 30:329–356, 1988.
- Forestry Canada Fire Danger Group. Development and structure of the Canadian forest fire behavior prediction system. Information Report ST-X-3, Forestry Canada, Science and Sustainable Development Directorate, Ottawa, ON, 1992.
- P. Forster, V. Ramaswamy, B. Artaxo, J. Berntsen, R. Betts, D. W. Fahey, J. Haywood, J. Lean, D. C. Lowe, G. Myhre, J. Ngana, R. Prinn, G. Raga, M. Schulz, and R. van Dorland. *Changes in Atmospheric Constituents and in Radiative Forcing*. Cambridge University Press, Cambridge, United Kingdom and New York, NY, USA, 2007.

- J. E. Francis. The seasonal environment of the Purbeck (Upper Jurassic) fossil forests. *Palaeogeography, Palaeoclimatology, Palaeoecology*, 48:285–307, 1984.
- R. Frei, C. Gaucher, S. W. Poulton, and D. E. Canfield. Fluctuations in Precambrian atmospheric oxygenation recorded by chromium isotopes. *Nature*, 461:250–254, 2009. doi: 10.1038/nature08266.
- P. Friedlingstein, P. Cox, R. Betts, L. Bopp, W. von Bloh, V. Brovkin, P. Cadule, S. Doney, M. Eby, I. Fung, G. Bala, J. John, C. Jones, F. Joos, T. Kato, M. Kawamiya, W. Knorr, K. Lindsay, H. D. Matthews, T. Raddatz, P. Rayner, C. Reick, E. Roeckner, K.-G. Schnitzler, R. Schnur, K. Strassmann, A. J. Weaver, C. Yoshikawa, and N. Zeng. Climate-Carbon Cycle Feedback Analysis: Results from the C4MIP Model Intercomparison. *Journal of Climate*, 19:3337–3353, 2006.
- A. D. Friend, A. K. Stevens, R. G. Knox, and M. G. R. Cannell. A process-based, terrestrial biosphere model of ecosystem dynamics (Hybrid v3.0). *Ecological Modelling*, 95:249–287, 1997.
- J. N. Galloway, F. J. Dentener, D. G. Capone, E. W. Boyer, R. W. Howarth, S. P. Seitzinger, G. P. Asner, C. C. Cleveland, P. A. Green, E. A. Holland, D. M. Karl, A. F. Michaels, J. H. Porter, J. A. Townsend, and C. J. Vörösmarty. Nitrogen cycles: past, present, and future. *Biogeochemistry*, 70:153–226, 2004.
- L. Giglio, J. T. Randerson, G. T. van der Werf, P. S. Kasibhatla, G. J. Collatz, D. C. Morton, and R. S. DeFries. Assessing variability and long-term trends in burned area by merging multiple satellite fire products. *Biogeosciences*, 7:1171–118, 2010.
- I. Glasspool. A major fire event recorded in the mesofossils and petrology of the Late Permian, Lower Whybrow coal seam, Sydney Basin, Australia. *Palaeogeogr. Palaeoclim. Palaeoecol.*, 164:373–396, 2000.
- I. J. Glasspool, D. Edwards, and L. Axe. Charcoal in the Silurian as evidence for the earliest wildfire. *Geology*, 32:381–383, 2004.
- J. A. J. Gowlett. Out in the Cold. *Nature*, 413:33–34, 2001.
- J. A. J. Gowlett. The early settlement of northern Europe: Fire history in the context of climate change and the social brain. *Comptes Rendus Palevol*, 5(1-2):299–310, 2006.
- P. M. Groffman, J. P. Hardy, C. T. Driscoll, and T. J. Fahey. Snow depth, soil freezing, and fluxes of carbon dioxide, nitrous oxide and methane in a northern hardwood forest. *Global Change Biology*, 12:1748–1760, 2006.
- van Andel T. H. Reconstructing climate and landscape of the middle part of the last glaciation in Europe - The Stage 3 Project. *Quaternary Research*, 57:2–8, 2002.
- J. W. K. Harris. *The Karari industry: Its place in East African prehistory*. PhD thesis, University of California, Berkeley, 1978.

Bibliography

- J. W. K. Harris and J. A. J. Gowlett. Evidence of early stone industries at Chesowanja, Kenya. volume 8, pages 208–212, 1980.
- S. Harrison and I. C. Prentice. Climate and CO₂ controls on global vegetation distribution at the last glacial maximum: analysis based on palaeovegetation data, biome modelling and palaeoclimate simulations. *Global Change Biology*, 9:983–1004, 2003.
- M. Heimann and M. Reichstein. Terrestrial ecosystem carbon dynamics and climate feedbacks. *Nature*, 451:289–293, 2008. doi: 10.1038/nature06591.
- F. A. Heinsch and P. L. Andrews. BehavePlus Fire Modeling System, version 5.0: Design and Features. General Technical Report RMRS-GTR-249, United States Department of Agriculture. Forest Service, Rocky Mountain Research Station, Fort Collins, CO, December 2010.
- W. Hofmann. Response of the chydorid faunas to rapid climatic changes in four alpine lakes at different altitudes. *Palaeogeography, Palaeoclimatology, Palaeoecology*, 159:281–292, 2000.
- H. D. Holland. The oxygenation of the atmosphere and oceans. *Proceedings of the Royal Society B*, 361:903–915, 2006. doi: 10.1098/rstb.2006.1838.
- J. T. et al. Houghton, editor. *Climate Change 1995: The Science of Climate Change*. Cambridge University Press, 1995.
- E.A. Howard. A simple model for estimating the moisture content of living vegetation a potential wildfire fuel. 1978.
- B. A. Hungate, J. S. Dukes, M. R. Shaw, Y. Luo, and C. B. Field. Atmospheric Science: Nitrogen and climate change. *Science*, 302:1512–1513, 2003. doi: 10.1126/science.1091390.
- Intergovernmental Panel on Climate Change. *Climate Change 2001: The Scientific Basis. Contribution of Working Group I to the Third Assessment Report of the Intergovernmental Panel on Climate Change*. Cambridge University Press, New York, 2001.
- E. G. Jobbágy and R. B. Jackson. The uplift of soil nutrients by plants: biogeochemical consequences across scales. *Ecology*, 85(9):2380–2389, 2004.
- D. W. Johnson, R. B. Susfalk, R. A. Dahlgren, and J. M. Klopatek. Fire is more important than water for nitrogen fluxes in semi-arid forests. *Environmental Science and Policy*, 1:79–86, 1998.
- E. A. Johnson. *Fire and vegetation dynamics: studies from the North American boreal forest*. Cambridge University Press: Cambridge, 1992.
- E.-A. Kaiser, F. Eiland, J. C. Germon, M. A. Gispert, O. Heinemeyer, C. Henault, A. M. Lind, M. Maag, E. Sagner, O. Van Cleemput, A. Vermoesen, and C. Webster. What predicts nitrous oxide emissions and denitrification N-loss from European soils? *Zeitschrift für Pflanzenernährung und Bodenkunde*, 159:541–547, 1996.

- J. O. Kaplan, N. H. Bigelow, I. C. Prentice, S. P. Harrison, P. J. Bartlein, T. R. Christensen, W. Cramer, N. V. Matveyeva, A. D. McGuire, D. F. Murray, V. Y. Razzhivin, B. Smith, D. A. Walker, P. M. Anderson, A. A. Andreev, L. B. Brubaker, M. E. Edwards, and A. V. Lozhkin. Climate change and Arctic ecosystems: 2. Modeling, paleodata-model comparisons, and future projections. *Journal of Geophysical Research*, 108(D19):8171, 2003. doi: 10.1029/2002JD002559.
- J. O. Kaplan, K. M. Krumhard, E. C. Ellis, W. F. Ruddiman, C. Lemmen, and K. Klein Goldewijk. Holocene carbon emissions as a result of anthropogenic land cover change. *The Holocene*, 21(5):775–791, 2011.
- J. O. Kaplan, K. M. Krumhardt, and N. E. Zimmermann. The effects of land use and climate change on the carbon cycle of Europe over the past 500 years. *Global Change Biology*, 18: 902–914, 2012.
- C. E. Kay. Aboriginal Overkill: The Role of Native Americans in Structuring Western Ecosystems. *Human Nature*, 5(4):359–398, 1994.
- B. Kitzler, S. Zechmeister-Boltenstern, C. Holtermann, U. Skiba, and K. Butterbach-Bahl. Nitrogen oxides emission from two beech forests subjected to different nitrogen loads. *Biogeosciences*, 3:293–310, 2006.
- R. Knowles. Denitrification. *Microbiological Reviews*, 46(1):43–70, 1982.
- D. A. Kramer. Minerals Yearbook. Nitrogen. US Geological Survey Minerals Information, 1999. URL <http://minerals.usgs.gov/minerals/pubs/commodity/nitrogen/>.
- G. Krinner, N. Viovy, N. de Noblet-Ducoudré, J. Ogée, J. Polcher, P. Friedlingstein, P. Ciais, S. Sitch, and I. C. Prentice. A dynamic global vegetation model for studies of the coupled atmosphere-biosphere system. *Global Biogeochemical Cycles*, 19:GB1015, 2005. doi: 10.1029/2003GB002199.
- C. Kroeze, A. Mosier, and L. Bouwman. Closing the global N₂O budget: A retrospective analysis 1500 - 1994. *Global Biogeochemical Cycles*, 13(1):1–8, 1999.
- J. H. Kroll, L. N. Ng, S. M. Murphy, R. C. Flagan, and J. H. Seinfeld. Secondary organic aerosol formation from isoprene photooxidation under high-NO_x conditions. *Geophysical Research Letters*, 32:L18808, 2005. doi: 10.1029/2005GL023637.
- Christopher J. Kucharik, Jonathan A. Foley, Christine Delire, Veronica A. Fisher, Michael T. Coe, John D. Lenters, Christine Young-Molling, Navin Ramankutty, John M. Norman, and Stith T. Gower. Testing the performance of a dynamic global ecosystem model: Water balance, carbon balance, and vegetation structure. *Global Biogeochemical Cycles*, 14(3): 795–825, 2000. ISSN 1944-9224. doi: 10.1029/1999GB001138. URL <http://dx.doi.org/10.1029/1999GB001138>.

Bibliography

- L. R. Kump. Terrestrial feedback in atmospheric oxygen regulation by fire and phosphorus. *Nature*, 335:152 – 154, 1988. doi: 10.1038/335152a0.
- Lee R. Kump. Chemical stability of the atmosphere and ocean. *Palaeogeography, Palaeoclimatology, Palaeoecology*, 75(1-2):123 – 136, 1989. ISSN 0031-0182. doi: 10.1016/0031-0182(89)90187-9.
- J. Lathière, D. A. Hauglustaine, and N. de Noblet-Ducoudré. Past and future changes in biogenic volatile organic compound emissions simulated with a global dynamic vegetation model. *Geophysical Research Letters*, 32:L20818, 2005. doi: 10.1029/2005GL024164.
- G. Lemdahl. Lateglacial and Early Holocene insect assemblages from sites at different altitudes in the Swiss Alps—implications on climate and environment. *Palaeogeography, Palaeoclimatology, Palaeoecology*, 159:293–312, 2000.
- J. M. Lenihan, C. Daly, D. Bachelet, and R. P. Neilson. Simulating Broad-Scale Fire Severity in a Dynamic Global Vegetation Model. *Northwest Science*, 72:91–103, 1998.
- T. M. Lenton, M. Crouch, M. Johnson, N. Pires, and L. Dolan. First plants cooled the Ordovician. *Nature Geoscience*, 5:86–89, 2012.
- T.M. Lenton and A.J. Watson. Redfield revisited: 2. What regulates the oxygen content of the atmosphere. *Global Biogeochemical Cycles*, 14(1):249–268, 2000.
- S. Levis, G. B. Bonan, M. Vertenstein, and K. W. Oleson. The Community Land Model’s Dynamic Global Vegetation Model (CLM-DGVM): Technical Description and User’s Guide. Technical Report NCAR Tech. Note TN-459-IA, NCAR, Terrestrial Sciences Section, Boulder, Colorado, 2004.
- H. T. Lewis. *Before the Wilderness: Environmental Management by Native Californians*, chapter Patterns of Indian Burning in California: Ecology and Ethnohistory, pages 55–116. Ballena Press, Menlo Park, CA, 1973.
- H. T. Lewis, editor. *Why Indians burned: specific versus general reasons*, number GTR-INT-182, November, 15-18, 1983. 1985. Proceedings–Symposium and Workshop on Wilderness Fire: Missoula, Montana, Ogden, UT: USDA Forest Service, Intermountain Forest and Range Experiment Station.
- R. Linn, J. Reisner, J. J. Colman, and J. Wintercamp. Studying wildfire behavior using FIRETEC. *International Journal of Wildland Fire*, 11:233–246, 2002.
- H. Lischke, U. von Grafenstein, and B. Ammann. Forest dynamics during the transition from the Oldest Dryas to the Bølling-Allerød at Gerzensee - a simulation study. *Palaeogeography, Palaeoclimatology, Palaeoecology*, in press:14 p., PALAEO–06350, 2012. doi: 10.1016/j.palaeo.2012.12.001.

- A. F. Lotter, H. J. B. Birks, U. Eicher, W. Hofmann, J. Schwander, and L. Wick. Younger Dryas and Allerød summer temperatures at Gerzensee (Switzerland) inferred from fossil pollen and cladoceran assemblages. *Palaeogeography, Palaeoclimatology, Palaeoecology*, 159:349–361, 2000.
- A. F. Lotter, O. Heiri, S. Brooks, J. N. F. van Leeuwen, U. Eicher, and B. Ammann. Rapid summer temperature changes during Termination 1a: high-resolution multi-proxy climate reconstructions from Gerzensee (Switzerland). *Quaternary Science Reviews*, 36:103–113, 2012. doi: 10.1016/j.quascirev.2010.06.022.
- J. Lovelock. *The ages of gaia: A biography of our living planet*. Commonwealth Fund Book Program. W. W. Norton & Company, 1995.
- Y. Luo, B. Su, W. S. Currie, J. S. Dukes, A. Finzi, U. Hartwig, B. Hungate, R. E. Mc Murtie, R. Oren, W. J. Parton, M. R. Pataki, D. E. Shaw, D. R. Zak, and C. B. Field. Progressive Nitrogen Limitation of Ecosystem Responses to Rising Atmospheric Carbon Dioxide. *BioScience*, 54(8):731–739, 2004.
- M. Maag and F. P. Vinther. Nitrous oxide emission by nitrification and denitrification in different soil types and at different soil moisture contents and temperatures. *Applied Soil Ecology*, 4:5–14, 1996.
- M. Magny. Climatic and environmental changes reflected by lake-level fluctuations at Gerzensee from 14,850 to 13,050 yr BP. *Palaeogeography, Palaeoclimatology, Palaeoecology*, in press:7 p., PALAEO–06135, 2012. doi: 10.1016/j.palaeo.2012.05.003.
- M. Magny, N. Thew, and P. Hadorn. Late-glacial and early Holocene changes in vegetation and lake-level at Hauterive/Rouges-Terres, Lake Neuchâtel (Switzerland). *Journal of Quaternary Science*, 18:31–40, 2003.
- D. Magri. Interpreting long-term exponential growth of plant populations in a 250,000-year pollen record from Valle die Castiglione (Roma). *New Phytologist*, 112:123–128, 1989.
- J. Mandel, J. D. Beezley, J. L. Coen, and M. Kim. Data Assimilation for Wildland Fires: Ensemble Kalman filters in coupled atmosphere-surface models. *IEEE Control Systems Magazine*, 29(3):47–65, 2009.
- S. Manzoni, R. B. Jackson, J. A. Trofymow, and A. Porporato. The Global Stoichiometry of Litter Nitrogen Mineralization. *Science*, 321:684–686, 2008.
- C. A. McLaugherty, J. Pastor, J. D. Aber, and J. M. Melillo. Forest Litter Decomposition in Relation to Soil Nitrogen Dynamics and Litter Quality. *Ecology*, 66(1):266–275, 1985.
- J. M. Melillo, P. A. Steudler, J. D. Aber, K. Newkirk, H. Lux, F. P. Bowles, C. Catricala, A. Magill, T. Ahrens, and S. Morriseau. Soil Warming and Carbon-Cycle Feedbacks to the Climate System. *Science*, 298:2173–2176, 2002.

Bibliography

- W. Mell, M. A. Jenkins, J. Gould, and P. Cheney. A physics-based approach to modelling grassland fires. *International Journal of Wildland Fire*, 16:1–22, 2007.
- P. R. Moorcroft, G. C. Hurtt, and S. W. Pacala. A method for scaling vegetation dynamics: the ecosystem demography model (ED). *Ecological Monographs*, 71:557–586, 2001.
- K. L. Moulton and R. A. Berner. Quantification of the effect of plants on weathering: Studies in Iceland. *Geology*, 26, 10:895–898, 1998.
- A. Neftel, C. Flechard, C. Ammann, F. Conen, L. Emmenegger, and K. Zeyer. Experimental assessment of N₂O background fluxes in grassland systems. *Tellus*, 59B:470–482, 2007.
- R. P. Neilson and S. W. Running. *Global Change and Terrestrial Ecosystems*, chapter Global dynamic vegetation modelling: coupling biogeochemistry and biogeography models, pages 451–465. Cambridge University Press, Cambridge, 1996.
- M. Nelson. A dynamic system model of the limiting oxygen index test: II. Retardancy due to char formation and addition of inert fillers. *Combust. Theory Model*, 5:95–83, 2001.
- I. R. Noble, G. A. V. Bary, and A. M. Gill. McArthur's fire danger meters expressed as equations. *Australian Journal of Ecology*, 5:201–203, 1980.
- R. J. Norby, B. DeLucia, E. H. and Gielen, C. Calfapietra, C. P. Giardina, J. S. King, J. Ledford, H. R. McCarthy, D. J. P. Moore, R. Ceulemans, P. De Angelis, A. C. Finzi, D. F. Karnosky, M. E. Kubiske, M. Lukac, K. S. Pregitzer, G. E. Scarascia-Mugnozza, W. H. Schlesinger, and R. Oren. Forest response to elevated CO₂ is conserved across a broad range of productivity. *Proceedings of the National Academy of Sciences, USA*, 102(50):18052–18056, 2005. doi: 10.1073/pnas.0509478102.
- R. J. Norby, J. M. Warren, C. M. Iversen, B. E. Medlyn, and R. E. McMurtrie. CO₂ enhancement of forest productivity constrained by limited nitrogen availability. *Proceedings of the National Academy of Sciences, USA*, 107(45):19368–19373, 2010. doi: 10.1073/pnas.1006463107.
- S. Normand, U. A. Treier, and B. V. Odgaard. Tree refugia and slow forest development in response to post-LGM warming in North-Eastern European Russia. *Frontiers of Biogeography*, 2(4):91–93, 2011.
- K. Nováková, M. van Hardenbroek, and W. O. van der Knaap. Response of subfossil Cladocera in Gerzensee (Swiss Plateau) to early Late Glacial environmental change. *Palaeogeography, Palaeoclimatology, Palaeoecology*, in press:6 p., PALAEO–06301, 2012.
- K. W. Oleson, Lawrence D. M., G. B. Bonan, M. G. Flanner, E. Kluzek, P. J. Lawrence, S. Levis, S. C. Swenson, P. E. Thornton, A. Dai, M. Decker, R. Dickinson, J. J. Feddema, C. L. Heald, F. Hoffman, J.-F. Lamarque, N. Mahowald, G.-Y. Niu, T. Qian, J. T. Randerson, S. Running, K. Sakaguchi, A. Slater, R. Stöckli, A. Wang, Z.-L. Yang, X. Zeng, and X. Zeng. Technical Description of version 4.0 of the Community Land Model (CLM). *NCAR TECHNICAL NOTE, NCAR/TN-478+STR, Boulder, CO, 80307-3000*, 2010.

- W. J. Parton, E. A. Holland, S. J. Del Grosso, M. D. Hartman, R. E. Martin, A. R. Mosier, D. S. Ojima, and D. S. Schimel. Generalized model for NO_x and N₂O emissions from soils. *Journal of Geophysical Research*, 106(D15):17403–17420, 2001.
- T. G. A. Paungfoo-Lonhienne, D. Rentsch, N. Robinson, M. Christie, R. I. Webb, H. K. Gamage, B. J. Carroll, P. M. Schenk, and S. Schmidt. Plants can use protein as a nitrogen source without assistance from other organisms. *Proceedings of the National Academy of Sciences, USA*, 105:4524–4529, 2008.
- J. G. Pausas and J. E. Keeley. A burning story: The role of fire in the history of life. *BioScience*, 59(7):593–601, 2009.
- P. Pavlov, J. I. Svendsen, and S. Indrellid. Human presence in the European Arctic nearly 40,000 years ago. *Nature*, 413:64–67, 2001.
- D. L. Peterson and K. C. Ryan. Modeling postfire conifer mortality for long-range planning. *Environmental Management*, 10(6):797–808, 1986.
- M. Pfeiffer and J. O. Kaplan. SPITFIRE-2: an improved fire module for Dynamic Global Vegetation Models. *Geoscientific Model Development Discussions*, 5:2347–2443, 2012. doi: 10.5194/gmdd-5-2347-2012.
- M. Pfeiffer, J. van Leeuwen, W. O. van der Knaap, and J. O. Kaplan. The effect of abrupt climate warming on biogeochemical cycling and N₂O emissions in a terrestrial ecosystem. *Palaeogeography, Palaeoclimatology, Palaeoecology*, in press, PALAEO-06176:12 p., 2012. doi: 10.1016/j.palaeo.2012.06.015.
- K. Pilegaard, U. Skiba, P. Ambus, C. Beier, N. Brüggemann, K. Butterbach-Bahl, J. Dick, J. Dorsey, J. Duyzer, M. Gallagher, R. Gasche, L. Horvath, B. Kitzler, A. Leip, M. K. Pihlatie, P. Rosenkranz, G. Seufert, T. Vesala, H. Westrate, and S. Zechmeister-Boltenstern. Factors controlling regional differences in forest soil emission of nitrogen oxides (NO and N₂O). *Biogeosciences*, 3:651–661, 2006.
- D. Pollard and E. J. Barron. Causes of model-data discrepancies in European climate during Oxygen Isotope Stage 3 with insights from the last glacial maximum. *Quaternary Research*, 59:108–113, 2003.
- W. M. Post, T.-H. Peng, W. R. Emanuel, A. W. King, V. H. Dale, and D. L. DeAngelis. The Global Carbon Cycle. *American Scientist*, 78:310–327, 1990.
- C. S. Potter and S. A. Klooster. Interannual variability in soil trace gas (CO₂, N₂O, NO) fluxes and analysis of controllers on regional to global scales. *Global Biogeochemical Cycles*, 12(4): 621–635, 1998.
- C. S. Potter, P. A. Matson, P. M. Vitousek, and E. A. Davidson. Process modeling of controls on nitrogen trace gas emissions from soils worldwide. *Journal of Geophysical Research*, 101 (D1):1361–1377, 1996.

Bibliography

- I. C. Prentice, D. Jolly, and BIOME 6000 participants. Mid-Holocene and glacial-maximum vegetation geography of the northern continents and Africa. *Journal of Biogeography*, 27: 507–519, 2000.
- I. C. Prentice, D. I. Kelley, P. N. Foster, P. Friedlingstein, S. P. Harrison, and P. J. Bartlein. Modeling fire and the terrestrial carbon balance. *Global Biogeochemical Cycles*, 25:GB3005, 2011. doi: 10.1029/2010GB003906.
- S. J. Pyne. *Fire in America: A Cultural History of Wildland and Rural Fire*. Princeton University Press, Princeton, NJ, 1982.
- S. J. Pyne. Maintaining Focus: An Introduction to Anthropogenic Fire. *Chemosphere*, 29(5): 889–911, 1994.
- S. J. Pyne. *World Fire: The Culture of Fire on Earth*, 384 p. University of Washington Press, Seattle, WA, 1997.
- S. J. Pyne. *Vestal Fire: an Environmental History, told through Fire, of Europe and Europe's Encounter with the World*. University of Washington Press, Seattle, WA, 2000.
- S. J. Pyne, P. L. Andrews, and R. D. Daven. *Introduction to Wildland Fire*. Wiley, London, 1996.
- A. Quillet, P. Changhui, and M. Garneau. Toward dynamic global vegetation models for simulating vegetation-climate interactions and feedbacks: recent developments, limitations, and future challenges. *Environmental Reviews*, 18(NA):333–353, 2010.
- R. J. Raison. A review of the role of fire in nutrient cycling in Australian native forests, and of methodology for studying the fire-nutrient interaction. *Australian Journal of Ecology*, 5(1): 15–21, 1980.
- J. T. Randerson, Y. Chen, G. R. van der Werf, B. M. Rogers, and D. C. Morton. Global burned area and biomass burning emissions from small fires. *Journal of Geophysical Research*, 117: G04012, 2012. doi: 10.1029/2012JG002128.
- J. Reilly, M. Mayer, and J. Harnisch. The Kyoto Protocol and non-CO₂ greenhouse gases and carbon sinks. *Environmental Modeling and Assessment*, 7:217–229, 2002.
- E. D. Reinhardt, R. E. Keane, and J. K. Brown. First Order Fire Effects Model: FOFEM 4.0, User's Guide. General Technical Report INT-GTR-344, United States Department of Agriculture, Forest Service, Missoula, Montana 59807, Intermountain Research Station, 1997.
- M. E. Repo, S. Susiluoto, S. E. Lind, S. Jokinen, V. Elsakov, C. Biasi, T. Virtanen, and P. J. Martikainen. Large N₂O emissions from cryoturbated peat soil in tundra. *Nature Geoscience*, 2:189–192, 2009.
- E. Rigolot. Predicting post fire mortality of *Pinus halepensis* Mill. and *Pinus pinea* L. *Plant Ecology*, 171:139–151, 2004.

- J. M. Robinson. Phanerozoic O₂ variation, fire, and terrestrial ecology. *Paleogeography, Palaeoclimatology, Palaeoecology*, 75:223–240, 1989.
- W. Roebroeks and P. Villa. On the earliest evidence for habitual use of fire in Europe. *Proceedings of the National Academy of Sciences, USA*, 108(13):5309–5214, 2011.
- M. Rondon, J. A. Ramirez, and J. Lehmann. Charcoal additions reduce net emissions of greenhouse gases to the atmosphere. pages 21–24, Baltimore, MA, March 2005 2005. USDA.
- M. A. Rondon, J. Lehmann, J. Ramirez, and M. Hurtado. Biological nitrogen fixation by common beans (*Phaseolus vulgaris*) increases with bio-char additions. *Biology and Fertility of Soils*, 43:699–708, 2007.
- R. C. Rothermel. A mathematical model for predicting fire spread in wildland fuels. *USDA Forest Service Research Paper, Ogden, UT 84401*, INT-115:48, 1972.
- W. F. Ruddiman. The anthropogenic greenhouse area began thousands of years ago. *Climatic Change*, 61:261–239, 2003.
- W. F. Ruddiman. The Early Anthropogenic Hypothesis: Challenges and Responses. *Reviews of Geophysics*, 45:RG4001, 1–37, 2006RG000207, 2007.
- P. W. Rundel. Impact of fire on nutrient cycles in Mediterranean-type ecosystems with reference to chaparral. *Ecological Studies*, 1983.
- Emily W.B. Russell. Indian-Set Fires in the Forests of the Northeastern United States. *Ecology*, 64(1):78–88, 1983.
- N. R. Sampson. Forest management, wildfire, and climate change policy issues in the 11 western states. Technical report, American Forest, Forest Policy Center, Washington, D.C., 1997.
- H. Sato, A. Itoh, and T. Kohyama. SEIB-DGVM: A new Dynamic Global Vegetation Model using a spatially explicit individual-based approach. *Ecological Modelling*, 200:279–307, 2007.
- J. P. Schimel and J. Bennett. Nitrogen mineralization: Challenges of a changing paradigm. *Ecology*, 85:591–602, 2004.
- J. Schwander, U. Eicher, and B. Ammann. Oxygen isotopes of lake marl at Gerzensee and Leysin (Switzerland), covering the Younger Dryas and two minor oscillations, and their correlation to the GRIP ice core. *Paleogeography, Palaeoclimatology, Palaeoecology*, 159: 203–214, 2000.
- A. C. Scott and I. J. Glasspool. The diversification of Palaeozoic fire systems and fluctuations in atmospheric oxygen concentration. *Proceedings of the National Academy of Sciences, USA*, 103:10861–10865, 2006.

Bibliography

- L. Ségalen, J. A. Lee-Thorp, and T. Cerling. Timing of C₄ grass expansion across sub-Saharan Africa. *Journal of Human Evolution*, 53:549–559, 2007. doi: 10.1016/j.jhevol.2006.12.010.
- S. P. Seitzinger, J. Harrison, J. Bohlke, A. Bouwman, R. Lowrance, B. Peterson, C. Tobias, and G. Van Drecht. Denitrification across landscapes and waterscapes: A synthesis. *Ecological Applications*, 16:2064–2090, 2006.
- S. Sitch, B. Smith, I. C. Prentice, A. Arneth, A. Bondeau, W. Cramer, J. O. Kaplan, S. Levis, W. Lucht, M. T. Sykes, K. Thonicke, and S. Venevsky. Evaluation of ecosystem dynamics, plant geography and terrestrial carbon cycling in the LPJ dynamic global vegetation model. *Global Change Biology*, 9:161–185, 2003.
- U. Skiba, K. A. Smith, and D. Fowler. Nitrification and denitrification as sources of nitric oxide and nitrous oxide in a sandy loam soil. *Soil Biology and Biochemistry*, 25(11):1527–1536, 1993.
- B. Smith, I. C. Prentice, and M. T. Sykes. Representation of vegetation dynamics in the modelling of terrestrial ecosystems: comparing two contrasting approaches within European climate space. *Global Ecology and Biogeography*, 10:621–637, 2001.
- K. A. Smith, P. E. Thomson, H. Clayton, I. P. McTaggart, and F. Conen. Effects of temperature, water content and nitrogen fertilisation on emissions of nitrous oxide by soils. *Atmospheric Environment*, 32(19):3301–3309, 1998.
- A. P. Sokolov, D. W. Kicklighter, J. M. Melillo, B. S. Felzer, C. A. Schlosser, and T. W. Cronin. Consequences of considering carbon-nitrogen interactions on the feedbacks between climate and the terrestrial carbon cycle. *Journal of Climate*, 21:3776–3796, 2008.
- S. Solomon, D. Qin, M. Manning, Z. Chen, M. Marquis, K. B. Averyt, M. Tignor, and H. L. Miller, editors. *Climate Change 2007: The Physical Science Basis. Contribution of Working Group I to the Fourth Assessment Report of the Intergovernmental Panel on Climate Change*, 2007. Cambridge University Press, Cambridge, United Kingdom/New York, NY, USA.
- M. Sorai, N. Yoshida, and M. Ishikawa. Biogeochemical simulation of nitrous oxide cycle based on the major nitrogen processes. *Journal of Geophysical Research*, 112:G01006, 2007.
- T. Sowers, R. B. Alley, and J. Jubenville. Ice core records of atmospheric N₂O covering the last 106.000 years. *Science*, 301:945–948, 2003.
- R. Spahni, J. Chappelaz, T. F. Stocker, L. Loulergue, G. Hausammann, F. Kawamura, J. Flückiger, J. Schwander, D. Raynaud, V. Masson-Delmotte, and J. Jouzel. Atmospheric methane and nitrous oxide of the Late Pleistocene from Antarctic ice cores. *Science*, 310:1317–1321, 2005.
- A. Spessa and R. Fisher. On the relative role of fire and rainfall in determining vegetation patterns in tropical savannas: a simulation study. *Geophysical Research Abstracts*, 12: EGU2010–7142–6, 2010, 2010.

- S. L. Stephens and M. A. Finney. Prescribed fire mortality of Sierra Nevada mixed conifer tree species: effects of crown damage and forest floor combustion. *Forest Ecology and Management*, 162:261–271, 2002.
- R. J. Stevens, R. J. Laughlin, and J. P. Malone. Soil pH affects the processes reducing nitrate to nitrous oxide and di-nitrogen. *Soil Biology and Biochemistry*, 30(8/9):1119–1126, 1998.
- J. R. Stewart and A. M. Lister. Cryptic northern refugia and the origins of the modern biota. *Trends in Ecology and Evolution*, 16:608–613, 2001.
- G. Strandberg, J. Brandefelt, E. Kjellström, and B. Smith. High-resolution regional simulation of last glacial maximum climate in Europe. *Tellus*, 63A:107–125, 2011. doi: 10.1111/j.1600-0870.2010.00485.x.
- P. E. Tarasov, V. S. Volkova, T. Webb, J. Guiot, A. A. Andreev, L. G. Bezusko, T. V. Bezusko, G. V. Bykova, N. I. Dorofeyuk, E. V. Kvavadze, I. M. Osipova, N. K. Panova, and D. V. Sevastyanov. Last glacial maximum biomes reconstructed from pollen and plant macrofossil data from northern Eurasia. *Journal of Biogeography*, 27:609–620, 2000.
- B. R. Taylor, D. Parkinson, and W. F. J. Parsons. Nitrogen and Lignin Content as Predictors of Litter Decay Rates: A Microsoms Test. *Ecology*, 70(1):97–104, 1989.
- K. Thonicke, S. Venevsky, S. Sitch, and W. Cramer. The role of fire disturbance for global vegetation dynamics: coupling fire into a Dynamic Global Vegetation Model. *Global Ecology and Biogeography*, 10:661–677, 2001.
- K. Thonicke, A. Spessa, I. C. Prentice, S. P. Harrison, L. Dong, and C. Carmona-Moreno. The influence of vegetation, fire spread and fire behaviour on biomass burning and trace gas emissions: results from a process-based model'. *Biogeosciences*, 7:1991–2011, 2010.
- P. E. Thornton, B. E. Law, H. L. Gholz, K. L. Clark, E. Falge, D. S. Ellsworth, A. H. Goldstein, R. K. Monson, D. Hollinger, M. Falk, J. Chen, and J. P. Sparks. Modeling and measuring the effects of disturbance history and climate on carbon and water budgets in evergreen needleleaf forests. *Agricultural and Forest Meteorology*, 113:185–222, 2002.
- P. E. Thornton, J.-F. Lamarque, N. A. Rosenbloom, and N. Mahowald. Influence of carbon-nitrogen cycle coupling on land model response to CO₂ fertilization and climate variability. *Global Biogeochemical Cycles*, 21:GB4018, 2007.
- P. E. Thornton, S. C. Doney, K. Lindsay, J. K. Moore, N. Mahowald, J. T. Randerson, I. Fung, J.-F. Lamarque, J. J. Feddema, and Y.-H. Lee. Carbon-nitrogen interactions regulate climate-carbon cycle feedbacks: results from an atmosphere-ocean general circulation model. *Biogeosciences Discussions*, 6:3303–3354, 2009.
- K. Tobolsky and B. Ammann. Macrofossils as records of plant responses to rapid Late Glacial climatic changes at three sites in the Swiss Alps. *Palaeogeography, Palaeoclimatology, Palaeoecology*, 159:251–259, 2000.

Bibliography

- C. Tymstra, R. W. Bryce, B. M. Wotton, and O. B. Armitage. Development and structure of Prometheus: the Canadian wildland fire growth simulation model. Information Report NOR-X-417, Canadian Forest Service, Northern Forestry Centre, Edmonton, AB, 2009.
- U. van Raden, D. Colombaroli, A. Gilli, J. Schwander, S. M. Bernasconi, J. van Leeuwen, M. Leuenberger, and U. Eicher. High-resolution late-glacial chronology for the Gerzensee lake record (Switzerland): $\delta^{18}\text{O}$ correlation between a Gerzensee-stack and NGRIP. *Palaeogeography, Palaeoclimatology, Palaeoecology*, in press:12 p., ALAEO-06149, 2012.
- C. E. van Wagner. Development and structure of the Canadian Forest Fire Weather Index System. Technical Report 35, Canadian Forest Service, Ottawa, Ontario, 1987.
- C.E. van Wagner. Prediction of crown fire behavior in two stands of jack pine. *Canadian Journal of Forest Research*, 23(3):442–449, 1993. doi: 10.1139/x93-062. URL <http://www.nrcr.esearchpress.com/doi/abs/10.1139/x93-062>.
- S. Venevsky, K. Thonicke, S. Sitch, and W. Cramer. Simulating fire regimes in human-dominated ecosystems: Iberian Peninsula case study. *Global Change Biology*, 8:984–998, 2002.
- F. P. Vinther. Total denitrification and the ratio between N_2O and N_2 during the growth of spring barley. *Plant and Soil*, 76:227–232, 1984.
- P. M. Vitousek and R. W. Howarth. Nitrogen Limitation on Land and in the Sea: How Can It Occur? *Biogeochemistry*, 13(2):87–115, 1991.
- U. von Grafenstein, U. Eicher, H. Erlenkeuser, P. Ruch, J. Schwander, and B. Ammann. Isotope signature of the Younger Dryas and two minor oscillations at Gerzensee (Switzerland): palaeoclimatic and palaeolimnologic interpretation based on bulk and biogenic carbonates. *Paleogeography, Palaeoclimatology, Palaeoecology*, 159:215–229, 2000.
- E. S. Vrba. *Evolutionary history of the "robust" australopithecines*, chapter Late Pliocene climatic events and hominid evolution, pages 405–426. Hawthorne, N.Y.:Aldine, 1988.
- E. S. Vrba. *Paleoclimate and evolution, with emphasis on human origins*, chapter On the connections between paleoclimate and evolution, pages 24–45. Yale University Press, New Haven, 1995.
- S. Wan, D. Hui, and Y. Luo. Fire Effects on Nitrogen Pools and Dynamics in Terrestrial Ecosystems: A Meta-Analysis. *Ecological Applications*, 11(5):1349–1365, 2001.
- D. A. Wardle, O. Zackrisson, G. Hörnberg, and G. Gallet. The influence of island area on ecosystem properties. *Science*, 277:1296–1299, 1997.
- Andrew Watson, James E. Lovelock, and Lynn Margulis. Methanogenesis, fires and the regulation of atmospheric oxygen. *Biosystems*, 10(4):293 – 298, 1978. ISSN 0303-2647. doi: 10.1016/0303-2647(78)90012-6. URL <http://www.sciencedirect.com/science/article/pii/0303264778900126>.

- C. Werner, K. Butterbach-Bahl, E. Haas, T. Hickler, and R. Kiese. A global inventory of N₂O emissions from tropical rainforest soils using a detailed biogeochemical model. *Global Biogeochemical Cycles*, 21:GB3010, 2007.
- L. Wick. Vegetational response to climatic changes recorded in Swiss Late Glacial lake sediments. *Palaeogeography, Palaeoclimatology, Palaeoecology*, 159:231–250, 2000.
- M. Williams. *Deforesting the Earth: From Prehistory to Global Crisis*. University of Chicago Press, Chicago, IL, 2002.
- K. J. Willis and T. H. van Andel. Trees or no trees? The environments of central and eastern Europe during the Last Glaciation. *Quaternary Science Reviews*, 23:2369–2387, 2004. doi: 10.1016/j.quascirev.2004.06.002.
- K. J. Willis, E. Rudner, and Sümegi. The Full-Glacial Forests of Central and Southeastern Europe. *Quaternary Research*, 53:203–213, 2000.
- R. A. Wilson Jr. A reexamination of fire spread in free burning porous fuel beds. Technical Report UTINT-289, 28, United States Department of Agriculture, Forest Service, Intermountain Forest and Range Experiment Station, Ogden, UT, 1982.
- M.-N. Woillez, M. Kageyama, G. Krinner, N. de Noblet-Ducoudré, N. Viovy, and M. Mancip. Impact of CO₂ and climate on the Last Glacial Maximum vegetation: results from the ORCHIDEE/IPSL models. *Climate of the Past*, 7:557–577, 2011. doi: 10.5194/cp-7-557-2011.
- E. Wolff and R. Spahni. Methane and nitrous oxide in the ice core record. *Philosophical Transactions of the Royal Society*, 365:1775–1792, 2007.
- F. I. Woodward and M. R. Lomas. Vegetation dynamics - simulating responses to climatic change. *Biol. Rev.*, 79:643–670, 2004.
- F. I. Woodward, M. R. Lomas, and S. E. Lee. *Terrestrial Global Productivity*, chapter Predicting the future productivity and distribution of global vegetation, pages 521–541. Academic Press, New York, 2001.
- R. W. Wrangham, Jones J. H., G. Laden, D. Pilbeam, and N. L. Conklin-Brittain. The Raw and the Stolen: Cooking and the Ecology of Human Origins. *Current Anthropology*, 40(5):567–594, 1999.
- Xu-Ri and I. C. Prentice. Terrestrial nitrogen cycle simulation with a dynamic global vegetation model. *Global Change Biology*, 14:1745–1764, 2008.
- D. Yibarbuk, P. J. Whitehead, J. Russell-Smith, D. Jackson, C. Godjuwa, A. Fisher, P. Cooke, Choquenot D., and D. M. J. S. Bowman. Fire ecology and Aboriginal land management in central Arnhem Land, northern Australia: a tradition of ecosystem management. *Journal of Biogeography*, 28:325–343, 2002.

Bibliography

- O. Zackrisson, M. Nilsson, and D. Wardle. Key ecological function of charcoal from wildfire in the boreal forest. *Oikos*, 77:10–19, 1996.
- S. Zaehle and A. D. Friend. Carbon and nitrogen cycle dynamics in the O-CN land surface model: 1. Model description, site-scale evaluation, and sensitivity to parameter estimates. *Global Biogeochemical Cycles*, 24(1):GB1005, 2010a.
- S. Zaehle and A. D. Friend. Description of the O-CN model: Supplementary material to: Carbon and nitrogen cycle dynamics in the O-CN land surface model, I: Model description, site-scale evaluation and sensitivity to parameter estimates. *Global Biogeochemical Cycles*, 24(1):GB1005, 2010b.
- S. Zaehle, A. D. Friend, P. Friedlingstein, F. Dentener, P. Peylin, and M. Schulz. Carbon and nitrogen cycle dynamics in the O-CN land surface model: 2. Role of the nitrogen cycle in the historical terrestrial carbon balance. *Global Biogeochemical Cycles*, 24(1):GB1006, 2010.

2 The effect of abrupt climatic warming on biogeochemical cycling and N₂O emissions in a terrestrial ecosystem

M. Pfeiffer, J. van Leeuwen, W. O. van der Knaap, and J. O. Kaplan. The effect of abrupt climate warming on biogeochemical cycling and N₂O emissions in a terrestrial ecosystem. *Palaeogeography, Palaeoclimatology, Palaeoecology*, in press:12 p.,2012.
doi:10.1016/j.palaeo.2012.06.015

The large, rapid increase in atmospheric N₂O concentrations that occurred concurrent with the abrupt warming at the end of the last glacial period might have been the result of a reorganization in global biogeochemical cycles. To explore the sensitivity of nitrogen cycling in terrestrial ecosystems to abrupt warming, we combined a scenario of climate and vegetation composition change based on multiproxy data for the Oldest Dryas-Bølling abrupt warming event at Gerzensee, Switzerland, with a biogeochemical model that simulates terrestrial N uptake and release, including N₂O emissions. As for many central European sites, the pollen record at the Gerzensee is remarkable for the abundant presence of the symbiotic nitrogen fixer *Hippophaë rhamnoides* (L.) during the abrupt warming that also marks the beginning of primary succession on immature glacial soils. Here we show that without additional nitrogen fixation, climate change results in a significant increase of N₂O emissions of approximately factor 3.4 (from 6.4 ± 1.9 to 21.6 ± 5.9 mg N₂O-N m⁻²yr⁻¹). Each additional 1000 mg m⁻² yr⁻¹ of nitrogen added to the ecosystem through N-fixation result in additional N₂O emissions of 1.6 mg N₂O-N m⁻²yr⁻¹ for the time with maximum *H. rhamnoides* coverage. Our results suggest that local reactions of emissions to abrupt climate change could have been considerably faster than the overall atmospheric concentration changes observed in polar ice. Nitrogen enrichment of soils due to the presence of symbiotic N-fixers during early primary succession not only facilitates the establishment of vegetation on soils in their initial stage of development, but can also have considerable influence on biogeochemical cycles and the release of reactive nitrogen trace gases to the atmosphere.

2.1 Introduction

Nitrous oxide (N₂O) is an important greenhouse gas that over a 100-year interval has a global warming potential of 298 times that of CO₂ and at present has an atmospheric lifetime of 114 years [Forster et al., 2007, Ramaswamy et al., 2001]. Comparable to CH₄, ice core records of atmospheric N₂O concentrations show rapid variations on both glacial-interglacial and millennial timescales during the last glacial [Blunier and Brook, 2001, Sowers et al., 2003] when the full amplitude of preindustrial variability was achieved in a century or less. The high temporal variability in N₂O concentrations closely parallels polar temperature records [Flückiger et al., 1999, Schilt et al., 2010], indicating that nitrogen trace gas emissions may be very sensitive to climatic change.

During the transition from Oldest Dryas (18,000-14,650 cal. yr. BP) to Bølling (14,650-14,000 cal. yr. BP) abrupt climatic changes occurred simultaneously on a hemispheric scale [Benson et al., 1997, Severinghaus and Brook, 1999] as indicated by the very similar oxygen isotope records from Greenland ice cores, European lake sediments [Schwander et al., 2000], and a variety of other paleoclimatic proxies that can be used to reconstruct climatic change and concurrent environmental conditions, e. g., chironomids, pollen, ostracods, varves and lake level changes [Heiri and Millet, 2005, Lotter et al., 2012, Niessen et al., 1992, Peyron et al., 2005, von Grafenstein et al., 1992]. Over a 50 year period, Greenland summit warmed 9 ± 3 °C [Severinghaus and Brook, 1999], while an increase in summer temperatures between 3 °C [Heiri and Millet, 2005] and 5.5 °C [Peyron et al., 2005] in summer temperatures has been reconstructed for Western Europe north of the Alps. At Gerzensee Lotter et al. [2012] reconstructed an increase in July temperature between 2–3 °C (chironomids) and 4–5 °C (pollen) that parallels a shift of more than 3‰ in a high-resolution stable oxygen-isotope record from bulk carbonates in the same core. Concurrent with this abrupt warming, a significant increase in atmospheric N₂O concentration is recorded in Greenland ice, from approx. 220 ppbv to 263 ppbv [Flückiger et al., 1999, Schilt et al., 2010]. While this event is a typical example of the simultaneous changes in temperature and N₂O concentrations that occurred during the last glacial period and into the deglaciation, current interpretation of the ice-core record cannot specify the relative contributions of different sources, e.g., terrestrial or marine, that could have caused the rapid increase in atmospheric N₂O concentrations.

Before the industrial period (ca. AD 1850), and at steady-state conditions, terrestrial soils are considered to have been the main source of atmospheric N₂O, accounting for ca. two thirds of the total source [Kroeze et al., 1999], while the remaining third is attributed to the oceans [Flückiger et al., 2004]. In soils, N₂O emissions mainly result from the nitrification and denitrification that occurs during microbial respiration of soil organic matter [Ambus, 1998]. N₂O emissions from soils are influenced by soil physical properties including soil temperature, pH, and air-filled pore-space, and by biological factors including the availability of mineral nitrogen and labile carbon, and interactions between these factors [Burford and Bremner, 1975, Conrad et al., 1983, Granli and Bøckman, 1994, Müller and Sherlock, 2004, Nägele and Conrad, 1990]. The O₂ content of soils is particularly important for denitrification,

where temporally water-saturated soils tend to produce the largest N₂O emissions. We would therefore expect terrestrial N₂O emissions to react strongly to an abrupt climatic change that influenced both temperature and precipitation. At present, the interpretation of the ice-core record of changes in atmospheric N₂O is limited by our inability to quantify directly the response of terrestrial and marine sources to abrupt climatic change.

The goal of the current study is to investigate the sensitivity of terrestrial N₂O emissions to an abrupt warming and wetting event. Multiproxy analyses at the Gerzensee in central Switzerland have provided reconstructions of temperature anomalies and changes in vegetation composition at the time of the Last Glacial termination on the basis of records of $\delta^{18}\text{O}$ of lake carbonates and of pollen and chironomids [e.g. Lotter et al., 2000, 2012, Schwander et al., 2000]. Vegetation reconstruction from the pollen record at the Gerzensee site for the time of the Oldest Dryas/Bølling transition shows a shift from open, tundra-like vegetation to a more forested landscape with a characteristic peak in *Juniperus* pollen, followed by an increase in broadleaved tree taxa [Ammann et al., 2011, van der Knaap, 2009].

Remarkable, and important for nitrogen cycling, is the abundant appearance of pollen of *Hippophaë rhamnoides* approximately 50 years after the initial abrupt warming and the increase in *Juniperus* pollen. *H. rhamnoides* (L., Sea Buckthorn), is a heliophytic, nitrogen-fixing deciduous shrubby species known for its ability to colonize soils that are poor in nitrogen and deprived of organic matter [Reynauld, 1975]. The expansion of *H. rhamnoides* in the Late Glacial is well documented in the European fossil pollen record [Lang, 1994]. It was particularly abundant on immature glacial till and other substrates at an initial stage of soil development following the retreat of Pleistocene ice in both the Alps and northern Europe [Firbas, 1949, Peteet, 2000, Sandegren, 1943]. At present this poorly competitive species is restricted to coastal habitats or along mountain streams in the Alps, Pyrenees and Carpathians [Bartish et al., 2006]. The association Hippophaë-*Juniperus*, followed by an increase in birch pollen, is typical for the transition into the Bølling [Ammann et al., 1994, Peyron et al., 2005, Reynauld, 1975, Skogen, 1972] and not specific for the Gerzensee site.

Being a nitrogen-fixing species, *H. rhamnoides*, along with similar N-fixing shrubs such as *Alnus* spp., is likely to have played an important role in facilitating primary succession on immature soils after the melting of glacial ice. Low nutrient levels and nutrient limitations to plant growth have been identified as factors controlling the rate of early primary succession [Chapin et al., 1994, Lawrence et al., 1967, Schoenike, 1958, van Cleve et al., 1971, Viereck, 1966, Vitousek and Walker, 1987, Walker, 1989]. Symbiotic N-fixers are often prominent in early primary succession and can directly enhance growth of associated species [Binkley et al., 1984, Blundon and Dale, 1990, Lawrence, 1951, Stevens and Walker, 1970]. Moreover, the presence of nitrogen-fixers is closely associated with accumulation of soil nitrogen [Bormann and Sidle, 1990, Crocker and Major, 1955, Ugolini, 1966].

Given the record of rapid environmental change at the Gerzensee, its location in one of the parts of the Earth's land surface most extremely affected by the Bølling warming event, and

Chapter 2. The effect of abrupt climatic warming on biogeochemical cycling and N₂O emissions in a terrestrial ecosystem

the widespread appearance of a N-fixing plant species that is not common under present-day conditions, we use this site to illustrate the sensitivity of terrestrial N₂O emissions to abrupt climatic change. Specifically, we hypothesize that 1) the pronounced and abrupt change in climate at the transition from Oldest Dryas to Bølling included an increase in N₂O emissions at the Gerzensee, and 2) the high abundance of *H. rhamnoides* shortly after the warming and wetting contributed to an enrichment of nitrogen, therefore providing additional nitrogen for nitrification and denitrification and additionally enhancing the release of N₂O. To test these hypotheses, we combine a scenario of climate and land cover change based on a synthesis of high-resolution multiproxy data with process modeling of nitrogen cycling at Gerzensee and quantify the effect of abrupt climatic and land-cover change on N₂O emissions.

2.2 Methods

To drive a process-oriented nitrogen cycle model and simulate the effects of abrupt warming and the presence of a symbiotic N-fixer on N₂O emissions, we used the high-resolution bulk carbonate $\delta^{18}\text{O}$ and pollen records from Gerzensee to develop a scenario of changes in climate and land cover. We assembled soil-texture data from maps of the present day situation. Using these datasets to drive the nitrogen cycle scheme of the ORCHIDEE-CN (O-CN) dynamic global vegetation model [Zaehle and Friend, 2010a]), we made a number of simulations to test the sensitivity of N₂O emissions on soil properties, climate, and vegetation change.

2.2.1 Site location, period of interest, and soils

Gerzensee (46.830 °, 7.547 °E) is a kettle-hole lake located on the Swiss Plateau, ca. 15 km southeast of Bern. With a surface area of 0.27 km², a catchment area of 2.6 km² and a maximum water depth of 10 m it is a valuable archive of environmental change throughout the Late Glacial and Holocene. In recent years the Gerzensee record has been studied intensively on local to regional scales to infer the effects of past abrupt climate change on ecosystem behavior with focus on the time of the Younger Dryas by using multiproxy approaches [Ammann, 2000, Brooks, 2000, Hofmann, 2000, Lemdahl, 2000, Tobolsky and Ammann, 2000, Wick, 2000].

The Oldest Dryas/Bølling transition starts about 14680 yr BP and reaches peak warming about 110 years later (14670 BP). In order to include the period covered by ice core records and characterized important changes in vegetation cover, our model simulations cover the 400-year period between 14800 and 14400 BP. A chronology for the Gerzensee site for our period of interest has been developed by van Raden et al. [2012]. All temporal references in this paper are given in calendar years before AD 1950 (years BP) and refer to the van Raden et al. [2012] chronology.

N₂O emissions are known to react sensitively to soil physical and chemical parameters, specifically soil temperature, soil water content [Dobbie and Smith, 2003, Zhang and Han, 2008], and soil pH [Simek and Cooper, 2002, Simek et al., 2002]. Soil water affects nitrifier and denitrifier

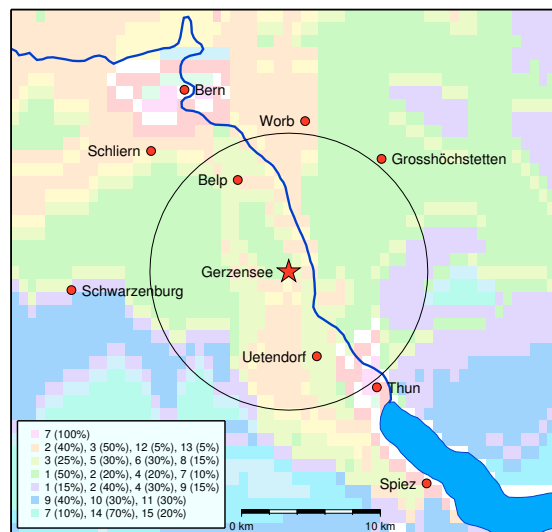


Figure 2.1: Map showing the spatial distribution of the major soil types at Gerzensee (star symbol) as derived from the Harmonized World Soil Database (HWSD). All soil types within a radius of 10 km to the Gerzensee site (circle) have been taken into account for this study. Most major soil types in the HWSD are subdivided into up to 4 sub-types. The numbers given in the legend of the soil map correspond to the soil numbers in Tab. 1, percentage numbers in brackets indicate the fraction that the corresponding soil takes up within the major category given through the assigned color in the map.

activity, nutrient concentration, redox conditions and gas diffusion [Weitz et al., 2001]. An increase in water filled pore space (WFPS) causes a shift from nitrification to denitrification as dominant source for N_2O emissions and leads to a pronounced increase in overall N_2O emissions [Davidson, 1992]. In order to take the influence of variable soil conditions on N_2O emissions into account, we assume that the pollen record at Gerzensee is representative within an area of 10 km around Gerzensee. Unfortunately, soil conditions at the time of Late Glacial are unknown and certainly differed from the present ones. It is likely that the freshly exposed glacial till at the time of the transitions was quite heterogeneous in terms of grain size distribution. Nevertheless, present-day soil conditions are the closest approximation available and therefore have been used to account for differences related to soil physics and chemistry. In order to test the effect of soil heterogeneity, all present-day soil types within a 10 km search radius (315 km², Fig. 2.1) around Gerzensee were extracted from the Harmonized World Soil Database [FAO et al., 2008]. We made separate model runs for each of the 15 soil types. The pH values of the soils were between 4.1 and 8.0, and sand contents between 20% and 87%, therefore displaying a large variety of different soil types. This allows us to evaluate the sensitivity of N_2O emissions to varying soil conditions. Depending on the mineral composition of the soils, the simulated hydrological conditions ranged from well drained on almost pure sand to poorly drained on very clayey soils. In a post-processing step, we averaged the N_2O emissions calculated for the 15 soil types tested, using the fraction of area that each soil took up within the 10 km search radius as weighting factor.

Chapter 2. The effect of abrupt climatic warming on biogeochemical cycling and N₂O emissions in a terrestrial ecosystem

2.2.2 Paleoclimate scenario for O-CN

O-CN requires daily hydro-meteorology (temperature and soil water content) to calculate nitrogen dynamics. For our experiments over the Bølling warming event, we developed a scenario of temperature and precipitation based on archives collected at Gerzensee and from other nearby sites. To estimate annual temperature anomalies, we used bulk carbonate $\delta^{18}\text{O}$ values from Gerzensee core GEJK [von Grafenstein et al., 2012]. This original time series has approximately decadal resolution. To create temperature anomalies with annual resolution we linearly interpolated between the points. This time series then was subtracted from the mean annual air temperature at Gerzensee at the present day in order to produce a time series of annual mean temperatures in the past. We reconstruct a mean temperature anomaly of -7.3 ± 0.5 °C for the 50 years prior to (14730-14680 BP) and -2.1 ± 0.3 °C for the 50 years around the peak of the transition (14600-14550 BP), resulting in a average increase in annual mean temperature of 5.2 °C. This increase is broadly consistent with the published estimates of July temperature changes reconstructed for this time period at Gerzensee of 4-5 °C for pollen, but higher than the 2-3 °C reconstructed from chironomids [Lotter et al., 2012], assuming that these reconstructed July temperature changes are also indicative for the range of change in mean annual temperature.

As daily variability in soil moisture, especially short-lived saturation events, are very important for soil N₂O emissions, we used a WGEN-based weather generator [Richardson and Wright, 1984] to create daily values for temperature and precipitation for the time period between 14800 BP and 14,000 BP. To generate precipitation anomalies, we used the pollen-based reconstruction of precipitation at Lac Lautrey [Peyron et al., 2005], located 130 km from Gerzensee (46.587 °N, 5.864 °E). Annual precipitation values reconstructed for Lac Lautrey before and after the transition were scaled to present day precipitation at Lac Lautrey. The resulting scaling factors then were applied to present day precipitation at Gerzensee to obtain the corresponding estimates for annual precipitation amounts at Gerzensee before and after the transition. With an annual precipitation of approx. 1700 mm at present day and a value of approx. 250 mm prior to and 800 mm after the transition for Lac Lautrey, this results in an increase of 360 mm for Gerzensee from 160 mm to 520 mm given a present day annual mean precipitation of 1100 mm. In order to produce an annually resolved timeseries of precipitation change at Gerzensee, we modulated the total change in precipitation inferred from the change reconstructed at Lac Lautrey with the high-resolution temperature reconstruction from Gerzensee. The monthly climatology used to drive the weather generator was derived from present day climatology for the Gerzensee adjusted by the reconstructed mean annual temperature and precipitation anomalies, i.e., the timing and magnitude of the seasonal cycle in our paleoclimate scenario are exactly the same as at present day. The number of days per year with precipitation is approximated as a linear function of total precipitation.

Daily values of climate produced by the weather generator were used as input for a simple soil hydrology model combining equations from BIOME 1 [Prentice et al., 1992] and pedotransfer functions from Saxton and Rawls [2006] to simulate daily values of soil-water content. The

hydrological dynamics simulated by this model produces daily values of soil water content and drainage loss depending on soil physical properties such as grain size distribution and organic matter content. Unsaturated hydraulic conductivity is updated every 30 seconds and water loss due to drainage is integrated over the course of a day. Daily soil water content is calculated based on the integrated loss of drainage and evapotranspiration, providing one value for soil moisture per day. The soil hydrology model does not calculate soil oxygen concentrations, but the nitrogen model includes functions to estimate anaerobic volumetric pore space and oxygen partial pressure depending on soil water content. Daily values of soil water content and temperature are required as abiotic drivers for the nitrogen dynamics model.

2.2.3 Vegetation change during the transition period

In order to generate an estimate of the vegetation composition in the region around Gerzensee, we used pollen percentages of selected taxa for the time of the transition [Ammann et al., 2012] to drive a biomization method [Peyron et al., 1998, Prentice et al., 1996] in order to generate a time series of Plant Functional Type (PFT) scores. We collapsed the 22 PFT scores delivered by the biomization method to the 3 PFTs required by O-CN (grass/herbaceous, needleleaf evergreen, broadleaf summergreen) and determined fractional values for each of the three PFTs (Fig. 2.2b) in order to know their contribution to the vegetation composition at a given time. As the original pollen record has a temporal resolution of ca. 15 years, we used linear interpolation in order to obtain annual fractions for the 3 collapsed PFTs. The annual PFT fraction values were used to calculate total annual N₂O emissions as a weighted average of the simulated annual PFT-specific emission values.

2.2.4 Biological nitrogen fixation

To test the effect of biological nitrogen fixation (BNF) by *H. rhamnoides* on N₂O emissions, we estimated the amount of nitrogen fixed by this species based on an approximation of its changing spatial coverage during the simulation. *H. rhamnoides* lives in symbiosis with nitrogen-fixing actinomycetes [Benson and Silvester, 1993], and is reported to fix between 300–1800 mg m⁻² yr⁻¹ of nitrogen [Dhyani et al., 2007, Stobdan et al., 2008, Zike et al., 1999] in pure culture. According to Lu [1992], *H. rhamnoides* capacity to fix nitrogen can be twice higher than that of soybean, and may increase the soil nitrogen content by 1.5 times within 3 years after establishment and 3-6 times within less than 50 years after establishment, although the nitrogen fixation activity may vary in response to environmental factors such as climate and nutrient status of the soil [Stewart and Pearson, 1967]. *H. rhamnoides* is a low pollen producer [Erdtman, 1969, Godwin, 1975], so any significant fraction of the total pollen spectrum belonging to this taxon indicates that its presence on the landscape was important. As we know the pollen percentages (see Fig. 2.2b) and accumulation rates of *H. rhamnoides*, but not the link between pollen percentages and landscape coverage of the species, we tested a number of different scenarios with different levels of nitrogen fixation accounting for a potential range of *H. rhamnoides* abundance on the landscape.

Chapter 2. The effect of abrupt climatic warming on biogeochemical cycling and N₂O emissions in a terrestrial ecosystem

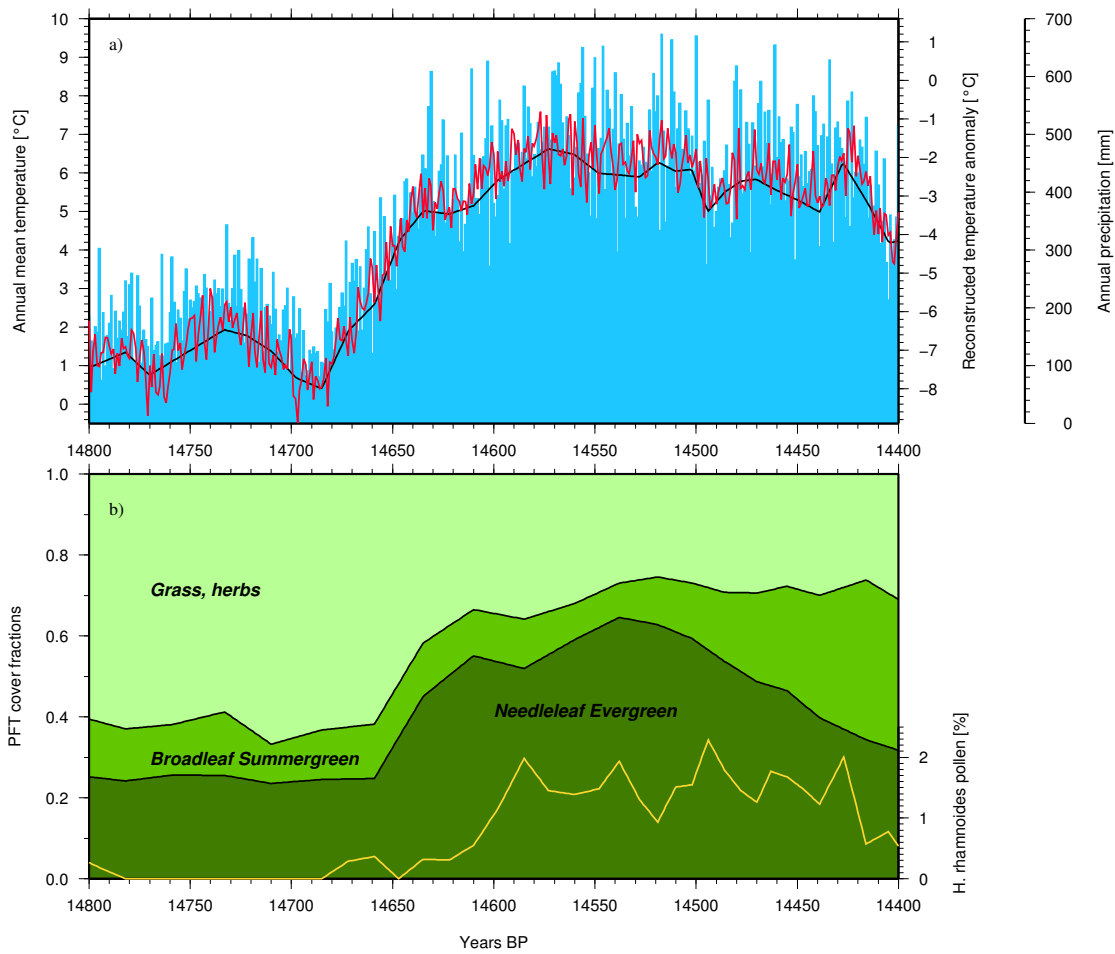


Figure 2.2: a) Annual mean temperature (red curve) simulated with the weather generator, temperature anomalies reconstructed from $\delta^{18}\text{O}$ values from ostracod shells at Gerzensee, (black curve) and annual precipitation simulated with the weather generator. b) Left axis: cover of the three PFT types used by O-CN, based on the pollen record derived from the Gerzensee core samples. Fractional contribution of PFTs to the overall vegetation cover has been estimated based on the biomization method described by Prentice et al. [1996], Peyron et al. [1998]. Right axis: Pollen percentage of *H. rhamnoides* (yellow curve).

In the baseline scenario, background nitrogen fixation by free-living soil organisms was set to $100 \text{ mg N m}^{-2} \text{ yr}^{-1}$, a value commonly suggested in the literature [Pühler, 1979]. Additional external nitrogen input was provided via atmospheric deposition, in the form of $200 \text{ mg N m}^{-2} \text{ yr}^{-1}$ each of ammonium and nitrate, respectively. These values correspond to low-level inputs reported for present-day areas that are very remote from human activities [Aber et al., 1989, Baron and Campbell, 1997, Blodau et al., 2006, Bowman, 1998]. This total baseline input of $500 \text{ mg N m}^{-2} \text{ yr}^{-1}$ was kept constant for all tested scenarios. In the baseline scenario, no additional BNF through *H. rhamnoides* was simulated (control). For the scenarios with additional BNF, annual BNF was correlated to the pollen percentage of *H. rhamnoides*, with the maximum BNF value corresponding to the year with the maximum pollen percentage for *H.*

rhamnoides. We tested 4 different levels of BNF, with maximum values between 2500 and 10000 mg N m⁻² yr⁻¹ in order to investigate the sensitivity of N₂O emissions to the presence of this nitrogen fixing shrub, and to take into account our inability to make a quantitative reconstruction of *H. rhamnoides* cover because its pollen productivity relative to other taxa in the record has never been characterized.

2.2.5 Simulation of N₂O emissions

The nitrogen model is an adaptation of the O-CN nitrogen model [Zaehle and Friend, 2010a,b, Zaehle et al., 2010] that dynamically simulates nitrogen concentrations in plants and soil, thereby allowing processes such as photosynthesis, autotrophic and heterotrophic respiration, plant allocation and nutrient turnover to respond to N status. Nitrogen inputs handled by O-CN include atmospheric deposition of nitrogen, fertilizer application and biological N fixation. Soil organic matter turnover is calculated for carbon and nitrogen pools based on the CENTURY scheme [Kirschbaum and Paul, 2002, Parton et al., 1993], while nitrification and denitrification are modeled following the DNDC-scheme by Li and Aber [2000], but without specifically calculating microbial growth. Concentrations for nitrate and ammonium are calculated as mass balance between mineralization and immobilization, adsorption of ammonium to clay minerals and drainage losses. Nitrogen losses from ecosystems to leaching and emission of trace gases from nitrification and denitrification are modeled mechanistically at a half-hourly time step [Zaehle and Friend, 2010a] and depend on factors such as soil water saturation / gas diffusivity, clay content and available substrate. For a more detailed description of O-CN including equations see [Zaehle and Friend, 2010b]. For the study at Gerzensee, we prescribe vegetation development over the time of the climatic transition as reconstructed from the pollen record instead of simulating vegetation development dynamically using a DGVG. Therefore, we are not using the part of ORCHIDEE-CN that simulates nitrogen cycling and allocation in plants. Instead, we parameterize the vegetation part of the model by prescribing typical values reported in literature for C/N ratios and biomass for each of the tree plant functional types (PFTs) grass/herbal, needleleaf evergreen and broadleaf summergreen. Due to PFT-specific differences in biomass and C/N ratios, litter amount and quality and consecutively soil organic matter decomposition, nitrification and denitrification vary between PFTs. N₂O emissions are simulated separately for each PFT using the subroutines for litter decomposition, soil organic matter dynamics and nitrogen dynamics in the soil on a daily basis. PFT-specific annual emission values are integrated in a post-processing step according to the fractional covers of the PFTs in order to obtain total emission values per unit area.

2.3 Results

The reconstructed temperature anomaly for the transition from Oldest Dryas to Bølling shows that the change in climate occurred very rapidly, within approx. 100 years (Fig. 2.2a). On average, the reconstructed temperature anomaly for the 50 years prior to the onset of the

Chapter 2. The effect of abrupt climatic warming on biogeochemical cycling and N₂O emissions in a terrestrial ecosystem

abrupt warming (14,730-14,680) was -7.3 ± 0.5 °C relative to present; in the 50 years around the peak of the warming period, temperature anomalies were -2.1 ± 0.3 °C (14,600-14,550 BP), resulting in an average increase of 5.2 °C as compared to the beginning of the warming. Using the weather generator, we simulated a mean temperature increase of 5.3 °C, from 1.2 ± 0.7 °C to 6.5 ± 0.6 °C, and a mean increase in precipitation of 316 mm, from 180 ± 63 mm to 496 ± 77 mm.

For the scenario with a constant background input of $500 \text{ mg N m}^{-2} \text{ yr}^{-1}$ provided by atmospheric deposition and nitrogen fixation by free-living soil organisms (baseline scenario), simulated total N₂O emissions (in the following always referred to in the unit of $\text{mg N}_2\text{O-N}$) for the area around Gerzensee increased significantly over the warming: We simulated a mean increase of $12.5 \text{ mg N m}^{-2} \text{ yr}^{-1}$, from $7.7 \pm 2.4 \text{ mg N m}^{-2} \text{ yr}^{-1}$ to $20.2 \pm 5.9 \text{ mg N m}^{-2} \text{ yr}^{-1}$. Maximum and minimum annual values simulated in the 50-year-period prior to the warming are $14.4 \text{ mg N m}^{-2} \text{ yr}^{-1}$ and $3.8 \text{ mg N m}^{-2} \text{ yr}^{-1}$, respectively, and $40.4 \text{ mg N m}^{-2} \text{ yr}^{-1}$ and $11.8 \text{ mg N m}^{-2} \text{ yr}^{-1}$ for the 50 years following the warming. Emissions between different soil types showed considerable variability, ranging between mean values of $1.0 \pm 0.5 \text{ mg N m}^{-2} \text{ yr}^{-1}$ and $11.8 \pm 3.5 \text{ mg N m}^{-2} \text{ yr}^{-1}$ prior to the transition, and $4.1 \pm 1.6 \text{ mg N m}^{-2} \text{ yr}^{-1}$ and $28.5 \pm 8.2 \text{ mg N m}^{-2} \text{ yr}^{-1}$ after the transition (Tab. 1). Emissions were lowest for a soil type with 73% sand and 6% clay with pH 4.1, and highest for a soil type with 37% sand, 23% clay and pH 6.2. Soil water content was the main soil physical property influencing emissions, followed by pH. For the very sandy soil, annual mean soil water saturation increased from $21.0 \pm 5.2\%$ to $40.3 \pm 4.2\%$, while an increase from $42.8 \pm 4.7\%$ to $60.3 \pm 3.8\%$ was simulated for the soil type with 37% sand.

During the first 50 years preceding the warming, from 14730 to 14680 BP, pollen percentages for *H. rhamnoides* were zero and then started to increase slightly. Therefore differences between the baseline scenario without additional BNF and the scenarios with different levels of BNF are not significant. For the BNF100-scenario (100 kg ha⁻¹ yr⁻¹ of additional nitrogen fixation at the time of maximum *H. rhamnoides* coverage) as well as for the baseline scenario (no additional BNF), the total average annual emissions prior to the warming are $7.7 \pm 2.4 \text{ mg N m}^{-2} \text{ yr}^{-1}$ as compared to $20.2 \pm 5.9 \text{ mg N m}^{-2} \text{ yr}^{-1}$ (baseline scenario) and $31.3 \pm 7.7 \text{ mg N m}^{-2} \text{ yr}^{-1}$ (BNF100 scenario) for the 50 years around the peak of the warming and wetting. This is a slight increase in emissions as compared to the baseline scenario, but still lies within the range of uncertainty. *H. rhamnoides* pollen percentages start to increase around 14,646 BP and exceed 1% around 14,600 BP, reaching a first maximum of 1.98% around 14,585 BP (Fig. 2.2b). They reach their maximum value of 2.29% around year 14,494 BP, but stay higher than 1% until approx. year 14,420 BP.

In the range of the scenarios that we tested, simulated N₂O emissions react linearly to the additional supply of nitrogen provided by biological nitrogen fixation from *H. rhamnoides*. In average, an increase of $1000 \text{ mg N m}^{-2} \text{ yr}^{-1}$ in nitrogen supply causes an increase in emissions of $1.6 \text{ mg N m}^{-2} \text{ yr}^{-1}$. For the time with maximum cover of *H. rhamnoides*, simulated N₂O emissions are up to 1.89 times higher for the BNF100-scenario, and 1.45 times higher for the

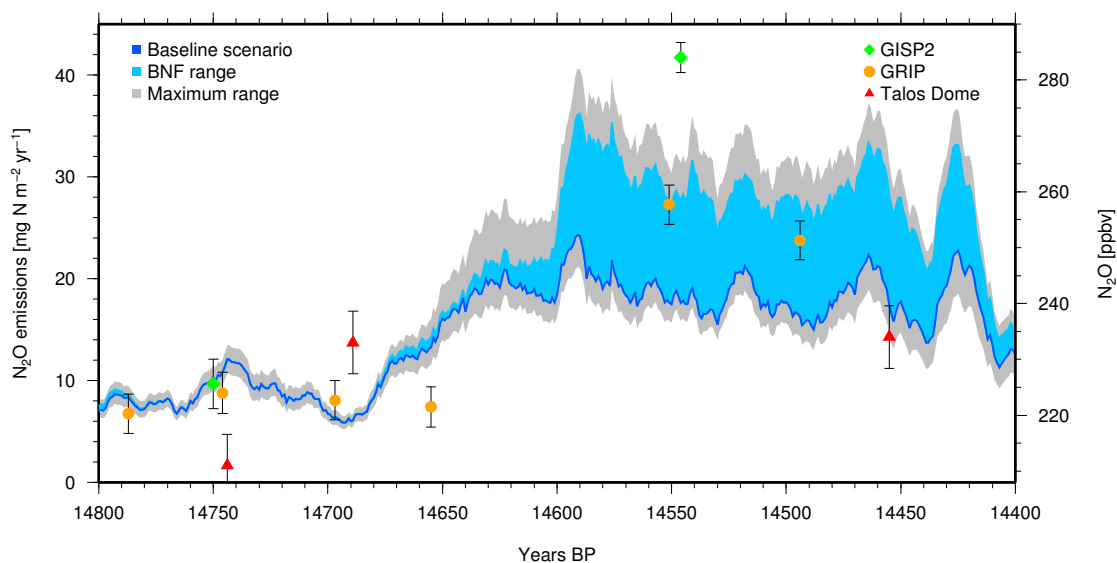


Figure 2.3: Simulated N_2O emissions for the time of the abrupt Bølling warming and atmospheric N_2O concentrations from ice core records. The blue line outlines the increase of N_2O emissions due to the warming and wetting with N-input kept at a constant, low level over time (baseline scenario). The upper edge of the light blue area corresponds to the N_2O emissions simulated for the BNF100 scenario. For the 4 tested BNF scenarios, emissions react linearly to additional nitrogen and lie within the blue area. The lower bound of the grey area corresponds to emissions from a pure coniferous evergreen forest stand under baseline conditions, while the upper bound corresponds to the emission line for a pure broadleaf summergreen forest under BNF100 conditions. Ice core data are from Sowers et al. [2003], Flückiger et al. [1999], Schilt et al. [2010]

BNF50-scenario as compared to the baseline scenario. Over the time period presented in Fig. 2.3, the total amount of N_2O emitted for the BNF100 scenario was 1.4 times higher than for the baseline scenario and 1.6 times higher over the time while the *H. rhamnoides* pollen percentages were higher than 1%.

PFT-specific emission values were highest for soils below broadleaf summergreen trees, followed by soils below herbaceous/grasses and needleleaf evergreen trees. Over the course of the 300 years from 14700 to 14400 cal. yr BP, total emissions for the grassland/herbaceous PFT-type were 1.2 times higher than those of the coniferous type, while emissions for the broadleaf summergreen type were 1.2 times higher than those of the grassland/herbaceous type. The lower boundary of the grey area in Fig. 2.3 corresponds to the emission line for coniferous evergreen forest under baseline conditions (no additional BNF), while the upper boundary corresponds to the emission line for broadleaf summergreen forest under BNF100 conditions (maximum tested BNF).

2.4 Discussion

Our simulations for the transition from the Oldest Dryas cold period to the Bølling warm period clearly suggest that N₂O emissions from the terrestrial biosphere reacted very sensitively to abrupt climatic warming and wetting. As hypothesized we found N₂O emissions to be responsive to a variety of different environmental factors that were included in our scenario of climatic and vegetation change at Gerzensee. Emissions reacted positively to increasing annual temperature and precipitation and on nutrient priming due to biological nitrogen fixation. Abiotic soil properties, e.g. soil pH, clay content and water retention capacity, caused considerable variability in simulated N₂O emissions. In the following sections, each of these aspects is discussed in more detail.

2.4.1 Uncertainties related to the climate reconstruction

With roughly decadal resolution, the $\delta^{18}\text{O}$ proxy record of the Gerzensee site is an exceptionally detailed record of the abrupt climatic change event in a terrestrial setting. Interpolation of this palaeoproxy record to annual time steps and the simulation of daily hydro-meteorology on these data by using a weather generator and a simple soil hydrology model introduce uncertainty in our results. As the $\delta^{18}\text{O}$ palaeoproxy record only allows a reconstruction for the temperature change but not for the change in precipitation, additional uncertainty arises from the need to scale the Lac Lautrey change in annual precipitation to the Gerzensee. Peyron et al. reconstructed values for annual precipitation at Lac Lautrey before and after the transition which provides a framework for the overall range of change in annual precipitation, but we had no information on how the increase happened in detail. The forced correlation between precipitation change and temperature change assumes a connection between both parameters that may not have existed in this form and also makes it difficult to separate the effect caused by the temperature increase from the effect triggered by the increase in annual mean precipitation. It is also uncertain if the ratio between annual precipitation amounts at Gerzensee and Lac Lautrey were the same at the time of the glacial termination as at present day. Moreover, since the only palaeoclimate reconstruction we had was mean annual temperature, and linked to it precipitation, we were not able to take into account potential changes in seasonality in the climate data we used to drive the nitrogen model. Changes in seasonality could have an impact on N₂O emissions, in particular if precipitation seasonality was different, e.g., if summers were relatively drier (or wetter) than at present. In this case we might expect less (more) N₂O emissions than the ones that we simulated, as soil microbial sensitivity is expected to be highest when temperatures are high, i.e. in summer. Nevertheless, the resulting data used to drive our model represent a plausible scenario of the climatic changes that occurred during the Bølling warming event, as the mean temperature increase simulated by the weather generator differs only slightly from the reconstructed mean (5.7 °C as compared to 5.5 °C, respectively). It is also important to note that the magnitude of the mean annual temperature rise during the abrupt warming (0.06 °C yr⁻¹) is smaller than the reconstructed inter-annual variability in temperature from either before (0.5 °C) or after

Table 2.1: Simulated N₂O emissions before and after the 30-year-transition period for the baseline scenario and the BNF100 scenario for the 15 different soil types extracted from the HWSD within a 10-km-radius around the Gerzensee site.

#	Soil characteristics [%]					50-year-av. N ₂ O emissions [mg m ⁻² yr ⁻¹]			
	Sand	Clay	Corg	pH	Area	BNF0		BNF100	
						before	after	before	after
1	42	20	1.5	5.1	25.6	7.9 ± 2.5	20.3 ± 5.9	7.9 ± 2.5	31.7 ± 7.8
2	45	19	1.0	6.4	19.1	8.4 ± 2.7	21.4 ± 6.5	8.4 ± 2.7	33.7 ± 8.6
3	42	22	1.0	6.4	14.1	10.5 ± 3.1	25.5 ± 7.3	10.5 ± 3.1	40.0 ± 9.5
4	40	21	1.0	5.1	11.7	8.6 ± 2.6	21.6 ± 6.2	8.6 ± 2.6	33.8 ± 8.1
5	37	23	1.1	6.2	6.8	11.8 ± 3.5	28.5 ± 8.2	11.8 ± 3.5	45.2 ± 10.6
6	80	8	0.6	6.8	6.8	2.2 ± 1.1	7.6 ± 3.3	2.2 ± 1.1	11.3 ± 4.5
7	20	40	33.6	4.3	5.0	2.1 ± 0.8	10.9 ± 5.3	2.1 ± 0.8	18.0 ± 8.4
8	39	22	1.7	6.6	3.4	10.3 ± 3.2	26.1 ± 7.6	10.3 ± 3.2	41.2 ± 9.9
9	73	6	1.2	4.1	2.7	1.0 ± 0.5	4.1 ± 1.6	1.0 ± 0.5	5.8 ± 2.1
10	75	10	0.9	5.1	1.3	2.7 ± 1.2	8.6 ± 3.3	2.7 ± 1.2	12.8 ± 4.4
11	87	4	2.2	4.4	1.3	1.3 ± 0.7	5.5 ± 2.4	1.3 ± 0.7	7.8 ± 3.1
12	34	18	0.6	8.0	0.8	5.9 ± 2.0	15.6 ± 4.9	5.9 ± 2.0	25.1 ± 6.7
13	44	21	0.8	8.0	0.8	7.3 ± 2.2	17.7 ± 5.1	7.3 ± 2.2	27.7 ± 6.7
14	38	20	4.6	5.2	0.4	7.5 ± 2.7	22.5 ± 7.1	7.5 ± 2.7	35.2 ± 9.7
15	24	12	3.0	4.6	0.1	3.4 ± 1.4	11.8 ± 4.7	3.4 ± 1.4	18.9 ± 6.8
Overall emissions:						7.7 ± 2.4	20.2 ± 5.9	7.7 ± 2.4	31.3 ± 7.7

the warming event (0.5 °C).

2.4.2 Influence of soil properties on N₂O emissions

Soil pH is known to influence N₂O production, as microbial nitrification and denitrification and chemical denitrification all react sensitively to changing pH values. Although the effect of pH on N₂O emissions from soils in detail can be complex [Yamulki et al., 1997], nitrification and denitrification rates generally tend to increase with pH with nitrifiers being more sensitive to acidic conditions than denitrifiers, but at the same time, the mole fraction of N₂O/ (N₂O + N₂) is known to decrease as pH increases [e.g. Firestone et al., 1980, Nömmik, 1956]. Simulating N₂O release for 15 different soil types with pH values ranging between 4.1 and 8.0, our model could reproduce the general pattern of decreasing N₂O emissions with decreasing pH, but this was dampened by the effect that varying soil moisture in the different soil types (textures) had on emissions. Due to their higher water retention capacity, soils with higher clay contents drain more slowly than sandy soils and stay wet for a longer time. This is reflected in the N₂O emission values presented in Table 2.1 and illustrated in Fig. 2.4b, which tend to increase with increasing clay contents of the soil with exception of soil 7 that has a clay content of 40%, but low emissions. The reason for this is due to fact that the simple water bucket model that we are using to simulate daily soil water content estimates a very high porosity and fast drainage

Chapter 2. The effect of abrupt climatic warming on biogeochemical cycling and N₂O emissions in a terrestrial ecosystem

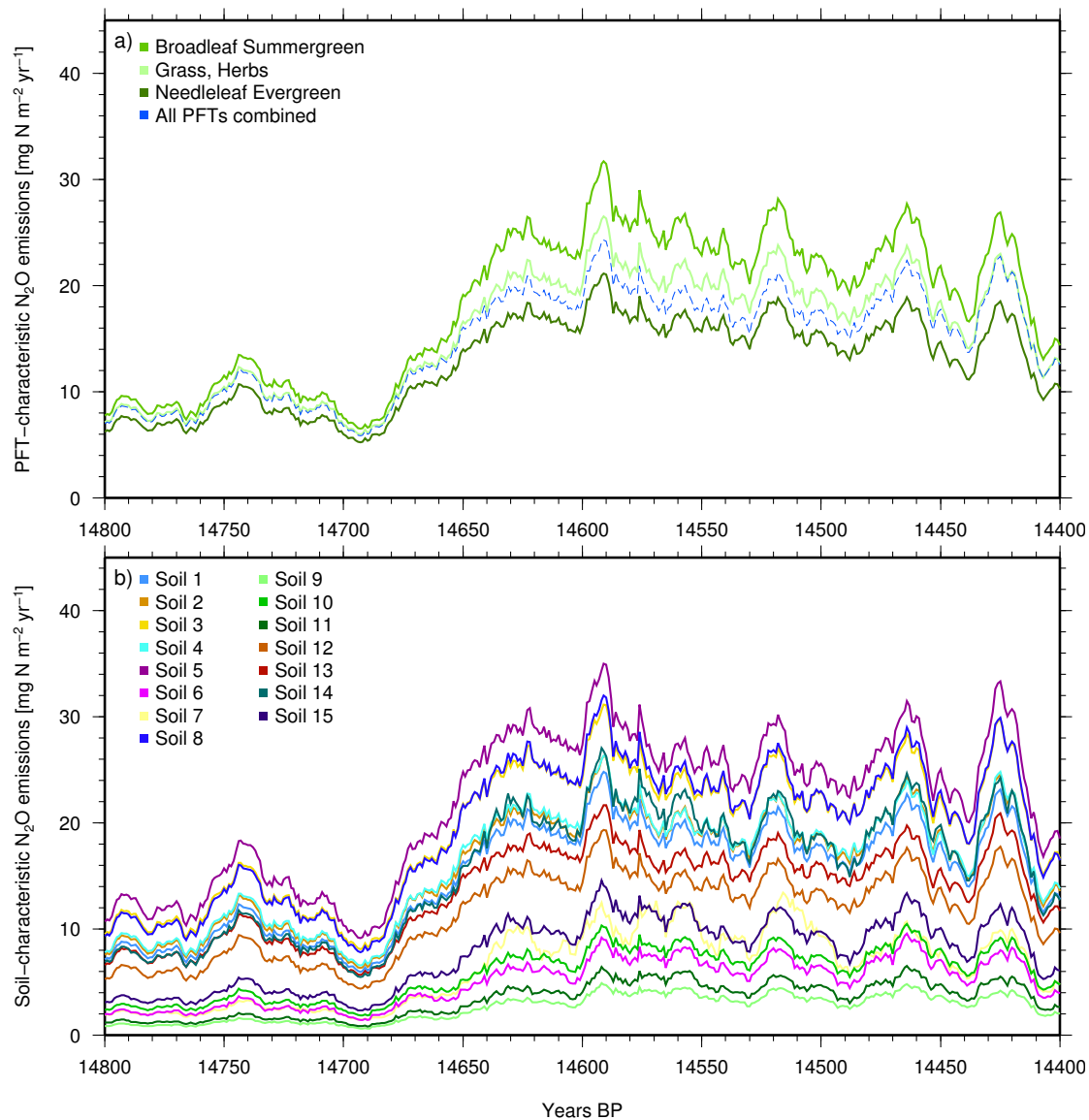


Figure 2.4: a) Green lines: characteristic emissions for the three simulated PFTs (BNF0 scenario). The blue line represents the emissions integrated over all three PFTs, weighed according to their contribution to the reconstructed vegetation cover. PFT-specific differences in N₂O emissions are due to differences in C/N ratios and biomass, i.e. litter quantities and qualities are different thereby influencing nitrogen mineralization, nitrification, denitrification and emissions. b) Characteristic emission signals for all 15 of the tested soils (BNF0 scenario). Differences in N₂O emissions are caused by differences in pH as well as grain size distribution and soil organic matter content, i.e. soil water retention capacity and absorption of ammonium.

for this soil because of its high organic matter content. A more realistic simulation of soil hydrology in organic soils is likely to produce more realistic estimates of N₂O emissions for these kinds of soils. In order to clearly and quantitatively disentangle the effects of pH and soil

moisture, further sensitivity studies with both parameters being tested separately would be required. In combination, pH and soil moisture caused significant variability in N₂O release, with emissions varying by almost one order of magnitude among soils. Although we had to use present-day soil data for our simulations, we are confident that by testing the sensitivity of N₂O emissions over a broad range of different soils within a larger area around Gerzensee we can take into account the fact that uncertainties due to exact soil conditions at the time of the transition are unknown. As soils developed from glacial till at the Gerzensee site, the mineral composition likely did not change considerably. Over the course of the Holocene, the depth of the soils is likely to have increased due to bedrock weathering, while at the same time soil organic matter accumulated as vegetation developed on the soils. Naturally the largest part of the N₂O emissions caused by soils stem from the topsoil layers where organic matter content and microbial activity is highest [Luo et al., 1998]. For the Gerzensee site, we simulated N₂O emissions in the top 30 cm of the soil column where the majority of the biological activity occurs. The area around Gerzensee is largely covered by thick layers of till and fluvial deposits and we do not expect shallower soils to have been widespread at any time since deglaciation.

2.4.3 Comparison of simulated N₂O emissions to present day measurements

Annual N₂O emission values reported in the literature for grassland and temperate and boreal forest ecosystems and tundra range over several orders of magnitude. Martikainen et al. [1993] report values that range from less than 4 to a maximum of 143 mg N₂O-N m⁻²yr⁻¹ for peatland sites in eastern and central Finland. Schulte-Bisping et al. [2003] estimated mean annual N₂O emission fluxes from German forest soils to be 32 mg N m⁻² yr⁻¹, with a range between 17 and 205 mg N m⁻² yr⁻¹, while Kesik et al. [2005] calculated average emission values between 55 and 62 mg N m⁻² yr⁻¹ for European forest soils, with lower emissions for the UK and some boreal forest areas, being in accordance with the values reported by Brumme et al. [2005] ranging between 10 and 30 g m⁻² N yr⁻¹. In a data compilation by Papen and Butterbach-Bahl [1999] N₂O emissions from temperate forest soils are reported over a wide range from 0 to 2000 mg N m⁻² yr⁻¹, with a mean range of 20 to 200 mg N m⁻² yr⁻¹, while Klemetsson et al. [1997] measured N₂O emissions between 2.5 and 25.4 mg N m⁻² yr⁻¹ for Norway spruce forest in southeast Sweden. Compared to these literature values, our simulated annual baseline emission values for the Late Glacial are within the range of observations, but towards the lower end. In this context it is important to emphasize that late-glacial ecosystems in central Europe were at an early stage of development, while much of the same region at the present day is nitrogen-saturated or close to a state of nitrogen saturation [Aber et al., 1989, Brumme and Khanna, 2008, Cannell and Thornley, 2000, Corre et al., 2003, Skeffington and Wilson, 1988, Tietema et al., 1998] due to high anthropogenic deposition since industrialization. Moreover, temperatures and precipitation for the time simulated in this study are still considerably lower than present day values even at the peak of warming with simulated annual mean temperature being approx. 2 °C less than at present and annual mean precipitation being half the amount reported for Gerzensee at present. Offline testing with the nitrogen model revealed that the model tends to react more sensitively to changes in soil moisture (precipitation) than to

Chapter 2. The effect of abrupt climatic warming on biogeochemical cycling and N₂O emissions in a terrestrial ecosystem

changes in temperature, although the simulated increase in emissions at Gerzensee is the synergistic product of both temperature and precipitation change. As the effect of changing precipitation from low to high on simulated N₂O emissions is higher at high temperatures due to the temperature dependency of soil microbial activity, and changes in temperature from low to high are more effective at high rather than low precipitation, especially the still considerably dry conditions at the peak of the warming may have limited N₂O emissions compared to present day conditions. Given these different ecosystem trajectories, we expect present-day nitrogen-saturated ecosystems in central Europe to have N₂O emissions that clearly exceed emission values for nutrient-limited, cooler and drier late-glacial ecosystems. It is likely that present-day boreal and tundra ecosystems with lower emission values are better modern analogues for these late-glacial ecosystems than central-European temperate forests under strong human influence. On the other hand, our simulations could underestimate N₂O fluxes by missing out on sub-daily peak emission events, e.g. linked to freeze-thaw events, due to the use of a daily rather than, e.g., half-hourly time step for the N-cycling calculations.

2.4.4 Vegetation succession and nitrogen enrichment by symbiotic fixation

Reconstructions of the ice extent in the north of the Swiss Alps indicate that the Gerzensee site probably already was ice-free between 17,000 and 18,000 cal. yr BP [Ivy-Ochs et al., 2008], but at the latest around ca. 16,000 cal. yr BP [Schlüchter, 1988], exposing glacial till as substrate for soil development, vegetation establishment and succession processes. Young substrates released by retreating glaciers are commonly poor in nutrients. Therefore plant growth in such pioneer soils tends to be limited by nitrogen [Chapin et al., 1994], which favors the presence of symbiotic N-fixing species in early primary succession [Gorham et al., 1979, Lawrence et al., 1967, Stevens and Walker, 1970]. These facilitate establishment of later-successional species by improving environmental conditions, while frequently placing themselves at a competitive disadvantage [Chapin et al., 1994] by accumulating nitrogen in the soil. The widespread presence of *H. rhamnoides* indicated in European pollen records from late-glacial times prior to the expansion of broadleaved forest tree species suggests such a mechanism, leading to an enrichment of nitrogen content in immature glacial soils. From a biogeochemical point of view, the enrichment of soil-nitrogen pools not only provides nutrients for plant growth, but also additional substrate for nitrification and denitrification, ultimately leading to an increase in N₂O emissions. Our sensitivity study clearly shows that nutrient priming by nitrogen fixers could have contributed to a significant release of N₂O from soils.

2.4.5 Simulated N₂O increase at Gerzensee and ice core records

The N₂O emissions simulated at Gerzensee represent the reaction of one relatively small, specific region and show that at small scales climate change as reconstructed from high-resolution $\delta^{18}\text{O}$ bulk carbonate and pollen records can happen very quickly and trigger very fast biogeochemical responses from ecosystems within a time scale of decades. The N₂O concentrations measured in polar ice are not always capable of resolving the full speed of

ecosystem responses to climatic change as can be seen from the N₂O concentration values from three different cores plotted in Fig. 2.3 alongside with the simulated emissions from Gerzensee. For the GRIP core, concentrations were approx. 200 ppbv at 16 ka BP, then gradually increased to 222 ppbv at 14655 BP, followed by a rapid increase to 257.7 ppbv in 14551. After this rapid increase, concentrations start to fluctuate but reach a maximum value of 268.3 ppbv in 14136. Similarly, concentrations from the GISP2 core start of with 183 ppbv at 16500 BP, then gradually increase to 225.6 ppbv at 14750 BP, followed by a rapid increase in concentrations to a maximum of 284 ppbv in 14546 BP before gradually dropping off again. For the Southern Hemisphere Talos Dome the increase in N₂O concentration is noticeable as well, but happens more gradually over a longer time span, although it is important to note that the resolution of the Talos Dome samples seem to be lower than, e.g., the resolution of the samples from the GRIP core. At Talos Dome, concentrations start to gradually increase at 15650 BP from 194.7 ppbv to a maximum of 251 ppbv at 13140 BP, which is outside the time frame visualized in Fig. 2.3. So although there is a visible reaction even for the Southern Hemisphere, it seems that the reaction was even slower than the one observed in the Greenland cores.

Compared to the speed of the reaction observed in the ice core records the reaction simulated for the Gerzensee site is very fast. It can be debated that the overall slower reactions observed in the ice cores is due to the fact that concentrations in the ice integrate over large areas with different regional responses happening at slightly different times, and gas diffusion and mixing before bubble close-off in glacier ice tends to smooth the temporal resolution of ice core gas records. It is well possible that for this reason the changes at Gerzensee seem to occur much faster than the atmospheric record indicates. Unfortunately, the ice core measurements do not better bracket the actual Bølling warming event, though this may improve in the future using continuous measurement techniques currently under development.

Although we cannot make an estimate of the total contribution of the terrestrial biosphere to the N₂O concentrations observed in polar ice in this regional scale study, we find that the very sensitive and pronounced reaction of N₂O emissions simulated for this site indicates that the role of the terrestrial land surface as a source of N₂O should not be underestimated. For a global quantification of all terrestrial sources as compared to the contribution of the oceans, a global paleoclimate reconstruction or simulation, e.g., from a GCM scenario, covering the time of the Oldest Dryas to Bølling transition would be required to drive a full DGVM such as O-CN in order to simulate vegetation dynamics and nitrogen cycling between vegetation, soils and atmosphere. Given the sensitivity of the response to abrupt climate change we find at Gerzensee, such a global-scale modeling experiment should be a priority for future research.

Chapter 2. The effect of abrupt climatic warming on biogeochemical cycling and N₂O emissions in a terrestrial ecosystem

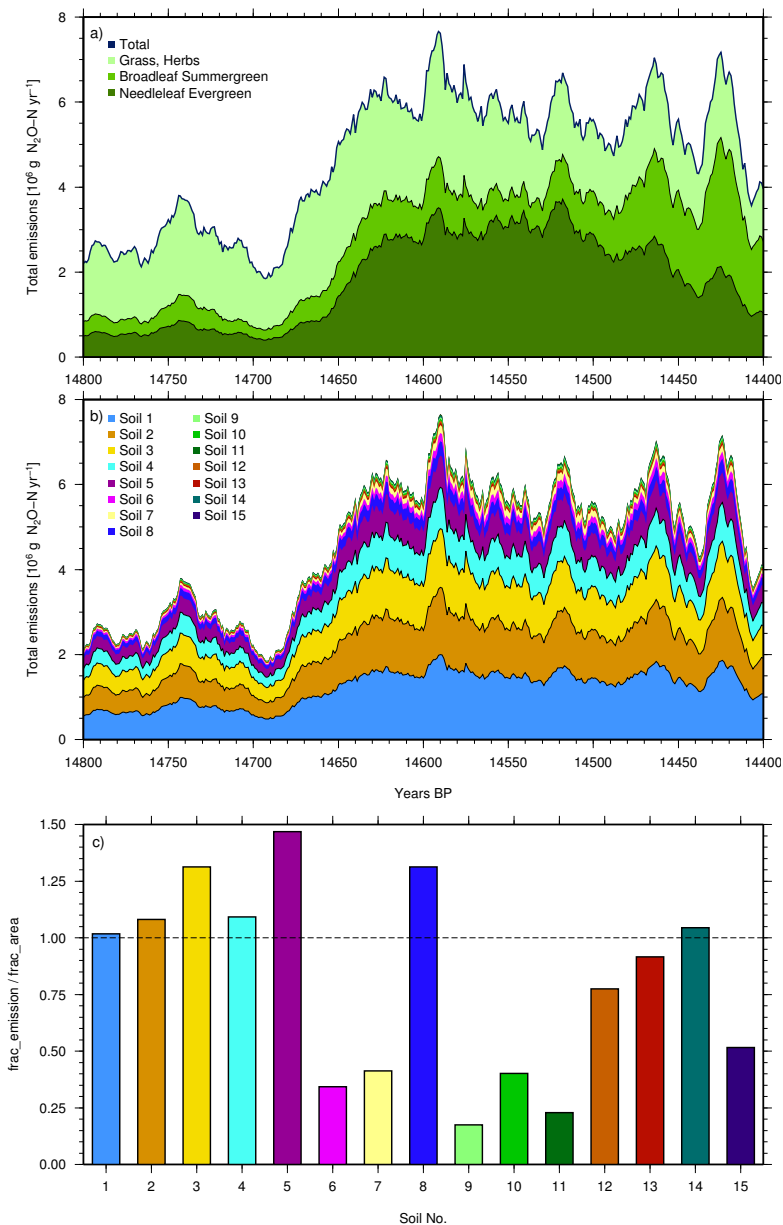


Figure 2.5: a) Total regional emissions for the 10-km area around Gerzensee stacked according to the contributions of the three PFTs (BNF0 scenario). Relative contributions of the three PFTs change over time due to the shift in vegetation composition and because PFTs do not react equally sensitive to the warming and wetting. b) Total regional emissions for the 10-km area around Gerzensee stacked according to contributions of the 15 soil types (BNF0 scenario). Differences between soils are due to their varying sensitivity and the relative contribution of the area taken up by the soil compared to the total area. c) Comparison of fraction of area occupied by soils to their fractional contribution to the total regional emissions (BNF0 scenario), integrated over the time period from 14800 BP to 14400 BP. Soils with a value of smaller (greater) than one contribute less (more) to the regional emissions than could be expected according to the fraction of area that they occupy.

2.5 Conclusions

Using a combination of modeling approaches and high-resolution multiproxy data we demonstrate that the pronounced increase in temperature and precipitation at the time of the transition from the Oldest Dryas cold phase to the Bølling warm phase caused a significant increase of terrestrial N₂O emissions from soils around the Gerzensee site in Switzerland. We are able to show that emissions react very sensitively to changes in soil moisture and vegetation composition and can vary significantly within a very short time span. For the baseline scenario with no additional BNF, we simulated an increase in emission by factor of 3.4 when comparing average emissions of the 20 years at the beginning of the transition to the 20 years at the peak of the transition.

By combining pollen records and biogeochemical modeling of the terrestrial nitrogen cycle, we show that facilitation by the presence of symbiotic nitrogen fixers such as *H. rhamnoides* in early phases of primary succession not only has important implications for initial stages of vegetation establishment on newly developing soils, but also for biogeochemical cycling and greenhouse gas emissions. By enriching soils with nitrogen and therefore providing additional substrate for nitrifying and denitrifying bacteria, the widespread presence of *H. rhamnoides* at the Gerzensee site during the Bølling warming event on average contributed an additional factor 1.5 to the release of N₂O in addition to the emissions caused by the warming and wetting when compared to the BNF100 scenario of the 20 years at the peak of the transition to the baseline scenario. Besides the unknown exact mineral composition of soils, the major uncertainty in estimating this additional N₂O release quantitatively is due to the problem that at present there is no quantitative way to reconstruct the spatial cover of *H. rhamnoides*. Consequently, only a range can be given as based on different scenarios of *H. rhamnoides* N-fixation.

The N₂O emissions that we simulate for the Gerzensee site are conservative estimates compared to the full range of emissions observed in field measurements at the present day, which range over more than three orders of magnitude depending on environmental conditions. It is therefore very likely that we underestimate the contribution of the terrestrial land surface to the overall change in atmospheric N₂O concentration observed in polar ice for the transition into the Bølling warm period by only looking at one regional-scale site. Future simulations on a global scale are needed in order to clarify the role of terrestrial soils as source of N₂O during abrupt climate change, and to contribute to an explanation of the observed concentration changes in polar ice.

Bibliography

- J. D. Aber, K. J. Nadelhoffer, P. Steudler, and J. M. Melillo. Nitrogen saturation in Northern forest ecosystems. *BioScience*, 39(6):378–386, 1989.
- P. Ambus. Nitrous oxide production by denitrification and nitrification in temperate forest, grassland and agricultural soils. *European Journal of Soil Science*, 49:495–502, 1998.
- B. Ammann. Biotic responses to rapid climatic changes: Introduction to a multidisciplinary study of the Younger Dryas and minor oscillations on an altitudinal transect in the Swiss Alps. *Palaeogeography, Palaeoclimatology, Palaeoecology*, 159:191–201, 2000.
- B. Ammann, A. F. Lotter, U. Eicher, M.-J. Gaillard, B. Wohlfahrt, W. Haeberli, G. Lister, M. Maisch, F. Niessen, and Ch. Schlüchter. The Würmian Late-glacial in lowland Switzerland. *Journal of Quaternary Science*, 9(2):119–125, 1994.
- B. Ammann, J. N. F. van Leeuwen, and W. O. van der Knaap. Vegetation response to the early rapid warming at the transition from the Oldest Dryas to the Bölling at Gerzensee (Switzerland) as recorded in a high-resolution pollen stratigraphy. *Paleogeography, Palaeoclimatology, Palaeoecology*, this volume(this issue), 2011.
- B. Ammann, J. F. N. van Leeuwen, van der Knaap. W. O., H. Lischke, O. Heiri, and W. Tinner. Vegetation responses to rapid warming and to minor climatic fluctuations during the Late-Glacial Interstadial (GI-1) at Gerzensee (Switzerland). *Paleogeography, Palaeoclimatology, Palaeoecology*, in press:20 p., PALAEO–06206, 2012. doi: 10.1016/j.palaeo.2012.07.010.
- J. S. Baron and D. H. Campbell. Nitrogen fluxes in a high elevation Colorado Rocky Mountain Basin. *Hydrological Processes*, 11:783–799, 1997.
- I. V. Bartish, J. W. Kadereit, and H. P. Comes. Late Quaternary History of *Hippophae rhamnoides* L. (Elaeagnaceae) inferred from chalcone synthase intron (Chsi) sequences and chloroplast DNA variation. *Molecular Ecology*, 15:4065–4083, 2006.
- D. R. Benson and W. B. Silvester. Biology of *Frankia* strains, actinomycete symbionts of actinorhizal plants. *Microbiological Reviews*, 57(2):293–319, 1993.
- L. Benson, J. Burdett, S. Lund, M. Kashgarian, and S. Mensing. Nearly synchronous climate change in the Northern Hemisphere during the last glacial termination. *Letters to Nature*, 388:263–265, 1997.

Bibliography

- D. Binkley, J. D. Lousier, and Jr. Cromack, K. Ecosystem effects of Sitka alder in a Douglas-fir plantation. *Forest Science*, 30:26–35, 1984.
- C. Blodau, N. Basiliko, B. Mayer, and T. R. Moore. The fate of experimentally deposited nitrogen in mesocosms from two Canadian peatlands. *Science of the Total Environment*, 364:215–228, 2006.
- D. J. Blundon and M. R. T. Dale. Dinitrogen fixation (acetylene reduction) in primary succession near Mount Robson, British Columbia, Canada. *Arctic and Alpine Research*, 22:255–263, 1990.
- T. Blunier and E. Brook. Timing of millennial-scale climate change in Antarctica and Greenland during the last glacial period. *Science*, 291:109–112, 2001.
- B. T. Bormann and R. C. Sidle. Changes in productivity and distribution of nutrients in a chronosequence at Glacier Bay National Park, Alaska. *Journal of Ecology*, 78:561–578, 1990.
- D. M. J. S. Bowman. Tansley Review No. 101 - The impact of Aboriginal landscape burning on the Australian biota. *New Phytologist*, 140:385–410, 1998.
- S. J. Brooks. Late-glacial fossil midge stratigraphies (Insecta: Diptera: Chironomidae) from the Swiss Alps. *Palaeogeography, Palaeoclimatology, Palaeoecology*, 159:261–279, 2000.
- R. Brumme and P. K. Khanna. Ecological and site historical aspects of N dynamics and current N status in temperate forests. *Global Change Biology*, 14:125–141, 2008.
- R. Brumme, L. V. Verchot, P. J. Martikainen, and C. S. Potter. *Contribution of trace gases nitrous oxide (N₂O) and methane (CH₄) to the atmospheric warming balance of forest biomes*, pages 293–318. Taylor & Francis Group, Oxon, New York, 2005.
- J. R. Burford and J. M. Bremner. Relationship between the denitrification capacities of soils and total, water-soluble and readily decomposable soil organic matter. *Soil Biology and Biochemistry*, 7:389–394, 1975.
- M. G. R. Cannell and J. H. M. Thornley. Nitrogen States in Plant Ecosystems: A Viewpoint. *Annals of Botany*, 86:1161–1167, 2000.
- F. S. Chapin, L. R. Walker, C. L. Fastie, and L. C. Sharman. Mechanisms of primary succession following deglaciation at Glacier Bay, Alaska. *Ecological Monographs*, 64(2):149–157, 1994.
- R. Conrad, W. Seiler, and G. Bunse. Factors influencing the loss of fertilizer nitrogen into the atmosphere as N₂O. *Journal of Geophysical Research*, 88(C11):6709–6718, 1983.
- M. D. Corre, F. Beese, and R. Brumme. Soil nitrogen cycle in high nitrogen deposition forest: changes under nitrogen saturation and liming. *Ecological Applications*, 13(2):287–298, 2003.
- R. L. Crocker and J. Major. Soil development in relation to vegetation and surface age at Glacier Bay, Alaska. *Journal of Ecology*, 43:427–448, 1955.

- E. A. Davidson. Sources of nitric oxide and nitrous oxide following wetting of dry soil. *Soil Science Society of America Journal*, 56:95–102, 1992.
- D. Dhyani, R. K. Maikhuri, K. S. Rao, L. Kumar, V. K. Purohit, M. Sundriyal, and K. G. Saxena. Basic nutritional attributes of *Hippophae rhamnoides* (Seabuckthorn) populations from Uttarakhand Himalaya, India. *Current Science*, 92(8):1148–1152, 2007.
- K. E. Dobbie and K. A. Smith. Nitrous oxide emission factors for agriculture soils in Great Britain: the impact of soil water filled pore space and other controlling variables. *Global Change Biology*, 9(204-218), 2003.
- G. Erdtman. *Handbook of Palynology*. Munksgaard, Copenhagen, 1969.
- FAO, IIASA, ISRIC, ISSCAS, and JRC. Harmonized World Soil Database (version 1.0), 2008.
- F. Firbas. *Spät- und nacheiszeitliche Waldgeschichte Mitteleuropas nördlich der Alpen*. Gustav Fischer Verlag, Jena, Germany, 1949.
- M. K. Firestone, R. B. Firestone, and J. M. Tiedje. Nitrous oxide from soil denitrification: factors controlling its biological production. *Science*, 208:749–751, 1980.
- J. Flückiger, A. Dällenbach, T. Blunier, B. Stauffer, T. F. Stocker, D. Raynaud, and J.-M. Barnola. Variations in atmospheric N₂O concentration during abrupt climatic changes. *Science*, 285: 227–230, 1999.
- J. Flückiger, T. Blunier, B. Stauffer, J. Chappelaz, R. Spahni, K. Kawamura, J. Schwander, T. F. Stocker, and D. Dahl-Jensen. N₂O and CH₄ variations during the last glacial epoch: Insight into global processes. *Global Biogeochemical Cycles*, 18:GB1020, 2004.
- P. Forster, V. Ramaswamy, B. Artaxo, J. Bernsten, R. Betts, D. W. Fahey, J. Haywood, J. Lean, D. C. Lowe, G. Myhre, J. Ngana, R. Prinn, G. Raga, M. Schulz, and R. van Dorland. *Changes in Atmospheric Constituents and in Radiative Forcing*. Cambridge University Press, Cambridge, United Kingdom and New York, NY, USA, 2007.
- H. Godwin. *Eleagnaceae*, pages 207–208. 1975.
- E. Gorham, P. M. Vitousek, and W. A. Reiners. The regulation of chemical budgets over the course of terrestrial ecosystem succession. *Annual Review of Ecology and Systematics*, 10: 53–84, 1979.
- T. Granli and O. C. Bøckman. Nitrous oxide from agriculture. *Norwegian Journal of Agricultural Sciences Suppl.*, 12:1–128, 1994.
- O. Heiri and L. Millet. Reconstruction of Late Glacial summer temperatures from chironomid assemblages in Lac Lautrey (Jura, France). *Journal of Quaternary Science*, 20(1):33–44, 2005.
- W. Hofmann. Response of the chydorid faunas to rapid climatic changes in four alpine lakes at different altitudes. *Palaeogeography, Palaeoclimatology, Palaeoecology*, 159:281–292, 2000.

Bibliography

- S. Ivy-Ochs, H. Kerschner, A. Reuther, F. Preusser, K. Heine, M. Maisch, P. W. Kubik, and Ch. Schlüchter. Chronology of the last glacial cycle in the European Alps. *Journal of Quaternary Science*, 23(6-7):559–573, 2008.
- M. Kesik, P. Ambus, R. Baritz, N. Brüggemann, K. Butterbach-Bahl, M. Damm, J. Duyzer, L. Horvath, R. Kiese, B. Kitzler, A. Leip, C. Li, M. Pihlatie, K. Pilegaard, G. Seufert, D. Simpson, U. Skiba, G. Smiatek, T. Vesala, and S. Zechmeister-Boltenstern. Inventories of N₂O and NO emissions from European forest soils. *Biogeosciences*, 2:353–375, 2005.
- M. U. F. Kirschbaum and K. I. Paul. Modelling C and N dynamics in forest soils with a modified version of the CENTURY model. *Soil Biology and Biochemistry*, 34(3):341–354, 2002.
- L. Klemetsson, A. K. Klemetsson, F. Moldan, and P. Weslien. Nitrous oxide emission from Swedish forest soils in relation to liming and simulated increased N-deposition. *Biology and Fertility of Soils*, 25:290–295, 1997.
- C. Kroeze, A. Mosier, and L. Bouwman. Closing the global N₂O budget: A retrospective analysis 1500 - 1994. *Global Biogeochemical Cycles*, 13(1):1–8, 1999.
- G. Lang. *Quartäre Vegetationsgeschichte Europas*. Gustav Fischer Verlag, Jena, Germany, 1994.
- D. B. Lawrence. Recent glacier history of Glacier Bay, Alaska and development of vegetation on deglaciated terrain with special reference to the importance of alder in the succession. *Yearbook of the American Philosophical Society 1950*, pages 175–176, 1951.
- D. B. Lawrence, R. E. Schoenike, A. Quispel, and G. Bond. The role of *Dryas drummondii* in vegetation development following ice recession at Glacier Bay, Alaska, with special reference to its nitrogen fixation by root nodules. *Journal of Ecology*, 55:793–813, 1967.
- G. Lemdahl. Lateglacial and Early Holocene insect assemblages from sites at different altitudes in the Swiss Alps—implications on climate and environment. *Palaeogeography, Palaeoclimatology, Palaeoecology*, 159:293–312, 2000.
- C. Li and J. Aber. A process-oriented model of and NO emissions from forest soils: 1. Model development. *Journal of Geophysical Research*, 105(D4):4369–4384, 2000.
- A. F. Lotter, H. J. B. Birks, U. Eicher, W. Hofmann, J. Schwander, and L. Wick. Younger Dryas and Allerød summer temperatures at Gerzensee (Switzerland) inferred from fossil pollen and cladoceran assemblages. *Palaeogeography, Palaeoclimatology, Palaeoecology*, 159:349–361, 2000.
- A. F. Lotter, O. Heiri, S. Brooks, J. N. F. van Leeuwen, U. Eicher, and B. Ammann. Rapid summer temperature changes during Termination 1a: high-resolution multi-proxy climate reconstructions from Gerzensee (Switzerland). *Quaternary Science Reviews*, 36:103–113, 2012. doi: 10.1016/j.quascirev.2010.06.022.
- R. S. Lu. Seabuckthorn: A multipurpose plant species for fragile mountains. *ICIMOD occasional paper*, 20, 1992.

- J. Luo, R. W. Tillman, R. E. White, and P. R. Ball. Variation in denitrification activity with soil depth under pasture. *Soil Biology and Biochemistry*, 30(7):897–903, 1998.
- P. J. Martikainen, H. Nykänen, P. Crill, and J. Silvola. Effect of a lowered water table on nitrous oxide fluxes from northern peatlands. *Nature*, 366:51–53, 1993.
- C. Müller and R. R. Sherlock. Nitrous oxide emissions from temperate grassland ecosystems in the Northern and Southern Hemispheres. *Global Biogeochemical Cycles*, 18:GB1045, 2004.
- W. Nägele and R. Conrad. Influence of pH on the release of NO and N₂O from fertilized and unfertilized soil. *Biology and Fertility of Soils*, 10:139–144, 1990.
- F. Niessen, G. Lister, and F. Giovanoli. Dust transport and palaeoclimate during the Oldest Dryas in Central Europe - implications from varves (Lake Constance). *Climate Dynamics*, 8: 71–81, 1992.
- H. Nömmik. Investigation on denitrification in soil. *Acta Agriculture Scandinavica*, 6:195–227, 1956.
- H. Papen and K. Butterbach-Bahl. A 3-year continuous record of nitrogen trace gas fluxes from untreated and limed soil of N-saturated spruce and beech forest ecosystem in Germany, 1. N₂O emissions. *Journal of Geophysical Research*, 104(D15):18487–18503, 1999.
- W. J. Parton, J. M. O. Scurlock, D. S. Ojima, T. G. Gilmanov, R. J. Scholes, D. S. Schimel, T. Kirchner, J.-C. Menaut, T. Seastedt, E. Garcia Moya, A. Kamnalrut, and J. I. Kinyamario. Observations and modelling of biomass and soil organic matter dynamics for the grassland biome worldwide. *Global Biogeochemical Cycles*, 7(4):785–809, 1993.
- D. Peteet. Sensitivity and rapidity of vegetational response to abrupt climate change. *Proceedings of the National Academy of Sciences, USA*, 97:1359–1361, 2000.
- O. Peyron, J. Guiot, R. Cheddadi, P. Tarasov, M. Reille, J.-L. de Beaulieu, S. Bottema, and V. Andrieu. Climatic reconstruction in Europe for 18000 yr B.P. from pollen data. *Quaternary Research*, 49:183–196, 1998.
- O. Peyron, C. Bégeot, S. Brewer, O. Heiri, M. Magny, L. Millet, P. Ruffaldi, E. van Campo, and G. Yu. Late-Glacial climatic changes in Eastern France (Lake Lautrey) from pollen, lake-levels and chironomids. *Quaternary Research*, 64:197–211, 2005.
- I. C. Prentice, W. Cramer, S. P. Harrison, R. Leeman, R. A. Monserud, and A. M. Solomon. A global biome model based on plant physiology and dominance, soil properties and climate. *Journal of Biogeography*, 19:117–134, 1992.
- I. C. Prentice, J. Guiot, B. Huntley, D. Jolly, and R. Cheddadi. Reconstructing biomes from palaeoecological data: a general method and its application to European pollen data at 0 and 6 ka. *Climate Dynamics*, 12:185–194, 1996.

Bibliography

- A. Pühler. Die Molekularbiologie der Stickstofffixierung bei *Klebsiella pneumoniae*. *Biologie in unserer Zeit*, 9(1):14–23, 1979.
- V. Ramaswamy, O. Boucher, J. Haigh, D. Hauglustaine, J. Hatwood, G. Myhre, T. Nakajima, G. Y. Shi, and S. Solomon. *Radiative forcing of climate change*, pages 349–416. Cambridge University Press, New York, 2001.
- Ch. Reynauld. Palaeoecological significance of *Hippophae rhamnoides*, with an example of the protocratic vegetational stage in NE Fennoscandia. *Boreas*, 5:9–24, 1975.
- C. W. Richardson and D. A. Wright. WGEN: A Model for Generating Daily Weather Variables. Technical Report ARS-8, United States Department of Agriculture, Agricultural Research Service, Springfield, VA. 22161, 1984.
- R. Sandegren. *Hippophae rhamnoides* L. i Sverige under Senkvartär tid. *Svensk Botansk Tidskrift*, 37:1–26, 1943.
- K. E. Saxton and W. J. Rawls. Soil water characteristic estimates by texture and organic matter for hydrologic solutions. *Soil Science Society of America Journal*, 70:1569–1578, 2006.
- A. Schilt, M. Baumgartner, J. Schwander, D. Buiron, E. Capron, J. Chappellaz, L. Loulergue, S. Schüpbach, R. Spahni, H. Fischer, and T. F. Stocker. Atmospheric nitrous oxide during the last 140,000 years. *Earth and Planetary Science Letters*, in press:11, 2010.
- Ch. Schlüchter. The deglaciation of the Swiss-Alps: A paleoclimatic event with chronological problems. *Bulletin de l'Association française pour l'étude du Quaternaire*, 2(3):141–145, 1988.
- R. E. Schoenike. Influence of mountain avens (*Dryas drummondii*) on growth of young cottonwoods (*Populus trichocarpa*) at Glacier Bay, Alaska. *Proceedings of the Minnesota Academy of Science*, 26:55–58, 1958.
- H. Schulte-Bisping, R. Brumme, and E. Priesack. Nitrous oxide emission inventory of German forest soils. *Journal of Geophysical Research*, 108(D4):4132, 2003.
- J. Schwander, U. Eicher, and B. Ammann. Oxygen isotopes of lake marl at Gerzensee and Leysin (Switzerland), covering the Younger Dryas and two minor oscillations, and their correlation to the GRIP ice core. *Palaeogeography, Palaeoclimatology, Palaeoecology*, 159:203–214, 2000.
- J. P. Severinghaus and E. J. Brook. Abrupt climate change at the end of the last glacial period inferred from trapped air in polar ice. *Science*, 2865:930–934, 1999.
- M. Simek and J. E. Cooper. The influence of soil pH on denitrification - progress towards the understanding of this interaction over the last 50 years. *European Journal of Soil Science*, 53:345–354, 2002.

- M. Simek, L. Jisova, and D. W. Hopkins. What is the so-called optimum pH for denitrification in soil? *Soil Biology and Biochemistry*, 34:1227–1234, 2002.
- R. A. Skeffington and E. J. Wilson. Excess nitrogen deposition: issues for consideration. *Environmental Pollution*, 54:159–184, 1988.
- A. Skogen. The Hippophae rhamnoides alluvial forest at Leimöra, Central Norway, a phytosociological and ecological study. *Det. K. Nor. Vidensk. Selsk.*, 4:1–115, 1972.
- T. Sowers, R. B. Alley, and J. Jubenville. Ice core records of atmospheric N₂O covering the last 106.000 years. *Science*, 301:945–948, 2003.
- P. R. Stevens and T. W. Walker. The chronosequence concept and soil formation. *Quarterly Review of Biology*, 45:333–350, 1970.
- W. D. P. Stewart and M. C. Pearson. Nodulation and nitrogen fixation by Hippophae rhamnoides, L., in the field. *Plant and Soil*, 26:348–360, 1967.
- T. Stobdan, D. Angchuk, and S. B. Singh. Seabuckthorn: An emerging storehouse for researchers in India. *Curr. Sci. India*, 94(10):1236–1237, 2008.
- A. Tietema, A. W. Boxman, M. Bredemeier, B. A. Emmett, F. Moldan, P. Gundersen, P. Schleppei, and R. F. Wright. Nitrogen saturation experiments (NITREX) in coniferous forest ecosystems in Europe: a summary of results. *Environmental Pollution*, 102(S1):433–437, 1998.
- K. Tobolsky and B. Ammann. Macrofossils as records of plant responses to rapid Late Glacial climatic changes at three sites in the Swiss Alps. *Palaeogeography, Palaeoclimatology, Palaeoecology*, 159:251–259, 2000.
- F. C. Ugolini. *Soils*, pages 20–72. Institutes of Polar Studies Report Number 20, Columbus, Ohio, USA, 1966.
- K. van Cleve, L. A. Viereck, and R. L. Schlentner. Accumulation of nitrogen in alder (*Alnus*) ecosystems near Fairbanks, Alaska. *Arctic and Alpine Research*, 3(101-114), 1971.
- W. O. van der Knaap. Estimating pollen diversity from pollen accumulation rates: a method to assess taxonomic richness in the landscape. *The Holocene*, 19(1):159–163, 2009.
- U. van Raden, D. Colombaroli, A. Gilli, J. Schwander, S. M. Bernasconi, J. van Leeuwen, M. Leuenberger, and U. Eicher. High-resolution late-glacial chronology for the Gerzensee lake record (Switzerland): $\delta^{18}\text{O}$ correlation between a Gerzensee-stack and NGRIP. *Palaeogeography, Palaeoclimatology, Palaeoecology*, in press:12 p., ALAEO-06149, 2012.
- L. A. Viereck. Plant succession and soil development on gravel outwash of the Muldrow Glacier, Alaska. *Ecological Monographs*, 36:181–199, 1966.
- P. M. Vitousek and L. R. Walker. *Colonization, succession and resource availability: ecosystem-level interactions*, pages 207–224. Blackwell Scientific, Oxford, England, 1987.

Bibliography

- U. von Grafenstein, H. Erlenkeuser, J. Müller, and A. Kleinmann-Eisenmann. Oxygen isotope records of benthic ostracods in bavarian lake sediments - Reconstruction of late and post glacial air temperatures. *Naturwissenschaften*, 79:145–152, 1992.
- U. von Grafenstein, S. Belmecheri, U. Eicher, U. van Raden, H. Erlenkeuser, N. Andersen, and B. Ammann. The oxygen and carbon isotope signature of biogenic carbonates in Gerzensee, Switzerland, during the rapid warming around 14.55 ka BP and the following interstadial. *Palaeogeography, Palaeoclimatology, Palaeoecology*, this volume(this issue), 2012.
- L. R. Walker. Soil nitrogen changes during primary succession on a floodplain in Alaska, U.S.A. *Arctic and Alpine Research*, 21:341–349, 1989.
- A. M. Weitz, E. Linder, S. Frohling, P. M. Crill, and M. Keller. N₂O emissions from humid tropical agricultural soils: effects of soil moisture, texture and nitrogen availability. *Soil Biology and Biochemistry*, 33:1077–1093, 2001.
- L. Wick. Vegetational response to climatic changes recorded in Swiss Late Glacial lake sediments. *Palaeogeography, Palaeoclimatology, Palaeoecology*, 159:231–250, 2000.
- S. Yamulki, R. M. Harrison, K. W. T. Goulding, and C. P. Webster. N₂O, NO and NO₂ fluxes from a grassland: effect of soil pH. *Soil Biology and Biochemistry*, 29(8):1199–1208, 1997.
- S. Zaehle and A. D. Friend. Carbon and nitrogen cycle dynamics in the O-CN land surface model: 1. Model description, site-scale evaluation, and sensitivity to parameter estimates. *Global Biogeochemical Cycles*, 24(1):GB1005, 2010a.
- S. Zaehle and A. D. Friend. Description of the O-CN model: Supplementary material to: Carbon and nitrogen cycle dynamics in the O-CN land surface model, I: Model description, site-scale evaluation and sensitivity to parameter estimates. *Global Biogeochemical Cycles*, 24(1):GB1005, 2010b.
- S. Zaehle, A. D. Friend, P. Friedlingstein, F. Dentener, P. Peylin, and M. Schulz. Carbon and nitrogen cycle dynamics in the O-CN land surface model: 2. Role of the nitrogen cycle in the historical terrestrial carbon balance. *Global Biogeochemical Cycles*, 24(1):GB1006, 2010.
- J. Zhang and X. Han. N₂O emission from the semi-arid ecosystem under mineral fertilizer (urea and superphosphate) and increased precipitation in northern China. *Atmospheric Environment*, 42:291–302, 2008.
- W. Zike, B. Guo, L. Yan, F. Zhou, and Y. Zhai. Study of Seabuckthorn root nodule nitrogen fixation. Beijing, China, 28 August - 2 September 1999 1999.

3 **LMfire: An improved fire module for Dynamic Global Vegetation Models**

M. Pfeiffer and J.O Kaplan. SPITFIRE-2: an improved fire module for Dynamic Global Vegetation Models. *Geoscientific Model Development Discussions*, 5:2347-2443.

doi:10.5194/gmdd-5-2347-2012

Resubmitted after revision as:

M. Pfeiffer, A. Spessa, and J. O. Kaplan. LMfire: an improved fire module for Dynamic Global Vegetation Models

Fire is the primary disturbance factor in many terrestrial ecosystems. Wildfire alters vegetation structure and composition, affects carbon storage and biogeochemical cycling, and results in the release of climatically relevant trace gases including CO₂, CO, CH₄, NO_x, and aerosols. One way of assessing the impacts of global wildfire on centennial to multi-millennial timescales is to use process-based fire models linked to Dynamic Global Vegetation Models (DGVMs). Here we present an update to the LPJ-DGVM and a new fire module based on SPITFIRE that includes several improvements to the way in which fire occurrence, behavior, and the effects of fire on vegetation are simulated. The new LPJ-LMfire model includes explicit calculation of natural ignitions, the representation of multi-day burning and coalescence of fires, and the calculation of rates of spread in different vegetation types. We describe a new representation of anthropogenic biomass burning under preindustrial conditions that distinguishes the different relationships between humans and fire among hunter-gatherers, pastoralists, and farmers. We evaluate our model simulations against remote-sensing based estimates of burned area at regional and global scale. While wildfire in much of the modern world is largely influenced by anthropogenic suppression and ignitions, in those parts of the world where natural fire is still the dominant process, e.g., in remote areas of the boreal forest and subarctic, our results demonstrate a significant improvement in simulated burned area over the original SPITFIRE. The new fire model we present here is particularly suited for the investigation of climate-human-fire relationships on multi-millennial timescales prior to the Industrial Revolution.

3.1 Introduction

Fire is one of the most important disturbance processes affecting the terrestrial biosphere. Fires affect most ecosystems from tropical forests to tundra [Bond and van Wilgen, 1996, Dwyer et al., 2000], and the evolution of fire over the Phanerozoic is likely to have had a major control on both the global carbon budget and the present distribution of plants on Earth [Bond and Keeley, 2005, Pausas and Keeley, 2009, Bond and Scott, 2010, Bond and Midgley, 2012]. Wildfires alter vegetation composition, structure, and distribution, biomass productivity, plant diversity and biogeochemical cycles [Johnson et al., 1998, Moreira, 27, Ojima et al., 1994, Wan et al., 2001, Neary et al., 2005, Bond et al., 2005]. Biomass burning (both wildfires and intentional combustion of biofuels) influences the spatial and interannual variability in the emissions of climatically relevant trace gases and aerosols, including CO₂, CO, CH₄, NO_x, and black carbon [Crutzen and Andreae, 1990, Penner et al., 1992, Andreae and Merlet, 2001, Jain et al., 2006]. Because of the close relationship between fire, vegetation, and climate, understanding the causes and consequences of fires are critical for any assessment of the past, present, and future state of the Earth System [Bowman et al., 2009].

Quantitative observations of wildfire are severely limited both in time and space; coverage in global datasets based on satellite observations begin in the last decades of the 20th century. To improve our understanding of the drivers of fire and fire-related trace gas and aerosol emissions, it is therefore imperative to use numerical models of fire occurrence, behavior, and impacts. But process-based modeling of fire and fire emissions is challenging. Fire occurrence is influenced by climate, vegetation structure and composition, and human activities; fire behavior is affected by weather, topography, and the characteristics of the fuel; fire disturbance alters vegetation composition and structure, and ultimately climate [Archibald et al., 2009, Bowman et al., 2009, Spessa et al., 2012]. Thus, modeling fire requires representations of vegetation, fire, and climate that interact and feed back upon one another.

Mathematical models of wildfire dynamics have existed for over 40 years [Rothermel, 1972]. The original models of fire behavior were motivated by needs for operational fire forecasting for firefighting and forest management applications. These models were applied at relatively small spatial scales of 10⁰-10³ ha, and have been extensively revised and updated over subsequent years [Burgan and Rothermel, 1984, Andrews, 1986, Burgan, 1987, Andrews and Chase, 1989, Reinhardt et al., 1997, Finney, 1998, Andrews et al., 2003, Andrews, 2007, Andrews et al., 2008, Heinsch and Andrews, 2010]. Fire modeling at field scale is an essential part of fire management and mitigation worldwide, and modern operational fire models such as BehavePlus [Heinsch and Andrews, 2010] can be used for a wide range of fire management applications, including projecting the behavior of ongoing fire, planning prescribed fire, assessing fuel-hazard, and training.

More recently, fire models have been developed for application at larger spatial scales, e.g., for integration into Dynamic Global Vegetation Models (DGVMs) in order to simulate the fundamental ecosystem disturbance process that fire represents, and in some cases, to es-

estimate the emissions of climate-relevant trace gases and aerosols at continental to global scale. Depending on the goals for application of the particular DGVM, the detail with which fire is represented varies, but all large-scale fire models include a representation of three key processes:

1. fire occurrence
2. fire behavior
3. fire impacts on vegetation

The most complex representations of fire currently adapted for DGVMs incorporate and generalize many of the concepts and equations developed for operational fire forecasting models into a large-scale framework. The RegFIRM fire model [Venevsky et al., 2002], originally developed as an embedded module within the Lund-Potsdam-Jena DGVM [LPJ, Sitch et al., 2003], was one of the first global fire models that contained explicit representations of climatic fire danger and lightning- and human-caused wildfire ignitions. Building on RegFIRM, the SPITFIRE (SPread and InTensity of FIRE) fire model [Thonicke et al., 2010] included a more complete process representation of fire ignitions and behavior, and further contained new representations of the impacts of fire on vegetation including plant mortality as a result of crown scorch and cambial damage, and routines for estimating trace gas and aerosol emissions. SPITFIRE was designed to overcome many of the limitations in previous fire models set within DGVM frameworks, and be flexible enough to permit simulation analyses at sub-continental to global scales with minimal input data requirements.

SPITFIRE is one of the most comprehensive fire modules for DGVMs currently available, and has been the focus of numerous studies on the role of fire in terrestrial ecosystems and the Earth System. Thonicke et al. [2010] presented the SPITFIRE model description and global assessments of simulated burned area and wildfire trace gas emissions. Gomez-Dans et al. [2013] used SPITFIRE in combination with MODIS burned area and tree cover data to improve the model's predictions of burned area at selected sites in different biomes using parameter calibration-optimization techniques. SPITFIRE has also been driven with L3JRC burned area data [Tansey et al., 2008] and MODIS burned area data [Roy et al., 2008, Roy and Boschetti, 2009] as part of the LPJ-GUESS vegetation model [Smith et al., 2001, Hickler et al., 2006] in a study examining emissions from biomass burning in Africa [Lehsten et al., 2009]. Using LPJ-GUESS-SPITFIRE, Lehsten et al. [2013] examined how changes to fire frequency, including fire exclusion, affects tree-grass ratios in Africa. Recently, Spessa et al. [2012] benchmarked LPJ-GUESS-SPITFIRE against remote sensing-based tree biomass data for pan-tropical forests and savannas [Saatchi et al., 2011, Baccini et al., 2012]. The model was driven by a combination of monthly burned area from the Global Fire and Emissions Database [GFEDv3.1, Giglio et al., 2010, van der Werf et al., 2010] and long-term annual fire statistics [Mouillot and Field, 2005].

In addition to LPJ and its variants, SPITFIRE has been incorporated into other vegetation models. Spessa and Fisher [2010] coupled SPITFIRE to a global version of the Ecosystem

Demography (ED) vegetation model [Moorcroft et al., 2001]. ED has been incorporated into the MOSES2.2 land surface model [Met Office Surface Exchange Scheme, Essery et al., 2001, Fisher et al., 2010], and the Community Land Surface Model [CLM, Oleson et al., 2010]. SPITFIRE is currently being integrated into ED-CLM (Spessa and Fisher, in preparation). With minor modifications, SPITFIRE has also been incorporated into the LPX DGVM and applied in global experiments to quantify the contribution of wildfires to the global land-atmosphere CO₂ flux [Prentice et al., 2011].

In the following sections, we describe LPJ-LMfire, which is a revised version of LPJ-SPITFIRE that we designed for simulating global fire and vegetation-fire interactions on centennial to multi-millennial timescales, primarily during prehistoric and preindustrial time. The purpose of this manuscript is to present a complete description of our current model code to facilitate referencing of the model in our future publications, and promote easier dissemination of our methods to other researchers who may be interested in using our model. We perform a detailed evaluation of the new model based on simulations and observations of fire in Alaska, and compare the results of a global simulation over recent decades to datasets of observed burned area. We conclude with recommendations for future model development.

3.2 Rationale for modifying SPITFIRE

We were motivated to modify SPITFIRE for two main reasons: 1) In some parts of the world with very little human impact on the landscape, most notably in boreal and subarctic North America, both LPJ-SPITFIRE and LPX simulated little or no burned area where observations show that large fires do occur, however infrequently. This indicated to us that the fundamental behavior of the model and/or the datasets used to drive the model could be improved. 2) We wanted to describe a scheme for simulating anthropogenic fire during the preindustrial period. The formulation for anthropogenic fire ignitions based on population density and a single spatially variable parameter $a(N_d)$ did not seem appropriate to us based on what is known about the way humans used fire during preindustrial time. In updating SPITFIRE to tackle these goals, we had to make several changes to the fire module and to LPJ itself. In addition to these changes, we introduce new formulations for lightning occurrence, rate of spread in herbaceous fuels, and anthropogenic burning. A detailed description of our changes from the original SPITFIRE follows.

3.3 Methods

Here we present a new fire module, LPJ-LMfire, that is designed to be used with LPJ and similar DGVMs. The module is largely based on SPITFIRE [Thonicke et al., 2010], but has been substantially altered in a number of important ways. We made changes that improved the simulation of daily lightning ignitions, fuel bulk density, fire rate of spread, and fire mortality. In order to simulate human fire during preindustrial and prehistoric time, we replace the

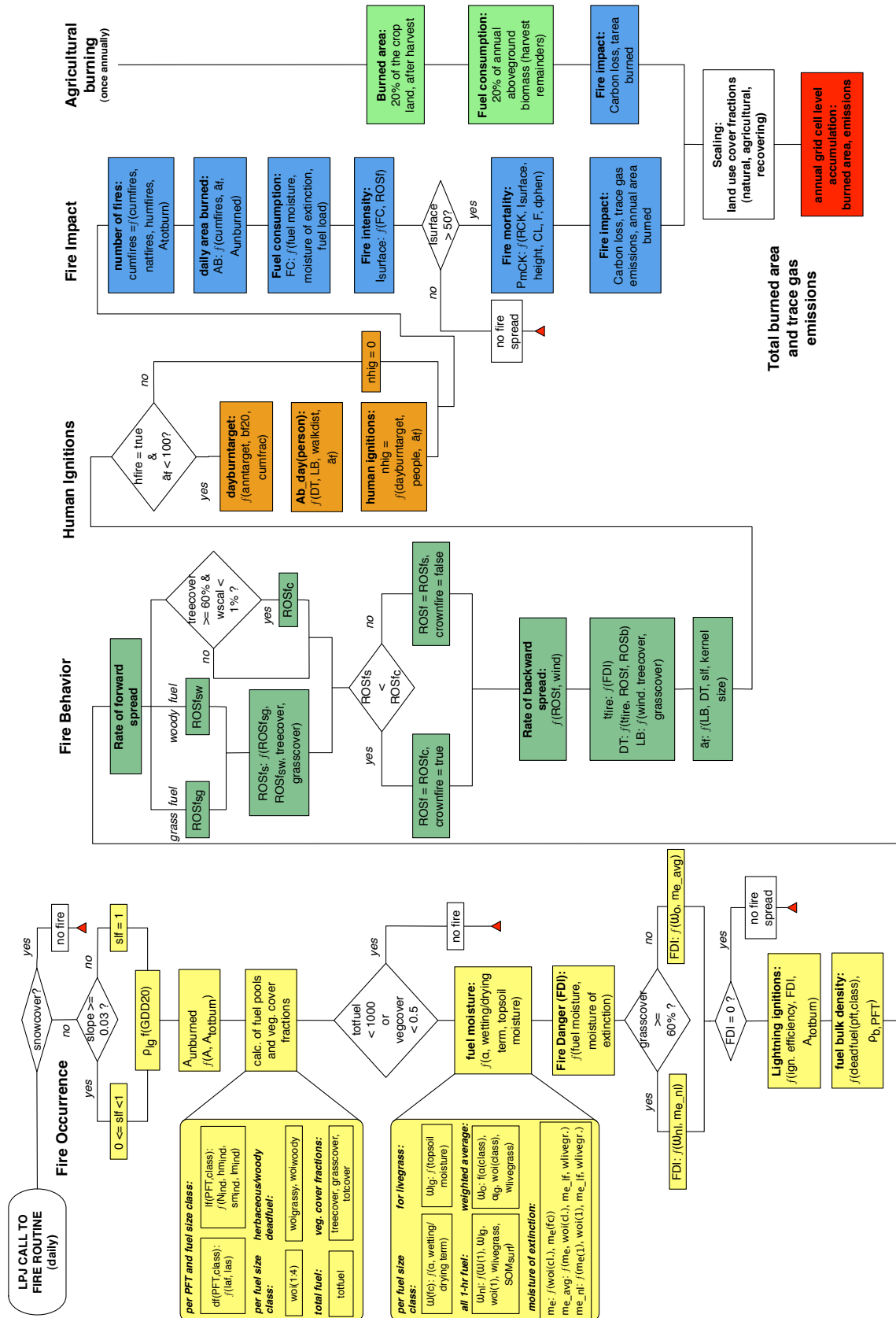


Figure 3.1: Flowchart of LPJ-LMfire

Chapter 3. LMfire: An improved fire module for Dynamic Global Vegetation Models

simple population density-based formulation for anthropogenic ignitions with a classification of humans by their subsistence lifestyle and introduce specific goals for each group in terms of fire management of their landscape. We further introduce a new scheme to track the progression of individual fires over the entire fire season and simulate smoldering ignitions. Fires in LPJ-LMfire continue burning for multiple days once ignited and are extinguished only by changes in weather, by merging with other active fires, or by running out of fuel when encountering previously burned area. Finally, we account for passive fire suppression as a result of landscape fragmentation from anthropogenic land use. These new methods for calculating wildfire occurrence, behavior, and impacts required changes not only to SPITFIRE, but also to LPJ, which we detail below.

The model description that follows is presented in the following order:

- Fire occurrence and ignitions (section 3.3.1)
- Fire behavior (section 3.3.2)
- Fire impacts on vegetation (section 3.3.3)

In each section we detail the representations in LPJ-LMfire that are different from the original SPITFIRE, followed by any changes we needed to make to LPJ to accommodate the requirements of the fire model. The description below is intended to stand alone, i.e., the entire model can be reconstructed on the basis of the equations and parameters presented in this paper without relying on earlier published descriptions. A comprehensive list of abbreviations is provided in Table 1, a flowchart illustrating the structure of LPJ-LMfire is depicted in Fig. 3.1, and a table listing the Plant Functional Type (PFT)-specific parameters is presented in Table A1. The remaining equations that were unchanged from original SPITFIRE are detailed in an Appendix, along with a table of supplementary symbols and abbreviations (Table 3.6).

A note on random numbers: LPJ-LMfire, as with SPITFIRE and some versions of LPJ [e.g., Gerten et al., 2004], uses random numbers to calculate certain processes, including precipitation occurrence and daily precipitation amount. In LPJ-LMfire we additionally use random numbers in the calculation of lightning fire ignitions. In this paper when we describe the use of random numbers, we are referring to values drawn from a pseudo-random sequence that displays statistical randomness. To guarantee reproducibility of simulation runs in LPJ-LMfire across platforms, rather than using a built-in function, we include random number generators in the model code for sampling uniform distributions [Marsaglia, 1991], and for other distributions based on the uniformly distributed sequence [Dagpunar, 1988]. We seed the random sequence at the beginning of each model run using a four-byte integer hash that is calculated from the geographic coordinates of the gridcell and is unique to at least 30 arc seconds of precision. The state of the random number sequence is stored separately for each gridcell, so the sequence of random numbers is preserved even if the model runs gridcells in parallel or a different order. This procedure ensures that every gridcell run with the same longitude and latitude will have exactly the same sequence of random numbers every time the model is run.

Table 3.1: Explanation of LMfire variable and parameter abbreviations

variable	variable explanation	variable unit
l_m	monthly number of lightning flashes	[grid cell ⁻¹ month ⁻¹]
LISOTD _m	monthly number of lightning flashes from LIS/OTD data set	[grid cell ⁻¹ month ⁻¹]
CAPE _{anom}	normalized CAPE anomaly of given month	[grid cell ⁻¹ month ⁻¹]
ieff _{avg}	average ignition efficiency	[-]
ieff _{pft}	PFT-specific ignition efficiency	[-]
fpc _{grid}	foliar projected cover fraction of PFT on grid cell	[-]
ieff _{bf}	ignition efficiency determined by burned area fraction of grid cell	[-]
ieff	overall ignition efficiency	[-]
burnedf	cumulative fraction of total grid cell area burned during the year	[-]
FDI	Fire danger index	[-]
rf	risk factor	[-]
ig _p	number of ignitions per fire-lighting person	[person ⁻¹ day ⁻¹]
D _{walk}	average walking distance per fire-lighting person	[m]
W _f	width of a single fire (shorter axis of burn ellipse)	[m]
DT	distance travelled by fire (length of major axis of burn ellipse)	[m]
LB	length-to-breadth ratio of the burn ellipse	[-]
Ab _{pd}	potential area that one person can burn	[ha day ⁻¹]
\bar{a}_f	average size of a single fire on a given day	[ha]
target _{d,group}	daily burning target	[ha day ⁻¹ group ⁻¹]
target _{y,group}	annual burning target	[ha year ⁻¹ group ⁻¹]
bf ₂₀	20-year running mean of annual burned area fraction	[-]
n _{hig}	number of human-caused ignitions	[d ⁻¹]
people	10% of all people within a given lifestyle group	[-]
ac _{area}	average contiguous area size of patches with natural veget.	[ha]
f _{nat}	fraction of gridcell covered with natural vegetation	[-]
A _{gc}	grid cell area	[ha]
$\rho_{livegrass}$	fuel bulk density of live grass	[kg m ⁻³]
GDD ₂₀	20-year-average number of growing degree days	[°C]
U _f	mean wind speed	[m min ⁻¹]
ROS _{fsg}	forward rate of spread of fire in herbaceous fuels	[m min ⁻¹]
rm	relative moisture of the fuel relative to its moisture of extinction	[-]

Chapter 3. LMfire: An improved fire module for Dynamic Global Vegetation Models

Table 3.1: Explanation of LMfire variable and parameter abbreviations (continued)

variable	variable explanation	variable unit
ω_{nl}	mean relative moisture content of 1-hr fuel class and live grass	[-]
me_{nl}	mass-weighted average moisture of extinction for live grass and 1 hr fuel	[-]
$\omega(1)$	moisture content of the 1-hour fuel class	[-]
$woi(1)$	dead fuel mass in 1-hour fuel class	[g m ⁻²]
ω_{lg}	relative moisture content of live grass	[-]
$W_{lifegrass}$	mass of live grass	[g m ⁻²]
$W_{finefuel}$	sum of live grass mass and 1-hour dead fuel class	[g m ⁻²]
SOM_{surf}	mass of organic matter in the O-horizon	[g m ⁻²]
$me_{fc}(1)$	moisture of extinction for 1-hour fuel size class (0.404)	[-]
me_{lf}	moisture of extinction for live grass fuels (0.2)	[-]
ω_o	relative daily litter moisture	[-]
me_{avg}	mass-weighted average moisture of extinction over all fuels	[-]
α	drying parameter for the fuel size classes ($1.5 * 10^{-3}, 8.13 * 10^{-5}, 2.22 * 10^{-5}, 1.5 * 10^{-6}$)	[°C ⁻²]
wn	total fuel (live mass of herbaceous, plus dead mass including all PFTs and fuel size classes 1-3)	[g m ⁻²]
$woi(1:3)$	1-, 10- and 100-hour dead fuel mass summed across all PFTs	[g m ⁻²]
wo	total mass of dead fuel summed across the first three fuel classes and all PFTs	[g m ⁻²]
$wtot$	total dead fuel mass within the first three fuel size classes, plus mass of the live grass	[g m ⁻²]
me_{fc}	moisture of extinction for the four fuel size classes (0.404, 0.487, 0.525, 0.5440)	[-]
me_{lf}	moisture of extinction for live grass / herbaceous fuels (0.2)	[-]
$ROS_{f_{sw}}$	surface forward rate of spread in woody fuels	[m min ⁻¹]
$ROS_{f_{sg}}$	surface forward rate of spread in herbaceous fuels	[m min ⁻¹]
$treecover$	fraction of grid cell area covered by tree pfts	[-]
$grasscover$	fraction of grid cell covered by grass pfts	[-]
$livefuel_{1hr}$	1-hour live fuel summed across all tree PFTs	[g m ⁻²]
ROS_f	Rate of forward spread	[m min ⁻¹]
ROS_s	Rate of surface forward spread	[m min ⁻¹]
slf	slope factor	[-]
γ	slope angle	[degrees]

Table 3.1: Explanation of LMfire variable and parameter abbreviations (continued)

variable	variable explanation	variable unit
fires_d	number of fires on current day	$[\text{day}^{-1}]$
fires_{d-1}	number of fires on previous day	$[\text{day}^{-1}]$
$\text{fires}_{\text{new}}$	newly ignited fires on current day	$[\text{day}^{-1}]$

3.3.1 Fire occurrence and ignitions

Factors excluding fire

As with SPITFIRE, the LMfire routine is designed to operate on a daily timestep. However, to save computation time we implemented several checks to ensure that the fire routine is only called when fires are possible. We exclude fire when there is snow cover in the model, assuming that a snow layer will not allow the ignition and spread of surface fires. As the current version of LPJ updates living biomass and the litter pools annually, we further skip calling the fire routine if the total vegetation foliar projected cover (FPC) of the gridcell is less than 50%, or if the total amount of fuel, including live fuel, all four dead fuel classes and the soil surface carbon pool, is less than 1 kg m^{-2} . These thresholds, similar to those used in LPX [Prentice et al., 2011], are based on the assumption that if fuels are discontinuous or insufficient in quantity a fire might start, but will not be able to spread far enough from the starting point to cause a significantly large wildfire. We calibrated our thresholds by running the model for individual gridcells and evaluating the modeled fireline intensity (I_{surface}) in environments with low vegetation cover and/or total fuel load. These minimum fuel load and continuity thresholds are almost always met except in hot and polar deserts where vegetation reaches its bioclimatic limits. Finally, we exclude anthropogenic ignitions of fire in the model spinup state before year 800 of the simulation in order to allow the development of a stable vegetation cover.

Calculation of daily lightning ignitions

Lightning ignitions in SPITFIRE are calculated from a satellite-based climatology of monthly lightning flash density [Christian et al., 2003] that is interpolated between months and scaled to yield a quasi-daily climatology of lightning strikes [Thonicke et al., 2010]. This daily number of lightning strikes is further reduced to fire ignitions based on a constant scaling factor. This approach neither takes into account the observation that lightning can be highly variable from year to year, particularly in regions where the total amount of lightning strikes is comparably low, nor that lightning occurrence is clustered in time, i.e., it is linked to precipitation events and times of atmospheric instability, nor that observations of fire ignitions suggest that a certain amount of stochasticity characterizes lightning caused fires. Here we describe our new approach for estimating the interannual variability of lightning, its daily occurrence, and a representation of the stochastic nature of lightning fire ignitions.

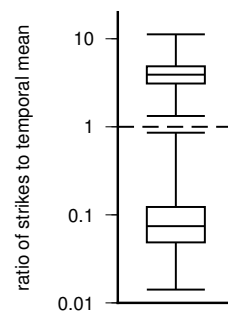


Figure 3.2: Maximum-to-mean-ratio (top boxplot) and minimum-to-mean-ratio (bottom boxplot) for ALDS strike data in June between 1986 and 2010, based on approx. 1750 gridcells with more than 5 years of observations.

Thonicke et al. [2010] argued that they expected the model sensitivity to inter-annual variability in lightning ignitions to be small compared to the overall model outcome and thus neglected interannual variability in lightning. However, we found that in places where fires are infrequent but important in terms of ecosystem impacts, and are generally caused by lightning, e.g., in boreal and subarctic North America, interannual variability in lightning occurrence is a key component of fire occurrence. In these regions, between 72% and 93% of all fires observed at present day are attributed to lightning ignitions [Stocks et al., 2003, Boles and Verbyla, 2000], and large interannual variability in burned area is visible in the GFEDv3 dataset [Giglio et al., 2010]. However, using the original SPITFIRE formulation for lightning ignitions meant that in much of boreal and subarctic North America and Siberia lightning-caused fires were never simulated.

We therefore believe that it is essential to capture interannual variability in lightning activity in order to simulate fire in boreal and subarctic regions that is consistent with observations. The only globally homogenized observation of lightning occurrence that is currently freely available is the LIS/OTD satellite-based dataset [Christian et al., 2003], though other datasets, e.g., WLLN [Virts et al., 2012] and GLD360 [Holle et al., 2011] are under development and could be applied in the future. The LIS/OTD data are available at the 0.5° spatial resolution we use for LPJ-LMfire, but only as a climatology (the HRMC dataset). Lower resolution LIS/OTD data are available as a multi-year monthly time series. However, for the extratropics (north and south of 42° latitude) this timeseries, and the climatology, is based on only four years of satellite observations. Because of the limited temporal coverage and low spatial resolution of available global lightning data, we developed a method of imposing interannual variability on climatological mean lightning frequency using ancillary meteorological data.

Peterson et al. [2010] describe the correlation between convective available potential energy (CAPE) and cloud-to-ground lightning flashes for Alaska and northern Canada, indicating that lightning strikes are more common at times with positive CAPE anomalies. Based on this observation, we produce an interannually variable time series of lightning by scaling the climatological mean lightning flash rate with monthly anomalies of CAPE. The magnitude

of the imposed variability is based on observed lightning strikes from the Alaska Lightning Detection System [ALDS, Alaska Bureau of Land Management, 2013].

To estimate the range of interannual variability in lightning amount, we analyzed ALDS strike data for the time period between 1986 and 2010 for June, the peak lightning month in most of Alaska. Point observations of lightning strikes in the ALDS were aggregated on a 0.5° grid, and gridcells with more than five years of lightning strike observations (approx. 1,750 valid cells) were analyzed with respect to the minimum, maximum, and mean number of observed lightning strikes over all available years. For each grid cell, the minimum and maximum observed values were set into a ratio to the temporal mean. The two boxplots in Fig. 3.2 show the minimum-to-mean ratio and maximum-to-mean ratio distribution for all grid cells. The total range in interannual variability spanned four orders of magnitude, from 1% of to 10-times the mean. We used this range to scale climatological mean lightning strikes based on CAPE anomalies.

Using CAPE from the 20th Century Reanalysis Project [Compo et al., 2011], we determined monthly anomalies on a gridcell level compared to the 1961-1990 mean CAPE value for a given month. The largest positive or negative CAPE-anomaly value within the time series for a specific grid cell is used to normalize CAPE anomalies to a range between -1 and $+1$ for the entire time series available for a given grid cell. Applying the normalized CAPE-anomaly with the scaling factor described above, the monthly number of lightning flashes is estimated as

$$I_m = \begin{cases} \text{LISOTD}_m \cdot (1 + 9 \cdot \text{CAPE}_{\text{anom}}), & \text{CAPE}_{\text{anom}} \geq 0 \\ \text{LISOTD}_m \cdot (1 + 0.99 \cdot \text{CAPE}_{\text{anom}}), & \text{CAPE}_{\text{anom}} < 0 \end{cases} \quad (3.1)$$

With the lightning flash density given by Eqn. 3.1, we disaggregate the monthly values to a daily amount and scale lightning flashes to cloud-to-ground lightning strikes. Noting that lightning and precipitation are closely correlated [see e.g. Jayaratne and Kuleshov, 2006, and references therein; Michaelides et al., 2009, Katsanos et al., 2007], we allow lightning strikes to occur only on days with precipitation. Daily precipitation occurrence is simulated with a weather generator following the original SPITFIRE formulation [Thonicke et al., 2010]. Simultaneous observations show that the quantity of lightning strikes is further positively correlated with precipitation amount [Piepgrass et al., 1982, Rivas Soriano et al., 2001, Zhou et al., 2002, Lal and Pawar, 2009]. Therefore, to estimate the number of daily lightning strikes, we scale the total monthly lightning amount by the daily fraction of monthly total precipitation as simulated by the weather generator. With daily lightning flashes, we estimate ground strikes by using a flash-to-strike ratio of 20% as in the original SPITFIRE. We confirmed this flash-to-strike ratio as realistic through a qualitative comparison of satellite-derived lightning flash density in the LIS/OTD LRMTS monthly timeseries with lightning ground-strike observations from the ALDS and from an extract of the North American Lightning Detection Network [NALDN Orville et al., 2011] dataset covering the southeastern United States.

With an estimate of lightning ground strikes, SPITFIRE calculates fire starts as a function of

Chapter 3. LMfire: An improved fire module for Dynamic Global Vegetation Models

a fixed ignition efficiency of 4%, yielding a total lightning flash-to-ignition ratio of 0.8%. In contrast, the LPX fire model specifies a 3% flash-to-ignition ratio, and further reduces the number of fire starts using the factor P_+ , which reduces the effectiveness of ignition events in wet months [Prentice et al., 2011, Eqn. 1]. Both of these methods result in a deterministic simulation of fire starts on any given day that is directly linked to lightning amount. The initiation of lightning-ignited fires is, however, also influenced by other factors, including the spatial distribution of lightning on the landscape, the temporal evolution of burned area during the fire season, and by a component that is observed but cannot be explained by large-scale variables, something that we term stochastic ignition efficiency.

These additional controls on fire starts are apparent when analyzing patterns of lightning strikes and burned area in boreal and subarctic regions where lightning is rare but large fires develop; these are places where human impact is low but both SPITFIRE and LPX fail to simulate burned area in agreement with observations. In attempting to improve our ability to model lightning-caused fire in the high latitudes, we made a series of changes to the way fire starts are calculated in LPJ-LMfire. Our new formulation accounts for the differential flammability of different plant types, fuel moisture, the spatial autocorrelation of lightning strikes, and previously burned area. All of these terms are combined to an estimate of ignition probability, against which we compare a uniformly distributed random number that represents the stochastic component of wildfire ignition.

Plant types differ in their intrinsic flammability as a result of leaf and stem morphology, typical canopy hydration status, and presence of phenols and other flammable compounds in the fuel [Diaz-Avalos et al., 2001]. We noticed that treating all PFTs the same way with respect to ignition efficiency was problematic, especially when comparing the tropics where lightning strikes are extremely frequent, to the extratropics where fewer strikes appear in some cases to cause equal or more amounts of fire. In assigning PFT-specific ignition efficiency parameters, we took a top-down approach, where we attempted to match the performance of the model with field observations of fire behavior. This optimization of the parameters led to a large range of values between 0.05 and 0.5 ($ieff_{pft}$, Table 3.5). The individual ignition efficiencies are combined into an FPC-weighted average

$$ieff_{avg} = \frac{\sum_{pft=1}^{npft} (fpc_{grid} \cdot ieff_{pft})}{\sum_{pft=1}^{npft} fpc_{grid}} \quad (3.2)$$

Lightning strikes display a large degree of spatial autocorrelation, tending to cluster on mountaintops and other high terrain, tall buildings, water bodies, etc. [Kotroni and Lagouvardos, 2008, Mazarakis et al., 2008, Uman, 2010]. Because of this autocorrelation, successive thunderstorms over the course of a fire season become less likely to start new fires because lightning will strike places that have already burned. As such, we decrease the likelihood of lightning-

ignited fires as a function of the area already burned to date:

$$ieff_{bf} = \frac{1 - burnedf}{1 + 25 \cdot burnedf} \quad (3.3)$$

This equation is based on an empirical evaluation of NALDN data for Florida where we investigated the spatial autocorrelation of lightning strikes in relation to strike density.

Similarly to LPX, the probability that a lightning strike will result in an ignition also depends on fuel moisture. In LPJ-LMfire we use the fire danger index (FDI) as an indicator of overall wetness. This has the advantage of not introducing yet another parameter, which, in the case of LPX was based on a single transect across the Sahel although it was intended to be used globally. The overall ignition probability on a given day is therefore calculated as:

$$ieff = FDI \cdot ieff_{avg} \cdot ieff_{bf} \quad (3.4)$$

As explained above, this probability is compared with a uniformly distributed random number that represents the stochastic component of wildfire ignitions that helps to explain why in certain cases a single lightning strike can be sufficient to cause a fire, whereas in other cases many lightning strikes within one thunderstorm do not cause a single fire [Nickey, 1976, Keeley et al., 1989, Kourtz and Todd, 1992, Jones et al., 2009, Hu et al., 2010]. The net effect of this approach is that lightning will sometimes cause a fire even though conditions are not very favorable, and vice-versa. By allowing either zero or one ignition per grid cell and day, we reflect the fact that lightning ignitions are discrete events.

Anthropogenic ignitions

Humans have used fire since the Paleolithic as a tool for managing landscapes, optimizing hunting and gathering opportunities, cooking, hunting and defense, and communication [Pyne, 1994, Anderson, 1994, Pyne, 1997, Carcaillet et al., 2002, Tinner et al., 2005, Roos et al., 2010]. The relationship of humans with fire has changed over history; particularly after the Neolithic revolution when people began cultivating domesticated plants and animals [Iversen, 1941, Kalis and Meurers-Balke, 1998, Lüning, 2000, Rösch et al., 2002, Kalis et al., 2003], and during the 20th century following the widespread mechanization of agriculture and institution of industrial fire suppression. Since our goal is to develop a model capable of simulating fire in prehistoric and preindustrial time, we attempt to quantify the way in which humans in the past used fire. For us the main question is not simply how much fire people can cause, as it only takes a few dedicated individuals to cause significant amounts of fire [e.g., Eva et al., 1998], but rather: how much fire would humans want to cause, given certain environmental conditions and subsistence lifestyles? We further account for the physical limits to anthropogenic fire ignitions.

Subsistence lifestyle is a very important factor determining why humans light fires and to what extent they light fires in order to manage their environment [Head, 1994, Bowman, 1998,

Chapter 3. LMfire: An improved fire module for Dynamic Global Vegetation Models

Bowman et al., 2004]. Hunter-gatherers use fire to promote habitat diversity and grass for game, keep landscapes open to ease their own mobility, and help prevent high-intensity wildfires late in the season that could totally destroy vegetation resources. They accomplish these goals by lighting low-intensity fires early in the fire season that remove only understory vegetation and prevent dangerous buildup of fuels [Lewis, 1985, Pyne, 1997, Williams, 2000, Kimmerer and Lake, 2001, Stewart et al., 2002]. Pastoralists use fire to kill unpalatable species and stop woody encroachment, to promote the growth of fresh grass, to control parasites and animal movements, and to increase visibility while mustering [Crowley and Garnett, 2000, Wincen, 1993]. Farmers will burn crop residues after harvest and pastures for domesticated grazers, and depending on population density and availability of unused land, may use fire to prepare new cropland while old areas are abandoned, e.g., in systems of shifting cultivation.

Thus modeling human burning in preindustrial time is complex, as different groups of people had different goals for fire management and these probably changed in space and time, and because few quantitative observations exist that enable us to directly calibrate our model. It is therefore necessary to make assumptions on the relationship between humans and fire based on qualitative information, e.g., from ethnographic, anthropological, and archaeological studies. Theoretically, the only limit to how much people can burn depends on population density, average daily walking range of people, fire weather conditions, and fuel availability and structure. In most cases, people will not fully exploit the potential maximum amount of fires they can cause, as they will try to use fire in a constructive way to manage their habitat rather than destroying it by over-burning [Head, 1994, Bowman, 1998, Bowman et al., 2004]. We define this constructive use of fire in terms of burn targets for the three subsistence lifestyle groups described above.

For foragers, we assume that their goal is to use fire to create and maintain semi-open landscapes, as this was the habitat most preferred by prehistoric people because habitat diversity and foraging opportunities increase with moderate disturbance, but decrease again if disturbance becomes too severe [e.g. Grime, 1973, Connell, 1978, Huston, 1979, Collins, 1992, Roxburgh et al., 2004, Perry et al., 2011, Faivre et al., 2011]. We therefore link the annual amount that foragers will try to burn to the simulated degree of landscape openness, i.e., tree cover, and the effectiveness of fires to open up forest, i.e., the rate of change of vegetation cover over time. The annual burn target for foragers is calculated as

$$t_{\text{ann}} = \max(\min((1 - \text{grass}) \cdot \max(\frac{d(\text{grass})}{dt}, 0) \cdot 20, 1), 0), \quad (3.5)$$

with the change in grasscover being estimated as

$$\frac{d(\text{grass})}{dt} = \text{grass}_{(t-1)} - (0.9 \cdot \text{grass}_{(t-1)} + 0.1 \cdot \text{grass}_t). \quad (3.6)$$

These equations imply that foragers living in an area with high forest cover will initially try to use fire to open the landscape. As the forest cover is reduced, the annual amount of anthropogenic fire will be reduced to maintain an equilibrium level of openness of the

landscape. Alternatively, if anthropogenic burning has little effect on forest cover, e.g., in wet environments, humans will “give up” trying to burn their landscape after a short period of time. This quantification of hunter-gatherer fire use is based on suggestions that native North Americans repeatedly made controlled surface burns on a cycle of one to three years, broken by occasional catastrophic fires that escaped the area intended to burn and periodic conflagrations during times of drought [Pyne, 1982, Williams, 2002b].

Pastoralists are assigned a constant burn target of 20% (equal to a 5-year fire return interval) that they will try to reach before they stop igniting fires, assuming that their interest in causing fires is less pronounced as they will try to preserve biomass for their domesticated grazers, while at the same time trying to maintain good pasture quality and avoid fuel accumulation in fire-prone environments. Present-day recommendations for prescribed fire maintenance of prairies and pastures suggest that a fire return interval target of five years may even be on the more conservative side of estimates [Prairiesource.com, 1992, Government of Western Australia, Department for Agriculture and Food, 2013].

Farmers may burn unused land to expand their area under cultivation or prepare new fields as old ones are abandoned, e.g., in shifting cultivation systems. They may also light fires to control fuel buildup and mitigate the possibility of devastating wildfires in areas adjacent to their cultivated land, or use fire to maintain pastures. To account for these processes, we assign farmers an annual burn target of 5% on land not used for agriculture, corresponding to a fire return interval of 20 years.

Given the assumption that people burn purposely to achieve a certain goal, it is unlikely that all people who are present in a grid cell will cause fire. When 10 or more people are present in a gridcell, we therefore allow only every 10th person present to purposely ignite fires. Among all groups of people, cognitive, genetic, and economic factors mean that human social organization leads to hierarchies of group sizes. Numerous archaeological and ethnographic studies have demonstrated that these relationships are remarkably stable over time [see, e.g., Hamilton, 2007, Whiten and Erdal, 2012]. Marlowe [2005] suggests that the optimal size of a hunter-gatherer group is 30 persons. We assume that three members of this group, e.g., able-bodied young males, will be responsible for fire management in the territory of the group. We allow for the possibility that the total number could be smaller at times, e.g., during colonization of new territory; if less than 10 people are present in a gridcell, then one person is responsible for fire ignitions. This 10% scaling factor on active human agents of fire is most important when calculating ignitions among forager populations. In agricultural and pastoral groups, population density will nearly always be high enough to ensure that an overabundance of potential arsonists is available to aim for the burn targets we specify.

Anthropogenic ignitions are determined after the calculation of the average size of single fires and their geometry on a given day. The number of individual ignitions per fire-lighting person

Chapter 3. LMfire: An improved fire module for Dynamic Global Vegetation Models

is calculated as

$$ig_p = \frac{D_{walk}}{W_f}, \quad (3.7)$$

where

$$W_f = \frac{DT}{LB} \quad (3.8)$$

The area that one fire-lighting person potentially can burn in one day is given by the equation

$$Ab_{pd} = ig_p \cdot \bar{a}_f, \quad (3.9)$$

where the average distance that one person lighting fire walks in one day is limited to 10 km.

How much fire people will start on a given day will depend on the environment in which they live. People who live in an environment that naturally has a lot of fire will take into account that some part of the landscape will burn naturally and adjust their burn target accordingly in order to avoid over-burning. In order to take into account that people have a collective memory of the fire history in their habitat, we keep track of the 20-year running mean of the burned area fraction in a given grid cell, and define the daily burn target for a given lifestyle group as

$$target_{d,group} = A_{gc} \cdot \max(target_{y,group} - bf_{20} - burnedf), \quad (3.10)$$

with A_{gc} being the grid cell area in ha. This function serves to reduce the target over the course of the year as people approach it. Once the target has been reduced to zero, people will stop igniting fires. The 20-year-average burned area fraction is subtracted to let people stay conservative with their burning by taking into account that there can be some baseline amount of lightning-caused fire as well, thereby avoiding overburning of their target.

Ethnographic and historical studies have shown that preindustrial humans lit fires for landscape management purposes when fires were not likely to become severe, i.e., when meteorological conditions allowed burning but the overall fire danger was not too high. To represent this observation, we restrict anthropogenic burning to days when the average size of single fires, \bar{a}_f , will not become larger than 100 ha. Additionally, the number of fires started by people on a given day is linked to the FDI via a multiplication factor that reduces the ignitions as FDI increases.

$$rf = \begin{cases} 1, & FDI \leq 0.25 \\ \frac{1}{1.22 \cdot \pi \cdot FDI} \cdot e^{-\frac{(\ln(FDI+1.29))^2}{0.18}}, & FDI > 0.25 \end{cases} \quad (3.11)$$

The decline of the risk factor, rf , follows a lognormal distribution with a maximum value of 1 at an FDI of 0.25 that then declines toward zero as FDI increases, which therefore makes it increasingly unlikely that people will keep causing fires when conditions for causing out-of-

control fires become more risky. We developed this equation based on ethnographic studies from Australia showing that aborigines preferentially cause fires at the beginning of the dry season when fire danger is still moderate, and decrease their ignition activities as FDI increases [Bowman, 1998, Yibarbuk et al., 2002, Bowman et al., 2004]. We chose a lognormal curve to describe the relationship between anthropogenic ignitions and FDI because even with high fire risk the chance that someone causes a fire will not be completely zero.

In cases where enough fire-lighting people are available to reach or exceed the burn target for the given day, the number of human-caused ignitions is derived from

$$n_{\text{hig}} = \text{rf} \cdot \frac{\text{target}_{\text{d,group}}}{\bar{a}_{\text{f}}}, \quad (3.12)$$

and in cases where the burn target of the day cannot be achieved due to a lack of enough fire-lighting people from

$$n_{\text{hig}} = \text{ig}_{\text{p}} \cdot \text{people} \cdot \text{rf} \quad (3.13)$$

Burning of cropland

All of the equations presented in section 3.3.1 concern anthropogenic burning on the fraction of the gridcell where potential natural vegetation is simulated by LPJ. We prescribe additional burn targets to account for anthropogenic burning on the part of the gridcell that is occupied by cropland. Evidence suggests that the usage of fire in cropland management was widespread in preindustrial times [see, e.g., Dumond, 1961, Sigaut, 1979, Otto and Anderson, 1982, Johnston, 2003, Williams, 2002a], and even nowadays is common in parts of the world where agriculture is largely unmechanized, e.g., in Sub-Saharan Africa, and parts of south and Southeast Asia, Indonesia and Latin America [Conklin, 1961, Seiler and Crutzen, 1980, Dove, 1985, Smittinand et al., 1986, Unruh et al., 1987, Kleinman et al., 1995, Van Reuler and Janssen, 1996, Cairns and Garrity, 1999, Akanvou et al., 2000, Fox, 2000, Rasul and Thapa, 2003].

Depending on agricultural practices, crop residues may be burned in situ or collected and burned throughout the year, e.g., as a fuel [Yevich and Logan, 2003]. Fields that are burned may be burned immediately after harvest or shortly before planting, and in some places where double or triple cropping is practiced possibly even several times per year. Cropland burning can be achieved largely independently of fire weather, e.g., managed fire was historically important in places with hypermaritime climate such as the uplands of northwestern Europe [Mather, 2004, Dodgshon and Olsson, 2006].

In LPJ-LMfire, 20% of the total simulated crop biomass produced within one year remains on the fields as residues, and this remaining biomass becomes potential fuel for agricultural burning. Farmers are assumed to burn 20% of the total cropland area within a grid cell every year. We derived this value from a qualitative comparison between total annual area burned observed in GFEDv3 and our simulated burning on natural land for regions in Africa

where agricultural burning is commonly practiced after harvest. It is a conservative first approximation for the past when people did not have modern day technology available to prepare fields for the next crop planting after harvest, and likely could be much higher in places where, e.g., multi-cropping is practiced and all fields are burned after every harvest.

As described above, cropland and crop residue burning practices vary with space and time. We therefore make no attempt to estimate the seasonality of cropland burning, aside from excluding cropland burning when snow cover is present or temperatures are below 0°C, and assume that burning is evenly distributed across all other days of the year. Future improvements to the model could attempt to resolve the temporal pattern of cropland burning by using a more sophisticated crop module for LPJ [e.g., Bondeau et al., 2007]. For studies that focus on fire seasonality or trace gas emissions from biomass burning on a sub-annual scale, the timing of anthropogenic activities affecting seasonal patterns of fire cannot be neglected and will need to be accounted for explicitly.

3.3.2 Fire behavior

As described above, boreal and subarctic regions are characterized by infrequent lightning ignitions that may still lead to large amounts of burned area because individual fires persist over the course of several weeks or months [Alaska Fire Service, 2013]. On the other hand, both SPITFIRE and LPX [Prentice et al., 2011] allow fires to burn for a maximum duration of 241 minutes, after which individual fire starts are extinguished. This representation of fire duration is likely the primary reason these models simulate burned area that is inconsistent with observations. The largest change we made from the original SPITFIRE was the implementation of a scheme for multi-day burning and the coalescence of fires. After making this fundamental change to the model, we had to revise other SPITFIRE formulations to make them consistent with our new approach. These revisions included changes to the representation of fuel composition and amount, to meteorological influences on fuel moisture and rate of spread, and the introduction of representation of the role of topography in influencing fire size. The new functionality and changes are detailed below.

Multi-day burning and coalescence of fires

Once a wildfire is started, it typically continues burning as long as fire weather conditions and availability of fuel do not restrict the progress of the fire [see, e.g., Todd and Jewkes, 2006, Desiles et al., 2007, Jones et al., 2009]. Wildfires display a characteristic diurnal cycle, with the most active period being around midday and early afternoon when humidity is at a minimum and wind speeds are higher [Pyne et al., 1996]. To account for these observations, we remove the 241-minute limitation on fire duration specified in SPITFIRE, but maintain this value as an active burning period on any given day in calculating daily burned area. Individual ignitions persist from one day to the next until they are extinguished due to 1) merging with other fires, 2) running out of fuel from burning into areas already burned during the current year, or 3) as

a result of sustained precipitation.

In LPJ-LMfire, the total number of fires burning on a specific day is therefore defined as the number of fires that were started on previous days that have not yet been extinguished, plus any potential additional ignitions on the current day. As individual fires grow in size, the likelihood of one fire burning into another or into an area that has already burned increases. To take this into account, we reduce the number of fires burning on any given day by the product of the gridcell fraction that has already burned in the current year and the total number of fires on this day. Thus, the total number of fires on any given day is calculated as:

$$\text{fires}_d = \text{fires}_{d-1} + \text{fires}_{\text{new}} - \text{burnedf} \cdot (\text{fires}_{d-1} + \text{fires}_{\text{new}}) \quad (3.14)$$

In allowing fires to burn for multiple days we needed to define threshold amounts of precipitation above which ongoing fires will be extinguished. Field observations have shown that while small amounts of precipitation will impede fire spread, fires may keep smoldering and start spreading as soon as conditions dry out again, and that the amount of precipitation required to slow or stop wildfires differs depending on the type of fuel that is burning [Latham and Rothermel, 1993, Hall, 2007, Hadlow, 2009, Pyne et al., 1996]. LPJ-LMfire extinguishes burning fires when the precipitation sum over consecutive days exceeds 10 mm for grid cells that have a grass cover of less than 60%, and 3 mm for grid cells with more than 60% grass cover.

Fuel quantity and density

While testing development versions of LPJ-LMfire, we noticed that simulated burned area greatly exceeded GFEDv3 observations in parts of Siberia and the seasonal tropical forests of South America. We diagnosed the cause as very high simulated fuel loads that in turn propagated extremely large fires. High fuel loads in the tropics were the result of unrealistic accumulation of biomass in living vegetation, whereas in the boreal regions slow decomposition of litter with low bulk density led to an unrealistically deep and loosely packed fuel bed. To improve the simulation of fire we therefore made several changes to the way LPJ simulates biomass and fuel bed density.

In LPJ, the amount of live woody biomass in a gridcell is determined by the PFT state variables of the average individual that represents the mean of the PFT-population with respect to all state variables describing the PFT, and by the individual density that represents the number of individuals in a unit area [Sitch et al., 2003]. Accumulation of biomass in the average individual is limited by the maximum crown area parameter. Density is limited by space in the gridcell, with the assumption that individuals do not overlap in space (packing constraint). Thus, at equilibrium, individual density stabilizes as the size of the average individual approaches maximum crown area. In our tests, simulated biomass accumulated to very high levels in areas where disturbance is rare and growth rates are high, such as the perennially humid parts of the Amazon basin.

Chapter 3. LMfire: An improved fire module for Dynamic Global Vegetation Models

To reduce biomass in LPJ-LMfire, we allow trees to reach a maximum crown area of 30 m², instead of the 15 m² used in the original LPJ parameterization. At the same time, we increased the maximum sapling establishment rate from 0.12 individuals m⁻² to 0.15 individuals m⁻². As leaves have less biomass per unit area than stems, increasing the maximum crown area parameter in the model decreases density and therefore simulated total biomass. Adjusting these two parameters leads to an overall decrease in total biomass between 5 and 15% for the area shown in Fig. 3.3, with highest reduction percentages in areas of high biomass such as the upper Amazon Basin. As described above, the reduction effect caused by the increase of maximum crown area is most relevant for the wet tropics where trees experience little disturbance and optimal growth conditions. In most extra-tropical regions, the new limit for maximum crown area is usually not reached due to climate-induced mortality and disturbance.

In boreal regions where we noticed very high amounts of burned area in our development simulations, we traced this back to high rates of fire spread simulated in an unrealistically deep and loosely packed fuel bed. In LPJ, litter decomposition is controlled by temperature and moisture so that under cold, dry conditions, very slow effective decomposition rates are simulated and litter tends to accumulate for decades to centuries. In boreal regions, particularly in the drier parts of Alaska and Siberia, the model therefore simulated large accumulations of aboveground litter, with values as high as 7 kg C m⁻². Following the original SPITFIRE parameterization, fuel bulk density is relatively low: 2 kg m⁻³ for herbaceous litter and 25 kg m⁻³ for woody litter. Large accumulations of litter therefore lead to the formation of a deep, loosely packed fuel bed. This problem is exacerbated when frequent fires result in widespread tree mortality and shift the vegetation cover towards being dominated by herbaceous PFTs.

Cold, dry climates lead to the accumulation of large amounts of organic matter, but the assumption that these would not be mechanically and chemically altered with time is unrealistic [Berg, 2000, Berg et al., 2001, Akselsson et al., 2005]. To account for changes in the physical properties of the fuel bed with time, we introduce an aboveground organic matter pool in LPJ that schematically represents an O-horizon. After having calculated decomposition in the three litter pools (fast litter, slow litter and belowground fine litter) following Sitch et al. [2003], the remaining carbon in the fast litter pool is transferred to the O-horizon where it decomposes with a nominal turnover time of 2 years at a temperature of 10°C. This way, an organic layer can build up in cold places where litter decomposition is slow, and unrealistically large accumulations of litter are avoided. Carbon that was transferred to the O-horizon does not contribute to the rate of spread calculations as it is considered to be densely packed compared to the fuels in the regular fuel size classes, but it is included into the overall fuel combustion term. As shown in Table 3.2, reducing the amount of dead fuel by transferring older litter into the O-horizon strongly affects the simulated rate of spread, and therefore fire size and burned area.

We also noticed that our implementation of the original SPITFIRE resulted in high rates of

Table 3.2: Rate of Spread calculations before and after implementation of the O-horizon. All calculations performed with wind speed of 3 m s^{-1} and fine fuel bulk density of 2 kg m^{-3} .

relative fuel moisture (%)	ROS (m s^{-1})
<i>without O-horizon, fine fuel load 4.2 kg m^{-2}</i>	
10	9.29
50	5.14
<i>with O-horizon, fine fuel load 0.2 kg m^{-2}</i>	
10	0.47
50	0.24

fire spread in tundra ecosystems and consequently simulation of burned area that exceeded observations (GFEDv3, Alaska Fire Service, 2013). As the standard version of LPJ does not have a tundra shrub PFT, subarctic vegetation is primarily represented by the C_3 -grass PFT, for which SPITFIRE assigns a constant fuel bulk density of 2 kg m^{-3} . In tundra ecosystems, herbaceous plants and shrubs grow close to the ground and typically have a dense life form, e.g., as tussocks, as an adaptation against damage from frost and snow burden [Bliss, 1962, Sonesson and Callaghan, 1991, Sturm et al., 2000]. To account for the dense growth form of tundra and the general tendency of herbaceous vegetation to grow more densely and closer to the ground with decreasing temperatures, we introduced a dependency between the bulk density of the two herbaceous PFTs and the 20-year running mean of the annual sum of degree-days on a 5°C base [GDD₂₀, Sitch et al., 2003]:

$$\rho_{\text{livegrass}} = \frac{20000}{\text{GDD}_{20} + 1000} - 1 \quad (3.15)$$

In the tropics, the annual GDD sum can be as high as 10,000, whereas in high latitudes values are typically 1000 or less. With fewer GDDs, we decrease bulk density from typical values in tundra areas of $10\text{--}12 \text{ kg m}^{-3}$, to $1\text{--}2 \text{ kg m}^{-3}$ in warm tropical regions where tall grasses grow. These endpoint values are estimated based on abundant field evidence demonstrating that tropical grasses are typically tall, whereas herbaceous tundra is short and often grows in dense tussocks [see, e.g., Breckle, 2002, Gibson, 2009]. We use GDD₂₀ because grass bulk density should not be influenced by interannual variability in climate, as individual species have a relatively stable growth habit over time. The modification of grass fuel bulk density affects simulated rate of spread. For example, given a fuel load of 1 kg m^{-2} , a wind speed of 3 m s^{-1} , and a fuel bulk density of 2 kg m^{-3} the resulting ROS is 2.36 m s^{-1} at an rm of 0.1 and 1.22 m s^{-1} at an rm of 0.5. With a fuel bulk density of 12 kg m^{-3} ROS is reduced by roughly one order of magnitude to 0.27 m s^{-1} and 0.14 m s^{-1} , respectively.

Fuel moisture

For herbaceous fuels, we set the relative moisture content of the fuel to be equal to the ratio

$$rm = \frac{\omega_{nl}}{me_{nl}}, \quad (3.16)$$

where ω_{nl} is the mean relative moisture content of the 1 h fuel class and the live grass, and me_{nl} is the mass-weighted average moisture of extinction for live grass and 1 hr fuel. ω_{nl} and me_{nl} are calculated as follows:

$$\omega_{nl} = \frac{\omega(1) \cdot woi(1) + \omega_{lg} \cdot (w_{livegrass} + SOM_{surf})}{w_{finefuel} + SOM_{surf}} \quad (3.17)$$

$$me_{nl} = \frac{me_{fc}(1) \cdot woi(1) + me_{lf} \cdot (w_{livegrass} + SOM_{surf})}{w_{finefuel} + SOM_{surf}} \quad (3.18)$$

As discussed above, the implementation of multi-day burning in LPJ-LMfire led to simulations of fires that were overly large and frequent compared to observations. This over-burning was partly solved by introducing the O-horizon for surface litter, and by adjusting the bulk density of live herbaceous fuels. However, in drier boreal and subarctic regions we also noticed that herbaceous live fuel moisture was very low in the middle of the growing season. This low moisture was a result of LPJ's standard representation of soil hydrology where all soils are considered to be free draining. In reality, much of the boreal and subarctic regions are underlain by permafrost, which acts as a barrier to water drainage [Kane and Stein, 1983, Niu and Yang, 2006]. To approximate the effects of permafrost on soil moisture, and therefore herbaceous live fuel moisture, we impede all drainage of soil water in LPJ where permafrost is present. We define permafrost as occurring in any gridcell where the 20-year running mean annual temperature is less than 0°C.

For woody fuels, relative moisture content is calculated as

$$rm = \frac{\omega_o}{me_{avg}} \quad (3.19)$$

Instead of resetting the relative daily litter moisture to saturation as soon as daily precipitation exceeds 3 mm, i.e., when the Nesterov Index (NI) is set to zero, we calculate ω_o as a mass balance between drying and wetting of the fuel, assuming that at a threshold of 50 mm precipitation all fuel will be completely wet, and lesser amounts of rain will partially wet the fuel according to the amount of precipitation. The drying term is estimated as a function of daily maximum and minimum temperature similar to the way the Nesterov Index is calculated in original SPITFIRE, based on the difference between the day's minimum and maximum temperature, the fuel water content, and a fuel drying parameter integrated over the alpha-

parameters given in Thonicke et al. [2010] according to fuel composition:

$$\text{dry}_o = t_{\max} \cdot (t_{\max} - t_{\min} - 4) \cdot \text{caf} \cdot \omega_{o,d-1} \quad (3.20)$$

$$\text{wet} = \begin{cases} 1, & \text{prec} > 50\text{mm} \\ \frac{\text{prec}}{50}, & \text{prec} \leq 50\text{mm}, \end{cases} \quad (3.21)$$

with 50 mm of daily precipitation being the threshold definition for heavy rain given by the World Meteorological Organization (<http://severe.worldweather.org/rain/>), at which we assume all fuel to be water-saturated, independent of its previous water status.

The water balance between drying and wetting is calculated as follows:

$$\text{balance} = \omega_{o,d-1} - \text{dry}_o + \text{wet}, \quad (3.22)$$

which is essentially a simple water bucket approach similar to the way the soil water balance is calculated in LPJ. The fuel moisture on the current day is defined as

$$\text{wet} = \begin{cases} 1, & \text{balance} > 1 \\ \text{balance}, & 0 \leq \text{balance} \leq 1 \\ 0, & \text{balance} < 0 \end{cases} \quad (3.23)$$

The variable *caf* represents α combined over all fuels, and is calculated as

$$\text{caf} = \frac{\sum_{i=1}^3 \alpha \cdot \text{woi}}{\text{wn}} \cdot \frac{\text{wo}}{\text{wtot}} + \alpha_{\text{lg}} \cdot \frac{\text{W}_{\text{livegrass}}}{\text{wtot}} \quad (3.24)$$

The mass-weighted average moisture of extinction over all fuels, me_{avg} , is calculated as

$$\text{me}_{\text{avg}} = \frac{\sum_{i=1}^{\text{fc}} (\text{woi} \cdot \text{me}_{\text{fc}})}{\sum_{i=1}^{\text{fc}} \text{woi}} \cdot \frac{\text{wo}}{\text{wtot}} + \frac{\text{me}_{\text{lf}} \cdot \text{W}_{\text{livegrass}}}{\text{wtot}} \quad (3.25)$$

Depending on the grasscover fraction of the grid cell, FDI is calculated as

$$\text{FDI} = \begin{cases} \max(0, (1 - \frac{\omega_{\text{nl}}}{\text{me}_{\text{nl}}}), & \text{grasscover} \geq 0.6 \\ \max(0, (1 - \frac{\omega_o}{\text{me}_{\text{avg}}}), & \text{grasscover} < 0.6 \end{cases} \quad (3.26)$$

Fire rate of spread

In contrast to SPITFIRE, we assume that fires will be mostly carried in light fuels as these are easily ignited due to their high surface area-to-volume (SAV) ratio and low fuel bulk density,

Chapter 3. LMfire: An improved fire module for Dynamic Global Vegetation Models

whereas heavier fuel components will sustain burning once fire has started at a given place. As each PFT in LPJ occupies an exclusive space on the gridcell, the possibility that their fuels are spatially collocated is also excluded. Our Monte Carlo simulations on the continuity of natural land depending on the fraction that is occupied by agricultural land (section 3.3.2, Eqn. 3.33) revealed that, in a randomly distributed spatial arrangement of two differing entities, the fractional occupation ratio has an influence on the continuity of both entities. This result also applies to the distribution of herbaceous versus woody PFTs and thus, fuels.

For example, if a herbaceous PFT occupies more than 60% of the grid cell, fire rate of spread is determined by the properties of the herbaceous fuel because it is not possible to arrange the remaining 40%, i.e., the woody PFTs, in a way that interrupts the continuity of the herbaceous fuel. Below 60% herbaceous cover, the average contiguous size of patches of herbaceous vegetation rapidly decreases as long as areas occupied by grass or trees are assumed to be distributed more or less randomly, and the influence of woody fuels on the overall rate of spread becomes more dominant. We therefore calculate rate of fire spread for herbaceous and woody fuel components separately and then average the two calculated rates of spread according to the coverage of the herbaceous and woody PFTs on the landscape.

To calculate rate of spread in grass, we use a modified form of the equation given in Mell et al. [2012], setting the fuel bulk density for these light fuels equal to the $\rho_{\text{livegrass}}$ value calculated in equation 3.15.

$$\text{ROS}_{\text{f}_{\text{sg}}} = \left((0.165 + 0.534 \cdot \frac{U_f}{60}) \cdot e^{-0.108 \cdot \text{rm} \cdot 100} \cdot g_s \cdot 60, \right) \quad (3.27)$$

where

$$g_s = -0.0848 \cdot \min(\rho_{\text{livegrass}}, 12) + 1.0848 \quad (3.28)$$

Equation 3.28 accounts for the variable density of live grass depending on GDD20 as calculated in Eqn. 3.15. Compared to SPITFIRE, the rate of spread in this new equation requires fewer parameters (wind speed, ratio of relative fuel moisture to its moisture of extinction, and fuel bulk density) and typically results in slower rate of spread when all other conditions are equal.

The rate of spread in woody fuel is calculated as in SPITFIRE, with the exception that we use a fixed value of $5 \text{ cm}^2 \text{ cm}^{-3}$ for SAV assuming that fire will be carried primarily by the finest component of the fuel bed. For details on the calculation of rate of spread, see the equations in Appendix 3.7.

We determine the surface forward rate of spread as the weighted average of the rate of spread in the woody and herbaceous fuel according to the cover fractions of tree- and grass-PFTs on the landscape:

$$\text{ROS}_{\text{f}_s} = \frac{\text{ROS}_{\text{f}_{\text{sw}}} \cdot \text{treecover} + \text{ROS}_{\text{f}_{\text{sg}}} \cdot \text{grasscover}}{\text{treecover} + \text{grasscover}} \quad (3.29)$$

In addition, we introduced a wind multiplier for high-wind conditions: at a wind speed of 10 m s^{-1} and above, the calculated ROS will be doubled, as the BEHAVE-based ROS is increasingly too low at higher wind speeds (see Fig. 13 in Morvan et al., 2008):

$$\text{windfact} = \begin{cases} 1 + e^{2 \cdot U_{\text{forward}} - 20}, & \frac{U_{\text{forward}}}{60} \leq 10 \\ 2, & \frac{U_{\text{forward}}}{60} > 10 \end{cases} \quad (3.30)$$

Effect of terrain on average fire size

Terrain can be an important factor influencing the spread of fires [Pyne et al., 1996]. We argue that areas with high relief energy should have smaller average fire sizes compared to areas that are completely flat as dissected topography will inhibit fire propagation. Although fire rate of spread is usually faster up-slopes due to more fuel surface being exposed to the flames than on flat terrain and additional upslope wind effects, at 0.5° spatial resolution no individual gridcell of $\sim 1000\text{-}3000 \text{ km}^2$ represents one single slope. Rather, all up-slopes will be accompanied by down-slopes on the opposing side where fire spread will be slowed or impeded. Terrain with high relief energy is also characterized by varying slope exposures. A dry sun-exposed slope will be opposed by a shady slope with wetter fuel conditions, different vegetation, and in some cases a sparsely vegetated crest that separates both slopes and impedes the spread of fires from one catchment into a neighboring one [Guyette et al., 2002]. Fuel continuity also can be broken by areas of unvegetated rock and cliffs, which are more likely to occur in complex terrain.

In LPJ-LMfire we calculate a terrain impedance factor based on our empirical observations, e.g., from evaluating burn scars on satellite imagery, that large fires are rare in mountainous regions. The factor *slf* is calculated as

$$\text{slf} = \begin{cases} 1, & \gamma < 1.7^\circ \\ \frac{1}{\frac{5}{9}\pi\gamma - 2}, & \gamma \geq 1.7^\circ, \end{cases} \quad (3.31)$$

and affects mean fire size \bar{a}_f as a downscaling factor:

$$\bar{a}_f = \bar{a}_f \cdot \text{slf} \quad (3.32)$$

We determined the median slope angle γ of a 0.5° gridcell by aggregating the maximum D8 slope [Zhang et al., 1999] at 1 arc minute resolution from the ETOPO1 global digital elevation model [Amante and Eakins, 2009]. Median slope angle at this scale ranges roughly from 0° to 17° from horizontal. A world map of *slf* is shown in Fig. S2.

With the size of individual fires scaled according to the average slope angle, more fires will be required to burn an equivalently sized total area in more complex terrain as compared to flat terrain.

Passive fire suppression through landscape fragmentation

For the first time in human history, modern technology allows people to actively suppress and extinguish wildfires to protect their lives and properties. In the past, possibilities to actively suppress and extinguish wildfires were limited [Skinner and Chang, 1996, Pausas and Keeley, 2009]. Nevertheless, increases in population densities and parallel increases in land use eventually contributed to landscape fragmentation and thereby indirect suppression of wildfires. Following Archibald et al. [2009] we simulate the effect that anthropogenic landscape fragmentation has on fire spread and therefore burned area.

In order to estimate the effects of anthropogenic landscape fragmentation, here defined as the fraction of cropland vs. unused land, we performed a Monte Carlo simulation on a grid of 100x100 pixels where we increased the fraction of cropland by 1% increments from 0 to 1. For each step, we randomly assigned pixels within the grid to either be cropland or unused land and calculated the average contiguous area size of natural patches based on an 8-cell neighborhood. To estimate the final average contiguous area size of natural patches, we performed 1000 repetitions of the experiment at each land use fraction. The resulting relationship between the cropland fraction of a grid cell and the average contiguous area size of unused patches can be approximated by the following equation:

$$ac_area = (1.003 + e^{(16.607 - 41.503 \cdot f_{nat})})^{-2.169} \cdot A_{gc}, \quad (3.33)$$

with A_{gc} being the grid cell area in ha. The equation accounts for changing land use as fragmentation is recalculated every year based on the information on how much land within a grid cell is agricultural land. The average contiguous area size of natural patches is used to set an upper limit to \bar{a}_f , the size of individual fires, in the fire routine. At very high land use fractions, we limit the minimum allowed averaged patch size to a kernel size of 10 ha, not allowing any fragmentation that causes natural patches smaller than this size. The concept of connectivity and fragmentation being related to the proportions of two different phases, in our case agricultural land and unused land, is well-known in other scientific contexts, e.g., in soil science where unsaturated soil water conductivity depends on the ratio between water-filled and air-filled pore space [Richards, 1931, Newman and Ziff, 2000]. For a detailed depiction of the Monte Carlo simulation results, see supplementary Figure S1.

3.3.3 Fire mortality

Fire mortality in the original version of SPITFIRE was simulated through a combination of cambial damage and scorching of tree crowns following Peterson and Ryan [1986], where tree kill is a function of fire intensity, bark thickness and tree height. Thus, to simulate realistic amounts of tree kill, it is essential to have a representation of the size and shape of trees in the model that is realistic. However, the population averaging of the allometric equations in LPJ leads to the simulation of average individuals that are much shorter and thinner than mature trees in nature. To overcome this limitation, SPITFIRE applied an unpublished scheme to

disaggregate the biomass represented by the average individual into a series of size classes with height and diameter that are relative to the height of the average individual simulated by LPJ. We use an adaptation of this scheme to approximate realistic tree heights in LPJ-LMfire.

We begin by prescribing a PFT-specific relationship between the simulated range in height for the average individual and the typical range in height from sapling to mature tree of a real individual of that PFT as it is observed in the field. Thus any given height of the average individual can be mapped to a “mean real height” (\bar{H}_{real}) for the PFT. Recognizing that the average individual represents a range of tree ages and sizes, we disaggregate the biomass of each average individual into seven height classes following a skew-normal distribution centered on \bar{H}_{real} estimated above. The heights of each height class are equally spaced and range from 50% of \bar{H}_{real} for the shortest class to 125% of \bar{H}_{real} for the tallest class.

Stem diameter is calculated separately for each height class based on the observed relationship between maximum tree height and diameter for each PFT. Bark thickness is calculated using the PFT-specific bark thickness parameters given in Thonicke et al. [2010] (par1, par2, Table 3.5). As in SPITFIRE, mortality resulting from cambial kill is calculated separately for each height class, and the total mortality over all classes is summed up across all classes per PFT. Apart from bark thickness, the probability of mortality due to cambial damage also depends on the residence time of the fire, τ_l , in relation to the critical time for cambial damage. Thonicke et al. [2010] do not provide the exact equation used in SPITFIRE to calculate τ_l , but refer to Peterson and Ryan [1986]. In LPJ-LPMfire we calculate τ_l using Eqn. 8 of Peterson and Ryan [1986]:

$$\tau_l = 39.4 \cdot \sum_{i=1}^{\text{fc}} \text{woi} \cdot (1 - (1 - \text{CF})^{0.5}) \quad (3.34)$$

With our revised height class scheme, we needed to re-parameterize the PFT-specific RCK- and p-values that describe the probability of mortality due to crown damage. When we used the SPITFIRE RCK parameters, close to 1 for all woody PFTs with the exception of the tropical broadleaf raingreen PFT, an undesired result of our multiple-day burning scheme was that excessive crown kill resulted in much of the simulated global vegetation cover being converted to grasslands in places with frequent fire occurrence. Observational data, e.g., from vegetation maps and the GLCF tree cover dataset [DeFries et al., 2000], showed that many of these places clearly should be forested. While we acknowledge that using parameters from observed plant traits is a good strategy, given the unrealistic allometry simulated for LPJ’s average individual and the simplification presented by our height class scheme, direct representation of the characteristics of individual trees is not strictly possible. Future model development should include better representation of the size and shape of trees in the model, e.g., by using a cohort-based approach such as that used in LPJ-GUESS [Smith et al., 2001]. In LPJ-LMfire, we set RCK to a constant value of 0.5 for all tree PFTs and p to a constant value of 0.3. We further add the restriction that deciduous trees can only be killed by crown scorch if green leaves are present at the time of fire occurrence.

Chapter 3. LMfire: An improved fire module for Dynamic Global Vegetation Models

In nature, most grasses grow quickly enough to finish their lifecycle within one growing season [Gibson, 2009]. Some herbs and grasses are annual species that sprout from seeds every year, while for many perennial herbaceous plants the entire aboveground biomass dies back after the growing season and then resprouts from the root mass during the next growing season [Cheney and Sullivan, 2008, Gibson, 2009]. In LPJ however, herbaceous PFTs take 3-10 years to reach equilibrium potential aboveground biomass under constant climate, soil and CO₂ forcing in part because establishment and allocation are updated only once annually. In SPITFIRE, herbaceous biomass is removed as a result of combustion. In areas with frequent fire, LPJ-SPITFIRE simulates herbaceous biomass and FPC that are lower than observations. This inconsistency affects not only fire behavior but also general biogeochemical cycling in ecosystems where herbaceous vegetation is present.

To avoid an unrealistic reduction in herbaceous biomass in LPJ-LMfire as a result of fire, we convert combusted live grass biomass to carbon, but do not remove the grass biomass from the live biomass pool at the end of year, similarly to the scheme used by Kaplan et al. [2011] to simulate the harvest of agricultural crops. This correction results in more realistic biomass and coverage of grasses when simulating fire. In the future, a new and more realistic implementation for the development and senescence of grasses within LPJ should be implemented, which will require moving to a daily time step for grass allocation, as, e.g., has been done for crops in LPJ-ML [Bondeau et al., 2007].

3.3.4 Datasets and model runs used for model evaluation

Evaluating a complex DGVM and fire model such as LPJ-LMfire requires suitable input data for driving the model, including information on climate including lightning, soils, topography, atmospheric CO₂ concentrations, and human population density and anthropogenic land use. Unfortunately, not all parts of the world where fire is observed are equally well represented in terms of quality data for driving and testing DGVMs with fire. In the simulations described below, we prepared a standard, global driver dataset for LPJ-LMfire using the datasets listed in Table 3.3. For the Alaska case study we replaced LIS/OTD with the ALDS dataset for the time period of record that overlapped with our experiments (1986-2010).

In all of the simulations presented in this paper, the model was spun up for 1020 years with a detrended version of the 20th Century Reanalysis climatology, with the atmospheric CO₂ concentrations of 1871, and then run in a transient simulation from 1871 to 2010.

Since we focus on the overall performance of the model in simulating fire behavior and impacts on ecosystems, and since the development of the demographic history datasets is the subject of a separate publication, we exclude anthropogenic ignitions from the simulations presented here.

We needed model-independent data to evaluate simulated fire frequency and behavior, e.g., satellite-derived or ground-based data of annual burned area. To evaluate LPJ-LMfire's per-

Table 3.3: Datasets used to drive LPJ-LMfire

Variables	Datasets	References
<i>Baseline climatology:</i>		
<i>Long-term monthly means</i>		
Temperature, Precipitation, Diurnal Temperature Range	WorldClim 2.1; Climate WNA	Wang et al. [2011], Hijmans et al. [2005]
Number of days per month with precipitation, Windspeed	CRU CL 2.0	New et al. [2002]
Total cloud cover	Wisconsin HIRS Cloud Climatology	Wylie et al. [2005]
Lightning flashes	LIS/OTD HRMC	Christian et al. [2003]
<i>Climate interannual variability:</i>		
<i>Detrended and transient (1871-2010)</i>		
Temperature, Precipitation, Cloud Cover, Windspeed, CAPE	20 th Century Reanalysis	Compo et al. [2011]
Elevation and Slope	ETOPO1	Amante and Eakins [2009]
Soil particle size distribution and volume fraction of coarse fragments	Harmonized World Soil Database	FAO et al. [2008]
Atmospheric CO ₂ concentrations	Composite CO ₂ timeseries	Krumhardt and Kaplan [2012]
Land Use	HYDE v3.1	Klein Goldewijk et al. [2010]

formance in Alaska, we compared simulated area burned between 1986 and 2010 with the AFS historical burned area polygon dataset [Alaska Fire Service, 2013]. For global model evaluation, we used GFEDv3 [Giglio et al., 2010] and the global burned area dataset published by Randerson et al. [2012].

3.4 Model results and evaluation

In the following sections, we first present and discuss LPJ results for simulated aboveground biomass and the O-horizon. We then present our case study for Alaska where we evaluate LPJ-LMfire simulation results with reference to the high quality datasets on lightning strikes that we used to drive the model, and detailed maps of annual burned area that we used to test model output. We present and discuss a world map of potential natural fire return interval that could be used for ecosystem management and restoration, and finally, compare a global fire scenario to global observations of burned area.

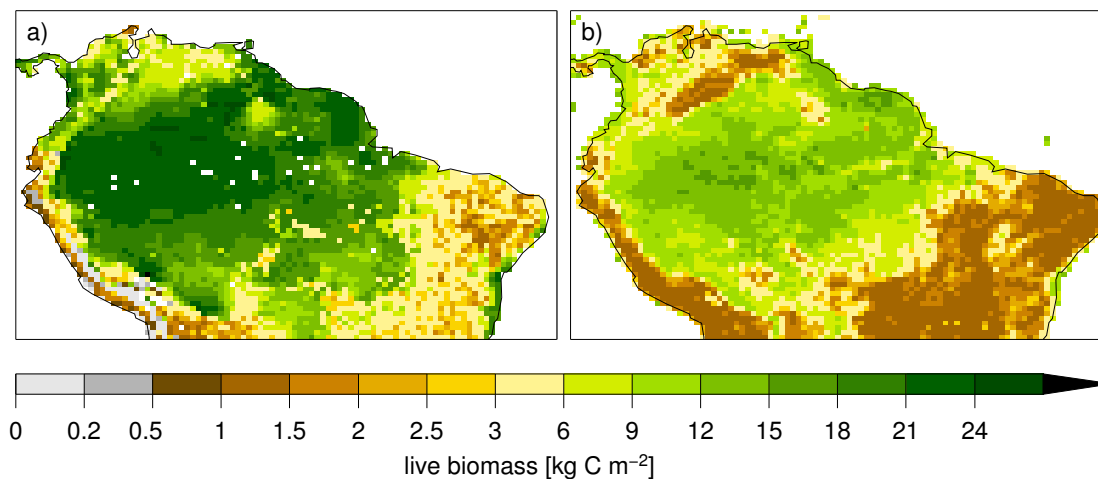


Figure 3.3: Simulated aboveground C-storage in living biomass (panel a)) after corrections to maximum establishment rate and maximum crown diameter in LPJ compared to aboveground live biomass values values derived from Saatchi et al. [2009] (panel b))

3.4.1 Aboveground biomass

As noted in section 3.3.2, living aboveground biomass simulated by LPJ was consistently overestimated compared to values reported in literature, especially in places with high biomass such as the Amazon Basin, where simulated values reached a maximum of more than 30 kg C m^{-2} . After the modifications we made to maximum crown radius and maximum establishment rate, aboveground biomass simulated in the central Amazon Basin ranged between 18 and 21 kg C m^{-2} (Fig. 3.3a). Comparisons of our simulated biomass with observations derived from satellite observations [Saatchi et al., 2009] show that even after the modifications, LPJ's estimates of aboveground live biomass are likely to be still on the high end of estimates. Aboveground biomass carbon estimates collected by Malhi et al. [2006] for old-growth Amazonian forests range between 8.5 and 16.7 kg C m^{-2} . Estimates of biomass carbon for tropical moist forests in the Brazilian Amazon collected by Houghton et al. [2001] range between 10 and 23.2 kg C m^{-2} , with a mean of 17.7 kg C m^{-2} . In regions with generally lower biomass, e.g., in the Caatinga of northeast Brazil or in the Andes, simulated and satellite-derived biomass values reported by Saatchi et al. [2009] are generally in good agreement, though the model underestimates biomass in parts of the Andes.

3.4.2 The organic soil layer

Figure 3.4 shows the global amount of carbon stored in the new LPJ O-horizon. The highest values are found in northeastern Siberia and northern North America, with values ranging between 2 and 3.5 kg C m^{-2} . In northern Europe, simulated values range between 1 and 2 kg C m^{-2} . These values do not capture the high end of values reported in literature, but are well within the observed range. For example, Mäkipää [1995] reported a range of 0.5 to

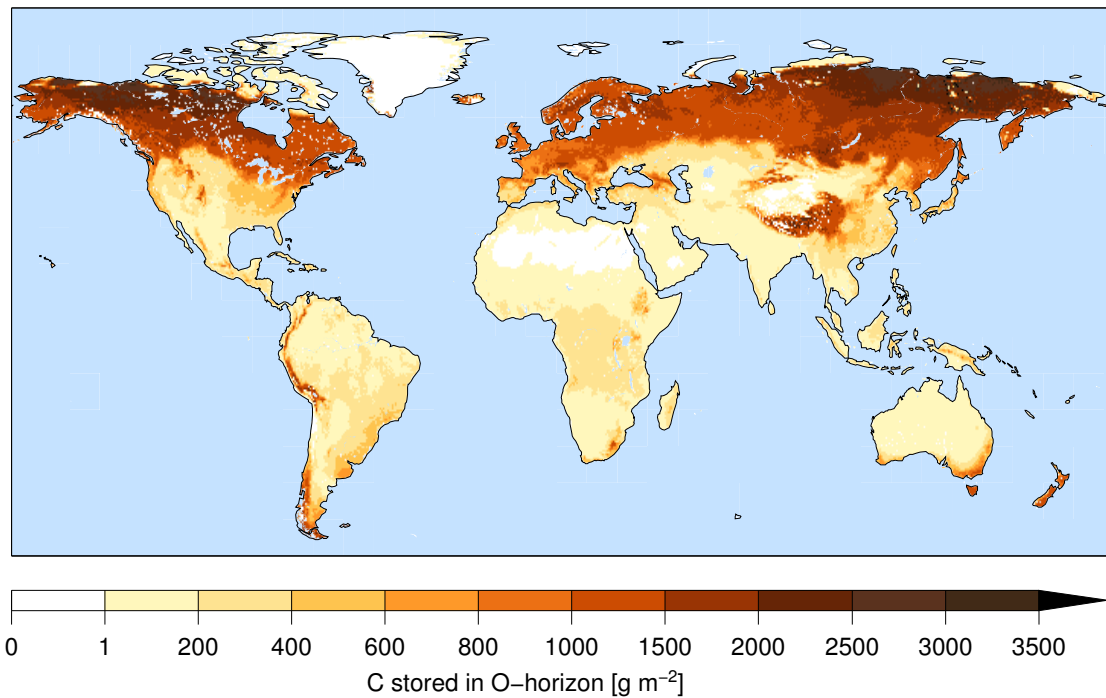


Figure 3.4: Simulated C-storage in the organic topsoil layer (O-horizon) newly implemented in LPJ

3 kg C m⁻² for the organic layers of forest soils in Southern Finland, depending on nutrient status and site wetness. For the arctic tundra of North America, Ping et al. (2008) reported values as low as 0.7 kg C m⁻² for mountain sites, and reaching 15.1 kg C m⁻² for lowland sites. Pregitzer and Euskirchen [2004] summarize organic soil horizon stocks from a number of studies, giving a range between 0.2 and 19.5 kg C m⁻² for boreal forests. The values simulated by LPJ are therefore within a realistic range, although site-specific variability cannot be reproduced at 0.5° spatial resolution.

3.4.3 Fire in boreal ecosystems: The Alaska case study

Fire is an important process in the boreal region and controls a variety of different ecosystem processes such as succession, tree recruitment, vegetation recovery, carbon storage, soil respiration and emission of atmospheric trace gases [Landhaeuser and Wein, 1993, Kurz and Apps, 1999, Johnson, 1992, Harden et al., 2000, Turetsky et al., 2002, Bergner et al., 2004, Kasischke et al., 2005]. Alaska was particularly suitable for our model evaluation, first because neither SPITFIRE nor LPX were able to simulate adequate amounts and realistic variability of burned area in boreal and subarctic environments, and also because the availability of data to drive and evaluate the fire model are excellent for this region.

Because sufficiently dry conditions occur comparatively rarely, fire is highly episodic in boreal

Chapter 3. LMfire: An improved fire module for Dynamic Global Vegetation Models

and subarctic Alaska and northern Canada [Kasischke et al., 2002], and hence the observational record is dominated by relatively few big fire years. Lightning is the main source of ignitions for large fires in boreal ecosystems. For the period 1950-1969, Barney [1971] showed that ~24% of all fire ignitions in Alaska were caused by lightning, but fires started by lightning accounted for more than 80% of total area burned. Todd and Jewkes [2006] provide an extensive year-by-year overview from 1950 to 2005, listing the total number of wildfires per year caused by humans and lightning, and the corresponding number of acres burned by these wildfires. 89% of all burned area between 1950 and 2005 can be attributed to lightning-caused fires [Todd and Jewkes, 2006]. From 1986 to 2005, 11 years had more than 95% of the total annual area burned attributed to lightning fires, 13 years had more than 90%, and 16 years had more than 80%. One of the reasons why the highly variable fluctuations in burned area could not be reproduced by the original version of SPITFIRE could be because interannual variability in lightning occurrence was neglected as described in section 3.3.1 above. Furthermore, smoldering fires are an important part of fire behavior in boreal and subarctic environments. For example, the recent Anaktuvuk River tundra fire smoldered for nearly two months as the tundra dried out before spreading rapidly at the end of the summer [Jones et al., 2009]. With the high-quality datasets that are available on fire in Alaska, we set out to see if the improvements we made to LPJ-LMfire substantially improved the model performance in this ecologically important region.

Simulated and observed area burned

Since the majority of burned area in Alaska is due to lightning-ignited fires [Todd and Jewkes, 2006], we set the model up to only simulate ignition and spread of naturally, i.e., lightning-ignited, fires on land not subject to human land use. We distinguish the following seven major ecoregions (Fig. 3.5) based on the ecoregions distinguished by the Alaska Interagency Coordination Center (2013):

1. Intermontane Boreal (IB)
2. Arctic Tundra (AT)
3. Arctic Range Transition (ART)
4. Bering Taiga (BTA)
5. Bering Tundra (BTU)
6. Coastal Rainforests (CR)
7. Aleutian Meadows (AM)

Depending on the ecoregion in consideration, the simulated and observed area burned on average over the time period from 1986 to 2010 varies considerably. In the following sections, we compare and discuss simulated fire occurrence with observed burned area by ecoregion.

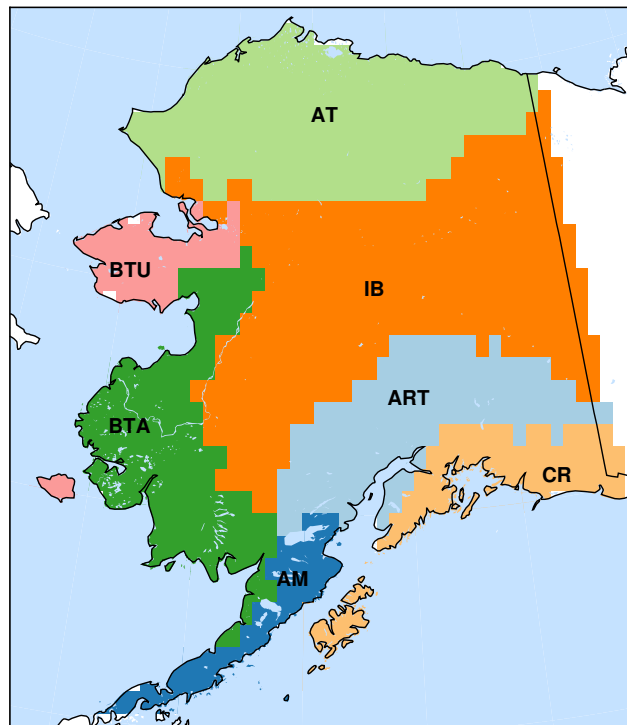


Figure 3.5: Alaska ecoregions following the scheme used by the Alaska Fire Service. IB=Intermontane Boreal; AT=Arctic Tundra; ART=Alaska Range Transition; BTA=Bering Taiga; BTU=Bering Tundra; CR=Coastal Rainforest; AM=Aleutian Meadows

Table 3.4: Observed and simulated mean (standard deviation) area burned and burned percent of total ecoregion area over the time period 1986-2010 by ecoregion

ecoregion	observation (km ²)	observation (% area)	simulated (km ²)	simulated (% area)
IB	4834 (6285)	0.96 (1.25)	4736 (5654)	0.94 (1.13)
AT	138 (281)	0.04 (0.08)	680 (1782)	0.19 (0.51)
ART	91 (109)	0.04 (0.05)	134 (393)	0.06 (0.19)
BTA	86 (146)	0.03 (0.06)	22 (70)	0.01 (0.03)
BTU	48 (104)	0.05 (0.10)	15 (33)	0.01 (0.03)
CR	13 (38)	0.01 (0.02)	10 (47)	0.01 (0.03)
AM	1 (5)	0.00 (0.00)	0 (0)	0.00 (0.00)

Intermontane Boreal ecoregion The intermontane boreal ecoregion, situated between the Alaska Range and the Brooks Range, is the most important region of Alaska for fire. On average, 93% of the total area burned in Alaska is located in this area. Both the observational data and the simulation results identify this area as the region most affected by fire. In this region, observations show an average annual burned area of 4,834 km² over 25 years and a standard deviation of 6,285 km² or $0.96 \pm 1.25\%$ of the total area of the region (Table 3.4). Our simulated

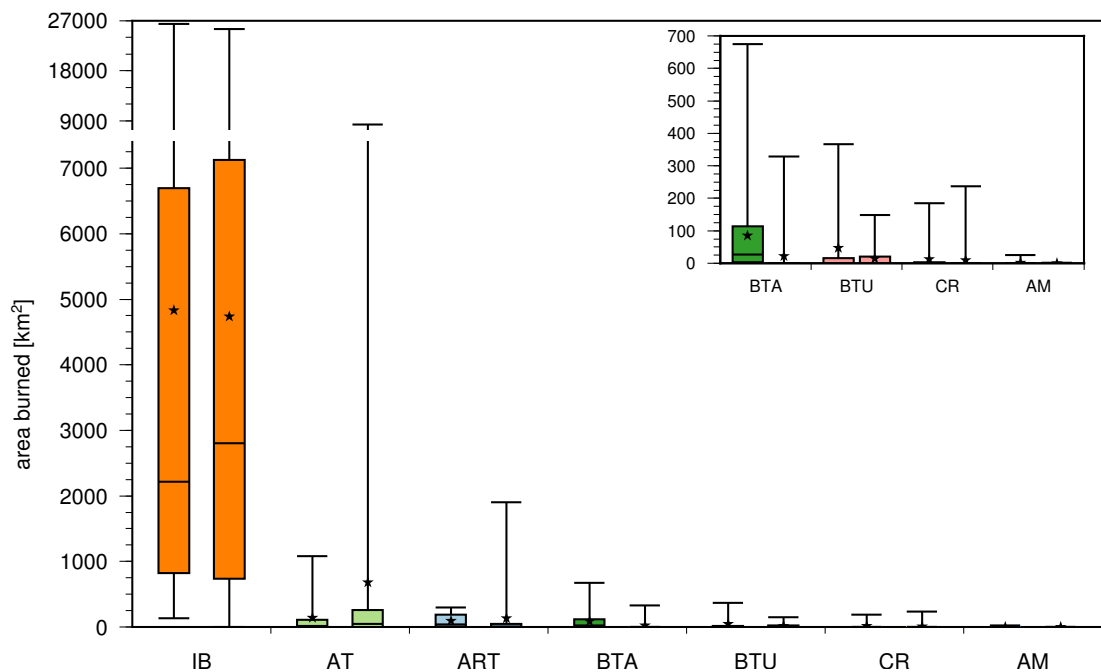


Figure 3.6: Boxplots showing the observed (left boxplot) and simulated (right boxplot) minimum, maximum, median and quartiles of area burned between 1986 and 2010 for each of the seven ecoregions. Black stars indicate the statistical mean value.

annual burned area of $4,736 \pm 5,654 \text{ km}^2$, or $0.94 \pm 1.13\%$, agrees well with observations, slightly underestimating both the total amount and the magnitude of the interannual variability in burned area. The absolute range of area burned in this region is approximately the same for both the observations and simulation, with a minimum of 136 vs. 0 km^2 and a maximum of 26,464 vs. 25,500 km^2 , respectively (Fig 3.6). For both observations and simulation, the annual mean burned area is larger than the median, indicating that the annual fire regime is characterized by relatively low area burned, occasionally interrupted by extreme years during which large areas burn. In contrast to the mean, where simulated burned area is slightly less than observations, the median and 75% percentile burned area are slightly higher in the simulation than the observations (Fig. 3.6). In Fig. 3.7 we show the simulated and observed timeseries of burned area in the Intermontane Boreal region. LPJ-LMfire reproduces observations of burned area well not only in terms of the average area burned over the 25 year period, but also in terms of the interannual variability.

Arctic Tundra Compared to the Intermontane Boreal ecoregion described above, burned area in the other six ecoregions is very small in terms of total area burned as well as percent of the ecoregion burned (Fig 3.6, Table 3.4). Our simulations therefore correctly identify the location of the most important ecoregion for fire in Alaska. However, our simulations overestimate the mean annual area burned as well as the maximum annual area burned for

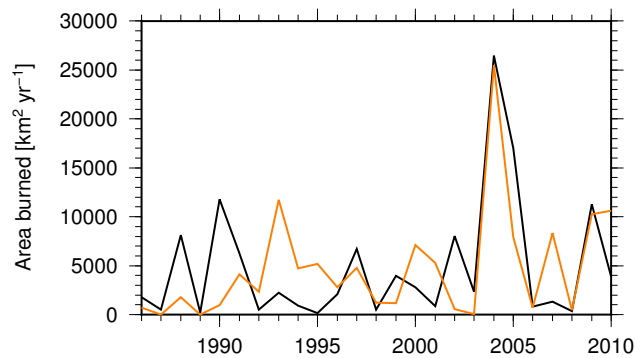


Figure 3.7: Simulated (orange) and observed (black) time series of total annual area burned in ecoregion IB between 1986 and 2010.

ecoregion AT (Arctic Tundra) compared to the observation data. This is due to two years within the simulated time series, 2008 and 2009, for which we largely overestimate the total area burned, whereas in most other years we simulate low amounts of burning that match the observational data in magnitude and variability. Exceptional years with very large single tundra fires are known to occur, e.g., the Anaktuvuk River Fire in 2007 [Jones et al., 2009]. Although LPJ-LMfire is capable of simulating years with exceptionally large amounts of fire in Alaska's arctic tundra, we are not able to reproduce burned area in exactly those years when large burned area was observed.

Bering Taiga and Bering Tundra Burning in the westernmost part of Alaska (ecoregions BTA and BTU) is generally low in the observational data (Fig. 3.6, Table 3.4), with a maximum of $675 \text{ km}^2 \text{ yr}^{-1}$ burned during the period 1986-2010, with an average of $86 \text{ km}^2 \text{ yr}^{-1}$, and a median of $27 \text{ km}^2 \text{ yr}^{-1}$ for the Bering Taiga, and a maximum of $367 \text{ km}^2 \text{ yr}^{-1}$, an average of $48 \text{ km}^2 \text{ yr}^{-1}$ and a median of $0 \text{ km}^2 \text{ yr}^{-1}$ for the Bering Tundra. This implies that an average of 0.03% of the Bering Taiga and 0.05% of the Bering Tundra region burned over the 25-year period. Our simulations underestimate burning in these regions, especially for the Bering Taiga, where the simulated maximum burned area is $329 \text{ km}^2 \text{ yr}^{-1}$, with an average of $22 \text{ km}^2 \text{ yr}^{-1}$ and a median of $0 \text{ km}^2 \text{ yr}^{-1}$. For the Bering Tundra, we simulate a maximum of $148 \text{ km}^2 \text{ yr}^{-1}$, an average of $15 \text{ km}^2 \text{ yr}^{-1}$, and a median of $0 \text{ km}^2 \text{ yr}^{-1}$, therefore also underestimating observations.

Ecoregions ART, CR and AM For ecoregion ART (Alaska Range Transition) LPJ-LMfire simulates a mean annual burned area of $134 \pm 393 \text{ km}^2 \text{ yr}^{-1}$ and a median of $4 \text{ km}^2 \text{ yr}^{-1}$ compared to an observed mean annual burned area of $91 \pm 109 \text{ km}^2 \text{ yr}^{-1}$ and a median of $37 \text{ km}^2 \text{ yr}^{-1}$ (Fig. 3.6, Table 3.4). We therefore underestimate the median while overestimating the mean, with the latter again being augmented due to one single fire year, 2007, for which we simulate a maximum of $1,907 \text{ km}^2 \text{ yr}^{-1}$ against an observation value of only $299 \text{ km}^2 \text{ yr}^{-1}$. All other 24 years for ecoregion ART are within the range of observation concerning total area burned

and interannual variability. Ecoregions CR (Coastal Rainforest) and AM (Aleutian Meadows) are ecoregions with extremely low amounts of burned area, both observed and simulated, in total as well as percentage of region's area. For ecoregion CR, an average of $13 \pm 38 \text{ km}^2 \text{ yr}^{-1}$ in the observation data compares to a simulated average of $10 \pm 47 \text{ km}^2 \text{ yr}^{-1}$. In ecoregion AM, burned area is recorded in four out of the 25 years of observation compared to two years of fire simulated by LPJ-LMfire. These results reveal that though we may not be able to reproduce exact numbers for area burned at the very low end of fire observations, we are still able to simulate fire occurrence behavior realistically even in areas where burning is rare and reproducing any fire at all in the simulations is challenging.

Discussion of Alaska burned area results

While overall mean simulated burned area was close to that observed, peak fire years in our simulated time series did not always match observed peak fire years (Fig. 3.7). The cause for this mismatch may be linked to the uncertainty in daily weather conditions resulting from the usage of a weather generator and monthly climate data. Using monthly climate forcing constrains total precipitation amount and number of wet days, but the timing of rainy days within a given month may be very different in the simulation compared to the true weather situation, e.g., if simulated wet days all come clustered at the beginning or end of the month whereas in reality they had been more equally distributed over the month. In such a case, the consequences for fuel wetting and drying are different between observation and simulation, with simulation overestimating fuel dryness and FDI and therefore leading to higher amounts of area burned. Moreover, the timing and amount of precipitation matters for simulating fire extinction in LPJ-LMfire, as either one day with more than 10 mm precipitation (3 mm precipitation with more than 60% grass cover) or several consecutive days with a sum of more than 10 mm precipitation are required to extinguish fires in our simulation. If, e.g., a fire is burning in a given month and the simulated clustering of rainy days within this month is less pronounced than the clustering that occurred in reality, the fire may continue burning although in reality it was extinguished. This may also be true for the opposite case, where fires are extinguished although they should have kept burning. Another uncertainty is linked to wind speed: as we lack the capability in our weather generator to disaggregate wind speed to daily or hourly values, we use climatological mean wind speed, which may underestimate the infrequent, high-wind events that are responsible for the largest episodes of fire spread. Finally, LPJ-LMfire does not simulate the feedback mechanism between fire and wind, e.g., large, intense fires such as those observed in boreal forests may produce strong convection that increases wind speeds in the vicinity of the fire, which in turn enhances fire spread.

Correct simulation of fires in tundra regions is challenging for several reasons. The most significant problem leading to a general overestimation of simulated burned area on the Alaska North Slope is the simple soil water scheme of LPJ that is neither able to explicitly simulate permafrost nor wetlands. Detailed analyses of grid pixels in Northern Alaska revealed that soils dry out very quickly as soon as all snow has melted in May or beginning of June, and,

because it is linked to soil moisture, the water content of the live grass drops quickly. Summers in Northern Alaska are dry, while at the same time day length is long and therefore simulated evapotranspiration is high and helps to draw down soil moisture in combination with surface runoff and drainage. Overall, this leads to simulation of environmental conditions that are far drier than in reality where thawing of the active layer proceeds slowly down the soil column over the course of the summer and, by limiting evapotranspiration, keeps soils and vegetation wetter than would otherwise be the case. If lightning occurs in the period between May and July, simulated fires spread very fast and therefore lead to an overestimation of burned area. In most of the cases where we overestimate burning, fires are ignited early in summer when in reality conditions are likely still too wet; the simulated fires spread quickly due to the fuel being dry and keep burning through summer due to the lack of precipitation. In addition to the poor representation of wetlands and permafrost in LPJ, the tundra on Alaska North Slope is characterized by a high density of water bodies including many lakes, peatlands, streams and rivers, which is not taken into account in LPJ. In reality, these water bodies will limit the spread of fires, as can be observed for the Anaktuvuk River fire which is bordered by rivers on its western and eastern margins. Future improvements to LPJ and the fire model therefore should focus on the implementation of adequate permafrost and wetland simulation modules [e.g., Wania et al., 2009, Koven et al., 2009, Ringeval et al., 2010] and the incorporation of some spatial statistic representing water body distribution on a grid cell level as a limiting factor to the spread of fires. This could be accomplished similarly to the way in which we account for the effects of landscape fragmentation on fire size as a result of topography (section 3.3.2) or land use (section 3.3.2). As LPJ-LMfire has no PFT that specifically represents it, tundra vegetation in the model is simulated with the C₃-grass PFT. As described in section 3.3.2, we tried to improve the representation of tundra vegetation with respect to fuel conditions by scaling the density of live grasses to the number of growing degree-days and by accounting for permafrost-impeded drainage of soil water. Eventually, woody shrub vegetation and tussocks could be represented by one or more separate tundra PFTs [see, e.g., Kaplan et al., 2003, Wania et al., 2009] as each of the constituent tundra vegetation plants have different density, height, and flammability that would affect fire spread.

Comparing the Bering Taiga and Bering Tundra ecoregion to the Arctic Tundra in Northern Alaska reveals that all three ecoregions are characterized by generally very low amounts of lightning. They can therefore all be classified as ignition-limited fire regimes. In contrast to the Arctic Tundra region, the two western regions have their precipitation maximum in summer, which coincides with the potential fire season. As a consequence of frequent rainfall events with often-substantial daily precipitation amounts, fuels stay wet and soil water status is high (Fig. 3.8). In the already rare case of a lightning ignition, fires therefore tend to spread slowly, stay small and are soon extinguished, especially when compared to fires started in the Arctic Tundra.

Rare but important fires in boreal and subarctic environments develop during particular conditions, e.g., an exceptionally long string of dry weather. As LPJ-LMfire uses a weather generator to disaggregate monthly climate variables to daily values, it is possible that the

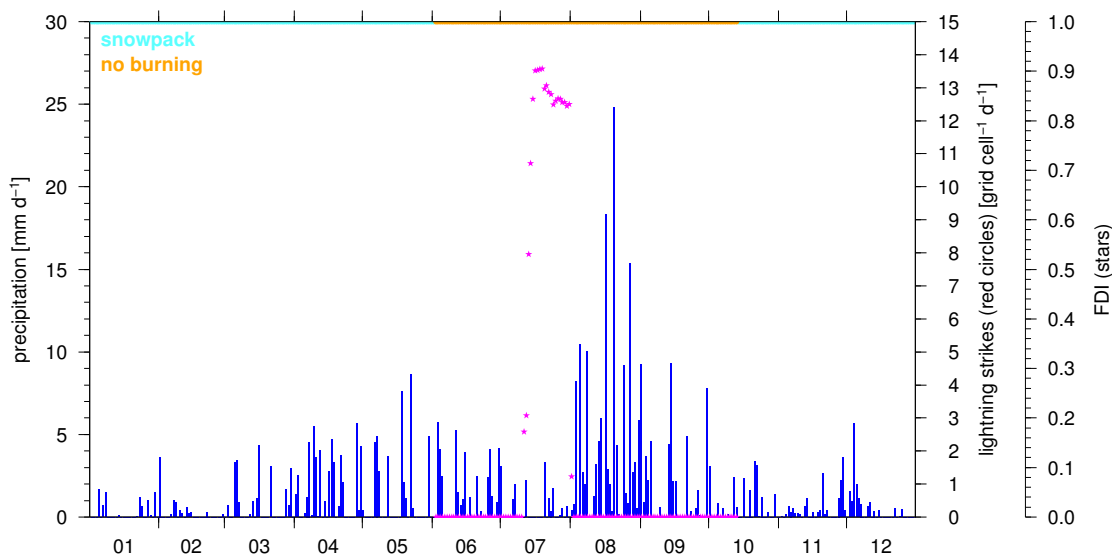


Figure 3.8: Typical daily diagnostics for a grid pixel located in ecoregion BTA, showing the daily amount of precipitation (blue bars), FDI (pink stars), lightning strikes (red circles), duration of snowcover (turquoise line at top of panel) and the snow-free time potentially available for burning (yellow line at top of panel). The year shown had a short dry period in July with FDI values high enough for burning, but no lightning strike that potentially could have started a fire occurred during this year.

specific circumstances that in reality led to a fire, i.e., having an ignition while at the same time simulating a sufficiently long dry period after the ignition so that the fire can spread, are not captured by the model simulation. With only few lightning sensors located in the far west of Alaska, it is also possible that the actual amount of lightning occurring in these two ecoregions is underestimated and not all lightning is recorded.

Apart from the limitations discussed here, using daily and interannually variable lightning as described in section 3.3.1 allows us to simulate fire in boreal regions, with results showing considerable interannual variability in total burned area. Although we may not be able to reproduce observed annual area burned exactly on a year-to-year basis because of the limitations highlighted above, with LPJ-LMfire we capture the overall behavior of boreal fires well in terms of being able to simulate long-term averages and variability that are consistent with observations.

Simulated fire return intervals in Alaska

Fire return interval (FRI), i.e., the number of years between successive fires in an area, is widely used to characterize natural fire regimes and assess the changes in fire frequency caused by climate change. For the recent past, efforts to reconstruct FRIs based on fire scar datasets have been performed by Balshi et al. [2007], who present maps of fire return intervals in boreal

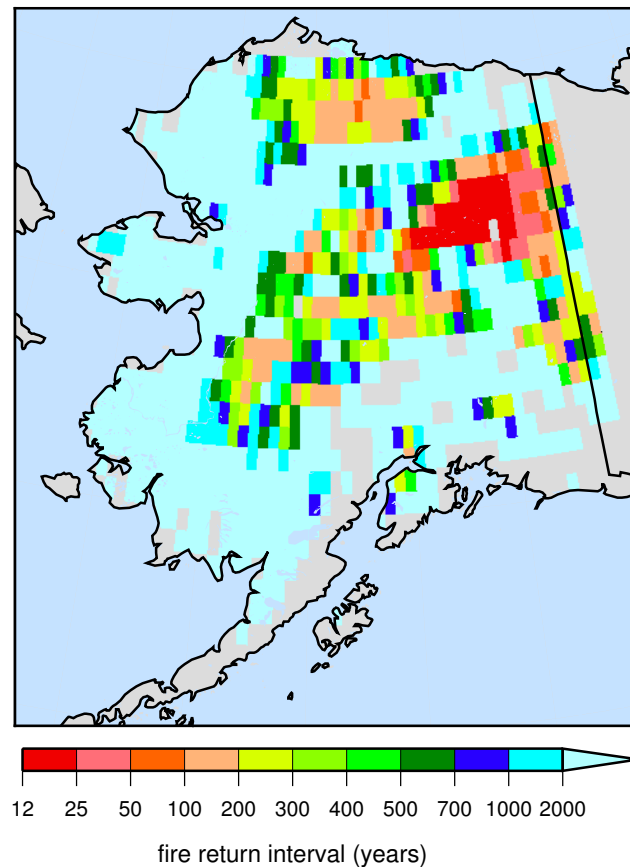


Figure 3.9: Simulated fire return intervals in Alaska for a 1000-year run with detrended 20th century climate.

North America and Eurasia using historical fire records for the 2nd half of the 20th century. In places where fire is infrequent, however, FRIs may exceed the period of modern observations. Detailed historical records of burned area in the boreal forest in the best case hold a little more than 70 years of data in Alaska and Canada and even less than that in Eurasia. Short records may be not representative of the overall average fire regime as by chance they may, e.g., represent a time of relatively high or low fire activity and therefore lead to an overestimation or underestimation of average FRIs over longer time scales. The need to perform spatial interpolation of FRIs over large spatial scales introduces further uncertainty.

Analysis of charcoal accumulation rates from sedimentary archives has been applied successfully on local to regional scales to reconstruct FRIs over longer time scales [e.g., Higuera et al., 2009, Lynch et al., 2004, Tinner et al., 2006, Higuera et al., 2008, Brubaker et al., 2009]. However, centennial to millennial scale climate variability probably affected FRIs as ecosystems adjusted to changing climate. It is therefore difficult to characterize steady-state equilibrium FRIs, or estimate how future climate changes could affect burning, based solely on paleo-archives. The advantage of DGVMs containing fire models is that they can be run for long time periods

Chapter 3. LMfire: An improved fire module for Dynamic Global Vegetation Models

using detrended steady-state climate, allowing vegetation and fire regime to equilibrate so that conclusions can be made as to what the equilibrium FRI would be if climate at any given time stayed constant.

To estimate FRIs for Alaska, we made a model run over 1,000 years with steady-state climate after vegetation and fire regime had equilibrated. Following Balshi et al. [2007], we define FRI as the time required to burn an area equal to the entire 0.5° grid cell. The FRI within a gridcell is consequently calculated as the ratio of 1,000 years and the number of times a gridcell area burned during these 1,000 years. We present our simulated fire return intervals in Fig. 3.9, using the same color scheme as in Balshi et al. [2007], but without applying any smoothing. Agreeing with Balshi et al. [2007], we simulate frequent burning with return intervals between 12 and 50 years in Eastern Alaska located in the Intermontane Boreal ecoregion between Brooks Range and Alaska Range. Towards the west of ecoregion IB, the FRIs predicted from our simulation become more heterogeneous, from less than 50 years to more than 500, therefore being slightly lower than the FRIs estimated by Balshi et al. [2007]. Towards the extreme west of mainland Alaska, we simulate FRIs between 900 and 2,000 years for some grid cells, but mostly FRIs are longer than 2000 years. Compared to Balshi et al. [2007] we estimate significantly longer FRIs in some gridcells, especially for ecoregion BTU (Bering Tundra). This may be linked to the possibility that the already low amounts of lightning is underestimated in the LIS/OTD lightning climatology used for this experiment, due to the limited four-year length of record of the lightning climatology and the low detection efficiency at high latitudes. In contrast, we simulate shorter fire return intervals for the Arctic Tundra, which typically fall in the 100-200 year and 500-700 year categories. Given the model shortcomings related to the simulation of tundra vegetation and permafrost (see section 3.4.3), these results may be biased somewhat towards shorter FRIs than are actually observed..

3.4.4 Global fire under natural conditions

The global effects of fire on aboveground live biomass are shown in Fig. 3.10. Both panels represent a world with potential natural vegetation and no anthropogenic land use. Panel (a) shows biomass with natural fires caused by lightning ignitions, while panel (b) shows a world without fire. Panel (c) shows the difference in biomass between a world with and without fire. The maps clearly reveal the parts of the world that are mostly affected by fire disturbance and therefore have less biomass than they potentially could have in a world without fire. On a 100-year basis the total amount of global carbon stored in aboveground living biomass is 208 ± 2 Pg less for the simulation with fire compared to the simulation without fire, totaling 948 ± 3 Pg C with fire. No impact of fire on biomass is simulated for the wet tropics where very little fire is simulated, such as the Amazon and Congo Basins or in Indonesia, all places that naturally store large amounts of carbon in forests. Most of the biomass loss related to fire disturbance is simulated in the seasonal tropics and subtropics: in the Miombo woodland region south of the Congo Basin, in the east and southeast of the Amazon Basin, in the Sahel, in India and Southeast Asia, and in Northern and Southern Australia. The impact of fire on

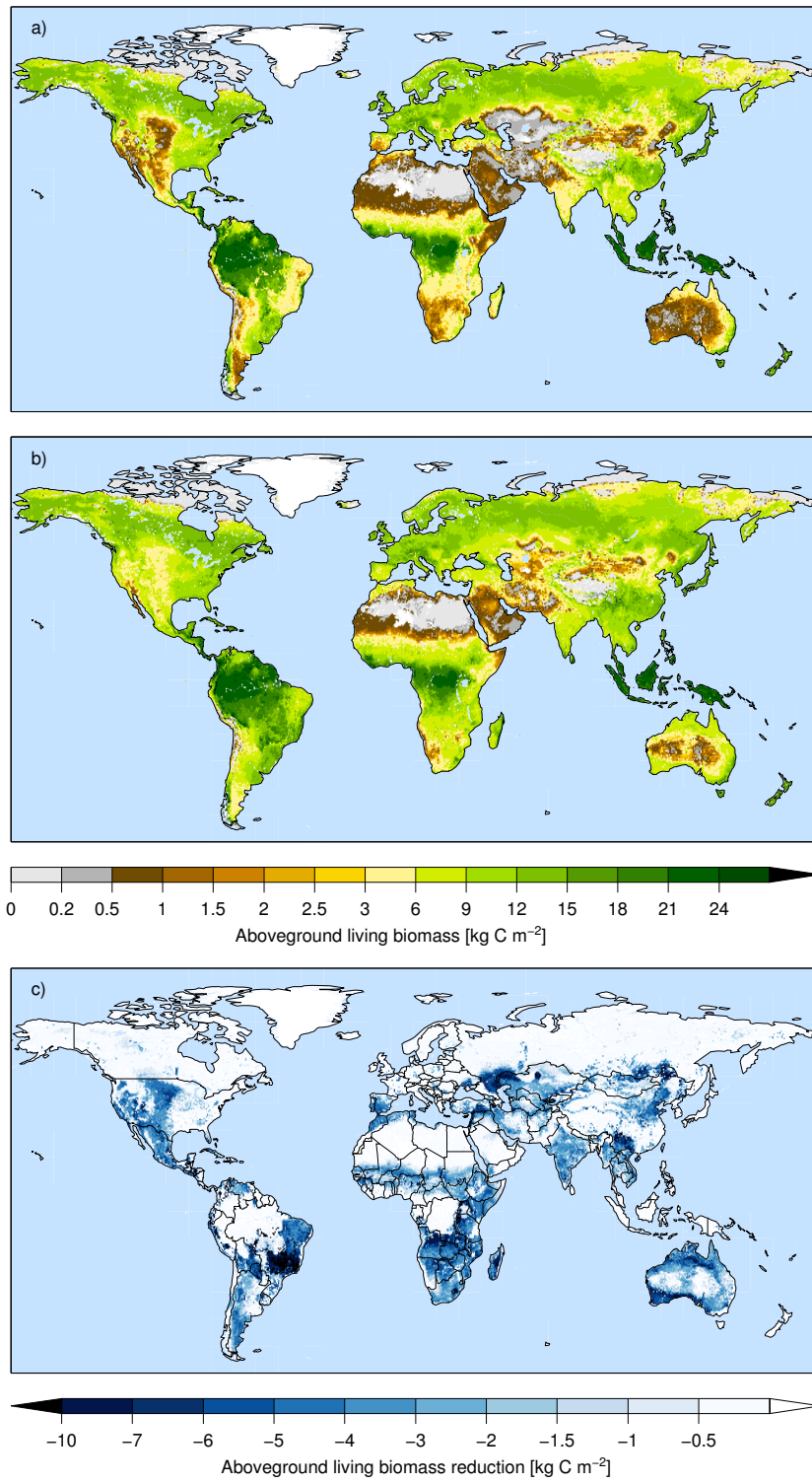


Figure 3.10: Simulated biomass C: a) human absence, lightning fires; b) human absence, no fire; c) reduction in biomass C between a) and b)

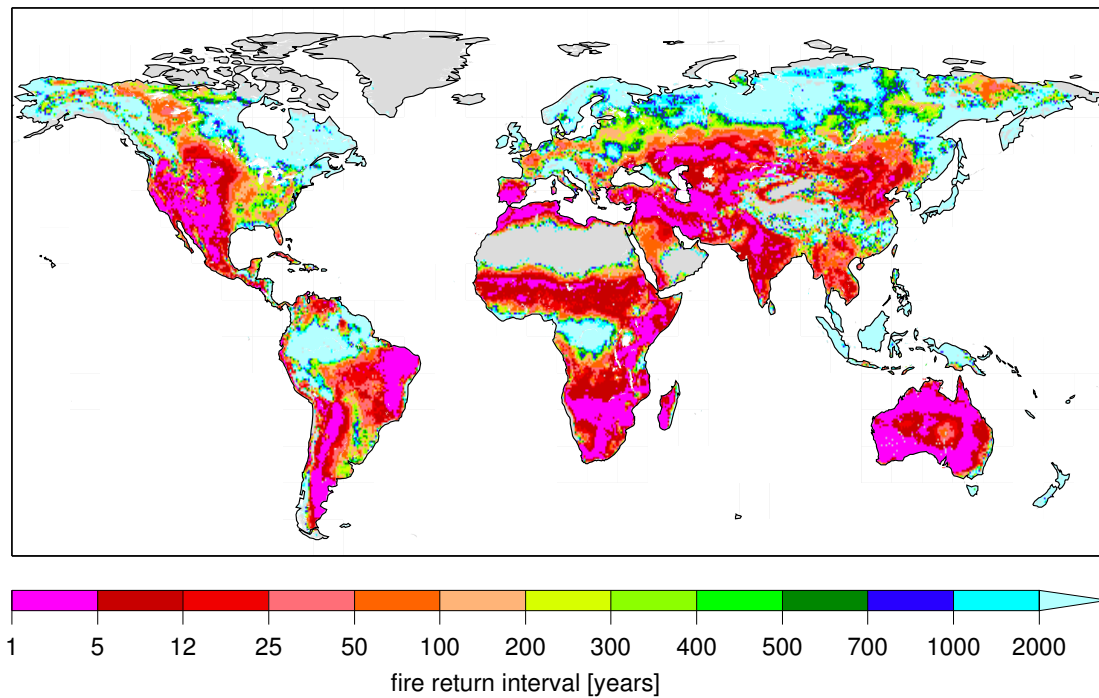


Figure 3.11: Simulated global fire return intervals for a model run over a time period of 1000 years using the detrended 20th century reanalysis and LIS/OTD-derived lightning climatology.

biomass is also clearly visible in the grassland regions of central and western North America, the Western Mediterranean, Southwestern Russia, Kazakhstan and Uzbekistan. Fires in the boreal regions can be extensive, but the return interval is too long to have a discernible impact on carbon storage in aboveground live biomass compared to ecosystems with short fire return intervals.

The results we present here are broadly consistent with those in Bond et al. [2005] who showed, in a series of experiments running a DGVM with and without fire, that the largest reductions in tree cover as a result of natural fire are in the seasonal subtropics. Bond et al. [2005, Fig. 6] also show a large reduction in forest cover in central Europe and the Eastern United States, areas where fire impacts in LPJ-LMfire are more muted. In contrast, LPJ-LMfire shows a large reduction in biomass in the grassland areas of central North America, on the Eurasian steppe, in central and southern Australia, and in southern South America when comparing "fire on" with "fire off" scenarios. Bond et al. [2005] state that FRIs simulated by their model in these natural grassland areas are much too long with respect to observations (75–200 years modeled where 2–5 years are observed). LPJ-LMfire shows much shorter FRIs (Fig. 3.11) of 1–5 years in much of these natural grassland regions that are more consistent with field observations.

The map of global FRIs in Fig. 3.11 shows that fires are most frequent in places where three factors are coincident:

- a) Enough biomass to sustain frequent burning
- b) Sufficient amounts of lightning ignitions
- c) Seasonally varying meteorological conditions, specifically a pronounced dry season that allows fuel drying.

If any of these three conditions is not present, wildfires are unlikely to occur. As noted above, fire is rare in the Amazon and Congo Basins and on the Indonesian archipelago. In these regions, lightning ignitions and biomass are not limiting, but meteorological conditions are typically too wet for the development of wildfires, with the exception of relatively infrequent severe drought events, e.g., in extreme El Niño years [Page et al., 2002, 2012]. In the desert and high-mountain regions of the world, e.g., in the Sahara desert, the southern part of the Arabian Peninsula, and on the Tibetan Plateau, the absence of biomass is the limiting factor for fire. Large parts of the world's boreal and subarctic ecosystems have enough biomass to support frequent burning, but the number of lightning ignitions generally tends to be low compared to lower latitudes, snow and temperatures below 0°C occur for half a year or more, and the summer season is frequently the wettest time of the year.

In contrast, in any part of the world where all three factors are met, fire return intervals are short, e.g., in the Sahel, the Western Mediterranean, the Near East, in the Miombo woodlands south and east of the Congo Basin, in most of Australia, and in the xerophytic Caatinga shrublands of Northeastern Brazil.

3.4.5 Comparison to contemporary observations of burned area

While LPJ-LMfire has been primarily designed to simulate fire behavior during preindustrial time, we compared the results of a global model run with satellite-based estimates of burned area that cover recent decades. In our model experiments we did not attempt to account for either anthropogenic ignitions or active suppression of wildfires, but we did account for passive fire suppression through landscape fragmentation as a result of agricultural land use. The differences between simulated and observed burned area therefore highlight the importance of human influence on the geographic distribution of fire at present. In a few parts of the world where human impact is minimal, we were further able to identify potential shortcomings of the current version of LPJ-LMfire and priorities for future model development.

As described in section 3.3.4 above, we ran LPJ-LMfire with climate and soils data that reflect the late 20th and early 21st centuries. The model was spun up for 1,020 years with 1871 CO₂ concentrations and land use, and then run in a transient climate, CO₂, and land use scenario for the period 1871–2010. Used land was defined as the sum of the agricultural and urban fractions and was specified from the HYDE v3.1 anthropogenic land cover change scenario [Klein Goldewijk et al., 2010]. In our simulations, fires were only allowed to burn on the unused fraction of each gridcell, and the only ignition source was lightning.

Chapter 3. LMfire: An improved fire module for Dynamic Global Vegetation Models

We compare our model results with the global burned area products GFEDv3.1 [Giglio et al., 2010, hereafter GFED] and the data set presented by Randerson et al. [2012, hereafter JR12]. GFED provides complete annual coverage for the years 1997–2011, while JR12 covers the period 2001–2010. The main difference between the two observational burned area products is that JR12 accounts for numerous additional small fires not included in GFED, which results in an increase in mean annual burned area of up to 30% in some regions, mainly in the tropics and subtropics.

We compare modeled with observed burned area on the basis of a multi-year mean of the annual total burned area fraction of each 0.5° gridcell. We extracted the time periods from our LPJ-LMfire run overlapping with the period covered by the observational datasets, summed the monthly values in the observational datasets to create annual totals, and calculated average burned area over the number of years of record. In comparing LPJ-LMfire with GFED, we masked the difference between model and observation where the differences were less than the aggregate uncertainty specified in the GFED database. For comparison with JR12, we masked areas where the model-data mismatch was less than 1%.

The differences between LPJ-LMfire and GFED are shown in panel **a** of Fig. 3.12; differences with JR12 are in Fig. S8. Overall, the spatial pattern and magnitude of the residual between model and observations are similar regardless of the observational data set we used. The greatest differences between model and observations are found in the seasonal tropics of Africa, both north and south of the Equator, where LPJ-LMfire shows substantially less burned area than the observations. Further large negative residuals are seen in northern Australia, along the steppe belt of Eurasia from Ukraine to Kazakhstan, in southeast Asia particularly in Cambodia, in the Amur region of the Russian far east, and in the lowlands of Bolivia and Paraguay. In contrast, the model shows relatively more burned area compared to observations in several regions, notably in the Caatinga region of northeastern Brazil, in Iran and western Turkmenistan, in most of southern Australia, in the western United States, and in the Chaco dry forest region of northwestern Argentina.

In panel **b** of Figs. 3.12 and S8, we place these differences between model and observations in the context of the anthropogenic imprint on the global land surface by means of a simple classification of the residual based on human impact. We specified human impact based on the GLOBIO methodology [Ahlenius, 2005, Fig. S9], which identifies the presence of anthropogenic features on the ground including urban areas, open cast mines, airports, roads, railroads, canals, and utility lines. Half-degree gridcells covered 1% or more by anthropogenic features were classified as being substantially influenced by human activities. On the basis of this classification, 75% (347 out of 464 Mha) of the mean annual global burned area in JR12 occurs on land influenced by human impact (for GFED the amount is 71% or 258 of 363 Mha). The areas of largest disagreement between model and observations are even more concentrated in regions of human impact. In gridcells where the difference between LPJ-LMfire and the observational datasets is greater than 1%, human impact is visible on 93% of the area.

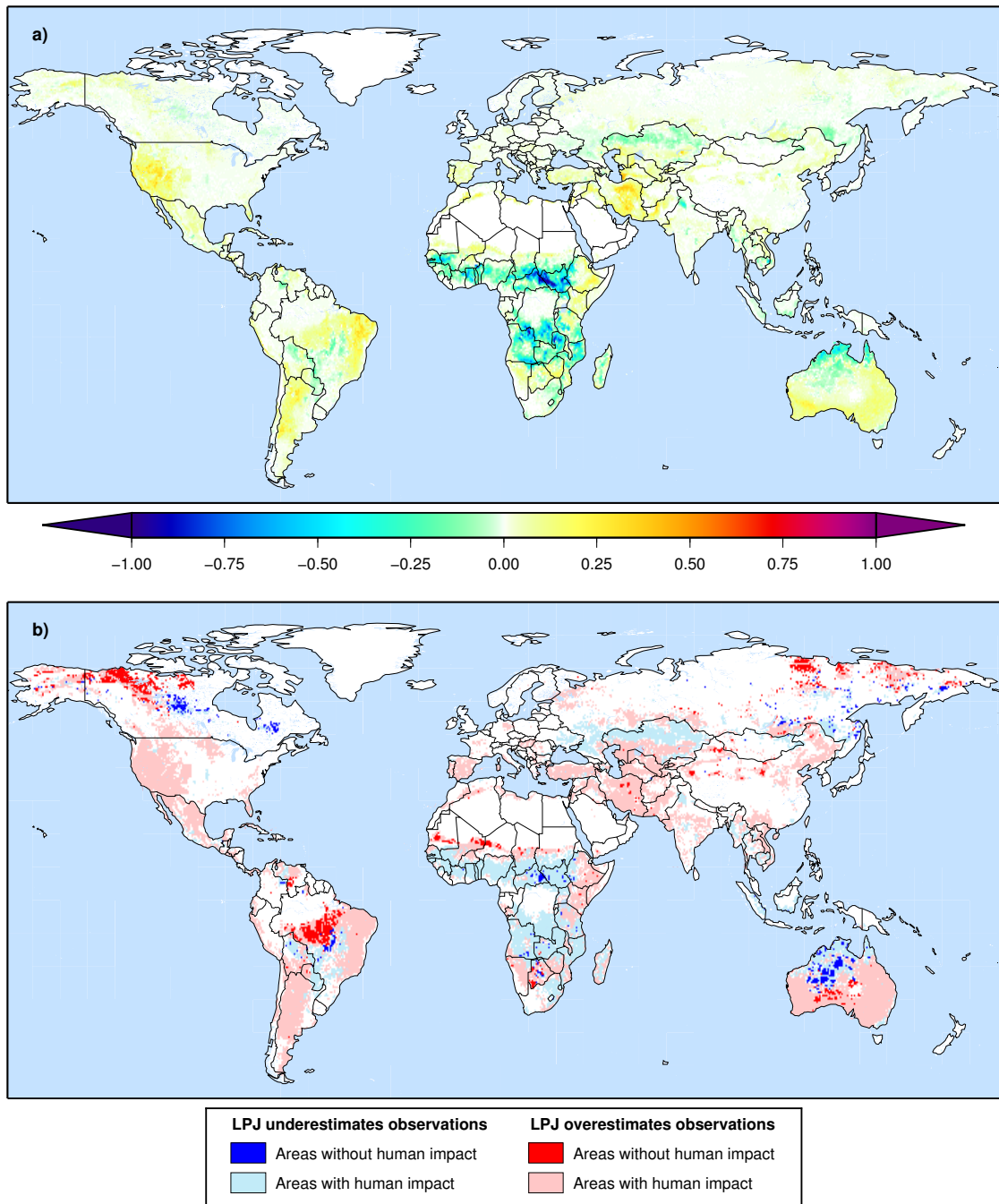


Figure 3.12: a) Residuals between observed average annual area burned in GFED and simulated burned area. b) Residuals between observed and simulated annual area burned in context of anthropogenic imprint on the global land surface.

As discussed above, where LPJ-LMfire underestimates observed burned area in much of the seasonal tropics, this is most likely the result of regular, intentional burning of cropland and pastures, and in some cases deforestation fires. In the Sahel, extensive agricultural burning is

Chapter 3. LMfire: An improved fire module for Dynamic Global Vegetation Models

common practice and occurs annually for several months during the Northern Hemisphere fall and winter when people ignite fires to remove crop residues, and to renew pasture grasses and stop woody encroachment on pastures, for hunting, and to control pests and wildfires [Menaut et al., 1991, Klop and Prins, 2008, Kull and Laris, 2009, NASA, 2011]. This is also the case for the Miombo woodlands south of the Congo basin and on Madagascar, where intentional burning plays an important role [Eriksen, 2007, Le Page et al., 2010]. van Wilgen et al. [1990] estimate that humans cause 70% of all annual fires in African savannas. Likewise, the large underestimate in burned area in the Eurasian steppe and Amur valley is related to agricultural burning [Tansey et al., 2004, Warneke et al., 2009].

In places where LPJ-LMfire overestimates burned area relative to observations and human impact is considered important, three processes that are not included in LPJ-LMfire may explain the differences: 1) removal of biomass from grazing and land degradation, 2) industrial fire suppression, and 3) landscape fragmentation from roads and other anthropogenic features that are not classified as agricultural land use by HYDE. Eastern Brazil, northern Argentina, southern Australia, East Africa, northern Mexico, and the western Great Plains of the United States are occupied by extensive open rangelands [Klein Goldewijk et al., 2010, Ramankutty et al., 2008] where livestock grazing leads to a reduction of fine fuel load that is not accounted for in our model simulations. Furthermore, the semiarid regions of the northern Sahel, Central Asia, and the Near East are characterized by extensive soil degradation as a result of overgrazing and millennia of land use [Dregne, 2002]. This degradation is not accounted for in our simulations, and the model simulates more biomass than is actually present, and therefore more fire. Industrial fire suppression is common in Europe, North America and Australia, and may explain much of the additional LPJ-LMfire overestimate relative to observations in these areas. In the U.S. alone, expenditure on wildfire suppression has increased continually over the last 70 years [Stephens and Ruth, 2005, Calkin et al., 2005, Westerling et al., 2006, Government Accounting Office, 2007, Gebert et al., 2007, 2008]. Finally, while we accounted for landscape fragmentation as a result of agricultural land use in our simulations, additional fragmentation effects caused by the presence of human infrastructure such as roads were not included. The combination of industrial fire suppression with a high magnitude of human impact is the likely cause for the overestimate in burned area in developed countries of the temperate regions.

On the remaining 7% of land area that may be classified as having insignificant human impact, we show overestimates in burned area in subarctic western Canada and eastern Siberia, in a small area along the southern margin of the Sahara in Mali and Niger, and markedly in the southeastern Amazon basin in the transition zone between tropical forests and the Cerrado savanna. In contrast, the model underestimates fire in boreal Canada, in the eastern Central African Republic, central Australia and in central Brazil. These residuals are useful for understanding the limitations of both our model and the observational datasets.

The unprojected maps in Figs. 3.12 and S8 exaggerate the area, but the overestimate in burned area in the subarctic may be caused by several factors that were already discussed in our

analysis of LPJ-LMfire results for Alaska. These include an inadequate representation of permafrost that influences soil hydrology and therefore fuel moisture, an overall overestimate in modeled aboveground biomass also caused by permafrost and/or lack of soil, and fine-scale landscape fragmentation caused by the rivers, lakes, and wetlands that are extensive in this region [Papa et al., 2010]. Permafrost is important in all of these northern areas where LPJ-LMfire overestimates observations [Tarnocai et al., 2009]. In areas of boreal Canada further south where LPJ-LMfire underestimates burned area, several factors not included in our simulations may influence the model results, including tree kill events as a result of insect infestations, and remote industrial activities including logging, and hydroelectric and oil and gas development. Furthermore, in the boreal and subarctic areas where modeled burned area is both under- and overestimated, the very short four-year period upon which our lightning climatology is based for the extratropics means that we may misestimate the number of ignitions in these regions. The large interannual variability and differences in spatial pattern in lightning we observed using the ALDS data for Alaska shows that the LIS/OTD climatology is at best a rough approximation of the actual amount of lightning strikes, and that in certain years, our LIS/OTD based estimates could result in a substantial over- or underestimate in the actual number of potential ignition events.

As described above, most of the temperate regions of the world are so extensively impacted by human activities, both at present and historically, that it is impossible to disentangle the natural fire regime from anthropogenic influences at the 0.5° spatial resolution used in our model simulations. A better test of our process fire model in mid-latitude settings could be to perform case studies in protected regions such as national parks or wilderness areas at very high (~1 km) spatial resolution.

In the subtropics and tropics, the largest area of disagreement between model and observations is in the transition zone between Cerrado savannas and tropical forests in the southeastern Amazon in northern Mato Grosso and southern Pará states of Brazil. In this region, a pronounced dry season of three to four months combined with high temperatures leads to rapid fuel drying and high FDI in our simulations. Combined with lightning activity in all seasons as seen in the LIS/OTD climatology, modeled fire frequencies and burned area in this region are high. In reality, several factors preclude the development of large fires in this region and should be included in future improvements to the model. In this region tropical forests tend to develop on lowland environments with deep soils; the maximum rooting depth in LPJ-LMfire is 2 m, but much more deeply rooted trees have been commonly observed in the Amazon [Kleidon and Heimann, 2000]. More deeply rooted trees would extend the period of greenness for tropical raingreen vegetation, the dominant PFT in this region in our model simulations, effectively limiting the length of the dry season for the vegetation.

Furthermore, green forest vegetation will effectively shade the litter and other fuel in the understory, reducing the rate at which it will dry out. In experiments in the seasonal tropics of the southeastern Amazon, Uhl and Kauffman [1990] showed that land cover controls fuel moisture, and that under equivalent climate conditions, fuels in intact forests would never

Chapter 3. LMfire: An improved fire module for Dynamic Global Vegetation Models

become dry enough to burn, while in grasslands only 24 hours of dry weather was required to support sustained burning. In this sense, the Nesterov Index approach used for estimating fuel moisture in SPITFIRE may be inadequate. We suggest that future models would benefit from an energy balance approach to estimating fuel moisture, particularly in forest understories. On the other hand, it is possible that the observations of burned area in this region are underestimates of the actual situation. Randerson et al. [2012] suggest that burned area in their dataset may be particularly underestimated in regions where small fires occur in forest understory. The combination of these limitations in both the model and the datasets probably leads to the large positive residual observed in this region.

Adjacent to this region of overestimated modeled burned area in central Brazil is a discontinuous region of underestimated burning in areas shown on our map to be largely free of human influence. This region in Mato Grosso, Goiás, and Tocantins states is an area where rapid land cover change, in the form of deforestation and conversion to agriculture and pasture, has been important in recent decades [de Souza et al., 2013]. This recent deforestation has been documented as being associated with an increase in burned area [Lima et al., 2012]. Our human influence map is based on the VMAP0 data product [NIMA, 2000] that was largely assembled from data collected during the period 1974–1994. We suggest that the negative residual in burned area in this region is a result of recent human activities not currently captured by our human impact database.

Similarly, the large areas of underestimated burned area in the easternmost Central African Republic and northern Australia have been attributed to human action, though not as a result of anthropogenic land cover change. In Africa, large savanna fires are intentionally lit to facilitate hunting in sparsely populated areas (Eva et al., 1998). Likewise, in northern Australia frequent intentional human burning is an important part of traditional landscape management that is widespread in sparsely populated areas at present [McKeon et al., 1990, Dyer, 1999, Yibarbuk et al., 2002, Bowman et al., 2004, Bowman and Prior, 2004, Crowley and Garnett, 2000].

In summary, our simulations of burned area over recent decades caused only by lightning ignitions and only passively suppressed through agricultural and urban land use shows substantial differences with observational datasets of fire. We expect these differences, because the complex human relationship with fire at present is well known, and we have made no attempt to prescribe this in our simulations. In parts of the world where human impact is limited, modeled mean burned area fraction often agrees within 10% of observations on a decadal average. In those areas of low human impact where we do show important disagreement between model and observations, we can identify limitations in our model and driver datasets. In boreal and subarctic Canada and Russia, we may overestimate fire because of our over-simplistic treatment of permafrost, and because of the presence of lakes, wetlands, and barren ground that are not accounted for in our model input. In the tropics and subtropics, we may overestimate burning because of an inadequate representation of the effects that canopy shading and deeply rooted vegetation have on fuel moisture. Future developments

to the model should address these issues by improving the soil hydrology scheme, by using recently developed methods for simulating permafrost [Wania et al., 2009] or deep tropical soils [Poulter et al., 2009].

3.5 General discussion

Realistic simulation of global vegetation dynamics requires the inclusion of disturbance regimes that influence vegetation development, alter vegetation structure and composition and affect global carbon budgets. Simulation of fire, arguably the most important disturbance process that affects the terrestrial biosphere, is of crucial importance for a complete model representation of terrestrial vegetation dynamics. Starting with SPITFIRE, we developed LPJ-LMfire to overcome some of the shortcomings of the original model. LPJ-LMfire includes major changes to the process representations of fire occurrence, fire spread and fire impact. In boreal and subarctic regions in particular, LPJ-LMfire results are in much better agreement with observations compared to SPITFIRE or LPX. In other parts of the world, the changes that we made to SPITFIRE in developing LPJ-LMfire are harder to distinguish at the coarse resolution at which we run the model, because of the pervasive nature of human impact on fire at present, both through ignitions and fire suppression.

Under a natural fire regime excluding human interference, lightning is the most common ignition source for wildfires. Accounting for interannual variability in lightning and the occurrence of lightning on a daily timescale is important, especially in regions where the total amount of monthly lightning strikes is low and therefore an equal distribution of lightning strikes on all days within a month may result in a significant underestimate of lightning ignitions. By correlating the occurrence of lightning strikes with the occurrence of precipitation, we provide a more realistic way to simulate lightning ignitions. The time series of burned area for central Alaska (Fig. 3.7) demonstrates that with daily and interannually variable lightning strikes, simulation of realistic fire behavior is possible even in boreal environments where simulating fire is challenging due to the stochastic nature of fire events, with single years showing significant amounts of area burned, while many other years have no or only very little fire.

By allowing the ignition of smoldering fires during wet conditions and simulating fires that persist over the course of multiple days instead of extinguishing each fire after a length of time that is limited to 241 minutes, LPJ-LMfire more closely reflects the true behavior of fire. Likewise, the calculation of fuel wetness as a mass balance function of wetting and drying in LPJ-LMfire, rather than relying on a precipitation threshold of 3 mm as suggested by Nesterov [1949] and used in SPITFIRE, made a substantial improvement in the agreement of the model results with observations.

Eventually, the introduction of additional shrub PFTs as intermediates between herbaceous vegetation and tree PFTs should be considered, especially for an appropriate representation of tundra and xerophytic vegetation. Introduction of shrub PFTs will help ameliorate the current

Chapter 3. LMfire: An improved fire module for Dynamic Global Vegetation Models

tendency of the model to overestimate herbaceous vegetation cover in fire prone areas and the strong positive feedback between fire and vegetation that results in an overestimate of fire frequency and the prevalence of grasses, a problem sometimes still observed, for example, in the Arctic tundra of Northern Alaska, or in southern Spain and central Australia. Further improvements should also focus on the inclusion of a scheme to simulate wetlands and permafrost in order to capture the way in which permafrost keeps tundra organic matter wet, even under dry meteorological conditions. Since our version of LPJ does not represent permafrost dynamics, soil and fuel drying and hence fire occurrence, are overestimated in tundra areas such as northern Alaska where wetlands and permafrost are common. Other future improvements to LPJ-LMfire should include development of a scheme to simulate of crown fires in addition to the surface fires simulated by the current version of the model.

By introducing a slope factor related to the median slope angle of each 0.5° grid cell, we present a simple way to account for the role that topographic complexity plays in limiting fire size and rate of spread. Eventually, a representation of other natural firebreaks such as rivers and lakes should be built into the fire module. An approximation of the number of rivers that could act as fire breaks could be handled by using drainage density information extracted from a DEM. That rivers constrain the spread of fires can be observed, for example, in case of the large Anaktuvuk River Fire from 2007 in the Alaskan tundra that was ultimately constrained by the two rivers: Nanushuk to the west and Itkillik to the east [Jones et al., 2009]. A measure of fragmentation by water bodies could be indirectly accounted for using Eqn. 3.14 which links the numbers of fires burning at any time to the degree to which the landscape has fragmented due to previous burns in the fire season.

Grass PFTs should be implemented such that they are able to reach full cover and complete their lifecycle within one growing season. Our overall simulation results indicate that this would be particularly important for mesic tropical savannas, where fire is a prevalent feature of the ecosystem and most species of grass have annual lifecycles [Scholes et al., 1997]. To accomplish this it would be necessary to run the entire model at a monthly or shorter timestep. Calculating processes such as allocation, turnover, and mortality that are currently updated annually in LPJ on a shorter timestep would also provide the additional advantage that burned area could be tracked continuously over time rather than resetting calculated burned area at the beginning of each calendar year. While the Northern Hemisphere summer fortunately roughly corresponds with the fire season for a large part of the world, it is not correct for southern south America, southern Australia, and parts of southeast Asia and the Sahel.

Our comparison of the LPJ-LMfire results with observational datasets of burned area shows the importance of anthropogenic impact on controlling the spatial pattern of fire observed in recent decades. About three-quarters of the Earth's surface where fire is observed at present occurs on lands influenced by human activities, and human interactions with fire range from rigorous suppression, e.g., in the U.S., Europe, or parts of Australia, to liberal intentional burning on agricultural and natural land, e.g., in sub-Saharan Africa. The sheer variety of examples for human-fire interactions makes it clear that modeling the spatial and temporal

pattern of fire at the present-day would require detailed parameterizations of the human relationships with fire at sub-national level. Prescription of human behavior with respect to fire could likely overcome most of the differences between observed and simulated results, but would no longer be process-based fire modeling. Moreover, such a detailed parameterization of anthropogenic behavior would reflect present-day customs and policies with respect to fire, but would have neither much predictive power for the future nor for the past, as human preferences and subsistence strategies change over time. Our main interest in developing LPJ-LMfire was to model fire, including anthropogenic fire, in the preindustrial past, when humans neither had present-day technology to suppress and control wildfires, nor modern day agricultural technologies that allow people to abstain from using fire for agricultural purposes.

We therefore decided to develop a more general scheme for representing human-fire-interactions in the past that is based on observations and knowledge on people who still use fire in traditional ways at present day, such as Australian Aborigines or subsistence farmers in developing countries, or on historical ethnographic observations of fire usage, e.g., of the North American Indians. Literature research, evidence from palaeoproxies such as charcoal preserved in sediments, and discussions with anthropologists and archaeologists led us to the conclusion that humans in the past used fire for a variety of different reasons, depending on their lifestyles and habitat, and that terrestrial biomass burning related to human activity must have been very common. By developing a method of representing the way in which people with different subsistence lifestyles interact with fire, with LPJ-LMfire we are able to perform quantitative estimates on the impact of anthropogenic burning on vegetation, carbon pools and trace gas emissions on a global scale during preindustrial time. We realize that this approach may be too simplistic to address specific local-scale peculiarities of human burning behavior, but believe nonetheless that our approach to classifying people's relationship with fire based on their subsistence lifestyle is a more appropriate way of addressing the implementation of human burning in the past than prescribing the patterns of human-influenced fire observed in the 21st century.

3.6 Conclusions

Beginning with LPJ-SPITFIRE [Thonicke et al., 2010], we made improvements to several aspects of the original formulation and achieved a more realistic process representation of fire occurrence, fire behavior, and fire impacts, particularly in boreal and subarctic ecosystems. With our updated model, LPJ-LMfire, we were able to simulate realistic fire regimes in Alaska, one of the key regions of the world where SPITFIRE results did not agree with observations. We also developed a scheme to distinguish among the ways in which preindustrial people with different subsistence strategies interact with fire to achieve their land management goals. LPJ-LMfire is a major improvement on past global fire models and will be particularly useful for studying changes in global fire on millennial timescales and provides a basis for further improvements, modifications and model development.

3.7 Appendix

In this appendix we provide the equations used in LPJ-LMfire that were not changed from the original SPITFIRE. With these, we provide a complete documentation of LPJ-LMfire. Variable and parameter abbreviations used in addition to those in Table 3.1 are provided in Table 3.6.

Table 3.5: PFT-specific parameters. TrBE=tropical broadleaf evergreen, TrBR=tropical broadleaf raingreen, TeNE=temperate needleleaf evergreen, TeBE=temperate broadleaf evergreen, TeBS=temperate broadleaf summergreen, BoNE=boreal needleleaf evergreen, BoS=boreal summergreen, C₃gr=C₃ perennial grass, C₄gr=C₄ perennial grass

	TrBE	TrBR	TeNE	TeBE	TeBS	BoNE	BoS	C ₃ gr	C ₄ gr
F	0.160	0.350	0.094	0.070	0.094	0.094	0.094	-	-
CLf	0.33	0.10	0.33	0.33	0.33	0.33	0.33	-	-
ieff _{pft}	0.05	0.40	0.10	0.10	0.50	0.44	0.44	0.50	0.50
emfact _{CO2}	1580	1664	1568	1568	1568	1568	1568	106	1664
emfact _{CO}	103	63	106	106	106	106	106	106	63
emfact _{CH4}	6.8	2.2	4.8	4.8	4.8	4.8	4.8	4.8	2.2
emfact _{VOC}	8.1	3.4	5.7	5.7	5.7	5.7	5.7	5.7	3.4
emfact _{TPM}	8.5	8.5	17.6	17.6	17.6	17.6	17.6	17.6	8.5
emfact _{NOx}	2.0	2.54	3.24	3.24	3.24	3.24	3.24	3.24	2.54
$\rho_{b,PFT}$	15	15	15	15	15	15	15	$\rho_{livegrass}$	$\rho_{livegrass}$
par1	0.0301	0.1085	0.0367	0.0451	0.0347	0.0292	0.0347	-	-
par2	0.0281	0.0281	0.0281	0.0281	0.0281	0.0281	0.0281	-	-

3.7.1 Fuel load and moisture

Fuel calculation by PFT and by fuel type ("slow aboveground litter" includes all woody litter, whereas "fast aboveground litter" is leaves only):

$$df(PFT,1) = 2.22 \cdot (s(1) \cdot las(PFT) + laf(PFT)) \quad (3.35)$$

$$df(PFT,2:4) = 2.22 \cdot (s(2:4) \cdot las(PFT)) \quad (3.36)$$

$$lf(PFT,1) = 2.22 \cdot N_{ind} \cdot (s(1) \cdot (hm_{ind}(PFT) + sm_{ind}(PFT)) + lm_{ind}(PFT)) \quad (3.37)$$

$$lf(PFT,2:4) = 2.22 \cdot N_{ind} \cdot s(2:4) \cdot (hm_{ind}(PFT) + sm_{ind}(PFT)) \quad (3.38)$$

$s = 0.045, 0.075, 0.21, 0.67$ for fuel size classes 1 - 4 (1: 1-hour fuel; 2: 10-hour fuel; 3: 100-hour fuel; 4: 1000-hour fuel).

Dead fuel load per fuel size class:

$$woi(class) = \sum_{pft=1}^{npft} df(pft,class) \quad (3.39)$$

Relative moisture content of live grass fuel:

$$\omega_{lg} = \frac{10}{9} \cdot \omega_{s1} - \frac{1}{9} \quad (3.40)$$

Recalculation of α_{lg} :

$$\alpha_{lg} = \begin{cases} \frac{-\log \omega_{lg}}{NI}, & \omega_{lg} > 0 \text{ and } NI > 0 \\ 0, & \text{else} \end{cases} \quad (3.41)$$

Calculation of total fine fuel amount:

$$W_{finefuel} = woi(1) + W_{livegrass} \quad (3.42)$$

Total mass of dead fuel summed across the first three fuel classes and all PFTs:

$$wo = \sum_{class=1}^3 (woi(class)) \quad (3.43)$$

Total dead fuel mass within the first three fuel size classes, plus mass of the live grass:

$$wtot = wo + W_{livegrass} \quad (3.44)$$

3.7.2 Rate of spread

For the calculation of $ROS_{f_{sw}}$, $\sigma = 5$,

$$rel_m = \frac{\omega_o}{me_{avg}} \quad (3.45)$$

$$wn = livemass + deadmass \quad (3.46)$$

$$livemass = \sum_{PFT=8}^9 pftlivefuel(PFT) \quad (3.47)$$

$$\text{deadmass} = \sum_{\text{PFT}=1}^9 \text{pftdeadfuel}(\text{PFT}) \quad (3.48)$$

$$\text{pftlivefuel}(\text{PFT}) = \sum_{\text{class}=1}^3 \text{lf}(\text{PFT}, \text{class}) \quad (3.49)$$

$$\text{pftdeadfuel}(\text{PFT}) = \sum_{\text{class}=1}^3 \text{df}(\text{PFT}, \text{class}) \quad (3.50)$$

$$\rho_{\text{PFT}(\text{PFT})} = \frac{\rho_{\text{b,PFT}(\text{PFT})} \cdot Z}{\sum_{\text{class}=1}^3 \text{df}(\text{PFT}, \text{class})} \quad (3.51)$$

$$Z = \text{df}(\text{PFT}, 1) + 1.2 \cdot \text{df}(\text{PFT}, 2) + 1.4 \cdot \text{df}(\text{PFT}, 3) \quad (3.52)$$

$$\rho_{\text{b}} = \frac{\rho_{\text{livegrass}} \cdot \text{livemass} + \sum_{i=1}^{\text{npft}} (\rho_{\text{PFT}(i)} \cdot \text{pftdeadfuel}(i))}{\text{wn}} \quad (3.53)$$

For the calculation of ROSf_c , $\sigma = 66$, $\text{rel}_m = 0.99$, $\rho_{\text{b}} = 0.1$, and

$$\text{wn} = \min\left(\sum_{\text{PFT}=1}^7 \text{lf}(\text{PFT}, 1), 8000\right) \quad (3.54)$$

The actual rate of spread calculation is based on equation (3.55) to (3.71).

Packing ratio:

$$\beta = \frac{\rho_{\text{b}}}{\rho_{\text{p}}} \quad (3.55)$$

Optimum packing ratio:

$$\beta_{\text{op}} = 0.200395 \cdot \sigma^{-0.8189} \quad (3.56)$$

Ratio of packing ratio to optimum packing ratio:

$$P_{\text{ratio}} = \frac{\beta}{\beta_{\text{op}}} \quad (3.57)$$

Maximum reaction velocity:

$$\Gamma'_{\text{max}} = \frac{1}{0.0591 + 2.926 \cdot \sigma^{-1.5}} \quad (3.58)$$

Optimum reaction velocity:

$$\Gamma' = \Gamma'_{\text{max}} \cdot P_{\text{ratio}}^A \cdot e^{A \cdot (1 - P_{\text{ratio}})} \quad (3.59)$$

$$A = 8.9033 \cdot \sigma^{-0.7913} \quad (3.60)$$

Moisture dampening coefficient:

$$v_M = 1 - 2.59 \cdot \text{rel}_m + 5.11 \cdot \text{rel}_m^2 - 3.52 \cdot \text{rel}_m^3 \quad (3.61)$$

Reaction intensity:

$$\text{IR} = \Gamma' \cdot \text{wn} \cdot \text{h} \cdot v_M \cdot v_s \quad (3.62)$$

Ratio of propagating flux to reaction intensity:

$$\xi = \frac{e^{(0.792 + 3.7597 \cdot \sqrt{\sigma} \cdot (\beta + 0.1))}}{192 + 7.9095 \cdot \sigma} \quad (3.63)$$

Wind coefficient:

$$\Phi_w = C \cdot (3.281 \cdot U_{\text{forward}})^B \cdot P_{\text{ratio}}^{-E} \quad (3.64)$$

$$C = 7.47 \cdot e^{-0.8711 \cdot \sigma^{0.55}} \quad (3.65)$$

$$B = 0.15988 \cdot \sigma^{0.54} \quad (3.66)$$

$$E = 0.715 \cdot e^{-0.01094 \cdot \sigma} \quad (3.67)$$

Chapter 3. LMfire: An improved fire module for Dynamic Global Vegetation Models

Effective heating number:

$$c = e^{\frac{-4.528}{\sigma}} \quad (3.68)$$

Heat of pre-ignition:

$$Q_{ig} = 581 + 2594 \cdot \omega_o \quad (3.69)$$

The rate of spread is then calculated as follows:

$$ROS_x = \frac{IR \cdot \xi \cdot (1 + \Phi_w) \cdot \text{windfact}}{\rho_b \cdot c \cdot Q_{ig}} \quad (3.70)$$

Backward rate of spread (decreases with increasing wind speed):

$$ROSB_s = ROSf_s \cdot e^{-0.012 \cdot U_{\text{forward}}} \quad (3.71)$$

3.7.3 Fire geometry and duration

Length-to-breadth ratio of burn ellipse in cases when wind speed exceeds 1 km hr⁻¹:

$$LB_{\text{tree}} = 1 + 8.729 \cdot (1 - e^{-0.03 - 0.06 \cdot U_{\text{forward}}})^{2.155} \quad (3.72)$$

$$LB_{\text{grass}} = 1.1 + 0.06 \cdot U_{\text{forward}}^{0.0464} \quad (3.73)$$

$$LB = \min(LB_{\text{tree}} \cdot \text{treecover} + LB_{\text{grass}} \cdot \text{grasscover}, 8) \quad (3.74)$$

In cases when wind speeds is slower than 1 km hr⁻¹, LB=1. The maximum daily fire duration is derived as a function of FDI:

$$t_{\text{fire}} = \frac{241}{1 + 240 \cdot e^{-11.06 \cdot \text{FDI}}} \quad (3.75)$$

The total distance traveled by a fire within a day is estimated as

$$DT = t_{\text{fire}} \cdot (ROSf + ROSb) \quad (3.76)$$

The mean area burned by one single fire is calculated as

$$\bar{a}_f = \min\left(\frac{\pi}{4 \cdot LB} \cdot DT^2 \cdot 0.0001, \text{ac_area}\right) \quad (3.77)$$

3.7.4 Combustion of dead fuel

Fraction of live grass consumed by surface fire:

$$rm = \frac{\omega_{lg}}{me_{ff}} \quad (3.78)$$

$$CF_{lg} = \begin{cases} 1, & rm \leq 0.18 \\ 2.45 - 2.45 \cdot rm, & rm > 0.73 \\ 1.10 - 0.62 \cdot rm, & \text{else} \end{cases} \quad (3.79)$$

Fraction of 1-hr fuel consumed by surface fire:

$$rm = \frac{\omega(1)}{me_{fc}(1)} \quad (3.80)$$

$$CF(1) = \begin{cases} 1, & rm \leq 0.18 \\ 2.45 - 2.45 \cdot rm, & rm > 0.73 \\ 1.10 - 0.62 \cdot rm, & \text{else} \end{cases} \quad (3.81)$$

Fraction of 10-hr fuel consumed by surface fire:

$$rm = \frac{\omega(2)}{me_{fc}(2)} \quad (3.82)$$

$$CF(2) = \begin{cases} 1, & rm \leq 0.12 \\ 1.47 - 1.47 \cdot rm, & rm > 0.51 \\ 1.09 - 0.72 \cdot rm, & \text{else} \end{cases} \quad (3.83)$$

Fraction of 100-hour fuel consumed by surface fire:

$$rm = \frac{\omega(3)}{me_{fc}(3)} \quad (3.84)$$

$$CF(3) = \begin{cases} 0.98 - 0.85 \cdot rm, & rm \leq 0.38 \\ 1.06 - 1.06 \cdot rm, & \text{else} \end{cases} \quad (3.85)$$

Fraction of 1000-hour fuel consumed by surface fire:

$$rm = \frac{\omega(4)}{me_{fc}(4)} \quad (3.86)$$

$$CF(4) = -0.8 \cdot rm + 0.8 \quad (3.87)$$

Total fuel consumed in each fuel size class ($g\ m^{-2}$):

$$FC(class) = CF(class) \cdot woi(class) \cdot (1 - ST) \quad (3.88)$$

To calculate how much fuel has been consumed in total within one gridcell over the course of a year, $FC(class)$ needs to be multiplied with the annual area burned (in m^{-2}).

Calculation of surface fire intensity:

$$I_{surface} = h \cdot ROSf_s \cdot \sum_{class=1}^3 FC(class) \cdot \frac{1}{60} \quad (3.89)$$

If the surface fire intensity is less than $50\ kW\ m^{-1}$, it is considered to be too low for burning and fires are extinguished.

3.7.5 Fire mortality and combustion of live fuel

Crown scorch is calculated per PFT. For seasonally leaf-bearing trees, crown scorch is relevant as long as there are leaves on the tree.

Probability of mortality due to crown damage, calculated per PFT:

$$P_{mCK}(PFT) = RCK(PFT) \cdot CK(PFT)^3 \cdot dphen(PFT) \quad (3.90)$$

$$CK(PFT) = \frac{SH(PFT) - height(PFT) + CL(PFT)}{CL(PFT)} \quad (3.91)$$

$$SH(PFT) = F(PFT) \cdot I_{surface}^{0.667} \quad (3.92)$$

$$CL(PFT) = \max(height(PFT) \cdot CLf(PFT), 0.01) \quad (3.93)$$

The probability of mortality due to cambial damage is given by:

$$P_m(\tau) = \begin{cases} 0, & \frac{\tau_l}{\tau_c} \leq 0.22 \\ 0.563 \cdot \frac{\tau_l}{\tau_c} - 0.125, & \frac{\tau_l}{\tau_c} > 0.22 \\ 1, & \frac{\tau_l}{\tau_c} \geq 2.0, \end{cases} \quad (3.94)$$

where τ_l/τ_c is the ratio of the residence time of the fire to the critical time for cambial damage [Peterson and Ryan, 1986]. The critical time for cambial damage τ_c (min) depends on the bark thickness BT (cm):

$$\tau_c = 2.9 \cdot BT^2, \quad (3.95)$$

[Peterson and Ryan, 1986, Johnson, 1992], which is calculated from the diameter at breast height (DBH, cm) using

$$BT = \text{par1} \cdot \text{DBH} + \text{par2}, \quad (3.96)$$

where par1 and par2 are PFT-specific constants (Table 3.5).

The total probability of mortality due to crown damage P_{mCK} and cambial damage $P_{\text{m}}(\tau)$ is calculated as:

$$P_{\text{m}} = P_{\text{m}}(\tau) + P_{\text{mCK}} - P_{\text{m}}(\tau) \cdot P_{\text{mCK}} \quad (3.97)$$

3.7.6 Fuel consumption

Biomass burned from dead fuel by fuel type and PFT:

$$BB_{\text{dead(PFT,1)}} = AB_{\text{frac}} \cdot CF(1) \cdot \text{laf(PFT)} \quad (3.98)$$

$$BB_{\text{dead(PFT,2)}} = AB_{\text{frac}} \cdot CF(1) \cdot \text{las(PFT)} \cdot 0.045 \quad (3.99)$$

$$BB_{\text{dead(PFT,3)}} = AB_{\text{frac}} \cdot CF(2) \cdot \text{las(PFT)} \cdot 0.075 \quad (3.100)$$

$$BB_{\text{dead(PFT,4)}} = AB_{\text{frac}} \cdot CF(3) \cdot \text{las(PFT)} \cdot 0.21 \quad (3.101)$$

$$BB_{\text{dead(PFT,5)}} = AB_{\text{frac}} \cdot CF(4) \cdot \text{las(PFT)} \cdot 0.67 \quad (3.102)$$

These are calculated on a daily basis. To calculate the annual total, the daily sum is accumulated over the course of the year:

$$\text{ann}BB_{\text{dead(PFT)}} = \text{ann}BB_{\text{dead(PFT)}} + BB_{\text{dead(PFT)}} \quad (3.103)$$

Chapter 3. LMfire: An improved fire module for Dynamic Global Vegetation Models

Biomass burned from live fuel by fuel type and PFT:

For tree-type PFTs:

$$BB_{\text{live(PFT,1)}} = AB_{\text{frac}} \cdot CK(\text{PFT}) \cdot lm_{\text{ind(PFT)}} \cdot N_{\text{ind(PFT)}} \quad (3.104)$$

$$BB_{\text{live(PFT,2)}} = AB_{\text{frac}} \cdot CK(\text{PFT}) \cdot sm_{\text{ind(PFT)}} \cdot N_{\text{ind(PFT)}} \cdot 0.04875 \quad (3.105)$$

$$BB_{\text{live(PFT,3)}} = AB_{\text{frac}} \cdot CK(\text{PFT}) \cdot hm_{\text{ind(PFT)}} \cdot N_{\text{ind(PFT)}} \cdot 0.04875 \quad (3.106)$$

For grass-type PFTs:

$$BB_{\text{live(PFT,1)}} = AB_{\text{frac}} \cdot CF(1) \cdot lm_{\text{ind(PFT)}} \quad (3.107)$$

Annual totals are continuously summed over the course of the year:

$$\text{ann}BB_{\text{live(PFT)}} = \text{ann}BB_{\text{live(PFT)}} + BB_{\text{live(PFT)}} \quad (3.108)$$

The annual running sum of mortality probability is calculated as:

$$\text{ann}_{\text{kill(PFT)}} = \text{ann}_{\text{kill(PFT)}} + P_{mCK(\text{PFT})} \cdot AB_{\text{frac}} \quad (3.109)$$

Updating of the litter pools is done once at the end of the year:

$$laf(\text{PFT}) = \max(laf(\text{PFT}) - \text{ann}BB_{\text{dead(PFT,1)}}, 0) \quad (3.110)$$

$$las(\text{PFT}) = \max(las(\text{PFT}) - \sum_{i=2}^5 \text{ann}BB_{\text{dead(PFT,i)}}, 0) \quad (3.111)$$

For the tree-type PFTs, live biomass that was killed but not consumed by burning is transferred to the litter pools and the individual density is updated based on the fraction of individuals that were killed over the course of the year:

$$N_{\text{ind-kill(PFT)}} = \text{ann}_{\text{kill(PFT)}} \cdot N_{\text{ind(PFT)}} \quad (3.112)$$

$$laf(\text{PFT}) = laf(\text{PFT}) + N_{\text{ind-kill(PFT)}} \cdot lm_{\text{ind(PFT)}} \quad (3.113)$$

$$\text{las}(\text{PFT}) = \text{las}(\text{PFT}) + N_{\text{ind-kill}(\text{PFT})} \cdot (\text{sm}_{\text{ind}(\text{PFT})} + \text{hm}_{\text{ind}(\text{PFT})}) \quad (3.114)$$

$$\text{lb}_g(\text{PFT}) = \text{lb}_g(\text{PFT}) + N_{\text{ind-kill}(\text{PFT})} \cdot \text{rm}_{\text{ind}(\text{PFT})} \quad (3.115)$$

$$N_{\text{ind}(\text{PFT})} = \max(N_{\text{ind}(\text{PFT})} - N_{\text{ind-kill}(\text{PFT})}, 0) \quad (3.116)$$

In case of a PFT being killed off completely by fire, reset presence to "false" and set all biomass pools of that PFT ($\text{lm}_{\text{ind}(\text{PFT})}$, $\text{sm}_{\text{ind}(\text{PFT})}$, $\text{hm}_{\text{ind}(\text{PFT})}$, $\text{rm}_{\text{ind}(\text{PFT})}$) to zero.

3.7.7 Trace gas emissions

Total carbon emissions from burning, across all PFTs:

$$\text{BB}_{\text{tot}} = \sum_{\text{PFT}=1}^{\text{npft}} \sum_{i=1}^5 \text{BB}_{\text{dead}(\text{PFT},i)} + \sum_{\text{PFT}=1}^{\text{npft}} \sum_{j=1}^3 \text{BB}_{\text{live}(\text{PFT},j)} \quad (3.117)$$

To calculate annual total carbon flux from biomass burning, keep updating the running sum:

$$\text{acflux}_{\text{fire}} = \text{acflux}_{\text{fire}} + \text{BB}_{\text{tot}} \quad (3.118)$$

Amount of carbon emissions from burning, per PFT:

$$\text{BB}_{\text{pft}(\text{PFT})} = 0.001 \cdot 2.22 \cdot \sum_{i=1}^5 \text{BB}_{\text{dead}(\text{PFT},i)} + \sum_{j=1}^3 \text{BB}_{\text{live}(\text{PFT},j)} \quad (3.119)$$

Daily trace gas emissions per species:

$$\text{Mx}(\text{spec}) = \sum_{\text{PFT}=1}^{\text{npft}} (\text{emfact}(\text{PFT},\text{spec}) \cdot \text{BB}_{\text{pft}(\text{PFT})}) \quad (3.120)$$

Annual trace gas emissions per species are calculated as running sum over the year:

$$\text{aMx}(\text{spec}) = \text{aMx}(\text{spec}) + \text{Mx}(\text{spec}) \quad (3.121)$$

Table 3.6: Explanation of SPITFIRE variable and parameter abbreviations

variable	variable explanation	variable unit
$\text{df}(\text{PFT},\text{class})$	dead fuel load per PFT in 1-, 10-, 100-, and 1000-hr fuel class	$[\text{g DM m}^{-2}]$

Chapter 3. LMfire: An improved fire module for Dynamic Global Vegetation Models

Table 3.6: Explanation of SPITFIRE variable and parameter abbreviations (continued)

variable	variable explanation	variable unit
lf(PFT,class)	live fuel load per PFT in 1-, 10-, 100-, and 1000-hr fuel class	[g DM m ⁻²]
laf(PFT)	fast-decomposing aboveground litter, per PFT	[g C m ⁻²]
las(PFT)	slow-decomposing aboveground litter, per PFT	[g C m ⁻²]
lbg(PFT)	belowground litter, per PFT	[g C m ⁻²]
N _{ind} (PFT)	individual density, per PFT	[m ⁻²]
lm _{ind} (PFT)	leaf mass of the average individual	[g C ind ⁻¹]
sm _{ind} (PFT)	sapwood mass of the average individual	[g C ind ⁻¹]
hm _{ind} (PFT)	heartwood mass of the average individual	[g C ind ⁻¹]
rm _{ind} (PFT)	root mass of the average individual	[g C ind ⁻¹]
woi(class)	1-, 10-, 100- and 1000-h dead fuel mass summed across all PFTs	[g m ⁻²]
ω_{s1}	relative moisture content of top soil layer	[-]
α_{ig}	drying parameter for live grass fuel	[°C ⁻²]
NI	Nesterov fuel dryness index	[°C ²]
rel _m	relative moisture content of the fuel relative to its moisture of extinction	[-]
ρ_b	fuel bulk density	[kg m ⁻³]
σ	surface-to-volume ratio of the fuel	[cm ² cm ⁻³]
ρ_{PFT} (PFT)	bulk density of dead fuel per PFT, mass-weighted over first 3 fuel size classes	[kg m ⁻³]
pftdeadfuel(PFT)	mass of dead fuel per PFT summed over the first 3 fuel size classes	[g m ⁻²]
β	packing ratio (fuel bulk density / oven dry particle density)	[-]
ρ_p	oven-dry particle density: 513	[kg m ⁻³]
β_{op}	optimum packing ratio	[-]
P _{ratio}	ratio of packing ratio to optimum packing ratio	[-]
Γ'_{max}	maximum reaction velocity	[min ⁻¹]
Γ'	optimum reaction velocity	[min ⁻¹]
ν_M	moisture dampening coefficient	[-]
IR	reaction intensity	[kJ m ⁻² min ⁻¹]
ν_s	mineral dampening coefficient, 0.41739	[-]
h	heat content of fuel: 18	[kJ g ⁻¹]
ξ	ratio of propagating flux to reaction intensity	[-]
Φ_w	wind coefficient	[-]
ϵ	effective heating number	[-]
Q _{ig}	heat of pre-ignition	[kJ kg ⁻¹]
ROsb _s	rate of backward surface spread	[m min ⁻¹]

Table 3.6: Explanation of SPITFIRE variable and parameter abbreviations (continued)

variable	variable explanation	variable unit
LB_{tree}	length-to-breadth ratio of burn ellipse with tree cover	[-]
LB_{grass}	length-to-breadth ratio of burn ellipse with grass cover	[-]
t_{fire}	fire duration	[min]
CF_{lg}	live grass fraction consumed by fire	[-]
$CF(class)$	fractional consumption of dead fuel, per fuel class	[-]
$\omega(class)$	moisture content, per fuel class	[-]
$FC(class)$	amount of dead fuel consumed	$g\ m^{-2}$
ST	mineral fraction of total vegetation mass, 0.055	[-]
$I_{surface}$	surface fire line intensity	$[kW\ m^{-1}]$
$P_{mCK}(PFT)$	probability of mortality due to crown damage	[-]
$RCK(PFT)$	PFT-specific crown damage parameter	[-]
$CK(PFT)$	crown scorch fraction	[-]
$dphen(PFT)$	leaf phenology status, per PFT	[-]
$SH(PFT)$	scorch height	[m]
$height(PFT)$	tree height	[m]
$CL(PFT)$	crown length of woody PFTs	[m]
$F(PFT)$	scorch height parameter	[-]
$BB_{dead}(PFT,1:5)$	biomass burned from dead fuel by PFT and fuel type	$[g\ m^{-2}]$
$BB_{live}(PFT,1:3)$	biomass burned from live fuel by PFT and fuel type	$[g\ m^{-2}]$
AB_{frac}	fractional area burned on the grid cell	$[day^{-1}]$
$ann_{kill}(PFT)$	annual total probability of mortality	[-]
$N_{ind-kill}(PFT)$	fraction of PFT killed by fire	[-]
BB_{tot}	total C-emissions from burning across all PFTs	$[g\ C\ m^{-2}]$
$BB_{pft}(PFT)$	total burned biomass, per PFT	$[kg\ dry\ matter\ m^{-2}]$
$acflux_{fire}$	annual C-flux from biomass burning	$[g\ m^{-2}]$
$Mx(spec)$	trace gas emissions, per species (CO_2 , CO , CH_4 , VOC , TPM , NO_x)	$[g\ x\ m^{-2}]$
$aMx(spec)$	annual trace gas emissions, per species	$[g\ x\ m^{-2}]$

3.8 Supplementary Figures

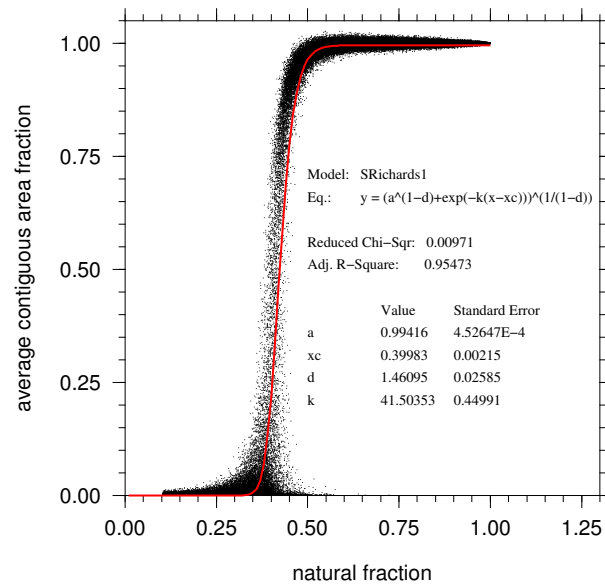


Figure 3.13: Scatterplot of Monte Carlo simulation results on a 100 x 100 grid. For each fractional combination of natural land vs. agricultural land on a step size of 0.01, pixels on the 100 x 100 grid were randomly assigned to be either natural land or cropland, and the average contiguous area fraction of natural patches was calculated based on an 8-cell neighborhood, for 1000 repetitions at each land use fraction.

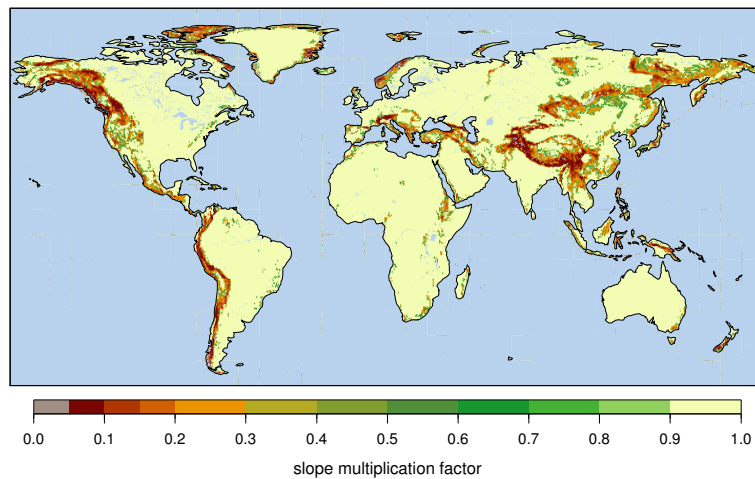


Figure 3.14: Spatial distribution of the slope factor (slf). Constraining effects of terrain size on the average size of fires are estimated by using slf as a multiplication factor on the default average fire size calculated by the fire model.

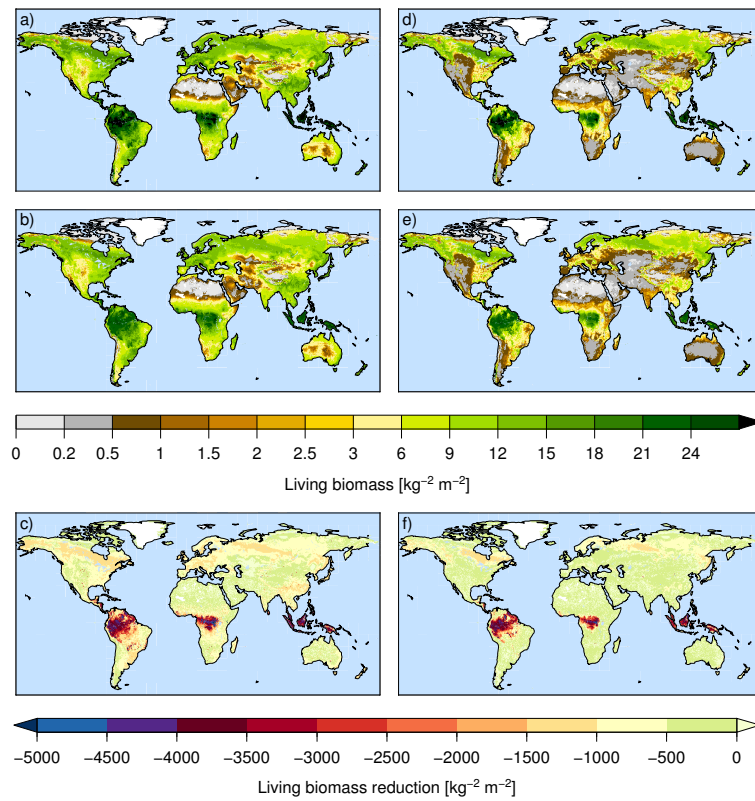


Figure 3.15: Effect on global biomass caused by the changes to maximum crown area and maximum establishment rate in LPJ. Panels a) to c): Scenario completely excluding fire, to illustrate how the underlying basis biomass for fires changes. Panel a): Old LPJ parameterization, with a maximum crown area constraint of 15 m^2 and a maximum establishment rate of $0.12 \text{ individuals m}^{-2}$. Panel b): New parameterization with a maximum crown area constraint of 30 m^2 and a maximum establishment rate of 0.15 . Panel c) Difference in biomass between b) and a): a reduction in living biomass can be observed globally, but total values of reduction are highest in the equatorial tropics where total biomass is highest. Panels d) to f) show global biomass for a simulation run including anthropogenic land use based on HYDE land use and lightning-caused burning on non-agricultural land, for the old parameterization of maximum crown area and maximum establishment rate in panel d) and the new parameterization in panel e), and the difference between e) and d) shown in panel f).

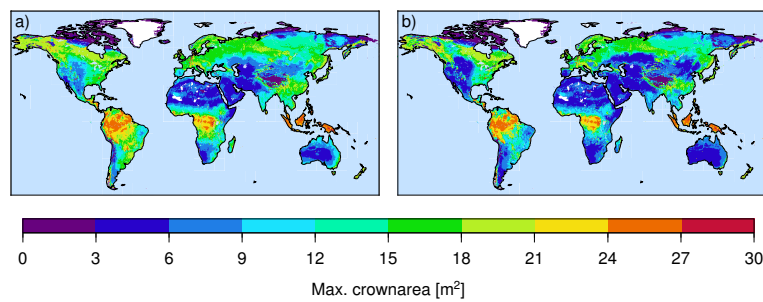


Figure 3.16: Panel a): Simulated maximum crown area for a world without fire after implementation of a maximum crown area threshold of 30 m^2 instead of 15 m^2 . Panel b): Simulated maximum crown area for a simulation run with lightning-caused fire. All places with maximum crown area between 15 m^2 and 30 m^2 are areas where the increase of maximum crown area contributes to the reduction of live biomass by decreasing individual density compared to the old parameterization.

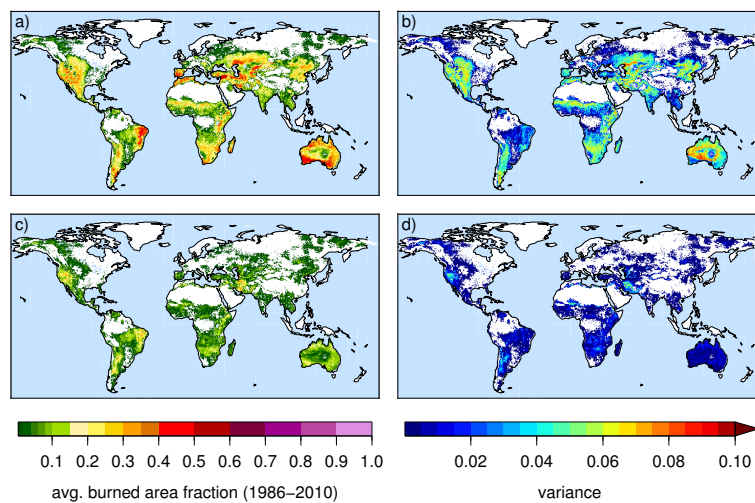


Figure 3.17: Panel a) Average annual burned area fraction for a simulation run without agricultural land use, and lightning-caused fires over 25 years. Panel b) Variance in annual burned area fraction in reference to panel a). Panel c) Average annual burned area fraction for a simulation run with lightning-caused fires, but fires being excluded from agricultural land. Panel d) Variance in annual burned area fraction in reference to panel c).

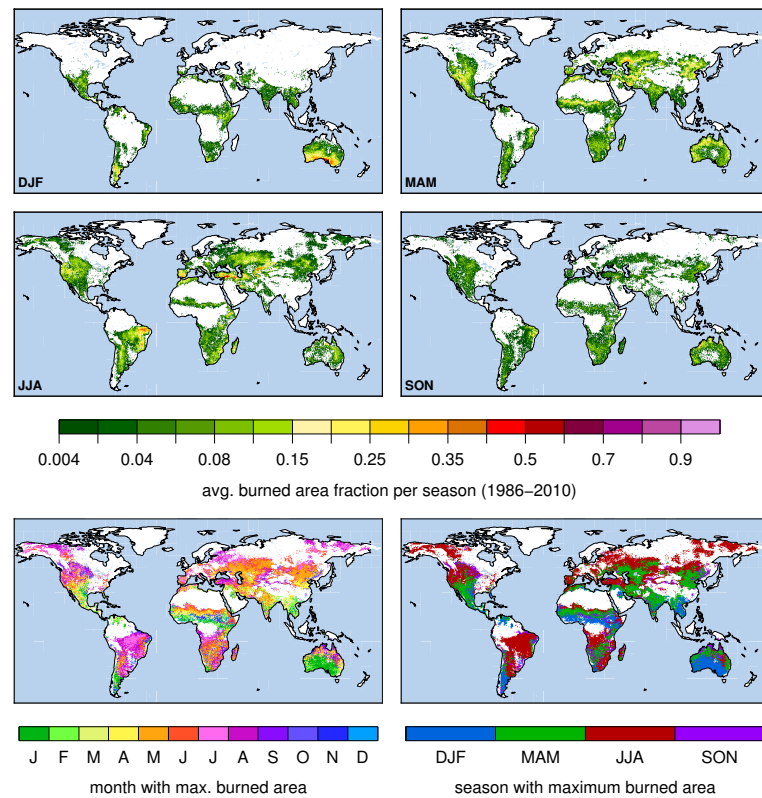


Figure 3.18: Seasonality of fire under natural conditions (no land use, lightning ignitions). The top four panels show the average burned area fraction per season over 25 years. The two bottom panels identify simulated peak fire month based on burned area fraction and a seasonal summary highlighting which season has the highest simulated burned area fraction at a given location.

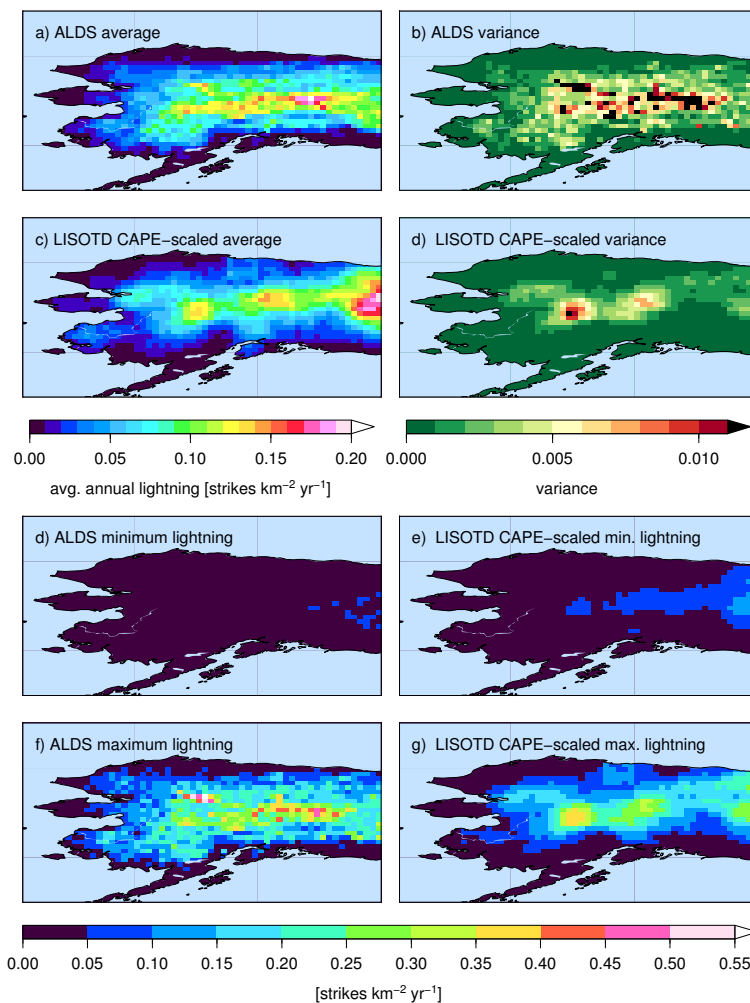


Figure 3.19: Statistical comparison between ALDS lightning observations and LIS/OTD-derived, CAPE-scaled lightning for the time period 2001-2010. While average annual lightning strikes between ALDS (panel a) and LIS/OTD-derived data (panel s) are comparable, the variance between years is higher for the ALDS data (Panel b) than for the LIS/OTD CAPE-scaled data, indicating that even with the scaling to CAPE anomalies the total range of interannual variability in lightning is still underestimated. Using LIS/OTD-data for Alaska is in general problematic as there are overall only four years of data available. Panels d) and e) compare the minimum lightning strike density for each grid cell between ALDS data and LIS/OTD-derived data, and panels f) and g) the maximum lightning strike density. The underestimate in interannual variability for the LIS/OTD-derived data is both due to an underestimate of maximum lightning strike density as well as a tendency to overestimate minimum lightning strike density.

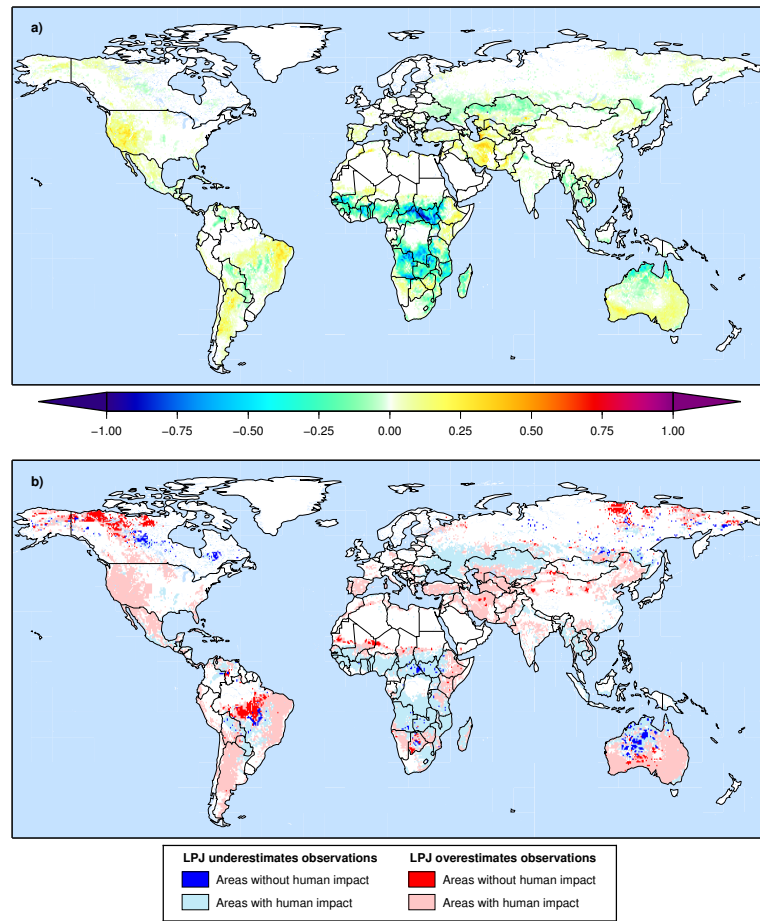


Figure 3.20: Panel a) Residuals between average annual area burned in Randerson et al. [2012] and LMfire simulation results; b) Residuals between observed and simulated annual area burned in context of anthropogenic imprint on the global land surface

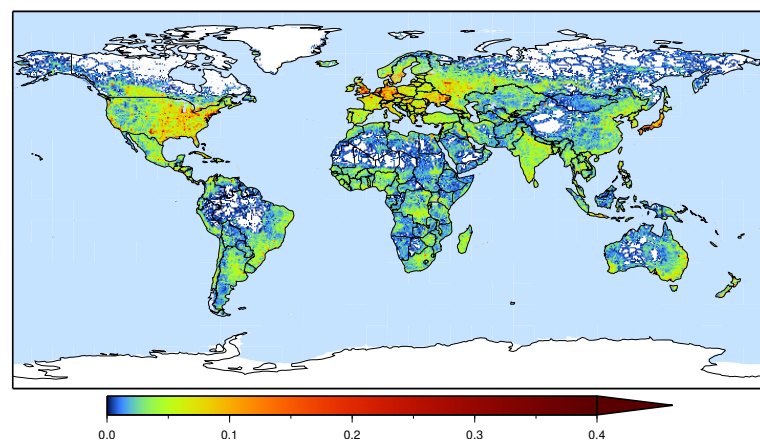


Figure 3.21: Human impact based on settlements and infrastructure (roads, powerlines, pipelines, etc.) [Ahlenius, 2005]

Bibliography

- H. Ahlenius. Human impact, year 2002 (Miller cylindrical projection), GLOBIO-2 model, 2005. URL http://www.grida.no/graphicslib/detail/human-impact-year-2002-miller-cylindrical-projection_7006.
- R. Akanvou, M. Becker, M. Chano, D. E. Johnson, H. Gbaka-Tcheche, and A. Toure. Fallow residue management effects on upland rice in three agroecological zones of West Africa. *Biology and Fertility of Soils*, 31:501–507, 2000.
- C. Akselsson, Berg. B., V. Meentemeyer, and O. Westling. Carbon sequestration rates in organic layers of boreal and temperate forest soils - Sweden as a case study. *Global Ecology and Biogeography*, 14:77–84, 2005.
- Alaska Bureau of Land Management. ALDS, 2013. URL <http://afsmaps.blm.gov/imf/imf.jsp?site=lightning>.
- Alaska Fire Service. Alaska Fire Service polygon maps of burned area, 2013. URL <http://afsmaps.blm.gov/imf/imf.jsp?site=firehistory>.
- C. Amante and B. W. Eakins. ETOPO1 1 Arc-minute Global Relief Model: Procedures, Data Sources and Analysis. Noaa technical memorandum nesdis ngdc-24, NOAA, 2009.
- M. K. Anderson. Prehistoric anthropogenic wildland burning by hunter-gatherer societies in the temperate regions: A net source, sink, or neutral to the global carbon budget? *Chemosphere*, 29:913–934, 1994.
- M. O. Andreae and P. Merlet. Emission of trace gases and aerosols from biomass burning. *Global Biogeochemical Cycles*, 15(4):955–966, 2001.
- P. L. Andrews. BEHAVE: Fire Behavior Prediction and Fuel Modeling System - Burn Subsystem, Part 1. General Technical Report INT-194, United States Department of Agriculture, Forest Service, Intermountain Research Station, Ogden, UT 84401, January 1986.
- P. L. Andrews. BehavePlus Fire Modeling System: Past, Present, and Future. Bar Harbor, ME, 23-25 October 2007. American Meteorological Society.

Bibliography

- P. L. Andrews and C. H. Chase. BEHAVE: fire behavior prediction and fuel modeling system - BURN subsystem, Part 2. General Technical Report INT-260, United States Department of Agriculture, Forest Service, Intermountain Research Station, Ogden, UT 84401, 1989.
- P. L. Andrews, C. D. Bevins, and R. C. Seli. BehavePlus Fire Modeling System, version 2.0: Users Guide. General technical report, United States Department of Agriculture, Forest Service, Rocky Mountain Research Station, Ogden, UT, 2003.
- P. L. Andrews, C. D. Bevins, and R. C. Seli. BehavePlus Fire Modeling System, version 4.0, User's Guide. General Technical Report RMRS-GTR-106WWW Revised, United States Department of Agriculture, Forest Service, Rocky Mountain Research Station, Ogden, UT, July 2008.
- S. A. Archibald, D. P. Roy, B. W. van Wilgen, and R. J. Scholes. What limits fire? An examination of drivers of burnt area in Southern Africa. *Global Change Biology*, 15:613–630, 2009.
- A. Baccini, S. J. Goetz, W. S. Walker, N. T. Laporte, M. Sun, D. Sulla-Menashe, J. Hackler, P. S. A. Beck, R. Dubayah, M. A. Friedl, S. Samanta, and R. A. Houghton. Estimated carbon dioxide emissions from tropical deforestation improved by carbon-density maps. *Nature Climate Change Letters*, 2:182–185, 2012.
- M. S. Balshi, A. D. McGuire, Q. Zhuang, J. Melillo, D. W. Kicklighter, E. Kasischke, C. Wirth, M. Flannigan, J. Harden, J. S. Clein, T. J. Burnside, J. McAllister, W. A. Kurz, M. Apps, and A. Shvidenko. The role of historical fire disturbance in the carbon dynamics of the pan-boreal region: A process-based analysis. *Journal of Geophysical Research*, 112:G02029, 2007. doi: 10.1029/2006JG000380.
- R. J. Barney. Wildfires in Alaska - some historical and projected effects and aspects. *Proceedings - Fire in the Northern Environment - A Symposium; U.S. Forest Service: Portland, OR, College AK 13-14 April 1971:51–59*, 1971.
- B. Berg. Litter decomposition and organic matter turnover in northern forest soils. *Forest Ecology and Management*, 133:13–22, 2000.
- B. Berg, C. McGlaugherty, A. V. De Santo, and D. Johnson. Humus buildup in boreal forests: effects of litter fall and its N concentration. *Canadian Journal of Forest Research*, 31(6): 988–998, 2001. doi: 10.1139/x01-031.
- B. Bergner, J. Johnstone, and K. K. Treseder. Experimental warming and burn severity alter CO₂ flux and soil functional groups in recently burned boreal forest. *Global Change Biology*, 10:1996–2004, 2004.
- L. C. Bliss. Adaptations of Arctic and Alpine Plants to Environmental Conditions. *Arctic*, 15(2): 117–144, 1962.
- S. H. Boles and D. L. Verbyla. Comparison of Three AVHRR-Based Fire Detection Algorithms for Interior Alaska. *Remote Sensing of Environment*, 72:1–16, 2000.

- W. J. Bond and J. E. Keeley. Fire as a global 'herbivore': the ecology and evolution of flammable ecosystems. *Trends in Ecology and Evolution*, 20(7):387–394, 2005.
- W. J. Bond and J. J. Midgley. Fire and the Angiosperm Revolutions. *International Journal of Plant Sciences*, 173(6):569–583, 2012.
- W. J. Bond and A. C. Scott. Fire and the spread of flowering plants in the Cretaceous. *New Phytologist*, 188:1137–1150, 2010.
- W. J. Bond and B. W. van Wilgen. *Fire and Plants*. Chapman & Hall, London, UK, 1996.
- W. J. Bond, F. I. Woodward, and G. F. Midgley. The global distribution of ecosystems in a world without fire. *New Phytologist*, 165:525–538, 2005. doi: 10.1111/j.1469-8137.2004.01252.x.
- A. Bondeau, P. C. Smith, S. Zaehle, S. Schaphoff, W. Lucht, W. Cramer, D. Gerten, H. Lotze-Campen, C. Müller, M. Reichstein, and B. Smith. Modelling the role of agriculture for the 20th century global terrestrial carbon balance. *Global Change Biology*, 13:679–706, 2007.
- D. M. J. S. Bowman. Tansley Review No. 101 - The impact of Aboriginal landscape burning on the Australian biota. *New Phytologist*, 140:385–410, 1998.
- D. M. J. S. Bowman and L. D. Prior. Impact of Aboriginal landscape burning on woody vegetation in *Eucalyptus tetrodonta* savanna in Arnhem Land, northern Australia. *Journal of Biogeography*, 31:807–817, 2004.
- D. M. J. S. Bowman, A. Walsh, and L. D. Prior. Landscape analysis of Aboriginal fire management in Central Arnhem Land, north Australia. *Journal of Biogeography*, 31:207–223, 2004.
- D. M. J. S. Bowman, J. K. Balch, P. Artaxo, W. J. Bond, J. M. Carlson, M. A. Cochrane, C. M. D'Antonio, R. S. DeFries, J. C. Doyle, S. P. Harrison, F. H. Johnston, J. E. Keeley, M. A. Krawchuck, C. A. Kull, J. B. Marston, M. A. Moritz, I. C. Prentice, C. I. Roos, A. C. Scott, T. W. Swetnam, G. R. van der Werf, and S. J. Pyne. Fire in the Earth System. *Science*, 324:481–485, 2009.
- S. W. Breckle. *Walter's Vegetation of the Earth: The Ecological Systems of the Geo-Biosphere*. Springer Verlag, Berlin, Heidelberg, 2002.
- L.B. Brubaker, P. E. Higuera, T. S. Rupp, M. A. Olson, P. M. Anderson, and F. S. Hu. Linking sediment-charcoal records and ecological modeling to understand causes of fire-regime change in boreal forests. *Ecology*, 90(7):1788–1801, 2009.
- R. E. Burgan. Concepts and Interpreted Examples In Advanced Fuel Modeling. General Technical Report INT-283, United States Department of Agriculture, Forest Service, Intermountain Research Station, Ogden, UT 84401, November 1987.
- R. E. Burgan and R. C. Rothermel. BEHAVE: Fire Behavior Prediction and Fuel Modeling System - Fuel Subsystem. General Technical Report INT-167, National Wildfire Coordinating Group, United States Department of Agriculture, United States Department of the Interior, Intermountain Forest and Range Experiment Station, Ogden, UT 84401, May 1984.

Bibliography

- M. Cairns and D. P. Garrity. Improving shifting cultivation in Southeast Asia by building on indigenous fallow management strategies. *Agroforestry Systems*, 47:37–48, 1999.
- D. E. Calkin, K. M. Gebert, J. G. Jones, and R. P. Neilson. Forest Service Large Fire Area Burned and Suppression Expenditure Trends, 1970-2002. *Journal of Forestry*, 103(4):179–183, 2005.
- C. Carcaillet, H. Almquist, H. Asnong, R. H. W. Bradshaw, J. S. Carrión, M.-J. Gaillard, K. Gajewski, J. N. Haas, S. G. Haberle, P. Hadorn, S. D. Müller, P. J. H. Richard, I. Richoz, M. Rösch, M. F. Sánchez Goñi, H. von Stedingk, A. C. Stevenson, B. Talon, C. Tardy, W. Tinner, E. Tryterud, L. Wick, and K. J. Willis. Holocene biomass burning and global dynamics of the carbon cycle. *Chemosphere*, 49:845–863, 2002.
- P. Cheney and A. Sullivan. *Grassfires: Fuel, Weather and Fire Behavior*, volume 2nd edition. CSIRO Publishing, 2008.
- H. J. Christian, Richard J. Blakeslee, Dennis J. Boccippio, William L. Boeck, Dennis E. Buechler, Kevin T. Driscoll, Steven J. Goodman, John M. Hall, William J. Koshak, Douglas M. Mach, and Michael F. Stewart. Global frequency and distribution of lightning as observed from space by the optical transient detector. *Journal of Geophysical Research*, 108(D1):4005, 2003. doi: 10.1029/2002JD002347. URL http://gcmd.nasa.gov/records/GCMD_lohrmc.html.
- S. L. Collins. Fire Frequency and Community Heterogeneity in Tallgrass Prairie Vegetation. *Ecology*, 73(6):2001–2006, 1992.
- G. P. Compo, J. S. Whitacker, P. D. Sardeshmukh, N. Matsui, R. J. Allan, X. Yin, B. E. Gleason Jr., R. S. Vose, G. Rutledge, P. Bessemoulin, S. Brönnimann, M. Brunet, R. I. Crouthamel, A. N. Grant, P. Y. Groisman, P. D. Jones, M. C. Kruk, A.C. Kruger, G. J. Marshall, M. Maugeri, H. Y. Mok, Ø Nordli, T. F. Ross, R. M. Trigo, X. L. Wang, S. D. Woodruff, and S. J. Worley. The Twentieth Century Reanalysis Project. *Quarterly Journal of the Royal Meteorological Society*, 137:1–28, 2011.
- H. C. Conklin. The Study of Shifting Cultivation. *Current Anthropology*, 2(1):27–61, 1961.
- J. H. Connell. Diversity in Tropical Rain Forests and Coral Reefs. *Science*, 199:1302–1310, 1978.
- G. M. Crowley and S. T. Garnett. Changing Fire Management in the Pastoral Lands of Cape York Peninsula of northeast Australia, 1623 to 1996. *Australian Geographical Studies*, 38(1): 10–26, 2000.
- P. J. Crutzen and M. O. Andreae. Biomass Burning in the Tropics: Impact on Atmospheric Chemistry and Biogeochemical Cycles. *Science*, 250(4988):1669–1678, 1990.
- J. Dagpunar. *Principles of Random Variate Generation*. Oxford Science Publications. Oxford: Clarendon Press, 1988.
- R. A. de Souza, F. Miziara, and P. De Marco Junior. Spatial variation of deforestation rated in the Brazilian Amazon: A complex theater for agrarian technology, agrarian structure and governance by surveillance. *Land Use Policy*, 30:915–924, 2013.

- R. S. DeFries, M. C. Hansen, J. R. G. Townshend, A. C. Janetos, and T. R. Loveland. A new global 1-km dataset of percentage tree cover derived from remote sensing. *Global Change Biology*, 6:247–254, 2000.
- S. L. E. Desiles, B. Nijssen, B. Ekwurzel, and T. P. A. Ferré. Post-wildfire changes in suspended sediment rating curves: Sabino Canyon, Arizona. *Hydrological Processes*, 21:1413–1423, 2007.
- C. Diaz-Avalos, D. L. Peterson, E. Alvarado, S. A. Ferguson, and J. E. Besag. Spacetime modelling of lightning-caused ignitions in the Blue Mountains, Oregon. *Canadian Journal of Forest Research*, 31(9):1579–1593, 2001.
- R. A. Dodgshon and G. A. Olsson. Heather moorland in the Scottish Highlands: the history of a cultural landscape, 1600-1880. *Journal of Historical Geography*, 32:21–37, 2006.
- M. R. Dove. *Swidden agriculture in Indonesia: the subsistence strategies of the Kalimantan Kantu*. Mouton de Gruyter, Berlin, Germany, 1985.
- H. E. Dregne. Land Degradation in the Drylands. *Arid Land Research and Management*, 16(2): 99–132, 2002.
- D. E. Dumond. Swidden agriculture and the rise of the Maya civilization. *Southwestern Journal of Anthropology*, 17(4):301–316, 1961.
- E. Dwyer, S. Pinnock, J.-M. Grégoire, and J. M. C. Pereira. Global spatial and temporal distribution of vegetation fire as determined from satellite observations. *International Journal of Remote Sensing*, 21(6-7):1289–1302, 2000.
- R. Dyer. The Role of Fire on Pastoral Lands in Northern Australia; in: Fire and Sustainable Agricultural and Forestry Development in Eastern Indonesia and Northern Australia. *ACIAR PROCEEDINGS*, 91:108–113, 1999.
- C. Eriksen. Why do they burn the 'bush'? Fire, rural livelihoods, and conservation in Zambia. *The Geographical Journal*, 173(3):242–256, 2007.
- R. Essery, M. Best, and P. Cox. MOSES 2.2 Technical Documentation. Technical report, Hadley Center Technical Note 30, Hadley Center, Met Office, Bracknell, UK, 2001.
- H. D. Eva, J. P. Malingreau, J. M. Gregoire, A. S. Belward, and C. T. Mutlow. Cover The advance of burnt areas in Central Africa as detected by ERS-1 ATSR-1. *International Journal of Remote Sensing*, 19(9):1635–1637, 1998.
- N. Faivre, Roche P., M. M. Boer, L. McCaw, and P. F. Grierson. Characterization of landscape pyrodiversity in Mediterranean environments: contrasts and similarities between south-western Australia and south-eastern France. *Landscape Ecology*, 26:557–571, 2011.
- FAO, IIASA, ISRIC, ISSCAS, and JRC. Harmonized World Soil Database (version 1.0), 2008.

Bibliography

- M. A. Finney. FARSITE: Fire Area Simulator - Model Development and Evaluation. *USDA Forest Service Research Paper, Missoula, MT, RMRS-RP-4 Revised:52*, 1998.
- J. B. Fisher, S. Sitch, Y. Malhi, R. A. Fisher, C. Hungtingford, and S.-Y. Tan. Carbon cost of plant nitrogen acquisition: A mechanistic, globally applicable model of plant nitrogen uptake, retranslocation, and fixation. *Global Biogeochemical Cycles*, 24:GB1014, 2010.
- J. M. Fox. How Blaming 'Slash and Burn' Farmers is Deforesting Mainland Southeast Asia. *AsiaPacific Issues*, 47:1–8, 2000.
- K. M. Gebert, D. E. Calkins, and J. Yoder. Estimating Suppression Expenditures for Individual Large Wildland Fires. *Western Journal of Applied Forestry*, 22(3):188–196, 2007.
- K. M. Gebert, D. E. Calkin, R. J. Huggett, and K. L. Abt. *The economics of forest disturbance: wild-fires, storms and invasive species*, chapter Economic analysis of federal wildfire management programs. Springer Verlag, Dordrecht, The Netherlands, 2008.
- D. Gerten, S. Schaphoff, U. Haberlandt, W. Lucht, and S. Sitch. Terrestrial vegetation and water balance - hydrological evaluation of a dynamic global vegetation model. *Journal of Hydrology*, 286:249–270, 2004.
- D. J. Gibson. *Grasses and grassland ecology*. Oxford University Press, Oxford, UK, 2009.
- L. Giglio, J. T. Randerson, G. T. van der Werf, P. S. Kasibhatla, G. J. Collatz, D. C. Morton, and R. S. DeFries. Assessing variability and long-term trends in burned area by merging multiple satellite fire products. *Biogeosciences*, 7:1171–118, 2010.
- J. Gomez-Dans, A. Spessa, M. Wooster, and P. Lewis. A sensitivity analysis study of the coupled vegetation-fire model, LPJ-SPITFIRE. *Ecological Modeling*, in review, 2013.
- Government Accounting Office. Wildland Fire Management Improvements Could Enhance Federal Agencies' Efforts to Contain the Costs of Fighting Fires. Technical Report GAO-07-922T, 15p, United States General Accounting Office, Washington, D.C. 20548, 2007.
- Government of Western Australia, Department for Agriculture and Food. Fire Management Guidelines for Kimberley Pastoral Rangelands: Best Management Practice Guide, 2013. URL http://www.agric.wa.gov.au/objtwr/imported_assets/content/lwe/regions/nrr/fire_management_guidelines_for_kimberley_pastoral_rangelands.pdf.
- J. P. Grime. Control of species density in herbaceous vegetation. *Journal of Environm. Management*, 1:151–167, 1973.
- R. P. Guyette, R. M. Muzika, and D. C. Dey. Dynamics of an Anthropogenic Fire Regime. *Ecosystems*, 5:472–486, 2002.
- A. M. Hadlow. *Changes in Fire Season Precipitation in Idaho and Montana from 1982-2006*. PhD thesis, Colorado Sate University, Fort Collins, Colorado, 2009.

- B. L. Hall. Precipitation associated with lightning-ignited wildfires in Arizona and New Mexico. *International Journal of Wildland Fire*, 16:242–254, 2007.
- M. J. Hamilton. The complex structure of hunter-gatherer social networks. *Proceedings of the Royal Society B*, (2195-2202), 2007.
- J. W. Harden, S. E. Trumbore, B. J. Stocks, A. Hirsch, S. T. Gower, K. P. O'Neill, and E. S. Kasischke. The role of fire in the boreal carbon budget. *Global Change Biology*, 6:174–184, 2000.
- L. M. Head. Landscapes socialised by fire: post-contact changes in Aboriginal fire use in northern Australia, and implications for prehistory. *Archaeology in Oceania*, 29:172–181, 1994.
- F. A. Heinsch and P. L. Andrews. BehavePlus Fire Modeling System, version 5.0: Design and Features. General Technical Report RMRS-GTR-249, United States Department of Agriculture. Forest Service, Rocky Mountain Research Station, Fort Collins, CO, December 2010.
- T. Hickler, I. C. Prentice, B. Smith, M. T. Sykes, and S. Zaehle. Implementing plant hydraulic architecture within the LPJ Dynamic Global Vegetation Model. *Global Ecology and Biogeography*, 15:567–577, 2006.
- P. E. Higuera, L. B. Brubaker, P. M. Anderson, T. A. Brown, A. T. Kennedy, and F. S. Hu. Frequent Fires in Ancient Shrub Tundra: Implications of Paleorecords for Arctic Environmental Change. *PLoS One*, 3(3):e0001744, 2008. doi: 10.1371/journal.pone.0001744.
- P. E. Higuera, L. B. Brubaker, P. M. Anderson, F. S. Hu, and T. A. Brown. Vegetation mediated the impacts of postglacial climate change on fire regimes in the south-central Brooks Range, Alaska. *Ecological Monographs*, 79(2), 2009.
- R. J. Hijmans, S. E. Cameron, J. L. Parra, P. G. Jones, and A. Jarvis. Very high resolution interpolated climate surfaces for global land areas. *International Journal of Climatology*, 25: 1965–1978, 2005.
- R. L. Holle, K. L. Cummins, and N. W. S. Demetriades. Monthly distribution of NLDN and GLD360 cloud-to-ground lightning. Technical report, Vaisala Inc., Tucson, Arizona 85756, 2011.
- R. A. Houghton, K. T. Lawrence, J. L. Hackler, and S. Brown. The spatial distribution of forest biomass in the Brazilian Amazon: a comparison of estimates. *Global Change Biology*, 7: 731–746, 2001.
- F. S. Hu, P. E. Higuera, J. E. Walsh, W. L. Chapman, P. A. Duffy, L. B. Brubaker, and M. L. Chipman. Tundra burning in Alaska: Linkages to climatic change and sea ice retreat. *Journal of Geophysical Research*, 115(G04002):8, 2010. doi: 10.1029/2009JG001270.
- M. Huston. A General Hypothesis of Species Diversity. *The American Naturalist*, 113(1):81–101, 1979.

Bibliography

- J. Iversen. Landnam i Danmarks Stenalder. En pollenanalytisk Undersøgelse over det første Landbrugs Indvirkning paa Vegetationsudviklingen, (Land occupation in Denmark's Stone Age. A Pollen-Analytical Study of the Influence of Farmer Culture on the Vegetational Development). *Danmarks Geologiske Undersøgelse*, Raekke II(66), 1941.
- A. K. Jain, Z. Tao, X. Yang, and C. Gillespie. Estimates of global biomass burning emissions for reactive greenhouse gases (CO₂, NMHCs, and NO_x) and CO₂. *Journal of Geophysical Research*, 111(D06304):14, 2006. doi: 10.1029/2005JD006237.
- E. R. Jayaratne and Y. Kuleshov. Geographical and seasonal characteristics of the relationship between lightning ground flash density and rainfall within the continent of Australia. *Atmospheric Research*, 79:1–14, 2006.
- D. W. Johnson, R. B. Susfalk, R. A. Dahlgren, and J. M. Klopatek. Fire is more important than water for nitrogen fluxes in semi-arid forests. *Environmental Science and Policy*, 1:79–86, 1998.
- E. A. Johnson. *Fire and vegetation dynamics: studies from the North American boreal forest*. Cambridge University Press: Cambridge, 1992.
- K. J. Johnston. The intensification of pre-industrial cereal agriculture in the tropics: Boserup, cultivation lengthening, and the Classic Maya. *Anthropological Archaeology*, 22:126–161, 2003.
- B. M. Jones, C. A. Kolden, R. Jandt, J. T. Abatzoglou, F. Urbans, and C. D. Arp. Fire Behavior, Weather, and Burn Severity of the 2007 Anaktuvuk River Tundra Fire, North Slope, Alaska. *Arctic, Antarctic, and Alpine Research*, 41(3):309–318, 2009. doi: 10.1657/1938-4246-41.3.309.
- A. J. Kalis and J. Meurers-Balke. Die "Landnam"-Modelle von Iversen und Troels-Smith zur Neolithisierung des westlichen Ostseegebietes - ein Versuch ihrer Aktualisierung. *Prähistorische Zeitschrift*, 73:1–24, 1998.
- A. J. Kalis, J. Merkt, and J. Wunderlich. Environmental changes during the Holocene climatic optimum in central Europe - human impact and natural causes. *Quaternary Science Reviews*, 22:33–79, 2003.
- D. L. Kane and J. Stein. Water Movement Into Seasonally Frozen Soils. *Water Resources Research*, 19(6):1547–1557, 1983.
- J. O. Kaplan, N. H. Bigelow, I. C. Prentice, S. P. Harrison, P. J. Bartlein, T. R. Christensen, W. Cramer, N. V. Matveyeva, A. D. McGuire, D. F. Murray, V. Y. Razzhivin, B. Smith, D. A. Walker, P. M. Anderson, A. A. Andreev, L. B. Brubaker, M. E. Edwards, and A. V. Lozhkin. Climate change and Arctic ecosystems: 2. Modeling, paleodata-model comparisons, and future projections. *Journal of Geophysical Research*, 108(D19):8171, 2003. doi: 10.1029/2002JD002559.

- J. O. Kaplan, K. M. Krumhard, E. C. Ellis, W. F. Ruddiman, C. Lemmen, and K. Klein Goldewijk. Holocene carbon emissions as a result of anthropogenic land cover change. *The Holocene*, 21(5):775–791, 2011.
- E. S. Kasischke, D. Williams, and D. Barry. Analysis of the patterns of large fires in the boreal forest of Alaska. *International Journal of Wildland Fire*, 11:131–144, 2002.
- E. S. Kasischke, E. J. Hyer, P. C. Novelli, L. P. Bruhwiler, N. H. F. French, A. I. Sukhinin, J. H. Hewson, and B. J. Stocks. Influences of boreal fire emissions on Northern Hemisphere atmospheric carbon and carbon monoxide. *Global Biogeochemical Cycles*, 19:GB1012, 2005. doi: 10.1029/2004GB002300.
- D. Katsanos, K. Lagouvardos, V. Kotroni, and A. A. Argiriou. Combined analysis of rainfall and lightning data produced by mesoscale systems in the central and eastern Mediterranean. *Atmospheric Research*, (55-63), 2007.
- J. E. Keeley, P. H. Zedler, C. A. Zammit, and T. J. Stohlgren. Fire and Demography. In S. C. Keeley, editor, *Science Series*, volume 34. Natural History Museum of Los Angeles County, 1989.
- R. W. Kimmerer and F. K. Lake. The Role of Indigenous Burning in Land Management. *Journal of Forestry*, 99(11):36–41, November 2001.
- A. Kleidon and M. Heimann. Assessing the role of deep rooted vegetation in the climate system with model simulations: mechanisms, comparison to observations and implications for Amazonian deforestation. *Climate Dynamics*, 16:183–199, 2000.
- K. Klein Goldewijk, A. Beusen, G. van Drecht, and M. de Vos. The HYDE 3.1 spatially explicit database of human-induced global land-use change over the past 12,000 years. *Global Ecology and Biogeography*, 20(1):73–86, 2010. doi: 10.1111/j.1466-8238.2010.00587.x.
- P. J. A. Kleinman, D. Pimentel, and R. B. Bryant. The ecological sustainability of slash-and-burn agriculture. *Agriculture, Ecosystems and Environment*, 52:235–249, 1995.
- E. Klop and H. H. T Prins. Diversity and species composition of West African ungulate assemblages: effects of fire, climate and soil. *Global Ecology and Biogeography*, 17:778–787, 2008.
- V. Kotroni and K. Lagouvardos. Lightning occurrence in relation with elevation, terrain slope, and vegetation cover in the Mediterranean. *Journal of Geophysical Research*, 113:D21118, 7p, 2008. doi: 10.1029/2008JD010605.
- P. Kourtz and B. Todd. Predicting the daily occurrence of lightning-caused forest fires. *For. Can. Petawawa Nat. For. Inst. Info. Rep. PI-X-112*, 1992.
- C. Koven, P. Friedlingstein, P. Ciais, Khvorostyanov D., G. Krinner, and C. Tarnocai. On the formation of high-latitude carbon stocks: Effects of cryoturbation and insulation by organic

Bibliography

- matter in a land surface model. *Geophysical Research Letters*, 36:L21501 5pp., 2009. doi: 10.1029/2009GL040150.
- K. M. Krumhardt and J. O. Kaplan. A spline fit to atmospheric CO₂ records from Antarctic ice cores and measured concentrations for the last 25,000 years. ARVE Technical Report 2, ARVE Group, Environmental Engineering Institute, Ecole Polytechnique Fédérale de Lausanne, EPFL, Station 2, 1015 Lausanne, 2012. URL http://grkapweb1.epfl.ch/pub/ARVE_tech_report2_co2spline.pdf.
- C. A. Kull and P. Laris. *Fire ecology and fire politics in Mali and Madagascar*; in: *Tropical Fire Ecology*, pages 171–226. Springer Verlag, Berlin, Heidelberg, 2009. doi: 10.1007/978-3-540-77381-8_7.
- W. A. Kurz and M. J. Apps. A 70-year retrospective analysis of carbon fluxes in the Canadian forest sector. *Ecological Applications*, 9:526–547, 1999.
- D. M. Lal and S. D. Pawar. Relationship between rainfall and lightning over central Indian region in monsoon and premonsoon seasons. *Atmospheric Research*, 92:402–410, 2009.
- S. M. Landhaeuser and R. M. Wein. Postfire vegetation recovery and tree establishment at the Arctic treeline: Climatic-change-vegetation-response hypothesis. *Journal of Ecology*, 81: 665–672, 1993.
- D. J. Latham and R. C. Rothermel. Probability of Fire-Stopping Precipitation Events. Technical report, U.S. Forest Service, Utah Regional Depository, Paper 354, 1993.
- Y. Le Page, D. Oom, J. N. M. Silva, P. Jönsson, and J. M. C. Pereira. Seasonality of vegetation fires as modified by human action: observing the deviation from eco-climatic fire regimes. *Global Ecology and Biogeography*, 19:575–588, 2010.
- V. Lehsten, K. Tansey, H. Baltzer, K. Thonicke, A. Spessa, U. Weber, Smith. B., and A. Arneth. Estimating carbon emissions from African wildfires. *Biogeosciences*, 6:349–360, 2009.
- V. Lehsten, A. Arneth, K. Thonicke, and A. Spessa. The effect of fire on tree-grass coexistence in savannas: a simulation study. *Journal of Vegetation Science*, in review, 2013.
- H. T. Lewis, editor. *Why Indians burned: specific versus general reasons*, number GTR-INT-182, November, 15-18, 1983. 1985. Proceedings–Symposium and Workshop on Wilderness Fire: Missoula, Montana, Ogden, UT: USDA Forest Service, Intermountain Forest and Range Experiment Station.
- A. Lima, T. S. Freire Silva, L. E. Oliveira, and C. de Aragão. Land use and land cover changes determine the spatial relationship between fire and deforestation in the Brazilian Amazon. *Applied Geography*, 34:239–246, 2012.
- J. Lüning. Steinzeitliche Bauern in Deutschland: die Landwirtschaft im Neolithikum. *Universitätsforschungen zur prähistorischen Archäologie, Bonn*, 58, 2000.

- J. A. Lynch, J. L. Hollis, and F. S. Hu. Climatic and landscape controls of the boreal forest fire regime: Holocene records from Alaska. *Journal of Ecology*, 92:477–489, 2004.
- R. Mäkipää. Effect of nitrogen input on carbon accumulation of boreal forest soils and ground vegetation. *Forest Ecology and Management*, 79:217–226, 1995.
- Y. Malhi, D. Wood, T. R. Bakers, J. Wright, O. L. Phillips, T. Cochrane, P. Meir, J. Chave, S. Almeida, L. Arroyo, N. Higuchi, T. J. Killeen, S. G. Laurance, W. F. Laurance, S. L. Lewis, A. Monteagudo, D. A. Neill, P. N. Vargas, N. C. A. Pitman, C. A. Quesada, R. Salomao, J. N. M. Silva, A. T. Lezama, J. Terborgh, R. Vasquez-Martinez, and B. Vinceti. The regional variation of aboveground live biomass in old-growth Amazonian forests. *Global Change Biology*, 12:1107–1138, 2006.
- F. W. Marlowe. Hunter-Gatherers and Human Evolution. *Evolutionary Anthropology*, 14:54–67, 2005.
- G. Marsaglia. Normal (Gaussian) Random Variables for Supercomputers. *The Journal of Supercomputing*, 5:49–55, 1991.
- A. S. Mather. Forest transition theory and the reforestation of Scotland. *Scottish Geographical Journal*, 120(1+2):83–98, 2004.
- N. Mazarakis, V. Kotroni, K. Lagouvardos, and A. A. Argiriou. Storms and Lightning Activity in Greece during the Warm Periods of 2003-06. *Journal of Applied Meteorology and Climatology*, 47(12):3089–3098, 2008.
- G. M. McKeon, K. A. Day, S. M. Howden, D. M. Mott, J. J. and Orr, and W. J. Scattini. Northern Australia savannas: management for pastoral production. *Journal of Biogeography*, 17: 355–372, 1990.
- W. E. Mell, J. J. Charney, M. A. Jenkins, P. Cheney, and J. Gould. *Numerical Simulations of Grassland Fire Behavior from the LANL - FIRETEC and NIST - WFDS Models; in: Remote Sensing Modeling and Applications to Wildland Fires*. Springer Verlag, Berlin, Heidelberg, 2012.
- J-C. Menaut, L. Abbadie, F. Lavenue, P. Loudjani, and A. Podaire. *Biomass burning in West African savannas*, pages 133–142. MIT Press, Cambridge, Massachusetts, USA, 1991.
- S. C. Michaelides, K. Savvidou, K. A. Nicolaidis, and M. Charalambous. In search for relationships between lightning and rainfall with a rectangular grid-box methodology. *Advances in Geosciences*, 20:51–56, 2009.
- P. R. Moorcroft, G. C. Hurtt, and S. W. Pacala. A method for scaling vegetation dynamics: the ecosystem demography model (ED). *Ecological Monographs*, 71:557–586, 2001.
- A. G. Moreira. Effects of Fire Protection on Savanna Structure in Central Brazil. *Journal of Biogeography*, 4:1021–1029, 27.

Bibliography

- D. Morvan, S. Méradji, and G. Accary. Physical modeling of fire spread in Grasslands. *Fire Safety Journal*, 44:50–61, 2008.
- F. Mouillot and C. B. Field. Fire history and the global carbon budget: a 1° x 1° fire history reconstruction for the 20th century. *Global Change Biology*, 11:398–420, 2005. doi: 10.1111/j.1365-2486.2005.00920.x.
- NASA. Understanding Earth Biomass Burning. Technical Report NP-2011-10-250-GSFC, National Aeronautics and Space Administration, Goddard Space Flight Center, Greenbelt, Maryland, 2011.
- D. G. Neary, K. C. Ryan, and L. F. DeBano. Wildland Fire in Ecosystems - Effects of Fire on Soil and Water. General Technical Report RMRS-GTR-42-volume4, United States Department of Agriculture, Forest Service, Rocky Mountain Research Station, Ogden, UT 84401, 2005.
- V. G. Nesterov. *Gorimost' lesa i metody eio opredelenia*. Goslesbumaga, Moscow, 1949.
- M. New, D. Lister, M. Hulme, and I. Makin. A high-resolution data set of surface climate over global land areas. *Climate Research*, 21:1–25, 2002.
- M. E. J. Newman and R. M. Ziff. Efficient Monte Carlo Algorithm and High-Precision Results for Percolation. *Physical Review Letters*, 85(19):4104–4107, 2000.
- B. B. Nickey. Occurrences of lightning fires - Can they be simulated? *Fire Technology*, 12(4): 321–330, 1976.
- NIMA. Vector Map Level 0 database (VMAP0), Digital Chart of the World, Edition 5. Technical report, National Imagery and Mapping Agency, Bethesda, MD, 2000.
- G.-Y. Niu and Z.-L. Yang. Effects of Frozen Soil on Snowmelt Runoff and Soil Water Storage at a Continental Scale. *Journal of Hydrometeorology*, 7:973–952, 2006.
- D. S. Ojima, D. S. Schimel, W. J. Parton, and C. E. Owensby. Long- and short-term effects of fire on nitrogen cycling in tallgrass prairie. *Biogeochemistry*, 24:67–84, 1994.
- K. W. Oleson, Lawrence D. M., G. B. Bonan, M. G. Flanner, E. Kluzek, P. J. Lawrence, S. Levis, S. C. Swenson, P. E. Thornton, A. Dai, M. Decker, R. Dickinson, J. J. Feddema, C. L. Heald, F. Hoffman, J.-F. Lamarque, N. Mahowald, G.-Y. Niu, T. Qian, J. T. Randerson, S. Running, K. Sakaguchi, A. Slater, R. Stöckli, A. Wang, Z.-L. Yang, X. Zeng, and X. Zeng. Technical Description of version 4.0 of the Community Land Model (CLM). *NCAR TECHNICAL NOTE, NCAR/TN-478+STR, Boulder, CO, 80307-3000*, 2010.
- R. E. Orville, G. R. Huffins, W. R. Burrows, and K. L. Cummins. The North American Lightning Detection Network (NALDN) - Analysis of Flash Data: 2001 - 09. *Monthly Weather Review*, 139:1305–1322, 2011.

- J. S. Otto and N. E. Anderson. Slash-and-Burn Cultivation in the Highlands South: A Problem in Comparative Agricultural History. *Comparative Studies in Society and History*, 24(1): 131–147, 1982.
- S. Page, F. Siegert, H. Boehm, A. Jaya, and S. Limin. The amount of carbon released from peat and forest fires in Indonesia during 1997. *Nature*, 420:61–65, 2002.
- S. Page, J. Rieley, A. Hoscilo, A. Spessa, and U. Weber. *Fire and Global Change*, chapter Chapter IV, Current Fire Regimes, Impacts and Likely Changes in Tropical Southeast Asia. Springer Verlag, Berlin, Heidelberg, 2012.
- F. Papa, C. Prigent, F. Aires, C. Jimenez, W. B. Rossow, and E. Matthews. Interannual variability of surface water extent at the global scale, 1993-2004. *Journal of Geophysical Research*, 115: D12111, 2010. doi: 10.1029/2009JD012674.
- J. G. Pausas and J. E. Keeley. A burning story: The role of fire in the history of life. *BioScience*, 59(7):593–601, 2009.
- J. E. Penner, R. E. Dickinson, and C. A. O’Neill. Effects of Aerosol from Biomass Burning on the Global Radiation Budget. *Science*, 256(5062):1432–1434, 1992.
- D. A. Perry, P. F. Hessburg, C. N. Skinner, T. A. Spies, S. L. Stephens, A. H. Taylor, J. F. Franklin, B. McComb, and G. Riegel. The ecology of mixed severity fire regimes in Washington, Oregon, and Northern California. *Forest Ecology and Management*, 262:703–717, 2011.
- D. Peterson, J. Wang, C. Ichoku, and L. A. Remer. Effects of lightning and other meteorological factors on fire activity in the North American boreal forest: implications for fire weather forecasting. *Atmospheric Chemistry and Physics*, 10:6873–6888, 2010.
- D. L. Peterson and K. C. Ryan. Modeling postfire conifer mortality for long-range planning. *Environmental Management*, 10(6):797–808, 1986.
- M. V. Piepgrass, E. P. Krider, and C. B. Moore. Lightning and Surface Rainfall During Florida Thunderstorms. *Journal of Geophysical Research*, 87(C13):11193–11201, 1982.
- B. Poulter, U. Heyder, and W. Cramer. Modeling the Sensitivity of the Seasonal Cycle of GPP to Dynamic LAI and Soil Depth in Tropical Rainforests. *Ecosystems*, 12:517–333, 2009.
- Prairiesource.com. Prescribed Burning 101: An Introduction to Prescribed Burning, Spring 1992, 1992. URL http://www.prairiesource.com/newsletters/92_spr01.htm.
- K. S. Pregitzer and E. S. Euskirchen. Carbon cycling and storage in world forests: biomae patterns related to forest age. *Global Change Biology*, 10:2052–2077, 2004.
- I. C. Prentice, D. I. Kelley, P. N. Foster, P. Friedlingstein, S. P. Harrison, and P. J. Bartlein. Modeling fire and the terrestrial carbon balance. *Global Biogeochemical Cycles*, 25:GB3005, 2011. doi: 10.1029/2010GB003906.

Bibliography

- S. J. Pyne. *Fire in America: A Cultural History of Wildland and Rural Fire*. Princeton University Press, Princeton, NJ, 1982.
- S. J. Pyne. Maintaining Focus: An Introduction to Anthropogenic Fire. *Chemosphere*, 29(5): 889–911, 1994.
- S. J. Pyne. *World Fire: The Culture of Fire on Earth*, 384 p. University of Washington Press, Seattle, WA, 1997.
- S. J. Pyne, P. L. Andrews, and R. D. Daven. *Introduction to Wildland Fire*. Wiley, London, 1996.
- N. Ramankutty, A. T. Evan, C. Monfreda, and J. A. Foley. Farming the planet: 1. Geographic distribution of global agricultural lands in the year 2000. *Global Biogeochemical Cycles*, 22: GB1003, 2008. doi: 10.1029/2007GB002952.
- J. T. Randerson, Y. Chen, G. R. van der Werf, B. M. Rogers, and D. C. Morton. Global burned area and biomass burning emissions from small fires. *Journal of Geophysical Research*, 117: G04012, 2012. doi: 10.1029/2012JG002128.
- G. Rasul and G. B. Thapa. Shifting Cultivation in the Mountains of South and Southeast Asia: Regional patterns and factors influencing the change. *Land Degradation and Development*, 14:495–508, 2003.
- E. D. Reinhardt, R. E. Keane, and J. K. Brown. First Order Fire Effects Model: FOFEM 4.0, User's Guide. General Technical Report INT-GTR-344, United States Department of Agriculture, Forest Service, Missoula, Montana 59807, Intermountain Research Station, 1997.
- L. A. Richards. Capillary conduction of liquids through porous mediums. *Physics*, 1(5):318–333, 1931.
- B. Ringeval, N. de Noblet-Ducoudré, P. Ciais, P. Bousquet, C. Prigent, F. Papa, and W. B. Rossow. An attempt to quantify the impact of changes in wetland extent on methane emissions on the seasonal and interannual time scales. *Global Biogeochemical Cycles*, 24:GB2003, 2010. doi: 10.1029/2008GB003354.
- L. Rivas Soriano, F. De Pablo, and E. García Díez. Relationship between Convective Precipitation and Cloud-to-Ground Lightning in the Iberian Peninsula. *Monthly Weather Review*, 129:2998–3003, 2001.
- C. I. Roos, A. P. Sullivan, and C. McNamee. Paleoecological Evidence for Systematic Indigenous Burning in the Upland Southwest. *The Archaeology of Anthropogenic Environments*, Southern Illinois University Press, Carbondale, pages 142–171, 2010.
- M. Rösch, O. Ehrmann, L. Herrmann, E. Schulz, A. Bogenrieder, J. P. Goldammer, M. Hall, H. Page, and W. Schier. An experimental approach to Neolithic shifting cultivation. *Vegetation History and Archaeobotany*, 11:143–154, 2002.

- R. C. Rothermel. A mathematical model for predicting fire spread in wildland fuels. *USDA Forest Service Research Paper, Ogden, UT 84401*, INT-115:48, 1972.
- S. H. Roxburgh, K. Shea, and J. B. Wilson. The Intermediate Disturbance Hypothesis: Patch Dynamics and Mechanisms of Species Coexistence. *Ecology*, 85(2):359–371, 2004.
- D. P. Roy and L. Boschetti. Southern Africa Validation of the MODIS, L3JRC, and GlobCarbon Burned-Area Products. *IEEE Transactions on Geoscience and Remote Sensing*, 47(4):1032–1044, 2009.
- D. P. Roy, L. Boschetti, C. O. Justice, and J. Ju. The collection 5 MODIS burned area product - Global evaluation by comparison with the MODIS active fire product. *Remote Sensing of Environment*, 112:3690–3707, 2008.
- S. S. Saatchi, R. A. Houghton, D. Alves, and B. Nelson. Amazon Basin Aboveground Live Biomass Distribution Map: 1999 - 2000. *Data Set from Oak Ridge National Laboratory Distributed Active Archive Center, Oak Ridge, Tennessee, U.S.A.*, 2009.
- S. S. Saatchi, N. L. Harris, S. Brown, M. Lefsky, and E. T. A. and Mitchard. Benchmark map of forest carbon stocks in tropical regions across three continents. *Proceedings of the National Academy of Sciences, USA*, 108:1–6, 2011. doi: 10.1073/pnas.1019576108.
- M. C. Scholes, R. Martin, R. J. Scholes, D. Parsons, and E. Winstead. NO and N₂O emissions from savanna soils following the first simulated rains of the season. *Nutrient Cycling in Agroecosystems*, 48:115–122, 1997.
- W. Seiler and P. J. Crutzen. Estimates of gross and net fluxes of carbon between the biosphere and the atmosphere from biomass burning. *Climatic Change*, 2:207–247, 1980.
- F. Sigaut. Swidden cultivation in Europe. A question for tropical anthropologists. *Social Science Information*, 18:679–694, 1979.
- S. Sitch, B. Smith, I. C. Prentice, A. Arneth, A. Bondeau, W. Cramer, J. O. Kaplan, S. Levis, W. Lucht, M. T. Sykes, K. Thonicke, and S. Venevsky. Evaluation of ecosystem dynamics, plant geography and terrestrial carbon cycling in the LPJ dynamic global vegetation model. *Global Change Biology*, 9:161–185, 2003.
- C. N. Skinner and C.-R. Chang. Fire Regimes, Past and Present. *Sierra Nevada Ecosystem Project: Final Report to Congress, vol. II, Assessments and scientific basis for management options*, 1996.
- B. Smith, I. C. Prentice, and M. T. Sykes. Representation of vegetation dynamics in the modelling of terrestrial ecosystems: comparing two contrasting approaches within European climate space. *Global Ecology and Biogeography*, 10:621–637, 2001.
- T. Smittinand, S. Ratanakhon, D. Banijbatana, T. Komkris, P. J. Zinke, P. Hinton, F.G. B. Keen, J. L. Charley, J. W. McGarity, and K. J. Pelzer. *Farmers in the Forest. Economic development*

Bibliography

- and marginal agriculture in Northern Thailand*. University of Hawai'i Press, Honolulu, HI 96822, 1986.
- M. Sonesson and T. V. Callaghan. Strategies of Survival in Plants of the Fennoscandian Tundra. *Arctic*, 44(2):95–105, 1991.
- A. Spessa and R. Fisher. On the relative role of fire and rainfall in determining vegetation patterns in tropical savannas: a simulation study. *Geophysical Research Abstracts*, 12: EGU2010–7142–6, 2010, 2010.
- A. Spessa, G. van der Werf, K. Thonicke, J. Gomez-Dans, R Fisher, and M. Forrest. *Fire and Global Change*, chapter Modeling Vegetation Fires and Emissions. Number Chapter XIV. Springer publishers, 2012.
- S. L. Stephens and L. W. Ruth. Federal Forest-Fire Policy in the United States. *Ecological Applications*, 15(2):532–542, 2005.
- O. C. Stewart, H. T. Lewis, and K. Anderson. *Forgotten Fires: Native Americans and the Transient Wilderness*. University of Oklahoma Press, 364 p., Norman, OK 73069, 2002.
- B. J. Stocks, J. A. Mason, J. B. Todd, E. M. Bosch, B. M. Wotton, B. D. Amiro, M. D. Flannigan, K. G. Hirsch, K. A. Logan, D. L. Martell, and W. R. Skinner. Large forest fires in Canada, 1959 - 1997. *Journal of Geophysical Research*, 108(D1):8149, 2003. doi: 10.1029/2001JD000484.
- M. Sturm, J. P. McFadden, G. E. Liston, F. S. Chapin, C. H. Racine, and J. Holmgren. Snow-Shrub Interactions in Arctic Tundra: A Hypothesis with Climatic Implications. *Journal of Climate*, 14:336–344, 2000.
- K. Tansey, J.-M. Grégoire, D. Stroppiana, A. Sousa, J. Silva, J. M. C. Pereira, L. Boschetti, M. Maggi, P. A. Brivio, R. Praser, S. Flasse, D. Ershov, E. Binaghi, D. Graetz, and P. Peduzzi. Vegetation burning in the year 2000: Global burned area estimates from SPOT VEGETATION data. *Journal of Geophysical Research*, 109:D14S03, 2004. doi: 10.1029/2003JD003598.
- K. Tansey, J.-M. Grégoire, P. Defourny, R. Leigh, J. Pekel, J. F. O. van Bogaert, E. van Bogaert, and E. Bartholomé. A new global, multi-annual (2000-2007) burnt area product at 1 km resolution. *Geophysical Research Letters*, 35:L01401, 2008. doi: 10.1029/2007GL031567.
- C. Tarnocai, J. G. Canadell, E. A. G. Schuur, P. Kuhry, G. Mazhitova, and S. Zimov. Soil organic carbon pools in the northern circumpolar permafrost region. *Global Biogeochemical Cycles*, 23:GB2023, 2009. doi: 10.1029/2008GB003327.
- K. Thonicke, A. Spessa, I. C. Prentice, S. P. Harrison, L. Dong, and C. Carmona-Moreno. The influence of vegetation, fire spread and fire behaviour on biomass burning and trace gas emissions: results from a process-based model'. *Biogeosciences*, 7:1991–2011, 2010.
- W. Tinner, M. Conedera, B. Ammann, and A. F. Lotter. Fire ecology north and south of the Alps since the last ice age. *Holocene*, 15:1214–1226, 2005.

- W. Tinner, F. S. Hu, R. Beer, P. Kaltenrieder, B. Scheurer, and U. Krähenbühl. Postglacial vegetational and fire history: pollen, plant macrofossil and charcoal records from two Alaskan lakes. *Vegetation History and Archaeobotany*, 15:279–293, 2006. doi: 10.1007/s00334-006-0052-z.
- S. K. Todd and H. A. Jewkes. Wildland Fire in Alaska: A History of Organized Fire Suppression and Management in the Last Frontier. Technical Report Bulletin No. 114, Agricultural and Forestry Experiment Station, University of Alaska, Fairbanks, 2006.
- M. Turetsky, K. Wieder, L. Halsey, and D. Vitt. Current disturbance and the diminishing peatland carbon sink. *Geophysical Research Letters*, 29:No. 11, 279–293, 2002. doi: 10.1007/s00334-006-0052-z.
- C. Uhl and J. B. Kauffman. Deforestation, Fire Susceptibility, and Potential Tree Responses to Fire in the Eastern Amazon. *Ecology*, 71(2):437–449, 1990.
- M. A. Uman. *The Art and Science of Lightning Protection*. Cambridge University Press: Cambridge, 2010.
- J. D. Unruh, J. M. Treacy, J. B. Alcorn, and S. Flores Paitán. *Swidden-fallow agroforestry in the Peruvian Amazon*, volume 5. New York Botanical Garden, 1987.
- G. R. van der Werf, J. T. Randerson, L. Giglio, G. J. Collatz, M. Mu, P. S. Kasibhatla, D. C. Morton, R. S. DeFries, Y. Jin, and T. T. van Leeuwen. Global fire emissions and the contribution of deforestation, savanna, forest, agricultural, and peat fires (1997-2009). *Atmospheric Chemistry and Physics Discussions*, 10:16153–16230, 2010. doi: 10.5194/acpd-10-16153-2010.
- H. Van Reuler and B. H. Janssen. Comparison of the fertilizing effects of ash from burnt secondary vegetation and of mineral fertilizers on upland rice in south-west Cote d’Ivoire. *Fertilizer Research*, 45:1–11, 1996.
- B. W. van Wilgen, C. S. Everson, and W. S. W. Trollope. *Fire Management in Southern Africa: Some Examples of Current Objectives, Practices and Problems*, pages 79–212. Springer Verlag, Berlin, 1990.
- S. Venevsky, K. Thonicke, S. Sitch, and W. Cramer. Simulating fire regimes in human-dominated ecosystems: Iberian Peninsula case study. *Global Change Biology*, 8:984–998, 2002.
- K. S. Virts, J. M. Wallace, M. L. Hutchins, and R. H. Holzworth. A new ground-based, hourly global lightning climatology. *Bull. Amer. Meteor. Soc.*, in review, 2012.
- S. Wan, D. Hui, and Y. Luo. Fire Effects on Nitrogen Pools and Dynamics in Terrestrial Ecosystems: A Meta-Analysis. *Ecological Applications*, 11(5):1349–1365, 2001.
- T. Wang, A. Hamann, D. L. Spittlehouse, and T. Q. Murdock. ClimateWNA - High-Resolution Spatial Climate Data for Western North America. *Journal of Applied Meteorology and Climatology*, 51:16–29, 2011.

Bibliography

- R. Wania, I. Ross, and I. C. Prentice. Integrating peatlands and permafrost into a dynamic global vegetation model: 1. Evaluation and sensitivity of physical land surface processes. *Global Biogeochemical Cycles*, 23:GB3014, 2009. doi: 10.1029/2008GB003412.
- C. Warneke, R. Bahreini, C. A. Brock, J. A. de Gouw, D. W. Fahey, K. D. Froyd, J. S. Holloway, A. Middlebrook, L. Miller, S. Montzka, D. M. Murphy, J. Peischl, T. B. Ryerson, J. P. Schwarz, J. R. Spackman, and P. Veres. Biomass burning in Siberia and Kazakhstan as important source for haze over the Alaskan Arctic in April 2008. *Geophysical Research Letters*, 36, L02813:6p, 2009. doi: 10.1029/2008GL036194.
- A. L. Westerling, H. G. Hidalgo, D. R. Cayan, and T. W. Swetnam. Warming and Earlier Spring Increase Western U.S. Forest Wildfire Activity. *Science*, 313(5789):940–943, 2006.
- A. Whiten and D. Erdal. The human socio-cognitive niche and its evolutionary origins. *Philosophical Transactions of the Royal Society B*, 367:2119–2129, 2012.
- G. W. Williams. Introduction to Aboriginal Fire Use in North America. *Fire Management Today*, 60:No. 3, 8–12, 2000.
- G. W. Williams. *Wilderness and Political Ecology: Aboriginal Land Management - Myths and Reality*, chapter Aboriginal use of fire: are there any "natural" plant communities? University of Utah Press, Logan, UT, 2002a.
- M. Williams. *Deforesting the Earth: From Prehistory to Global Crisis*. University of Chicago Press, Chicago, IL, 2002b.
- R. Wincen. The pastoral industry of Cape York Peninsula. *Cape York Peninsula Land Use Study Talkback, Brisbane*, 4:8–9, 1993.
- D. Wylie, D. L. Jackson, W. P. Menzel, and J. J. Bates. Trends in Global Cloud Cover in Two Decades of HIRS Observations. *Journal of Climate*, 18:3021–3031, 2005.
- R. Yevich and J. A. Logan. An assessment of biofuel use and burning of agricultural waste in the developing world. *Global Biogeochemical Cycles*, 17(4), 1095, 2003. doi: 10.1029/2002GB001952.
- D. Yibarbuk, P. J. Whitehead, J. Russell-Smith, D. Jackson, C. Godjuwa, A. Fisher, P. Cooke, Choquenot D., and D. M. J. S. Bowman. Fire ecology and Aboriginal land management in central Arnhem Land, northern Australia: a tradition of ecosystem management. *Journal of Biogeography*, 28:325–343, 2002.
- X. Zhang, N. A. Drake, J. Wainwright, and M. Mulligan. Comparison of slope estimates from low resolution DEMs: scaling issues and a fractal method for their solution. *Earth Surface Processes and Landforms*, 24:763–779, 1999.
- Y. Zhou, X. Qie, and S. Soula. A study of the relationship between cloud-to-ground lightning and precipitation in the convective weather system in China. *Annales Geophysicae*, 20: 107–113, 2002.

4 Role of humans and fire for vegetation in Europe during the Last Glacial Maximum

M. Pfeiffer and J. O. Kaplan, manuscript in preparation for submission to Nature Geoscience

Proxy-based vegetation reconstructions for the Last Glacial Maximum (LGM) in Europe suggest a high degree of landscape openness with a dominance of steppe-type vegetation. Dynamic Global Vegetation Models (DGVMs) have difficulties in reproducing this high degree of landscape openness and overestimate tree cover albeit colder and drier climatic conditions and lower CO₂ concentrations. Here we argue that inclusion of anthropogenic fire into DGVMs is essential to simulate vegetation patterns that are in better agreement with reconstructions. Using LPJ in combination with a process-based fire module that is capable of simulating natural as well anthropogenic burning, we test the hypothesis that fire usage by Paleolithic hunter-gatherers may be the key to simulating more open vegetation in Europe. We performed four model simulations to test the effect of naturally caused fires alone versus natural plus human fire for the LGM and preindustrial time. For all four simulations, we analyze quantities and changes in average annual area burned and simulated tree cover. Our results show that already relatively small total increases of average annual area burned due to additional human ignitions may result in a drastic reduction of tree cover and a dominance of grassy/herbaceous plant functional types as suggested by data-based vegetation reconstructions. We therefore conclude that the usage of fire by forager people in Europe during the LGM should not be overlooked, and that climatic conditions and low atmospheric CO₂ alone may not be sufficient to explain and realistically simulate the predominance of steppe-type vegetation.

4.1 Introduction

Vegetation reconstructions based on pollen and plant macrofossils for the time of the Last Glacial Maximum (LGM) show vegetation patterns that are very different from the patterns of potential natural vegetation at present day. Large parts of Eurasia that are forested at present

Chapter 4. Role of humans and fire for vegetation in Europe during the Last Glacial Maximum

day or would potentially be forested without human interference were characterized by the prevalence of shrubby and herbaceous vegetation types and reduced tree cover. Extensive areas of Eurasia that are classified as forest-type biomes at present day were steppe and tundra during LGM [Prentice et al., 2000b, Tarasov et al., 2000]. Biome reconstructions for Eurasia come to the conclusion that steppe was the dominant vegetation type across northern Eurasia south of ca. 57 °N, with tundra being adjacent in the north and the boreal forest being much reduced and discontinuous, while cool mixed and temperate deciduous forests were absent from the central part of the East European Plain and the southern Urals [Tarasov et al., 2000]. Mediterranean pollen sites indicate savanna-like ecosystems or steppe-type vegetation with a predominance of grassland and scrubland taxa, and pollen sites north of the Alps show steppe-type vegetation with mixed-in tundra features where trees were largely absent [Elena et al., 2000, and references therein].

Significantly lower levels of atmospheric CO₂ compared to present-day conditions reinforced interactions between plants and climate at the LGM [Monnin et al., 2001, Prentice and Harrison, 2009, Ramstein et al., 2007]. In combination with low CO₂ concentrations, cold and dry conditions at LGM [Wu et al., 2007] likely contributed to a remarkable expansion of tundra and steppe at the expense of forest biomes in Eurasia, which were shifted southward and fragmented relative to their present day extent [Prentice et al., 2000b]. Contrasting to vegetation reconstructions based on pollen, simulations of LGM vegetation in Europe using Dynamic Global Vegetation Models (DGVMs) or equilibrium biosphere models suggest a greater representation of trees than indicated by the proxy-based vegetation reconstructions [see, e.g. Harrison and Prentice, 2003, Kaplan et al., 2003, Lathière et al., 2005, Strandberg et al., 2011, Woillez et al., 2011]. This discrepancy with respect to tree representation between data-based reconstructions and modeled vegetation distribution may be due to biases in both methods and has not been definitively resolved. Explanation attempts point out that model calibrations for the cold distributional limits for trees are based on observed modern distributions in relation to mean temperature of coldest month instead to absolute minimum temperature, although trees may be more closely linked to the latter than the former [Strandberg et al., 2011, Woodward and Williams, 1987]. Moreover, most DGVMs distinguish herbaceous vegetation from woody vegetation, but lack an explicit incorporation of shrubby PFTs that could represent shrubland or woody tundra as an essential element of European vegetation during the LGM [Harrison and Prentice, 2003], therefore making it unclear what exactly the simulated woody vegetation actually represents.

Another key point for accurately simulating vegetation distribution is the adequate incorporation of disturbance factors, with fire being one of the major causes of vegetation disturbance with effects on vegetation productivity, composition and nutrient cycling [Bond et al., 2005, Bowman et al., 2009]. The occurrence of natural fires is largely controlled by climatic conditions [Pitman et al., 2007, van der Werf et al., 2008, Williams et al., 2001]. Analysis of sedimentary charcoal indicates consistently lower fire activity during glacial periods relative to interglacial periods, although considerable millennial-scale variability in glacial fire regimes is documented [Daniau et al., 2010, Power et al., 2008]. However, the impact of prehistoric fires

set by humans is debated among scientists and views diverge from negligible to substantial importance [Bowman et al., 2011]. Foragers can directly alter fire regimes by increasing the number of ignitions and by shifting their timing, and indirectly by altering fuel structure and availability through burning. Bowman et al. [2011] emphasize that the importance of human-caused ignitions will vary according to the saturation of environments with respect to natural ignitions, with effects being smaller in naturally ignition-saturated environments.

Based on the knowledge that hunter-gatherers use fire liberally for many different purposes [Lewis, 1985], and that at the time of the LGM fire had been an indispensable part of human life for probably more than 30 - 80 ka years [Pausas and Keeley, 2009, and references therein], we ask the question what role humans and their use of fire for landscape management may have had for LGM vegetation distribution in Europe. We hypothesize that natural and anthropogenic burning may have played an important role in creating the open types of landscapes indicated by vegetation reconstructions based on proxies, and that inclusion of a process-based representation of natural and anthropogenic burning into DGVMs may help to overcome the discrepancy between modeled and observed vegetation in Europe at LGM. To test the potential effect of anthropogenic and natural burning on LGM vegetation in Europe, we perform model simulations using LPJ in combination with the fire module described in chapter 3. To drive LPJ, we use GISS ModelE climate output [Schmidt et al., 2006, Murray et al., 2012] based on CLIMAP sea surface temperatures [Geological Society of America, 1981].

4.2 Methods

We performed four simulation runs for Europe to evaluate the effect of people and fire on glacial vegetation: two simulation runs for LGM climate and low CO₂, and for comparison two simulation runs for the preindustrial period (1770 AD) with corresponding climate and atmospheric CO₂ level. For each time slice, one simulation has been performed excluding people, i.e., allowing only natural ignitions, and a second simulation including additional fire caused by humans. At 21 ka BP, all people are considered to be hunters and gatherers living on natural land, whereas at 1770 farmers are the dominating lifestyle group in Europe. Based on an extensive literature review on population densities of more than 100 modern and historic hunter-gatherer peoples, we set a forager population density of 0.025 people km⁻² for the LGM runs. The simulation run for 1770 with presence of people includes land use and burning on agricultural land as described in chapter 3. We use the KK12 landuse dataset (publication in prep.) to parameterize population estimates and fraction of land being subject to agricultural land use at preindustrial. The CLIMAP GCM output [Murray et al., 2012, publication in prep.] used to drive LPJ and the linked fire module for the LGM includes anomalies of monthly mean temperature, diurnal temperature range, precipitation, number of wet days per month, cloud cover, wind speed and lightning relative to preindustrial climate.

Coastlines and outlines of ice sheets at LGM are used as mask to determine potentially vegetated land area at 21 ka BP. For each simulation run we performed a model spinup of 1020

Chapter 4. Role of humans and fire for vegetation in Europe during the Last Glacial Maximum

years and evaluate the last 150 years of spinup when vegetation is in equilibrium with climate and fire.

4.3 Results

We analyzed two different aspects with respect to simulated fire at the LGM and preindustrial: Patterns and changes in average annual area burned, and changes in simulated tree cover, with specific emphasis on the changes caused by anthropogenic fire.

4.3.1 Changes in average annual area burned

At LGM, lightning-caused fires occur in most parts of Europe (Fig. 4.1a), although the average percentage of area burned per year is below 10 % in most areas north of the Mediterranean. Areas with burned area percentages above 15 % are predominantly located around the coastlines of the Mediterranean Sea, with hotspots of burning along the coasts of the Iberian Peninsula, North Africa, and the eastern Mediterranean region. The presence of hunter-gatherers leads to an increase in burning in almost all parts of Europe, namely all places that naturally burn less than 10 % (Fig. 4.1b). For places around the Mediterranean that already burn frequently due to natural ignitions, the presence of people does not lead to a noticeable increase in total burning. Typically, the presence of humans leads to an increase in annual area burned of between 3 and 9 % in most parts of Europe north of the Mediterranean. For the land area shown in Fig. 4.1 (between 24 °W and 60 °E, and 30 °N and 60 °N), the simulated average annual area burned without people equals 768.338 km², and increases to 1.049.200 km² once people are included as ignition source, i.e., the average annual area burned over the shown area increases by factor 1.4. Without people, 25 % of the annual area burned is located between 30 °N and 34 °N, 50 % of the area between 30 °N and 37 °N, 75 % between 30 °N and 42 °N, making the Mediterranean the clear hotspot of burning. The relative contribution of Europe north of the Alps to the total area burned within a year is increased when including anthropogenic ignition sources. The limits of the quartiles are shifted towards the north, with 25 % of the total area being burned below 35 °N, 50 % below 39 °N, and 75 % below 49 °N. This implies that the presence of people has hardly any effect on the average amount of area burned each year for most of the Mediterranean region. For Europe north of the Alps, the amount of annual burned area caused by people varies between 5 and 10 % for most places. Compared to the average area burned in the Mediterranean region, the simulated total amount of area burned in Europe north of the Alps is low even when including anthropogenic burning, and varies between 2 and 15 % for most places. However, compared to the scenario with natural fire only where hardly any fire is simulated in many places of Europe north of the Alps, the presence of people more than doubles the total amount of area burned albeit total amounts being low even with the presence of people.

As depicted in Fig. 4.1c, most places in Europe experienced less fire during the LGM than at preindustrial. Strong negative anomalies in annual area burned were simulated were

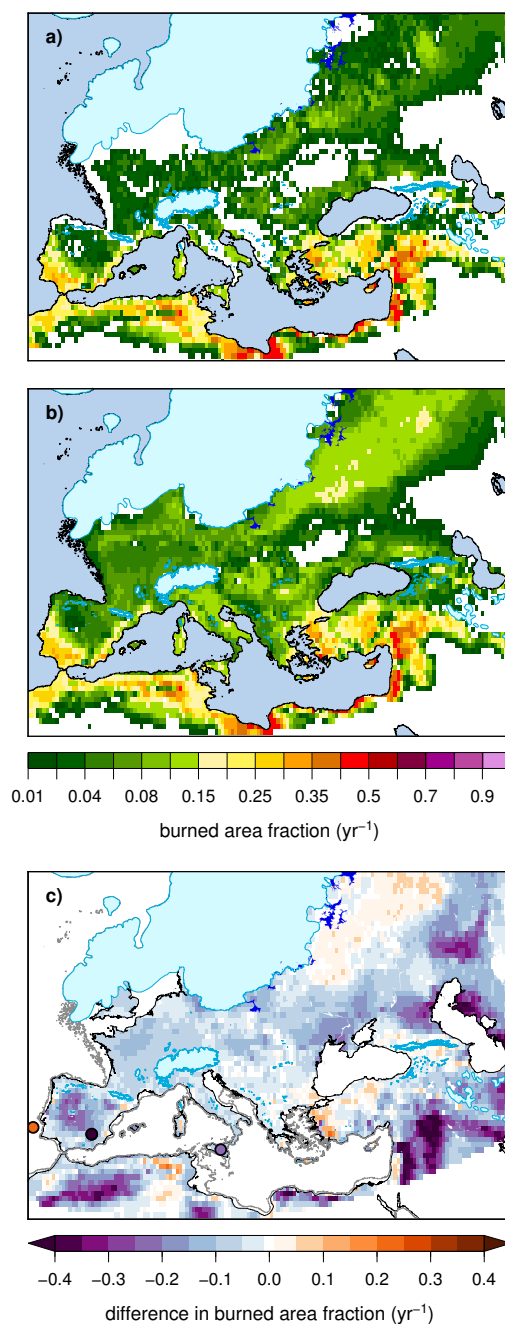


Figure 4.1: Panel a): Simulated annual area burned without anthropogenic ignitions at LGM. Panel b): Simulated annual area burned including additional ignitions from hunter-gatherers. Panel c) Difference in annual burned area between LGM and preindustrial (both scenarios including anthropogenic burning). The filled circles indicate charcoal anomalies between LGM and preindustrial.

simulated in the area of the Caspian Sea, the Eastern Mediterranean region, and the central part of the Iberian Peninsula. Slightly more fire than at preindustrial is simulated south of the

Chapter 4. Role of humans and fire for vegetation in Europe during the Last Glacial Maximum

Black Sea and the Aegean Region, and east of the Scandinavian ice sheet. For all area that was land and ice-free during both LGM and preindustrial between 24 °W – 60 °E, and 30 °N – 60 °N, the increase in average annual area burned from LGM to preindustrial amounts to a factor of 2.5 for the scenarios with natural burning only, and a factor of 2.2 for the scenarios including anthropogenic fire. For the preindustrial, 25 % of the annual area burned in the scenario with people is due to anthropogenic fire, with 16 % burning on agricultural land and 9 % burning on natural land, while 31 % of the annual area burned during the LGM can be attributed to anthropogenic burning. The increase in annual area burned from LGM to preindustrial is most pronounced between 45 °N and 51 °N for both the natural and anthropogenic scenario. At 45 °N, burning at preindustrial is 2.4 times (2.0 times) higher for the natural (anthropogenic) scenario than at LGM. This factor rapidly increases to 9.7 (5.5) at 48 °N and then drops again to 2.2 (2.5) at 51 °N. North of 51 °N the factor drops and reaches 1 at approx. 56 °N (54 °N). South of 45 °N the increase factor varies between 1.7 (1.6) and 3.8 (3.7), with an average of 2.6 ± 0.7 (2.3 ± 0.7).

For the LGM-scenario (preindustrial scenario) with people, anthropogenic fire is responsible for 6 ± 5 % (2 ± 5 %) of the total annual area burned between 30 °N and 40 °N. Between 40 °N and 53 °N, in average 48 ± 8 % (38 ± 9 %) of the annual area burned are due to human burning, with approx. 31 % (27 %) at 40 °N and 51 % (32 %) at 53 °N, and a maximum of 63 % at 43 °N (61 % at 43 °N). North of 51 °N, the relative contribution of anthropogenic burning rapidly increases from 36 % (34 %) to more than 64 % (94 %) between 57 °N and 60 °N. At preindustrial, anthropogenic burning on agricultural land dominates between 34 °N and 54 °N over anthropogenic burning on natural land.

4.3.2 Changes in simulated tree cover

Simulated tree cover at the LGM is spatially variable. For the scenario with natural fire only (Fig. 4.2a), areas of relatively high tree cover are located south and east of the Black Sea, in the Italian Apennines, the Dinaric Alps, the Carpathian Mountains, the northern Atlantic coast of the Iberian Peninsula, in western and central Europe, and east of the Scandinavian ice sheet. In comparison, the scenario including hunter-gatherer burning shows a considerable reduction in tree cover for most of Europe (Fig. 4.2b), leading to an overall more homogenous tree cover with a large degree of openness. Most places have no more than 10 – 30 % tree cover, with reductions in tree cover being most pronounced in places where higher tree cover was simulated without the presence of people (Fig. 4.2c). Anthropogenic burning decreases the area covered by trees by 38.5 %, from $3.698.562 \pm 124.641$ km² to $2.275.108 \pm 86.368$ km², compared to the scenario with natural burning only. Averaged over the total ice-free land area, 29.5 % of this land area is covered with trees when only taking into account lightning ignitions, whereas the presence of humans as additional ignition source reduced the area covered by trees to 18.2 %.

For both burning scenarios, tree cover in the Mediterranean region below 36 °N in average

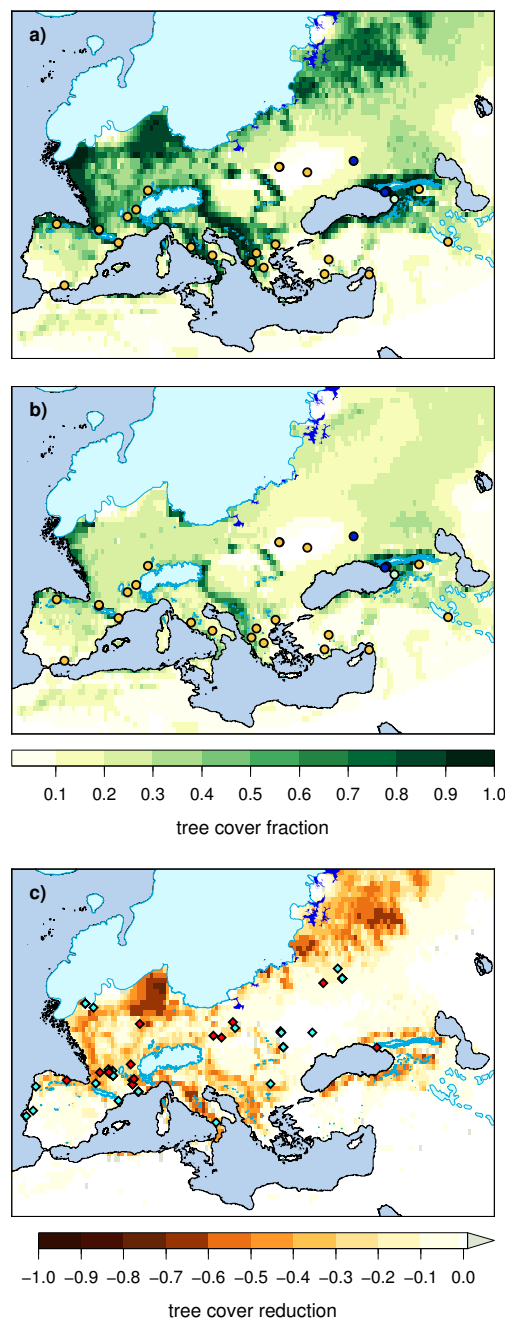


Figure 4.2: Panel a): Simulated LGM tree cover for the scenario without anthropogenic ignitions. The filled circles show the BIOME6000 biome classification for available pollen sites [Prentice et al., 2000b]. Yellow circles indicate steppe vegetation, blue circles cold evergreen needleleaf forest, and light green circles cool mixed forest. Panel b) Simulated tree cover at LGM including additional anthropogenic ignitions. Panel c) Reduction in tree cover due to hunter-gatherer burning. Diamonds indicate archaeological sites, red diamonds are sites with evidence for human fire use.

Chapter 4. Role of humans and fire for vegetation in Europe during the Last Glacial Maximum

does not exceed 10 %. For the scenario excluding anthropogenic burning, tree cover north of the Mediterranean region in average varies between 50 and 60 %, with some areas, e.g., south of the Scandinavian ice sheet, reaching values as high as 80 to 90 % where no fire is simulated under natural conditions. North of the Mediterranean region, inclusion of anthropogenic burning leads to a remarkable reduction in overall tree cover, with average values ranging between 20 and 30 % for most places in western and central Europe, and values between 10 and 20 % directly east of the Scandinavian ice sheet. South of 36 °N, human fire has only very little influence on simulated tree cover, causing an overall reduction between 2 and 4 %. In contrast, the reduction in tree cover caused by additional human burning north of the Alps varies between 20 and 60 % (Fig. 4.2c).

A comparison of simulated tree cover area in Europe during LGM and preindustrial for those regions that were land and ice-free at both times yields a tree cover increase by a factor of 1.2 from LGM to preindustrial, from $3.284.495 \pm 113.340 \text{ km}^2$ to $3.934.389 \pm 103.052 \text{ km}^2$ for the natural-only scenario. For the scenario including people, forest cover increases by a factor of 1.3, from $2.021.313 \pm 80.271 \text{ km}^2$ to $2.557.679 \pm 100.449 \text{ km}^2$. At preindustrial, the presence of people decreases the average forest cover in Europe by 35 % relative to the simulation without people. However, 67 % of the reduction in tree cover at preindustrial is due to deforestation linked to agriculture, i.e., conversion of natural land to agricultural fields, and only 33 % of the reduction in tree cover is due to human burning on non-agricultural land. Comparable to the tree cover situation at the LGM, tree cover is less than 10 % for latitudes below 36 °N for both scenarios. Tree cover rapidly increases between 36 °N and 43 °N, where it reaches a maximum value of 70 % for the natural scenario (52 % for the scenario with people) before gradually dropping off to a value of 33 % (21 %) at 47 °N. Between 48 °N and 51 °N values increase again to approx. 45 % (25 %), before dropping off to a minimum of 34 % (23 %) at 54 °N. North of 54 °N, the average latitudinal tree cover rapidly increases to more than 90 % (60 %) north of 57 °N.

4.4 Discussion

Charcoal records for the time of the LGM indicate reduced amounts of burning compared to preindustrial and present day for many extra-tropical sites [Power et al., 2008]. While offering valuable information on qualitative differences between fire regimes at LGM and preindustrial, charcoal records do not directly allow a quantitative assessment of changes in fire regimes. Moreover, charcoal evidence for Europe during the LGM is limited to a few sites (Fig. 4.1c) and therefore makes it difficult to draw quantitative conclusions for the entire area of Europe. Using a coupled vegetation-fire model enables us to produce a spatially coherent estimate of burning at the LGM. Using the fire model described in Chapter 3 and simulating forager burning as a dynamic reaction of humans to environmental conditions as depicted in section 2 enables us to assess burning caused by natural ignition sources as well as possible effects of Paleolithic hunter-gatherers on fire regimes and vegetation.

While previous studies have attempted to model the effect of natural fire regimes on LGM vegetation and trace gas emissions [Prentice et al., 2011, Thonicke et al., 2005], to our knowledge no study so far has included any parameterization or scheme to estimate the extent and effects of anthropogenic fires caused by hunter-gatherer people. Given the knowledge that we have, especially hunter-gatherer people use fire very liberally and for many different purposes to manage landscapes and ecosystems that are favorable for their own survival, with an innate preference for semi-open savanna-type landscapes [Balling and Falk, 1982, Gobster, 1994, 1995, Kaplan and Kaplan, 1989, Kaplan et al., 1989, Williams, 2002]. Arguably, this preference for semi-open landscape types is linked to modern humans having evolved in Africa's savanna ecosystems [Orians and Heerwagen, 1980]. Humanity's origin in highly flammable savannas probably contributed to an early mastery of fire [Ségalen et al., 2007], which eventually became a unique trait of humanity that was culturally framed and transmitted [Bowman et al., 2011, Pyne, 2000, Wrangham, 2009]. Once humans had added fire to their Paleolithic tool kit, fire was used liberally by hunter-gatherers for clearing habitat by opening up scrublands and woodlands, to facilitate travelling and hunting, to remove vermin, to promote plant food sources and habitat diversity for game, to reduce fuel loads and create landscape patchiness in order to avoid the risk of catastrophic fires, for cooking, as defense against wild animals, as a means of communication, and for warfare among tribes [Bird et al., 2008, Burney and Flannery, 2005, Kimmerer and Lake, 2001, Pyne, 1994, 1997, Roos et al., 2010, Stewart et al., 2002, Williams, 2000]. Generally speaking, hunter-gatherers prefer semi-open landscapes because they offer the advantage of being able to see approaching predators as well as prey, while at the same time being a refuge sheltering the observer from being seen [Appleton, 1975], and enabling people to move around quickly and with ease [Kaplan, 1991]. Even at present indigenous forager societies often show this innate preference for semi-open environments by describing "good country" as open and with little undergrowth [Stanley, 2000] and by actively promoting openness and patchiness by applying regular burning to vegetation [Barr and Cary, 1992].

Based on the overwhelming evidence of hunter-gatherers using fire to promote landscape openness and patchiness, we argue that ignoring anthropogenic fire dynamics at prehistoric times is likely to produce a biased picture of vegetation dynamics and may well be a reason why DGMVs tend to consistently overestimate tree cover specifically in Europe during the LGM. Archaeological evidence clearly shows that at the time of the LGM humans have been present in all parts of Europe (Fig. 4.2c), and very likely not only used fire for cooking, as indicated by findings of charred material in cave sites, but also for many other purposes to facilitate daily life. By incorporating a simple scheme of hunter-gatherer burning that mimics the interaction between fires, change in tree cover, and human ignitions we can show that additional fire caused by people leads to a significant decrease in tree cover especially in those places that originally had a high simulated tree cover. Our simulation results suggest that a moderate increase in burning frequency resulting in an increase in average annual burned area fraction of 0.05 to 0.1 in many places is already sufficient to cause a significant decrease in simulated tree cover. A comparison of Fig. 4.1a) and 4.1b) reveals that none of the grid pixels

Chapter 4. Role of humans and fire for vegetation in Europe during the Last Glacial Maximum

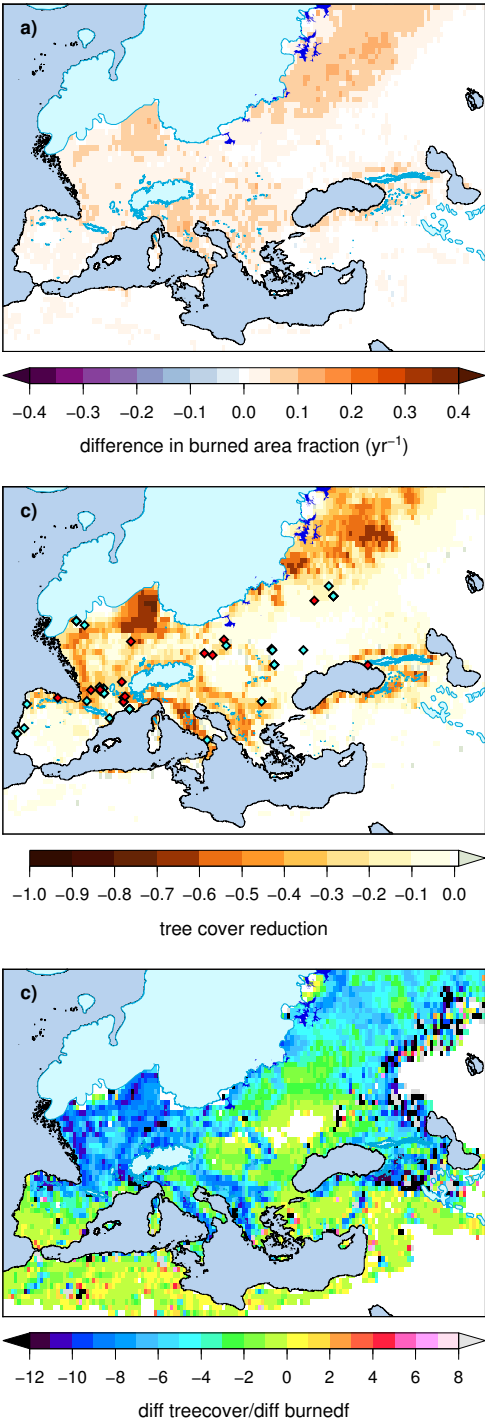


Figure 4.3: Panel a) Difference in annual burned area between the LGM scenarios without and including anthropogenic burning. Panel b) Reduction in tree cover due to hunter-gatherer burning. Diamonds indicate archaeological sites, red diamonds are sites with evidence for human fire use. Panel c) Ratio between treecover reduction and difference in burned area due to hunter-gatherers. Strong negative ratios indicate places where vegetation reacts particularly sensitive to hunter-gatherer burning.

within the simulation area experiences an increase in annual burned area fraction of more than 0.15 through the additional anthropogenic burning, with only few grid pixels showing an increase between 0.1 and 0.15, and the majority of the grid pixels showing an increase of less than 0.05 (see also Fig. 4.3a). Those areas that show the most drastic decrease in tree cover when introducing anthropogenic burning (Fig. 4.2c) are mostly characterized by extremely low amounts of natural burning (Fig. 4.1a) with often less than 4 % of grid cell area burned by year. A small increase of 0.05 to 0.1 in annual burned area fraction in these places is sufficient to decrease the average tree cover fraction by up to 0.5 or more (Fig. 4.2c), thereby causing a shift from tree-dominated landscape to a very open type of landscape with a domination in grassy and herbaceous PFTs (Fig. 4.2b). As indicated by the filled circles in Fig. 4.2a) and 4.2b), this simulated increase in openness is in good agreement with pollen-based biome reconstructions, which indicate steppe vegetation for most of the available sites in Europe [Bigelow et al., 2003, Harrison et al., 2001, Prentice et al., 2000a], whereas the simulated tree cover for the scenario with natural-burning only (Fig. 4.2a) suggests an underestimation of openness especially for western and central Europe, and the land area to the east of the Scandinavian ice sheet. At the same time, places that have been discussed as potential tree refugia, e.g., around the Black Sea or in the Dinaric Alps [Bennett et al., 1991, Brewer et al., 2002, Svenning et al., 2008], remain with a tree cover of at least 60 % even when including human burning.

4.5 Conclusions

The results of your study agree with evidence from charcoal records that suggests lower burning for the LGM compared to preindustrial, both when comparing scenarios excluding and including anthropogenic burning for both time slices. During the LGM simulated amounts of annual area burned are generally very low in most parts of Europe outside the Mediterranean when considering natural fire only. Concomitantly, simulated tree cover levels, specifically in western and central Europe, range between 40 and 80 %. This is in contradiction with available pollen records, which point to steppe-type vegetation for most of the available sites. With archaeological evidence clearly suggesting the presence of hunter-gatherers in Europe during the LGM, and based on extensive evidence of foragers using fire liberally to increase landscape openness, we argue that anthropogenic burning as disturbance factor in addition to natural burning may be a key factor for improving vegetation dynamics modeling for the LGM. We are able to show that adding anthropogenic fire as an additional vegetation disturbance component leads to a low to moderate total increase in average annual area burned, although the relative increase compared to the natural-only scenario is very pronounced especially for latitudes north of the Mediterranean where natural burning is very low. An increase in average annual burned fraction of 0.05 to 0.1 caused by human burning has proved to be sufficient for causing a reduction in tree cover fraction as high as 0.6. With anthropogenic burning being taken into account, extensive parts of Europe show a simulated tree cover of no more than 10 to 20 %. Such a high degree of landscape openness agrees well with the steppe-like

Chapter 4. Role of humans and fire for vegetation in Europe during the Last Glacial Maximum

conditions suggested by pollen-based vegetation reconstructions. Fire was likely the most indispensable tool of Paleolithic hunter-gatherers in a glacial world, and one would arguably not give these humans enough credit when assuming that they did not know how to use it for their benefits, e.g. to shape landscapes that improved their chances of survival. Although the absolute change in burning caused by humans may look small, the resulting change in vegetation cover shows that even neglecting seemingly small factors can lead to a considerable bias in the overall outcome. We therefore suggest that ignoring forager burning as disturbance factor in vegetation modeling can be responsible for the discrepancies between reconstructed and simulated vegetation cover, resulting in an overestimation of tree cover in Europe during the LGM.

4.6 Supplementary Figures

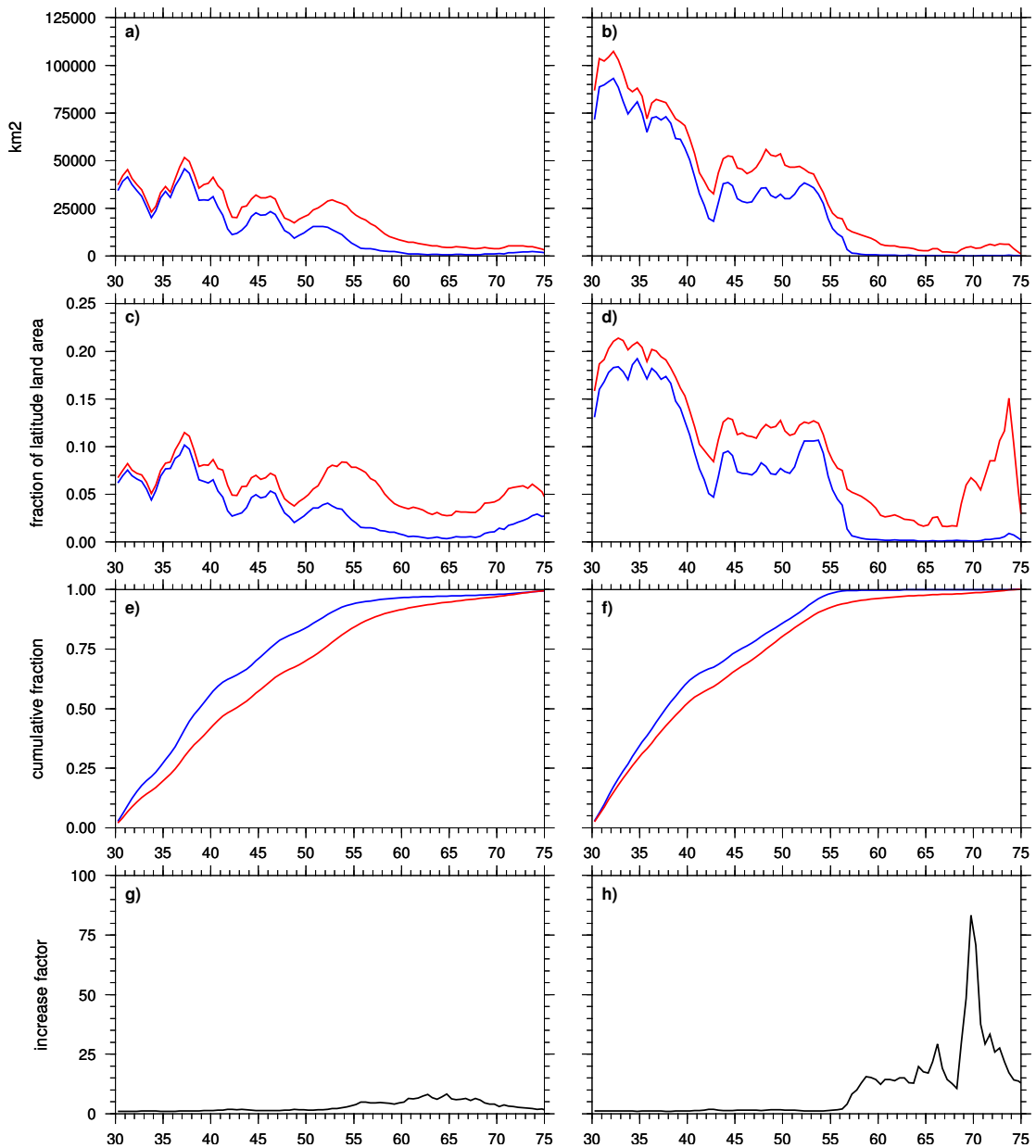


Figure 4.4: Panels in left column are for LGM, panels in right column for preindustrial. Blue curves are for scenarios with human absence, red curves for scenarios including human presence and burning. Panel a) and b): Annual area burned per 0.5° latitudinal band. Panel c) and d): Fraction of latitude land area burned per year. Panel e) and f): Cumulative fraction of annual burned latitude area between 30 and 75 °N. Increase in latitudinal burned area per year due to additional human burning.

Chapter 4. Role of humans and fire for vegetation in Europe during the Last Glacial Maximum

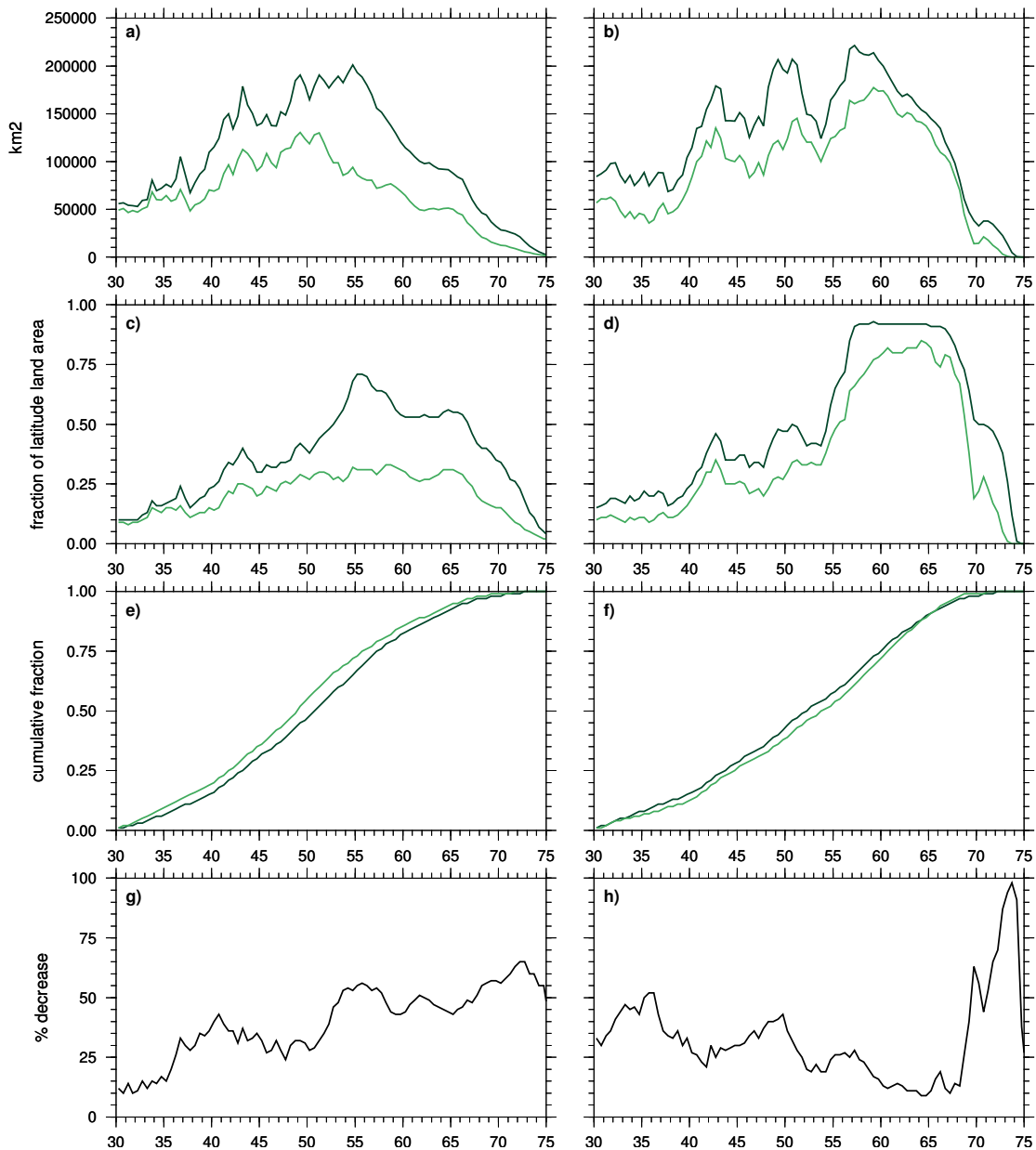


Figure 4.5: Panels in left column are for LGM, panels in right column for preindustrial. Dark green curves are for scenarios with human absence, light green scenarios include human presence and burning. Panel a) and b): Total forest area per 0.5° latitudinal band. Panel c) and d): Fraction of latitude land area covered by trees. Panel e) and f): Cumulative fraction of total forest cover between 30 and 75 °N. Panel g) and h): Decrease in latitudinal forest cover due to human presence and burning.

Bibliography

- J. Appleton. *The Experience of Landscape*. Wiley, London, 1975.
- J. D. Balling and J. H. Falk. Development of Visual Preference for Natural Environments. *Environment and Behavior*, 14:1:5–28, 1982. doi: 10.1177/0013916582141001.
- N. F. Barr and J. W. Cary. *Greening a Brown Land: The Australian Search for Sustainable Land Use*. Macmillan, Australia: Melbourne, 1992.
- K. D. Bennett, P. C. Tzedakis, and K. J. Willis. Quaternary refugia of north European trees. *Journal of Biogeography*, 18:103–115, 1991.
- N. H. Bigelow, L. B. Brubaker, M. E. Edwards, S. P. Harrison, I. C. Prentice, P. M. Anderson, A. A. Andreev, P. J. Bartlein, T. R. Christensen, W. Cramer, J. O. Kaplan, A. V. Lozhkin, N. V. Matveyeva, D. F. Murray, A. D. McGuire, V. Y. Razzhivin, J. C. Ritchie, B. Smith, D. A. Walker, K. Gajewski, V. Wolf, B. H. Holmqvist, Y. Igarashi, K. Kremenetskii, A. Paus, M. F. J. Pisaric, and V. S. Volkova. Climate change and Arctic ecosystems: 1. Vegetation changes north of 55 degrees N between the last glacial maximum, mid-Holocene, and present. *Journal of Geophysical Research-Atmospheres*, 108(D19):–, 2003. 732ER Times Cited:40 Cited References Count:414.
- R. B. Bird, D. W. Bird, B. F. Coddling, C. H. Parker, and J. H. Jones. The "fire stick farming" hypothesis: Australian Aboriginal foraging strategies, biodiversity, and anthropogenic fire mosaics. *Proceedings of the National Academy of Sciences, USA*, 105(39):14796–14801, 2008.
- W. J. Bond, F. I. Woodward, and G. F. Midgley. The global distribution of ecosystems in a world without fire. *New Phytologist*, 165:525–538, 2005. doi: 10.1111/j.1469-8137.2004.01252.x.
- D. M. J. S. Bowman, J. K. Balch, P. Artaxo, W. J. Bond, J. M. Carlson, M. A. Cochrane, C. M. D'Antonio, R. S. DeFries, J. C. Doyle, S. P. Harrison, F. H. Johnston, J. E. Keeley, M. A. Krawchuck, C. A. Kull, J. B. Marston, M. A. Moritz, I. C. Prentice, C. I. Roos, A. C. Scott, T. W. Swetnam, G. R. van der Werf, and S. J. Pyne. Fire in the Earth System. *Science*, 324: 481–485, 2009.
- D. M. J. S. Bowman, J. Balch, P. Artaxo, W. J. Bond, M. A. Cochrane, C. M. D'Antonio, R. DeFries, F. H. Johnston, J. E. Keeley, M. A. Krawchuck, C. A. Kull, M. Mack, M. A. Moritz, S. J. Pyne,

Bibliography

- C. I. Roos, A. C. Scott, N. S. Sodhi, and T. W. Swetnam. The human dimension of fire regimes on Earth. *Journal of Biogeography*, 38(12):2223–2236, 2011. doi: 10.1111/j.1365-2699.2011.02595.x.
- S. Brewer, R. Cheddadi, J.-L. de Beaulieu, M. Reille, and Data contributors. The spread of deciduous *Quercus* throughout Europe since the last glacial period. *Forest Ecology and Management*, 156:27–48, 2002.
- D. A. Burney and T. F. Flannery. Fifty millennia of catastrophic extinctions after human contact. *Trends in Ecology and Evolution*, 20(7):396–402, 2005. doi: 10.1016/j.tree.2005.04.022.
- A.-L. Daniau, S. P. Harrison, and P. J. Bartlein. Fire regimes during the Last Glacial. *Quaternary Science Reviews*, 29:2918–2930, 2010. doi: 10.1016/j.quascirev.2009.11.008.
- H. Elenga, O. Peyron, R. Bonnefille, D. Jolly, R. Cheddadi, J. Guiot, V. Andrieu, S. Bottema, G. Buchet, J.-L. de Beaulieu, A. C. Hamilton, J. Maley, R. Marchant, R. Perez-Obiol, M. Reille, G. Riollet, L. Scott, H. Straka, D. Taylor, E. van Campo, A. Vincens, F. Laarif, and H. Jonson. Pollen-based biome reconstruction for southern Europe and Africa 18,000 yr BP. *Journal of Biogeography*, 27:621–634, 2000.
- Geological Society of America. Seasonal reconstructions of the Earth's surface at the last glacial maximum. Map Series, Technical Report MC-36, Geological Society of America, Boulder, Colorado, 1981.
- P. H. Gobster. The Urban Savanna: Reuniting Ecological Preference and Function. *Restoration and Management Notes*, 12:64–71, 1994.
- P. H. Gobster. Aldo Leopold's Ecological Esthetic: Integrating Esthetic and Biodiversity Values. *Journal of Forestry*, 93(2):6–10, 1995.
- S. Harrison and I. C. Prentice. Climate and CO₂ controls on global vegetation distribution at the last glacial maximum: analysis based on palaeovegetation data, biome modelling and palaeoclimate simulations. *Global Change Biology*, 9:983–1004, 2003.
- S. P. Harrison, H. Takahara, and I. C. Prentice. Palaeovegetation - Diversity of temperate plants in east Asia. *Nature*, 413:129–130, 2001.
- J. O. Kaplan, N. H. Bigelow, I. C. Prentice, S. P. Harrison, P. J. Bartlein, T. R. Christensen, W. Cramer, N. V. Matveyeva, A. D. McGuire, D. F. Murray, V. Y. Razzhivin, B. Smith, D. A. Walker, P. M. Anderson, A. A. Andreev, L. B. Brubaker, M. E. Edwards, and A. V. Lozhkin. Climate change and Arctic ecosystems: 2. Modeling, paleodata-model comparisons, and future projections. *Journal of Geophysical Research*, 108(D19):8171, 2003. doi: 10.1029/2002JD002559.
- R. Kaplan and S. Kaplan. *The Experience of Nature: A Psychological Perspective*. Cambridge University Press: Cambridge, 1989.

- R. Kaplan, S. Kaplan, and T. Brown. Environmental preference: a comparison of four domains of predictors. *Environment and Behavior*, 21:509–530, 1989.
- S. Kaplan. *Beyond rationality: Clarity-based decision making; in: Environment, Cognition and Action*, pages 171–190. Oxford University Press, New York, 1991.
- R. W. Kimmerer and F. K. Lake. The Role of Indigenous Burning in Land Management. *Journal of Forestry*, 99(11):36–41, November 2001.
- J. Lathière, D. A. Hauglustaine, and N. de Noblet-Ducoudré. Past and future changes in biogenic volatile organic compound emissions simulated with a global dynamic vegetation model. *Geophysical Research Letters*, 32:L20818, 2005. doi: 10.1029/2005GL024164.
- H. T. Lewis, editor. *Why Indians burned: specific versus general reasons*, number GTR-INT-182, November, 15-18, 1983. 1985. Proceedings–Symposium and Workshop on Wilderness Fire: Missoula, Montana, Ogden, UT: USDA Forest Service, Intermountain Forest and Range Experiment Station.
- E. Monnin, A. Indermühle, A. Dällenbach, J. Flückiger, B. Stauffer, T. F. Stocker, D. Raynaud, and J.-M. Barnola. Atmospheric CO₂ Concentrations over the Last Glacial Termination. *Science*, 291:112–116, 2001.
- L. T. Murray, J. O. Kaplan, and L. J. Mickley. LGM CLIMAP dataset. pers. comm., 2012.
- G. H. Orians and J. H. Heerwagen. *Evolved responses to landscapes. In: The adaptive mind: Evolutionary psychology and the generation of culture*, pp. 555-579. Oxford University Press, New York, 1980.
- J. G. Pausas and J. E. Keeley. A burning story: The role of fire in the history of life. *BioScience*, 59(7):593–601, 2009.
- A. J. Pitman, G. T. Narisma, and J. McAneney. The impact of climate change on the risk of forest and grassland fires in Australia. *Climatic Change*, 84:383–401, 2007. doi: 10.1007/s10584-007-9243-6.
- M. J. Power, J. Marlon, N. Ortiz, P. J. Bartlein, S. P. Harrison, F. E. Mayle, A. Ballouche, R. H. W. Bradshaw, C. Carcaillet, C. Cordova, S. Mooney, I. C. Prentice, K. Thonicke, W. Tinner, C. Whitlock, Y. Zhang, Y. Zhao, A. A. Ali, R. S. Anderson, R. Beer, H. Behling, C. Briles, K. J. Brown, A. Brunelle, M. Bush, P. Camill, G. Q. Chu, J. Clark, D. Colombaroli, S. Connor, A.-L. Daniau, M. Daniels, J. Dodson, E. Doughty, M. E. Edwards, W. Finsinger, D. Foster, J. Frechette, M.-J. Gaillard, D. G. Gavin, E. Gobet, S. Haberle, D. J. Hallet, P. Higuera, G. Hope, S. Horn, J. Inoue, P. Kaltenrieder, L. Kennedy, Z. C. Kong, C. Larsen, C. J. Long, J. Lynch, E. A. Lynch, M. McGlone, S. Meeks, S. Mensing, G. Meyer, T. Minckley, J. Mohr, D. M. Nelson, J. New, R. Newnham, R. Noti, W. Oswald, J. Pierce, P. J. H. Richard, C. Rowe, M. F. Sanchez Goni, B. N. Shuman, H. Takahara, J. Toney, C. Turney, D. H. Urrego-Sanchez, C. Umbanhowar, M. Vandergoes, B. Vanniore, E. Vescovi, M. Walsh, X. Wang, N. Williams,

Bibliography

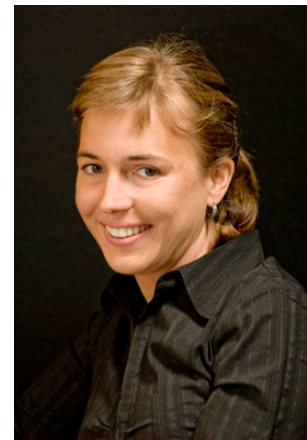
- J. Wilmshurst, and J. H. Zhang. Changes in fire regimes since the Last Glacial Maximum: an assessment based on a global synthesis and analysis of charcoal data. *Climate Dynamics*, 30:887–907, 2008.
- I. C. Prentice and S. P. Harrison. Ecosystem effects of CO₂ concentration: evidence from past climates. *Climate of the Past*, 5:297–307, 2009.
- I. C. Prentice, M. Heimann, and S. Sitch. The carbon balance of the terrestrial biosphere: Ecosystem models and atmospheric observations. *Ecological Applications*, 10:1553–1573, 2000a.
- I. C. Prentice, D. Jolly, and BIOME 6000 participants. Mid-Holocene and glacial-maximum vegetation geography of the northern continents and Africa. *Journal of Biogeography*, 27: 507–519, 2000b.
- I. C. Prentice, D. I. Kelley, P. N. Foster, P. Friedlingstein, S. P. Harrison, and P. J. Bartlein. Modeling fire and the terrestrial carbon balance. *Global Biogeochemical Cycles*, 25:GB3005, 2011. doi: 10.1029/2010GB003906.
- S. J. Pyne. Maintaining Focus: An Introduction to Anthropogenic Fire. *Chemosphere*, 29(5): 889–911, 1994.
- S. J. Pyne. *World Fire: The Culture of Fire on Earth*, 384 p. University of Washington Press, Seattle, WA, 1997.
- S. J. Pyne. *Vestal Fire: an Environmental History, told through Fire, of Europe and Europe's Encounter with the World*. University of Washington Press, Seattle, WA, 2000.
- G. Ramstein, M. Kageyama, J. Guiot, H. Wu, C. Hély, G. Krinner, and S. Brewer. How cold was Europe at the Last Glacial Maximum? A synthesis of the progress achieved since the first PMIP model-data intercomparison. *Climate of the Past*, 3:331–339, 2007.
- C. I. Roos, A. P. Sullivan, and C. NcNamee. Paleoecological Evidence for Systematic Indigenous Burning in the Upland Southwest. *The Archaeology of Anthropogenic Environments, Southern Illinois University Press, Carbondale*, pages 142–171, 2010.
- G. A. Schmidt, R. Ruedy, J. E. Hansen, I. Aleinov, N. Bell, M. Bauer, S. Bauer, B. Cairns, V. Canuto, Y. Cheng, A. Del Genio, G. Faluvegi, A. D. Friend, T. M. Hall, Y. Hu, M. Kelley, N. Y. Kiang, D. Koch, A. A. Lacis, J. Lerner, K. K. Lo, R. L. Miller, L. Nazarenko, V. Oinas, Ju. Perlwitz, Ja. und Perlwitz, D. Rind, A. Romanou, G. L. Russell, M. Sato, D. T. Shindell, P. H. Stone, S. Sun, N. Tausnev, D. Thresher, and M.-S. Yao. Present day atmospheric simulations using GISS ModelE: Comparison to in-situ, satellite and reanalysis data. *J. Climate*, 19:153–192, 2006.
- L. Ségalen, J. A. Lee-Thorp, and T. Cerling. Timing of C₄ grass expansion across sub-Saharan Africa. *Journal of Human Evolution*, 53:549–559, 2007. doi: 10.1016/j.jhevol.2006.12.010.

- A. Stanley. Indigenous Land Management Perspective on Conservation and Production. volume Proceedings of the Bushcare Grassy Landscapes Conference, Canberra, Australia, pages 89–100, 2000.
- O. C. Stewart, H. T. Lewis, and K. Anderson. *Forgotten Fires: Native Americans and the Transient Wilderness*. University of Oklahoma Press, 364 p., Norman, OK 73069, 2002.
- G. Strandberg, J. Brandefelt, E. Kjellström, and B. Smith. High-resolution regional simulation of last glacial maximum climate in Europe. *Tellust*, 63A:107–125, 2011. doi: 10.1111/j.1600-0870.2010.00485.x.
- J.-C. Svenning, S. Normand, and M. Kageyama. Glacial refugia of temperate trees in Europe: insights from species distribution modelling. *Journal of Ecology*, 96:1117–1127, 2008.
- P. E. Tarasov, V. S. Volkova, T. Webb, J. Guiot, A. A. Andreev, L. G. Bezusko, T. V. Bezusko, G. V. Bykova, N. I. Dorofeyuk, E. V. Kvavadze, I. M. Osipova, N. K. Panova, and D. V. Sevastyanov. Last glacial maximum biomes reconstructed from pollen and plant macrofossil data from northern Eurasia. *Journal of Biogeography*, 27:609–620, 2000.
- K. Thonicke, I. C. Prentice, and C. Hewitt. Modeling glacial-interglacial changes in global fire regimes and trace gas emissions. *Global Biogeochemical Cycles*, 19:GB3008, pp.12, 2005. doi: 10.1029/2004GB002278.
- G. R. van der Werf, J. T. Randerson, L. Giglio, N. Gobron, and A. J. Dolman. Climate controls on the variability of fires in the tropics and subtropics. *Global Biogeochemical Cycles*, 22:GB3028, 2008. doi: 10.1029/2007GB003122.
- A. A. J. Williams, D. J. Karoly, and N. Tapper. The sensitivity of Australian fire danger to climate change. *Climatic Change*, 49(1-2):171–191, 2001. doi: 10.1023/A:1010706116176.
- G. W. Williams. Introduction to Aboriginal Fire Use in North America. *Fire Management Today*, 60:No. 3, 8–12, 2000.
- M. Williams. *Deforesting the Earth: From Prehistory to Global Crisis*. University of Chicago Press, Chicago, IL, 2002.
- M.-N. Woillez, M. Kageyama, G. Krinner, N. de Noblet-Ducoudré, N. Viovy, and M. Mancip. Impact of CO₂ and climate on the Last Glacial Maximum vegetation: results from the ORCHIDEE/IPSL models. *Climate of the Past*, 7:557–577, 2011. doi: 10.5194/cp-7-557-2011.
- F. I. Woodward and B. G. Williams. Climate and plant distribution at global and local scales. *Vegetatio*, 69:189–197, 1987.
- R. W. Wrangham. *Catching Fire: How Cooking made us human*. Basic Books, New York, 2009.
- H. Wu, J. Guiot, S. Brewer, and Z. Guo. Climatic changes in Eurasia and Africa at the last glacial maximum and mid-Holocene: reconstructions from pollen data using inverse vegetation modelling. *Climate Dynamics*, 29:211–229, 2007. doi: 10.1007/s00382-007-0231-3.

Curriculum Vitae

Personal profile:

As a Geocologist (Diplom) I am interested in processes and linkages between processes in the Earth system. My specific goal is to study the connections between the different compartments of the Earth in order to understand the functioning of the Earth system as a whole. My expertise is in hydrogeology, biogeography, soil ecology, and vegetation modeling using Dynamic Global Vegetation Models. My key strengths include strong analytical and abstract skills, a strong ability for interdisciplinary thinking and collaboration with people from different scientific backgrounds, and the capability to quickly acquire new knowledge and skills. I enjoy working in an interdisciplinary team where I can exchange ideas and knowledge with others and benefit from synergy, but also have the possibility to work independently. Driven by curiosity, I am highly motivated to take up challenges and find unconventional approaches to tackle open questions.



Graduate Formation

Doctoral student in ARVE research group (start 1st October 2008)

Thesis Supervisor: Prof. Dr. Jed O. Kaplan

Thesis Exam: 21.03.2013

Modeling terrestrial Paleobiogeochemistry

Focus 1: The effect of abrupt climatic warming on biogeochemical cycling and N₂O emissions in a terrestrial ecosystem

Sensitivity study combining process-based simulation of terrestrial nitrogen cycling and multiproxy data from the Swiss Gerzensee data to study the effect of abrupt warming and vegetation change on terrestrial N₂O emissions during the Oldest Dryas/Bølling transition.

Focus 2: LMfire: an improved fire module for Dynamic Global Vegetation Models

Development of a new fire module for LPJ based on SPITFIRE with major changes to the calculation of natural and anthropogenic ignitions, fuel handling, fragmentation effects, fire duration and rate of spread with specific focus on simulating prehistoric anthropogenic burning.

Focus 3: Role of humans and fire for vegetation in Europe during the Last Glacial Maximum

Sensitivity study focussing on the role of European Paleolithic hunter-gatherer fire use in creating the steppe-type vegetation reconstructed from pollen data for the time of the LGM.

Undergraduate Formation

04/08 Master Title (Diplom) in Geoecology from University of Bayreuth (grade 1.0)

Diplomarbeit Master thesis in Hydrogeology, at University of Bayreuth: "Evaluation and Modeling of the Pumping Tests at Heinersreuther Forst" (grade 1.15), supervised by Prof. Dr. Klaus Bitzer

Exams Hydrogeology (major, grade 1.0)
 Soil Ecology (major, grade 1.0)
 Geoinformation Systems/Remote Sensing (minor, grade 1.0)
 Geology/Geomorphology (minor, grade 1.0)
 Biogeography (voluntary major without final examination)

Languages:

German Native language
English Excellent speaking and writing skills (worked four years in a research group with predominantly native English speakers)
French Fluent (speaking and writing)

Software skills:

Programming Languages, Frameworks and Tools:

Linux, Windows, OS X, Fortran 90, Shell Scripting, Open MPI (basic knowledge)

Data handling, processing, and illustration:

NetCDF, CDO, NCKS, PostgreSQL (basic knowlegdge), GMT

Conferences:

07/09 PAGES First Young Scientist Meeting and PAGES Third Open Science Meeting in Corvallis, Oregon (poster presentation)
02/10 1st TERRABITES Symposium, Hamburg, Germany (poster presentation)
07/11 XVIII INQUA-Congress, Bern, Switzerland (poster presentation)
02/12 2nd TERRABITES Symposium, Frascati, Italy (poster presentation)
 participation at TERRABITES 1st training school
07/12 3rd International Schöntal Conference, Farming in the Forest - Ecology of Fire in Prehistoric Agriculture, Kloster Schöntal, Germany (poster presentation)
04/12 ProClim 13th Swiss Global Change Day, Bern, Switzerland (awarded poster)

Publications:

M. Pfeiffer and J. O. Kaplan. Response of terrestrial N₂O and NO_x emissions to abrupt climate change. IOP Conference Series: Earth and Environmental Science. 9(1). 012001, 2012, doi:10.1088/1755-1315/9/1/012001

M. Pfeiffer, J. van Leeuwen, W. O. van der Knaap, and J. O. Kaplan. The effect of abrupt climate warming on biogeochemical cycling and terrestrial N₂O emissions in a terrestrial ecosystem. *Palaeogeography, Palaeoclimatology, Palaeoecology*. in press, PALAEO-06176, 12 p. 2012, doi:10.1016/j.palaeo.2012.06.015

M. Pfeiffer and J. O. Kaplan. SPITFIRE-2: an improved fire module for Dynamic Global Vegetation Models. *Geoscientific Model Development Discussions*. 5:2347-2443, 2012, 10.5194/gmdd-5-2347-2012; resubmitted to *Geoscientific Model Development* after review, 02/2013

M. Pfeiffer and J. O. Kaplan. The role of humans and fire for vegetation in Europe during the Last Glacial Maximum. manuscript in prep. for submission to *Nature Geoscience*.